Phosphine and allyl halocarbonyl complexes of molybdenum and tungsten

Hodson, Annabelle G. W.

Award date:
1988

Awarding institution:
University of Bath

PHOSPHINE AND ALLYL HALOCARBONYL COMPLEXES OF MOLYBDENUM AND TUNGSTEN

submitted by

Annabelle G.W. Hodson

for the Degree of Doctor of Philosophy

of the University of Bath

1988

ProQuest LLC
789 East Eisenhower Parkway
P.O. Box 1346
Ann Arbor, MI 48106-1346

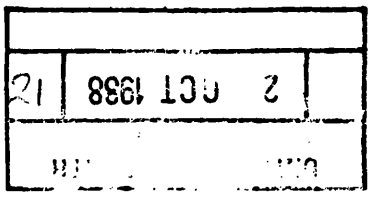

5023580

TO MY MOTHER AND FATHER

FOR THEIR HELP AND SUPPORT

ACKNOWLEDGEMENTS

I would like to thank my supervisor Dr. B.J.Brisdon for his encouragement and guidance throughout the course of this work and the University of Bath for the opportunity to undertake this research.

I would also like to thank Drs. M.F.Mahon and K.C.Molloy of the University of Bath for the structural studies undertaken.

SUMMARY

An investigation of the decarbonylation of $M(CO)_3(PR_3)_2X_2$ (M=Mo, W, PR_3=$PEtPh_2$, PEt_2Ph, $PMePh_2$, PMe_2Ph, X=halide) has shown that the ease of formation and stability of the products $[M(CO)_2(PR_3)_2X_2]_n$ (n=1 or ⩾2) are dependent upon the steric and electronic requirements of PR_3 and X. Analogous reactions in acetonitrile generated the mononuclear complexes $M(CO)_2(PR_3)_2X_2(MeCN)$, which reacted with alkynes R'C≡CR' or anions to yield complexes $M(CO)(PR_3)_2X_2(R'C{\equiv}CR')$ (R'=Me or Ph), $[M(CO)_2(PR_3)_2(SCN)_2]_n$ (n>1), $M(CO)_2(PR_3)_2(O_2CCF_3)_2$, $M(CO)_2(PR_3)_2(O_2CCF_3)Br$, $M(CO)_2(PR_3)(S_2CNEt_2)_2$, $M(CO)(PR_3)_2(S_2CNEt_2)_2$ and $\{MBr(CO)_2(PR_3)_2\}_2-(\mu-C_2O_4)$ respectively, whose structures and bonding were probed by spectroscopic methods. The molecular structure of $MoBr_2(CO)(PMePh_2)_2(MeC{\equiv}CMe)$ which contains a 4-electron donor alkyne ligand was established by X-ray diffraction analysis.

Examination of the solution properties of $MCl(CO)_2(\eta^3\text{-}2\text{-}C_3H_4R)(MeCN)_2$ (M=Mo, W, R=H, Me) dissolved in R'OH (R'=H, Me, Et) has produced evidence for the predominance of $[M(CO)_2(\eta^3\text{-}C_3H_4R)(solvent)_Y]^+$ (Y probably 3) cations under neutral conditions, and the binuclear anions $[M_2(CO)_4(\eta^3\text{-}C_3H_4R)_2(\mu\text{-}OR')_3]^-$ in the presence of base. The latter were isolated and characterised as their tetraphenylarsonium salts. Reactions of $MX(CO)_2(\eta^3\text{-}2\text{-}C_3H_4R)(MeCN)_2$ (X=halide) with 2,2'-bipyridyl, 2,2'-dipyridylamine (L_2) or diethylenetriamine, bis-(2-pyridylmethyl)amine (L_3) in water yielded complexes of the type $MX(CO)_2(\eta^3\text{-}C_3H_4R)L_2$ and $MX(CO)_2(\eta^3\text{-}C_3H_4R)L_3$ or $[M(CO)_2(\eta^3\text{-}C_3H_4R)L_3]^+X^-$. Anion exchange of the halide by hexafluorophosphate generated complexes $[M(CO)_2(\eta^3\text{-}C_3H_4R)L_3]PF_6$, whose dynamic behaviour in solution was demonstrated by variable temperature ^1H NMR spectroscopy, and an X-ray diffraction analysis of

$[W(CO)_2(\eta^3\text{-}C_3H_5)(\text{bis-(2-pyridylmethyl)amine})]PF_6$ showed that the tridentate was bonded to an asymmetric metal centre.

Reaction of $Ph_4P[MCl(CO)_3L_2]$ (M=Mo, L_2=phen, M=W, L_2=bipy) with methanolic $ClCH_2C{\equiv}CCH_2Cl$ generated complexes of the type $MCl(CO)_2(\eta^3\text{-}CH_2{=}C(CO_2Me){-}C{=}CH_2)L_2$ and $MCl(CO)_2(\eta^3\text{-}CH_2{=}C(CO_2Me){-}C(OMe)(Me))L_2$, whilst analogous reactions in the presence of thiols HSR' or amines HNRR' yielded the compounds $MoCl(CO)_2(\eta^3\text{-}CH_2{=}C(COSR'){-}C{=}CH_2)$bipy (R'=Et, Bu^n or Ph) and $MoCl(CO)_2(\eta^3\text{-}CH_2{=}C(CONRR'){-}C{=}CH_2)L_2$ (L_2=bipy, R=R'=Me, Et or Pr^n, R=H, R'=Me, Et, Pr^n, Ph, CH_2Ph, $CH_2CH{=}CH_2$ or $CH_2C{\equiv}CH$, L_2=phen, R=R'=Et). The roles of water, amine size and basicity in determining the type of product formed have been investigated and an order of amine reactivity proposed. Reaction of an amido complex, the heptafluorobutyrate anion and $AgBF_4$ in acetone generated the derivatives $Mo(CO)_2(\eta^3\text{-}CH_2{=}C(CONHR'){-}C{=}CH_2)(bipy)(O_2CC_3F_7)$, and the structure of $Mo(CO)_2(\eta^3\text{-}CH_2{=}C(CONHMe){-}C{=}CH_2)(bipy)(O_2CC_3F_7)$ containing an η^3-<u>trans</u>-butadienyl ligand was determined by an X-ray diffraction study.

TABLE OF CONTENTS

ABBREVIATIONS

acac	acetylacetonate anion
arphos	1-Diphenylphosphino-2-diphenylarsinoethane
bipy	2,2'-bipyridyl
bpma	bis(2-pyridylmethyl)amine
Bu	butyl
COC	capped octahedron
cod	cycloocta-1,5-diene
Cp	cyclopentadiene
CTP	capped trigonal prism
diars	o-phenylenebis(dimethlyarsine)
dien	diethylenetriamine
dme	dimethoxyethane
dmpe	bis-(dimethylphosphino)ethane
dpa	2,2'-dipyridylamine
dpae	bis-(diphenylarsino)ethane
dpam	bis-(diphenylarsino)methane
dppe	bis-(diphenylphosphino)ethane
dppm	bis-(diphenylphosphino)methane
en	1,2-diaminoethane
Et	ethyl
FAB	fast atom bombardment
L	Lewis base
Λ_M	molar conductivity
Me	methyl
m/z	mass per unit charge
MeCN	acetonitrile
mmol	millimole
O_h	octahedron
PB	pentagonal bipyramid
Ph	phenyl
phen	1,10-phenanthroline
Pr	propyl
py	pyridine
pz	pyrazolyl
R	alkyl or aryl
r.t.	ambient temperature
salal	salicylaldehydato anion
θ	Tolman cone angle
THF	tetrahydrofuran
tpma	tris-(2-pyridylmethyl)amine
TP	trigonal prism
ψ	molecular orbital

INFRA-RED (IR) SPECTRA

cm^{-1}	wavenumber
k	CO stretching force constant
m	medium
s	strong
v	very
w	weak
ν_s	symmetric stretching vibration
ν_{as}	asymmetric stretching vibration
2ϕ	calculated OC-M-CO angle

ULTRA-VIOLET (UV) SPECTRA

ϵ	molar extinction coefficient
E_h	transition energy
λ_{max}	wavelength at maximum absorbance

NUCLEAR MAGNETIC RESONANCE (NMR) SPECTRA

δ	chemical shift relative to TMS
d	doublet
J	coupling constant
m	multiplet
ppm	parts per million
q	quartet
s	singlet
t	triplet
TMS	tetramethyl silane

CHAPTER 1

AN INTRODUCTION TO Mo AND W PHOSPHINE HALOCARBONYL COMPLEXES

1.1 INTRODUCTION

The Group VI transition metals molybdenum and tungsten form an extensive range of complexes with coordination numbers from four to nine, resulting from the combination of coordinated ligands with differing σ- and π-bonding properties and the metal atom in formal oxidation states of -II to +VI. In accord with the effective atomic number rule, metal ions with d^6 or d^4 electronic configurations and ligands with strong π-acceptor abilities form stable six or seven coordinate complexes respectively. Of particular reference to the work described in this thesis are the carbonyl complexes of d^4 molybdenum and tungsten ions, which have been shown to exhibit interesting dynamic behaviour and stereochemistry [1-5], to be of considerable significance in oxidative addition reactions and catalytic processes [6] and to occur as intermediates in associative reactions of six coordinate complexes [7-9]. In order to more fully understand the role of such species, a large body of research has been devoted to the preparation and characterisation of stable seven coordinate Mo(II) and W(II) complexes, with the substituted halocarbonyls of general formulae $M(CO)_3L_2X_2$ and $M(CO)_2L_2(\eta^3$-allyl$)X$, where L or L_2 are Group V donor ligands and X is a halide, featuring prominently in these investigations.

In continuation of this work, two main areas of research have been undertaken and are presented in this thesis. These concern chemistry associated with the tertiary phosphine complexes $M(CO)_3(PR_3)_2X_2$ and two types of η^3-bonded organometallic species, the first of which contains symmetric η^3-allyl units, the second containing asymmetric, 2-substituted η^3-butadienyl moieties. This chapter constitutes a short review of the preparation, bonding and structure of the phosphine complexes and their decarbonylation

products and considers the electronic and steric factors which influence their adoption of six or seven coordinate geometries.

1.2 PREPARATIVE METHODS FOR $M(CO)_3(PR_3)_2X_2$

(M=Mo or W, PR_3=tertiary phosphine, X=halide).

The seven coordinate Mo(II) and W(II) halocarbonyls $M(CO)_3(EPh_3)_2X_2$ (E=P, As or Sb) were first prepared by Colton and coworkers [10-13] by reaction of the donor ligands EPh_3 with $[M(CO)_4X_2]_2$ and this general method with slight modification [14] has been used extensively by successive workers in this area. The parent halocarbonyls were first reported in 1966 and a halogen-bridged seven coordinate structure was postulated to account for their diamagnetism. Recently the dimeric nature of $W_2Br_4(CO)_8$ has been confirmed by X-ray crystallography [15] and reaction with EPh_3 therefore involves both the breaking of halogen bridges and carbon monoxide displacement. Another method frequently employed in the preparation of $M(CO)_3(ER_3)_2X_2$ (R=alkyl or aryl) involves the halogenation of cis-$M(CO)_4(ER_3)_2$ [16], and until recently this was the only useful route to the iodo complexes since $[M(CO)_4I_2]_2$ is particularly unstable.

Both these general synthetic methods have been extended to include a wide range of complexes of general formula $M(CO)_3L_2X_2$, containing either mono- or bidentate ligands of phosphorus, arsenic, antimony or nitrogen. Anker, Colton and Tomkins [17] provided an excellent early review of this area, describing both the optimum preparative route to each complex and the comparative properties of each species. However these routes do not always successfully yield the required pure product. Thus reaction of bromine or iodine with cis- or trans-$[M(CO)_4(PPh_3)_2]$ in dichloromethane or chloroform results in the formation of $[PPh_3H][M(CO)_3(PPh_3)X_3]$ (M=Mo

or W, X=Br or I) [18] (the proton is presumed to originate from the solvent since this product was not formed in carbon tetrachloride), whilst reaction of ligands of poor π-acceptor ability such as nitrile with $[Mo(CO)_4X_2]_2$ produces unstable Mo(II) species which disproportionate into Mo(0) and Mo(III) complexes [19] as shown in 1.1 below.

$$3[Mo(\mu\text{-}X)X(CO)_4]_2 + 12L \xrightarrow{-6CO} 6Mo(CO)_3X_2L_2$$

$$6Mo(CO)_3X_2L_2 \xrightarrow{-6CO} 2Mo(CO)_6 + 4MoX_3L_3 \qquad (1.1)$$

(X=Cl or Br, L=nitrile, pyridine, THF, etc.)

In addition, loss of CO during the preparation of $[M(CO)_4Br_2]_2$ may result in the formation of $M_2(CO)_7Br_4$ [15] as an impurity and produce unwanted by-products upon subsequent reaction with a donor ligand.

Recently halogenation of fac-$M(CO)_3(MeCN)_3$ has been shown to yield $M(CO)_3(MeCN)_2X_2$ [20], of which only the iodo complexes proved sufficiently stable to be fully characterised. Subsequent displacement of acetonitrile by ER_3 provided an alternative route to known iodo complexes [21,22] and a useful method for preparing new mono substituted species $M(CO)_3(MeCN)I_2L$ (M=Mo or W, L=EPh_3 or halo-sustituted pyridine) [23,24]. Finally for the preparation of some specific phosphine derivatives, reductive carbonylation of $M(PPh_3)_2Cl_4$ to $M(CO)_3(PPh_3)_2Cl_2$ has been successfully achieved [25], and reaction of EMe_3 with $M(CO)_4(E'Me_3)X_2$ provides a path to the mixed complexes $M(CO)_3(EMe_3)(E'Me_3)X_2$ (E,E'=P, As or Sb) [26].

1.3 BONDING IN $M(CO)_3(PR_3)_2X_2$.

1.3.1 THE METAL-CARBONYL BOND.

The molecular orbitals of an isolated carbon monoxide molecule can be illustrated by electron density plots of the frontier molecular orbitals [27] as shown in Fig. 1.1. The lowest unoccupied molecular orbitals are the degenerate set $2\pi^*$ (π anti-bonding), whilst the highest occupied molecular orbital is 5σ (σ bonding). The greater electronegativity of oxygen compared to carbon leads to localisation of 4σ and 1π electron density on the oxygen atom and 5σ and $2\pi^*$ on the carbon atom.

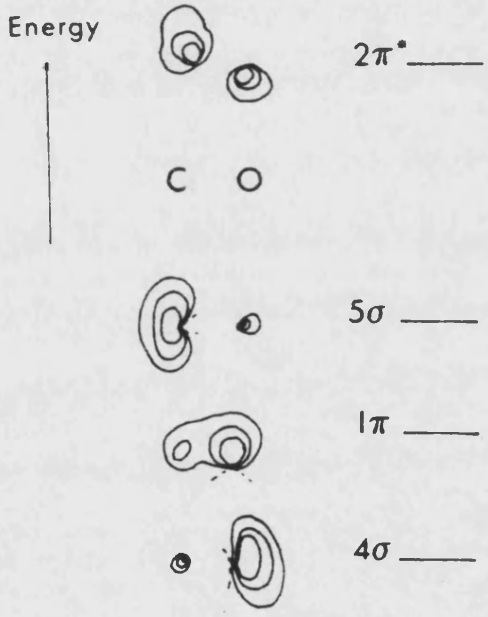

Fig. 1.1 Electron density plots of the frontier orbitals of CO.

Transition metal-carbonyl σ-interactions are dominated by donation of electron density from 5σ to an empty metal orbital, whilst of the two effects of 1π and $2\pi^*$ interaction with d-orbitals, the latter predominates and leads to transfer of electron density from the metal to the carbonyl ligand.

For $M(CO)_6$ the metal-ligand interactions can be illustrated in detail by Fig. 1.2. Six bonding and anti-bonding σ

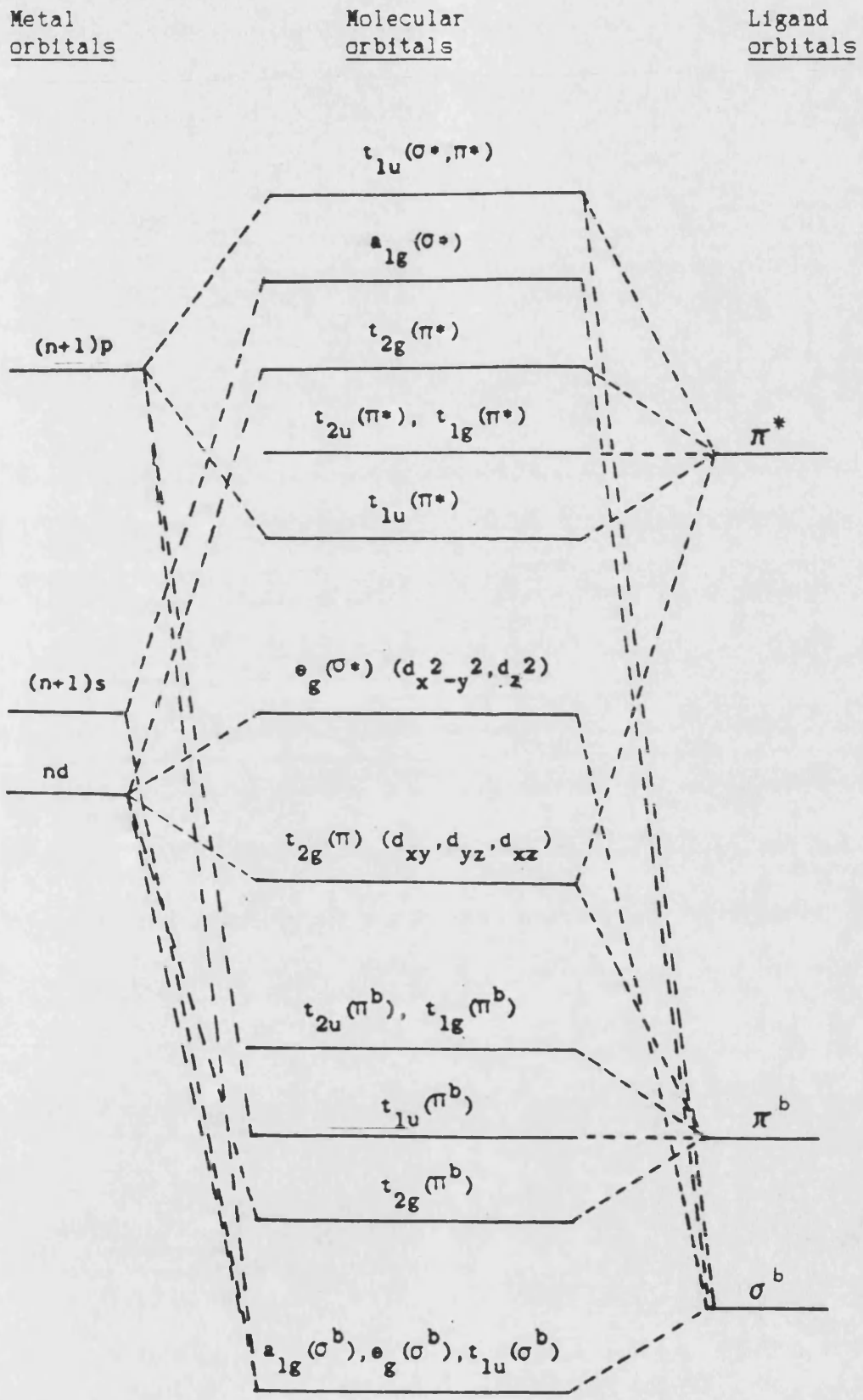

Fig. 1.2 Molecular orbital diagram for octahedral metal carbonyls and their derivatives.

molecular orbitals are generated by linear combinations of ligand σ orbitals and metal $nd_{x^2-y^2}$ and nd_{z^2} (e_g), (n+1)s (a_{1g}) and (n+1)p_x, (n+1)p_y and (n+1)p_z (t_{1u}) orbitals. The π molecular orbitals are composed of nd_{xy}, nd_{xz} and nd_{yz} (t_{2g}) metal orbitals and combinations with π and π^* ligand molecular orbitals. Metal (n+1)p orbitals interact with both ligand π and π^* orbitals yielding three bonding and three antibonding molecular orbitals, t_{1u} (π^b) and t_{1u} (π^*), and three strongly antibonding molecular orbitals, t_{1u} (σ^* and π^*), with both σ and π character. Finally t_{1g} and t_{2u}, π and π^* ligand orbital combinations have no interaction with metal orbitals.

In Group VI hexacarbonyls the metal and each carbonyl group contribute six and two electrons respectively, which fill the σ and π molecular orbitals up to and including the t_{2g} level. The formation of a partial double bond between metal and carbon (carbonyl) results in lowering of the bond order between carbon and oxygen as shown by comparison of the infra-red carbonyl stretching frquencies for free CO (2143cm^{-1}) and the t_{1u} mode of gaseous $Mo(CO)_6$ (2000cm^{-1}). In substituted metal carbonyl derivatives the ability of the non-carbonyl ligands to act as π-acceptors or donors should influence the amount of electron density which is dispersed from the metal into the carbonyl anti-bonding orbitals. This argument has been invoked to both explain differences in carbonyl stretching frequencies for analogous complexes $M(CO)_nL_{6-n}$, in which only the ligand L is changed and the successive lowering of CO stretching frequencies upon substitution of CO by PR_3 in the series $M(CO)_n(PR_3)_{6-n}$.

1.3.2 THE METAL-PHOSPHINE BOND

1.3.2.1 Π-BONDING EFFECTS

Until the early 1960's bonding between phosphines and transition metals was believed to consist of a combination of σ- and π-bonding analogous to that found in metal carbonyls. Interaction of a metal acceptor orbital with the lone-pair electrons of the phosphorus atom results in the formation of a σ-bond and a tetrahedral configuration at the phosphorus atom. The π-bonding component was assumed to arise from metal d_π donation to vacant 3d orbitals on phosphorus. However much controversy has arisen as to whether phosphines can, or do, utilise their 3d orbitals in this way and many investigations centred upon low valent metal-phosphine carbonyl derivatives have been carried out in order to resolve this problem.

Bigorgne [28] suggested that the linear relationship between Taft inductive constants (σ^*) of the X substituents in the phosphine PX_3 and the B, ν(CO) stretching frequency in $Ni(CO)_3(PX_3)$ or $Ni(CO)_2(PX_3)_2$, indicated an absence of metal-phosphine π-bonding in these complexes. However, not all PX_3 containing species fitted this plot and the use of Taft σ^* constants as a true measure of π-acceptance was criticised, since inductive effects cannot be assumed to be identical through carbon and phosphorus. Angelici and Ingemason [29] considered that the σ-donor ability of PX_3 was reflected by its ionisation energy or its pKa value and attempted to relate the equilibrium constant, K, to σ-bonding ability by consideration of the replacement reactions described in equation 1.2. Values of K were

$$W(CO)_5(\text{amine}) + PX_3 \xrightarrow{K} W(CO)_5(PX_3) + \text{amine} \qquad (1.2)$$

shown to decrease in the order PBu^n_3 > PPh_3 > $P(OPh)_3$, which is essentially the order of decreasing PX_3 basicity.

The π-bonding ability of PX_3 will be dependent upon both the metal to which it is coordinated and other ligands in the primary coordination sphere, and an order of phosphine π-acceptor ability might therefore be based upon variation of parameters such as ν(CO) or CO force constants for a constant electronic environment. Tolman [30] studied the variation in the A_1 ν(CO) stretching mode of some seventy $Ni(CO)_3(PX_3)$ complexes and by taking the value of 2056.1cm^{-1} for $Ni(CO)_3(PBu^t_3)$ which contains the most basic ligand of the series as zero, assigned a factor χ to each component X, Y or Z in $Ni(CO)_3(PXYZ)$ defined by equation 1.3. The value of ν(CO) A_1 for

$$\nu(CO)\ A_1 \quad Ni(CO)_3(PXYZ) = 2056.1 + \Sigma\chi_i\ cm^{-1} \qquad (1.3)$$

$Ni(CO)_3(PXYZ)$ was defined as the electronic parameter of PXYZ and although this allowed the calculation of unknown ν(CO) values, Tolman did not relate χ to σ or π effects. Values of ν_s(CO) and ν_{as}(CO) in complexes such as $Mo(CO)_3(PX_3)_3$ [31] and $Co(CO)_3(NO)(PX_3)$ [32] have been used to produce an order of π-bonding ability, however studies of ν(CO) and force constants for $M(CO)_5(PX_3)$ (M=Mo or W) [33,34] showed that their relationship to pKa was similar to that for the analogous amine complexes where π-bonding could not occur.

Despite evidence against π-bonding in PX_3 complexes in general, X-ray measurements of some phosphine and phosphite M-P bonds [35,36] indicate that a π-component does exist and it is now generally accepted that the order of π-acceptor ability is CO ≈ PF_3 >$P(OR)_3$ > PPh_3 ≈ PR_3 >PBu^t_3. This order reflects the effective electronegativity of X which has a strong effect upon the partial charge on phosphorus and hence on the 3d orbital size.

1.3.2.2 PHOSPHINE BASICITY AND STERIC EFFECTS

Of the four electron pairs associated with the phosphorus atom in PR_3, three are involved in P-R bonding, occupying orbitals which are primarily of 3p character, but also have some s-character, whilst the fourth is a lone-pair having largely s-character. The greater p-character of the lone-pair orbital in smaller phosphines increases the availability of these electrons, and consequently small phosphines are relatively stronger bases than large phosphines. Table 1.1 shows that in general phosphines are weaker bases than

Table 1.1 Comparison of pKa^ values of amines and phosphines.

	pKa		pKa
PH_3	-14.00	NH_3	9.21
$MePH_2$	-3.20	$MeNH_2$	10.62
Me_2PH	3.90	Me_2NH	10.64
Me_3P	8.65	Me_3N	9.76

^-pKa values of phosphines and amines throughout this thesis refer to the values of pKa for the conjugate acids

amines. The order of basicity for amines (secondary>primary>tertiary> NH_3) does not quite parallel that for phosphines (tertiary> secondary>primary>PH_3) and this may reflect the influence of greater steric crowding about the nitrogen upon protonation of the tertiary amine.

Although weaker bases, phosphines are more nucleophilic than amines as a result of the greater polarisability of the phosphorus lone pairs of electrons and the larger size of the phosphorus atom. Thus the basicity, nucleophilicity and formation of metal-phosphine bonds are strongly affected by the substituents R in PR_3, and the steric effect of PR_3 is one of the most important factors influencing the geometry of metal-phosphine complexes.

In order to discuss size effects, Tolman [37] defined the ligand cone angle, θ for a symmetrical phosphine PXYZ as the apex angle of a cylindrical cone centred 2.28Å from the phosphorus atom which just touched the outer edge of the Van der Waals radii of the groups attached to phosphorus (Fig.1.3).

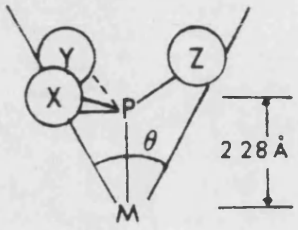

Fig.1.3 Pictorial definition of the cone angle, θ.

For a phosphine PXYZ (X≠Y≠Z), θ can be obtained from the angle $\theta_i/2$ for each substituent, i, by the equation $\theta = 2/3\Sigma\theta_i/2$, whilst for symmetrical phosphines (X=Y=Z) angles greater than 180° may be measured by trigonometry (Fig. 1.4).

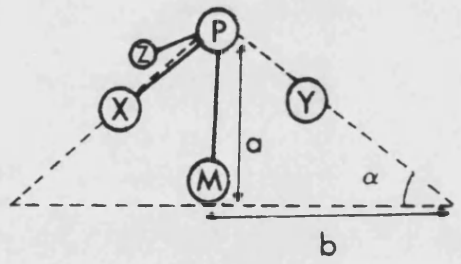

$$\tan\alpha = \frac{a}{b}$$

$$\theta = 180 + 2\alpha$$

Fig. 1.4 Measurement of θ for angles greater than 180°.

Values of θ for bidentate phosphines $X_2P(CH_2)_nPX_2$ (X=alkyl or aryl, n=integer) may be calculated from θ/2, taken as the angle between one M-P bond and the bisector of the PMP angle (Fig.1.5).

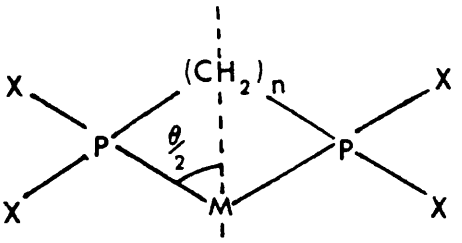

Fig.1.5 Measurement of θ for bidentate phosphines.

The importance of steric effects on stability can be illustrated by the complexes $M(CO)_3(P(tolyl)_3)_2X_2$, of which the P(p-tolyl)$_3$ products (θ=145°) are stable, but the P(o-tolyl)$_3$ complexes (θ=194°) rapidly decompose [38]. Table 1.2 shows that for analogous phosphines and phosphites, the oxygen atom for phosphites leads to smaller θ values, whilst in bidentate phosphines increasing the P-P separation has little effect on cone angle compared to the size of alkyl or aryl substituents.

Table 1.2 Cone angles for selected phosphines and phosphites.

			$R_2P-(CH_2)_n-PR_2$		
R	Phosphine PR_3	Phosphite $P(OR)_3$	n=1	n=2	n=3
Ph	145	128	121	125	127
Et	132	109		115	
Me	118	107		107	

The use of a constant M-P bond length of 2.28Å to define θ is not inappropriate, since this distance varies little in a range of transition metal-alkyl or aryl phosphine complexes [39].

1.4 SEVEN COORDINATION AND MOLECULAR SHAPE

In keeping with the demands of the effective atomic number rule, a large number of heptacoordinate carbonyl complexes of Mo(II) and W(II) are known [39]. The two types of complex which form the subject of this thesis may both be formally considered as seven coordinate metal(II) species. In addition to the phosphine carbonyl halides $M(CO)_3(PR_3)_2X_2$, the η^3-allyl complexes $M(CO)_2(\eta^3\text{-allyl})L_2X$ may be regarded as seven coordinate if the allyl group is considered as a bidentate ligand. Irrespective of geometry these d^4 complexes are diamagnetic with a pair of low energy metal orbitals being occupied by the four d-electrons.

Several methods have been used to try to predict the most stable geometries for seven coordination. Gillespie [40] considered that a series of charge points on the surface of a sphere would be under an energy law of the form $E=\Sigma r_{ij}^{-n}$ (r_{ij}= distance between two of the points i and j, n=positive integer), which for all n values up to six would have the same effect as maximising the least distance between any two of the point charges. Thus for n>6 and n=2 respectively, the capped octahedron and pentagonal bipyramid were predicted, whilst for n values between these extremes a capped trigonal prismatic form was indicated. Calculations of the relative repulsive energies for the three geometries by Britton [41] were in keeping with Gillespie's suggestions, however the relative energy differences between these forms were small, indicating that in real structures other factors may result in variations from these idealised forms. Subsequent calculations of energy E for differing values of n for a range of geometries [42,43] supported these earlier conclusions and in addition revealed that heptacoordinate

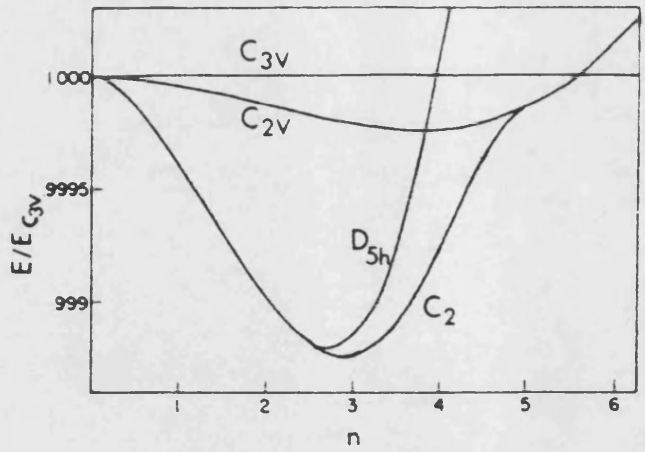

Fig.1.6 Energy diagram for seven coordinate geometries.

geometries of C_2 and C_s symmetries which had not previously been considered were of almost identical energy to that for the pentagonal bipyramid (D_{5h}) below n=2.5 (Fig.1.6). Thus as n decreased, the geometry altered from C_{3v} (capped octahedron) via C_{2v} (capped trigonal prism) and C_2 or C_s to D_{5h} (pentagonal bipyramid) (Fig.1.7) with small changes of energy.

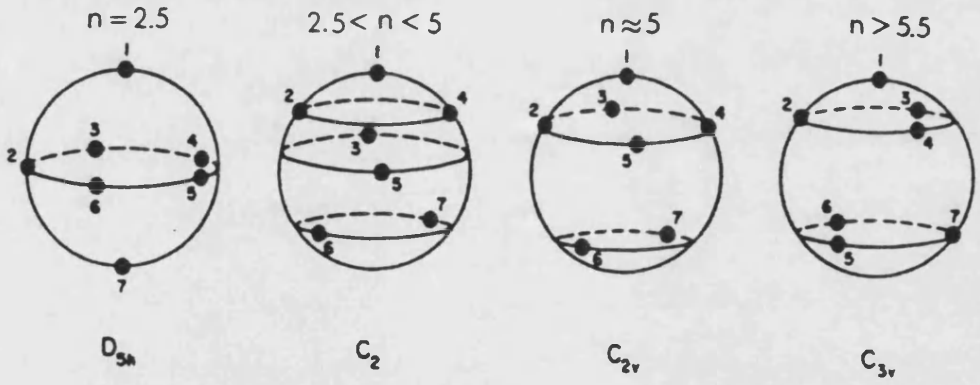

Fig.1.7 Predicted geometries for seven particles.

A review by Drew of seven coordinate structures determined by X-ray crystallography [39] showed that in addition to the commonly encountered structures of the capped octahedron (COC), pentagonal bipyramid (PB) and capped trigonal prism (CTP), some complexes can be usefully described in terms of a square anti-prism or 4:3 geometry (Fig. 1.8).

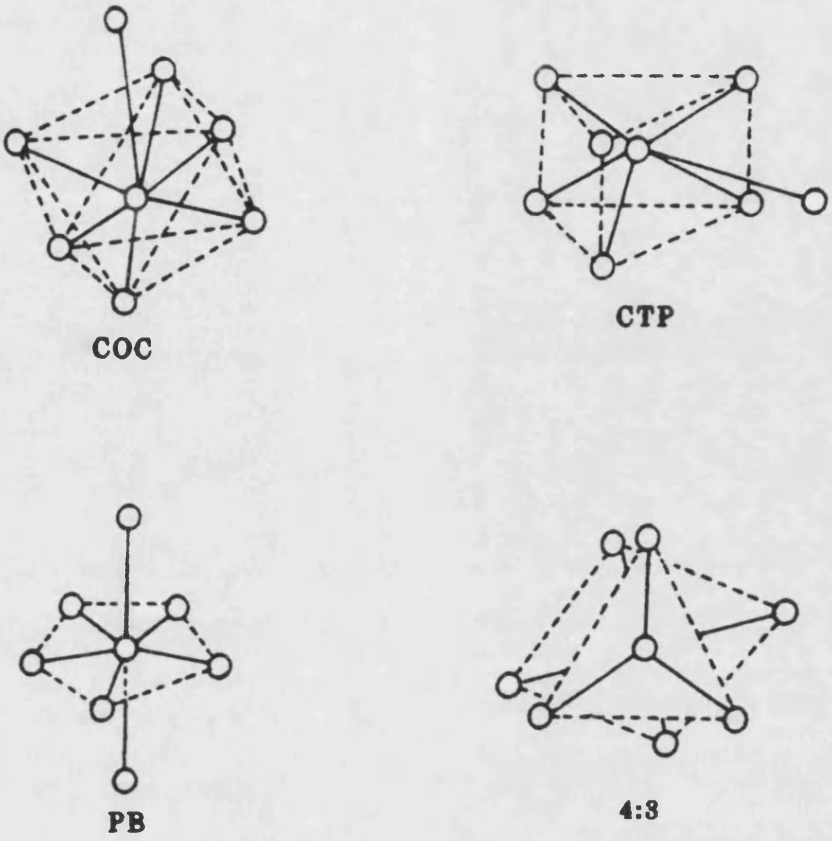

Fig. 1.8 The four major predicted seven coordinate geometries.

Intramolecular interconversion between the three major idealised geometries by edge stretching has been envisaged by Muetterties and Guggenberger [44] (Fig. 1.9). Only 6° in the average set of angles separate the CTP and COC, and intermediate geometries are commonly identified for Mo and W complexes $M(CO)_n(PR_3)_mX_2$ ($n \neq m = 2$ or 3). Two

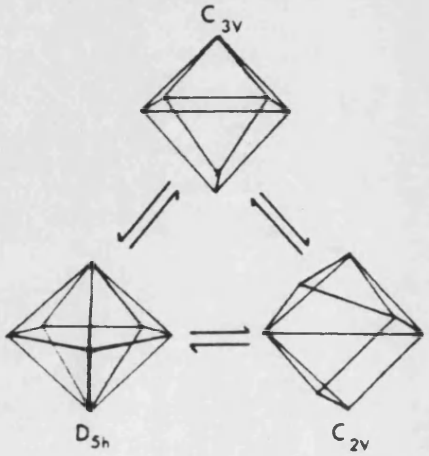

Fig. 1.9 Interconversion cycle between 7-coordinate geometries.

major methods have been suggested to quantify these observed distortions from the ideal geometries. Dollase [45] altered the coordinates of the observed ML_7 crystal structures to those of the ideal polyhedra by rotation and dilation, relating the real and ideal forms by root mean square (r.m.s) differences according to equation 1.4, in which d_i is the distance between the equivalent points in the two polyhedra.

$$\text{r.m.s.} = \left[\frac{\sum_{i=1}^{i=7} d_i^2}{7}\right]^{1/2} \qquad (1.4)$$

Muetterties and Guggenberger [44] used a hard sphere model and the n=6 exponent of the repulsive potentials to compare ideal and real dihedral angles, δ', defined as the angle between two normals of adjoining triangular faces. Table 1.3 shows how dihedral angles of a range of Mo(II) and W(II) seven coordinate complexes may be used to indicate their structure relative to ideal geometries. Distortions from idealised stereochemistries are dependent upon the electronic nature and size of the ligands, together with any ligand connectivities.

Table 1.3 Dihedral angles for some Mo and W seven-coordinate structures.

	δ'	Ref.
C_{3v} (COC) geometry	24.2 , 24.2 , 24.2	
$MoBr_2(CO)_2(dpam)_2$	6.3 , 5.2 , 47.3	46
$MoBr_2(CO)_3(dppe)$	5.4 , 13.2 , 19.0	47
$[W(CO)_3(PMe_2Ph)_3I]^+$	3.2 , 5.1 , 32.3	48
$[Mo(CNBu^t)_6I]^+$	0.3 , 0.3 , 45.0	49
$[Mo(CNBu^t)_7]^{2+}$	0 , 0 , 39.4	50
C_{2v} (CTP) geometry	0 , 0 , 41.5	
$W(CO)_2(CNBu^t)_3I_2$	4.8 , 2.3	51
4:3 geometry	0 , 0	

1.5 THE MOLECULAR GEOMETRY OF SEVEN-COORDINATE Mo AND W COMPLEXES

1.5.1 STERIC EFFECTS

Examples of monomeric or dimeric hepta-coordinate metal carbonyl complexes having PB, COC, CTP or 4:3 geometries are listed in Table 1.4. The presence of several bulky atoms, such as halogens or substituted phosphines, can be easily accommodated by the COC and CTP geometries and many M(unidentate)$_7$ complexes of this type have been described as intermediate between these two geometries, with the halogen frequently occupying the least crowded capping position. Substituted metal(II) carbonyl complexes are readily accommodated by the COC geometry, since the L-M-L angles are relatively flexible and up to four carbonyl groups can be mutually cis, thus avoiding competition for the metal dπ electrons. On purely steric grounds complexes with from two to four halogens should also favour this geometry, since the uncapped face can accommodate three bulky atoms (e.g. $[W(CO)_4Br_3]^-$ [52]), whilst a fourth halogen may be sited at the capping position (e.g. $[W(PMe_2Ph)_3Br_4]$ [53]).

Halocarbonyl Mo or W complexes having PB or 4:3 geometries are less common than those of COC or CTP and often contain a combination of bidentate or/and several bulky monodentate ligands as exemplified by $W(CO)_3(dppm)I_2$ (PB) or $W(CO)_2(CNBu^t)_3I_2$ (4:3) [55,51]. The small equatorial L-M-L angles in the PB form can result in steric crowding which may be reduced by buckling of the plane and hence distortion from idealised geometry. To assess the influence of a bidentate chelate upon geometry the concept of normalised bite was introduced. This was defined as the distance between the effective bond centres (L-L) divided by the M-L radius, r and is illustrated for bidentate $R_2E(CH_2)_nER_2$ (n=integer) in Fig. 1.10.

Table 1.4 Structures of some 7-coordinate Mo and W Carbonyl Complexes.

Complex	Structure	Ref.
Monomers		
$Mo(CO)_2(PPh_3)(SPPh_2)_2$	PB	54
$W(CO)_3(dppm)I_2$	PB	55
$Mo(CO)_2(PMe_2Ph)_3Br_2$	COC	56
$Mo(CO)_3(PEt_3)_2Cl_2$	COC	57
$W(CO)_3(dpam)_2Br_2$	COC	58
$W(CO)_3(dmpe)I_2$	COC	59
$Mo(CO)_2(PMe_3)_2(O_2CCF_3)_2$	CTP	60
$Mo(CO)_3(bipy)(HgCl)Cl$	CTP	61
$W(CO)_3(S_2CNEt_2)_2$	CTP	62
$W(CO)\{P(OMe)_3\}_2\{Me_2AsC(CF_3)=C(CF_3)AsMe_2\}Br_2$	CTP	63
$[Mo(CO)(CNBu^t)_3Cp]^+$	4:3	64
$W(CO)_2(CNBu^t)_3I_2$	4:3	51
$W(CO)_2(PPh_3)(S_2CNEt_2)_2$	4:3	65
Dimers		
$[Mo(\mu\text{-}CO_3)(CO)(PMe_2Ph)_3]_2$	COC	66
$[W(CO)_4Br_2]_2$	COC	15
$[Mo(CO)_2\{P(OMe)_3\}(O_2CCF_3)\{\mu\text{-}(P)(O)(OMe)_2\}]_2$	CTP	67
$[Mo_2(CO)_4\{P(OMe)_3\}_4Cl_3]^{n+}$	4:3	68

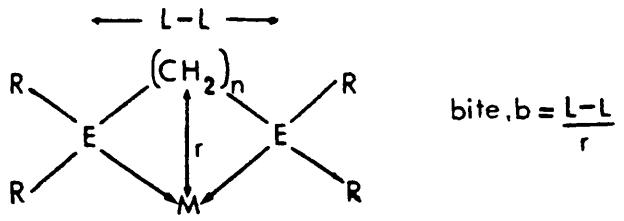

Fig. 1.10 Pictorial definition of normalised bite, b.

The bite, b is thus dependent upon the sizes of the atoms and chelate ring, although the metal exerts no influence over molecular geometry in analogous Mo(II) and W(II) complexes as a result of the Lanthanide contraction. Kepert [69] predicted a range of stereochemistries corresponding to potential energy minima for molecules of the type $[M(unidentate)_n(bidentate)_m]^{x+,o}$ (n=5, m=1; n=3, m=2; n=1, m=3) containing bidentates (L-L) of bite, b. Results for complexes with n=5, m=1 and n=3, m=2 only are discussed below, since this thesis is centred upon such complexes.

Fig. 1.11 shows the predicted forms for n=5, m=1. For bite

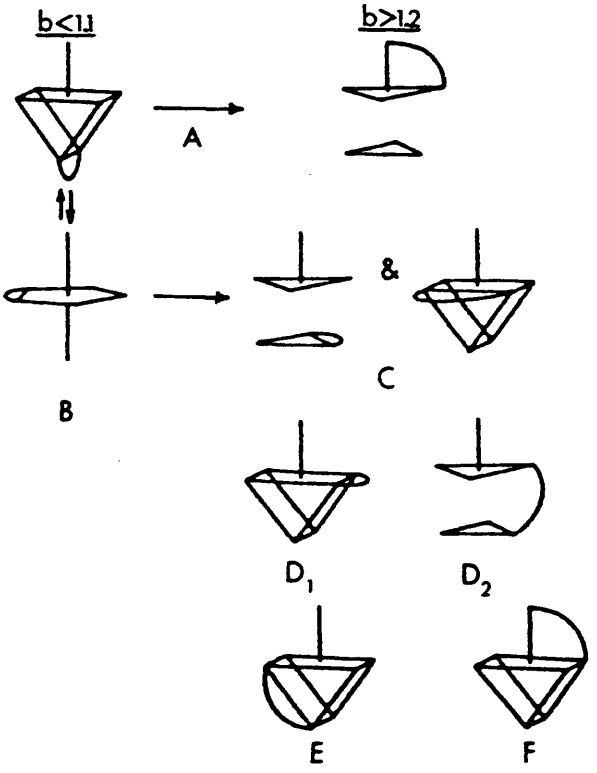

Fig. 1.11 Stereochemistries for $[M(unidentate)_5(bidentate)]^{x+,o}$

values below 1.1, a shallow potential energy trough was found to incorporate the CTP with (L-L) spanning the unique edge (A, Fig. 1.11) and the PB with (L-L) spanning two points in the girdle (B, Fig 1.11). Both these stereochemistries distorted progressively as the value of b increased, leading to stereochemistries C, D, E and F at very high values of b. In practice however these predictions may be overruled by the steric demands of other bulky monodentates within the molecule, as revealed by $WOCl_4$(diars) in which the bidentate ligand occupies one axial and one equatorial site with the oxygen atom in an axial position and the four chlorine atoms completing the PB girdle [70]. By far the most common structurally characterised Mo(II) and W(II) complexes containing one bidentate ligand are the substituted carbonyl halides containing a diarsine, diphosphine or bipyridyl (Table 1.5).

Table 1.5 Structures of some $M(unidentate)_4(bidentate)$ complexes.

Complex	b	Stereochemistry	ref.
$Mo(CO)_3(Ph_2POPPh_2)I_2$	1.03	B	71
$Mo(CO)_2(dppm)_2Cl_2.C_6H_6$	1.05	D	72
$W(CO)_3(dppm)I_2$	1.09	B	55
$Mo(CO)_2(dpam)_2Cl_2$	1.10	D	72
$Mo(CO)_2(dpam)_2Br_2$	1.18	D	46
$Mo(CO)_3(bipy)(HgCl)Cl$	1.18	D	73
$W(CO)_3(bipy)(GeBr_3)Br$	1.20	D	74
$W(CO)_3(dppe)I_2$	1.22	D	59
$Mo(CO)_3(dppe)Br_2.Me_2CO$	1.24	D	47
$Mo(CO)_3(Ph_2P(CH_2)_3PPh_2)I_2$	1.33	D	55

Complexes containing 5- or 6-membered rings often adopt COC or CTP geometries in which the bidentate spans one of the prism edges e.g. $Mo(CO)_3(dppe)I_2$ b=1.24 [55], whilst 4-membered chelate rings can be accommodated in the equatorial ring of the PB geometry, e.g. as in $Mo(CO)_3(Ph_2POPPh_2)I_2$ b=1.03 and $W(CO)_3(dppm)I_2$ b=1.09 [71,55].

The calculation of potential energy minima for complexes of general formula $[M(unidentate)_3(bidentate)_2]^{x\pm.0}$ led to the stereochemistries shown in Fig. 1.12. For normalised bite sizes below 1.1, a deep minimum on the potential energy surface corresponds to the PB (I,Fig. 1.12) which continuously distorts as b increases until a CTP is formed which alters again to a further PB with different ligand distribution from the first. Stereochemistry II (Fig. 1.12) demands 3 unidentate ligands, co-planar with the central metal atom and a 2-fold axis passing through the central atom and only occurs as a potential minimum for relatively high values of b. Variation of metal-ligand bond lengths may result in stabilisation of stereochemistries III and IV (Fig. 1.12), but they remain unstable with respect to I and II. Mo and W(II) complexes have not been

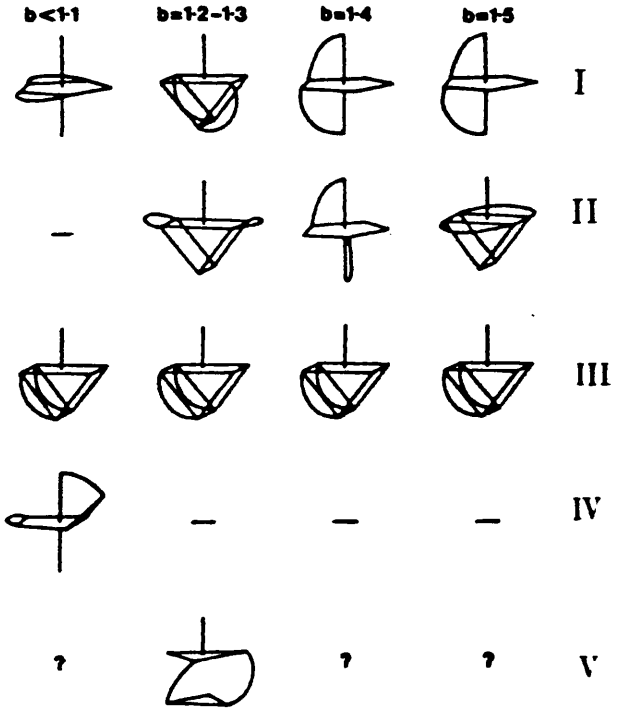

Fig. 1.12 Stereochemistries for $[M(unidentate)_3(bidentate)_2]^{x\pm.0}$

found which can be represented by V and the stability of such stereochemistries is uncertain. X-ray analyses of substituted Mo and W carbonyls with n=3,m=2 are less common than for n=5,m=1, but typical examples of stereochemistries I and II are respectively $W(CO)(dppm)_2I_2$ b=1.03 [75] and $[W(CO)_2(dppe)_2I]I$ b=1.21 [76].

The ratio, size and bite values of donor atoms not only strongly influence the solid state molecular structure, but will also influence the dynamic behaviour of the complex in solution. Thus the dynamic solution behaviour of several halocarbonyl complexes containing bidentate P or As donors have been examined by variable temperature ^1H NMR methods [77,78,79], which readily distinguished between mono- and bidentate chelation of the phosphine ligands and hence allowed the determination of the coordination number of the metal ion.

1.5.2 ELECTRONIC EFFECTS

The electronic preference of a ligand group for a particular site within the PB, COC or CTP forms will be dependent upon its relative donor-acceptor ability. Hoffmann et al [81] based their predictions for site preferences upon extended Hückel molecular orbital calculations for a hypothetical d^4 ML_7 species. Separation of σ and π effects was achieved by first considering L as a ligand bearing a single σ-orbital and 2 electrons. The orbital pattern and population analysis for such a PB are shown in Fig. 1.13 (I), and suggest that good σ-donors should favour the equatorial sites, whilst electronegative ligands should prefer the more negative apical sites. In Fig. 1.13 (II and III) the population analyses and orbital splitting patterns for such a system with COC or CTP geometries indicate that the more positive capping site or unique edge should be preferentially occupied by strong σ-donors.

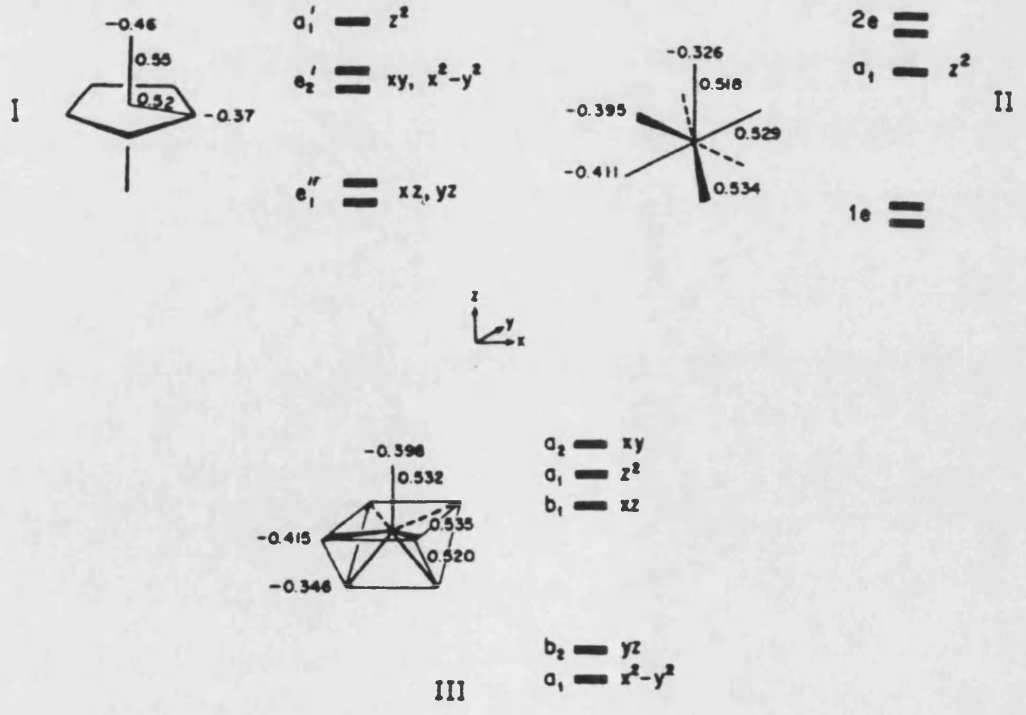

Fig. 1.13 Orbital patterns and calculated population analyses for PB, COC or CTP d^4 ML_7 species.

Hoffmann et al next considered the influence of π-interacting groups. The overlap between the p-orbitals of a π-donor (D) or π-acceptor (A) ligand and the two low-lying metal orbitals in d^4 ML_6D and ML_6A systems was considered by defining a local coordinate system x',y',z' (shown in III,Fig. 1.14) for each ligand L (x' is the M-L vector, y' is at right-angles to x' in the plane of M, L and the capping site and z' completes the right-handed coordinate system), and by definition of the orbital orientations as $\parallel$ for the ligand p orbital along the y' axis and as $\perp$ for the p orbital along z'. The COC and CTP forms are shown in (II) and (III) Fig. 1.14 and both possess three distinct sites: the apex, the capped face and the uncapped face (COC) or unique edge (CTP), which may be denoted respectively as c, cf, uf in the COC and c, qf(quadrilateral face) and e(edge) in the CTP.

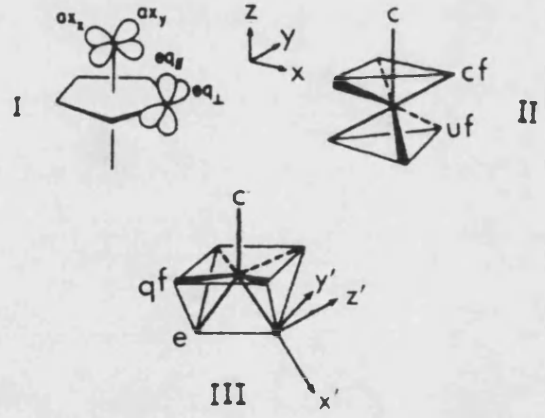

Fig. 1.14 Definitions for the PB, CTP and COC in ML_7 species.

The four possible orientations of a substituent orbital in a PB form are shown in Fig. 1.14 (I) and for COC (IA and IB) and CTP (IIA and IIB) forms in Fig. 1.15. Based upon these orbital interactions, a set of predictions for site preferences was devised by Hoffmann et al and is summarised in Table 1.6.

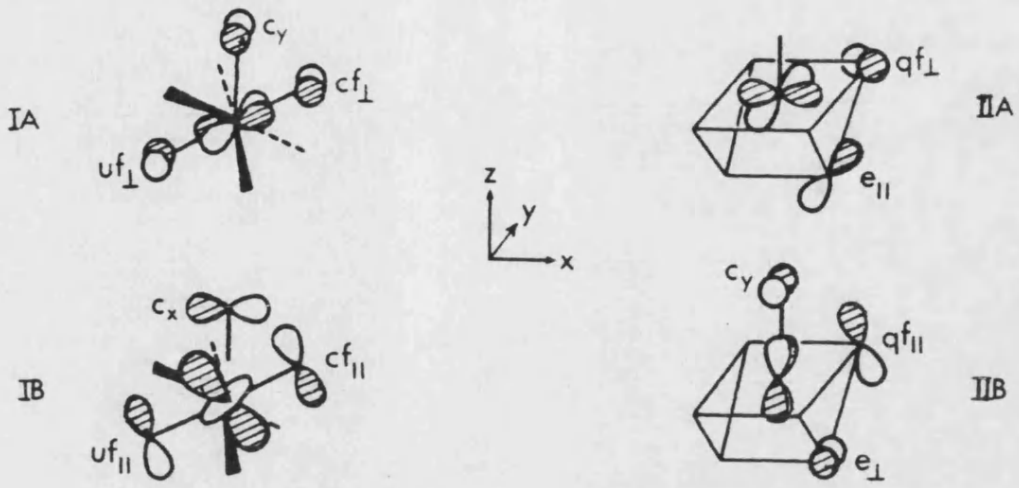

Fig. 1.15 Interactions between p- and d-orbitals in ML_7.

Table 1.6 Predicted site preferences of donors or acceptors in d^4 ML_7.

PB	Acceptor	ax > eq	$eq_{||}$ > $eq\perp$		
PB	Donor	eq > ax	$eq\perp$ > $eq_{||}$		
COC	Acceptor	cf > c > uf	$cf\perp$ > $cf_{||}$	$uf\perp$ > $uf_{||}$	
COC	Donor	uf > c > cf	$cf_{||}$ > $cf\perp$	$uf_{||}$ > $uf\perp$	
CTP	Acceptor	qf ≈ e > c	$qf\perp$ > $qf_{||}$	$e\perp$ > $e_{||}$	c_y > c_x
CTP	Donor	c > e ≈ qf	$qf_{||}$ > $qf\perp$	$e_{||}$ > $e\perp$	c_x > c_y

Although the stereochemical guide is in general accord with many structurally defined d^4 $M(CO)_3L_2X_2$ complexes, comparisons with these theoretical predictions are complicated by the fact that many of these complexes are intermediate between COC and CTP geometries and contain mixtures of weak and strong π-acceptors.

1.6 CHANGES BETWEEN SIX AND SEVEN COORDINATION IN MOLYBDENUM AND TUNGSTEN d^4 OR d^6 CARBONYL PHOSPHINE COMPLEXES.

1.6.1 BY HALIDE EXTRACTION OR OXIDATION

Six coordinate d^4 metal complexes are coordinatively unsaturated and therefore are expected to be highly electrophilic. Consequently oxidation of six coordinate molybdenum (0) complexes such as cis-$Mo(CO)_2(L\text{-}L)_2$ (L-L=dppe or bipy) with silver tetrafluoroborate in coordinating solvents affords a range of seven coordinate cations $[Mo(CO)_2(L\text{-}L)_2S]^{2+}$ (L-L=dppe, S=MeCN or PhCN [82], L-L=bipy, S=MeCN, acetone or water [83]), the dppe complexes also being obtained by halide extraction from cis-$[Mo(CO)_2(dppe)_2X]^+X^-$. In non-coordinating solvents however the weakly coordinating anion PF_6^- may exist in equilibrium with F^- ($PF_6^- = PF_5 + F^-$) and thus oxidation of cis-$Mo(CO)_2(dppe)_2$ in these solvents has been shown to result in the formation of $[Mo(CO)_2(dppe)_2F]PF_6$, clearly reflecting the strong drive for Mo(II) to increase its coordination number from six to seven [82].

1.6.2 BY REVERSIBLE LOSS OF CARBON MONOXIDE

Following the first preparation of the complexes $M(CO)_3(EPh_3)_2X_2$ (M=Mo or W, E=P, As or Sb, X=halogen), it was discovered that on heating the PPh_3 species only a molecule of carbon monoxide was lost to form a dark blue product $[M(CO)_2(PPh_3)_2X_2]_n$ [11,12]. Passage of CO through acetone or dichloromethane solutions of these products rapidly reformed the parent tricarbonyls [84] and these complexes were therefore termed carbon monoxide carriers (1.5). The inability of the analogous triphenylarsine or stibine species to lose CO was attributed to the greater sizes of the As and Sb atoms, which resulted in greater distances between the phenyl and carbonyl

groups and thus less steric strain within the molecule. The decarbonylation products were initially formulated as six coordinate 16-electron monomeric complexes of general formula $M(CO)_2(PPh_3)_2X_2$,

$$M(CO)_3(PPh_3)_2X_2 \underset{+CO}{\overset{-CO}{\rightleftharpoons}} [M(CO)_2(PPh_3)_2X_2]_n \qquad (1.5)$$

however their diamagnetism (in contrast to paramagnetic $Mo(CO)_2(py)_2X_2$) and coordinative unsaturation fuelled speculation that seven coordination of the metal atom was achieved by dimerisation. Both halogen-bridged and metal-metal bonded dimers [10] were considered, but a monomeric formulation was finally confirmed by X-ray analysis of $Mo(CO)_2(PPh_3)_2Br_2$ [85], which revealed an unusual non-octahedral arrangement of the six ligands around the metal atom. The diamagnetism of these species was attributed to a splitting of the degenerate t_{2g} orbitals due to the distortion, allowing pairing of the four metal d-electrons in the two lower energy orbitals. The paramagnetism of the pyridine analogue was explained by the presence of unpaired electrons arising from a smaller ligand field splitting within the t_{2g} set. Two other systems, $M(CO)_3(P(tolyl)_3)_2X_2$ [36] and $M(CO)_3(PEt_3)_2X_2$ [16] (M=Mo or W), were subsequently found to produce deep blue, diamagnetic dicarbonyls and act as CO carriers. The intense colouration is associated with a strong absorption in their UV spectra near 500nm which can be attributed to an electronic transition within the split t_{2g} orbitals and is diagnostic of these distorted 16-electron species.

Elimination of CO from tricarbonyl complexes does not however always result in monomer formation. Thus boiling, methanolic solutions of $Mo(CO)_3(PMe_2Ph)_2X_2$ (X=Cl,Br) yield diamagnetic products which have neither the intense colouration characteristic of the monomers nor their solubility in organic solvents [16]. A structure

determination by X-ray analysis or NMR spectroscopy was not possible, but the presence of both terminal and bridging metal-chlorine stretching frequencies in the far infra-red spectrum of the chloro complex suggested a halogen-bridged polymeric formula $[Mo(CO)_2(PMe_2Ph)_2X_2]_n$ (n=integer). This postulate has been given support by the recent X-ray analysis of $[W(CO)_4Br_2]_2$ [15], which contains two W-Br-W bridges within a dimeric unit. Analogous tricarbonyl tungsten complexes did not to lose CO. In the absence of accurate molecular weights the value of n cannot be assigned, however a value of n=2 has by convention been adopted by previous workers in this area and will be continued throughout this thesis.

Colton [79] examined the ^{13}C NMR spectrum of $Mo(CO)_3(ER_3)_2X_2$ (ER_3=P(tolyl)$_3$, $AsPh_3$ or $SbPh_3$) at -70°C and attributed the two resonances at ca. 200ppm to the carbonyl groups. For ER_3=P(tolyl)$_3$, the higher field resonance of intensity one was assigned to the unique carbonyl trans to P(tolyl)$_3$ (Fig. 1.17, isomer I) and it was suggested that this carbonyl was the least strongly bound and most likely to be lost by steric interaction, in accord with the known distorted structure of $Mo(CO)_2(PPh_3)_2X_2$ [85].

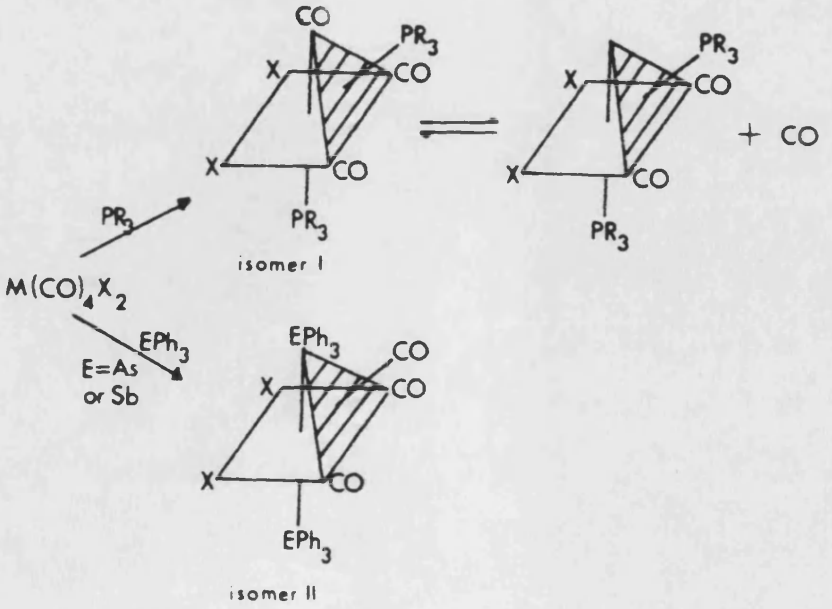

Fig. 1.17 Isomeric forms of $M(CO)_3(ER_3)_2X_2$ predicted by ^{13}C NMR data.

The lower field resonance of intensity two was therefore attributed to the two remaining carbonyl groups in the capped face. For the $AsPh_3$ and $SbPh_3$ complexes this pattern of carbonyl resonances was reversed, with the lower field, weaker resonance corresponding to the unique capping carbonyl (Fig. 1.17,isomerII). This suggests that it is the structure of the arsine and stibine complexes which inhibits their ability to lose CO. However a combination of heat and high vacuum has been reported to produce impure mixtures of parent tricarbonyl and dimeric $[Mo(CO)_2(EMe_3)_2X_2]_2$ (X=I,E=P,As or Sb;X=Cl or Br,E=As) or $[W(CO)_2(AsMe_3)_2X_2]_2$ (X=I,Br or Cl) [86] which were identified by elemental analysis, infra-red spectroscopy and their ability to reversibly take up CO. No reason was suggested to explain why these complexes lost CO, whilst the more sterically strained $AsPh_3$ and $SbPh_3$ complexes failed to do so, but these results suggest that steric arguements alone are not sufficient to explain the relative ease of CO loss.

^1H NMR studies of $M(CO)_3(dppm)X_2$ and $M(CO)_3(dpam)_2X_2$ [87,88,89] have shown that the former contains dppm in a bidentate mode, whilst two unidentate dpam units are present in the latter. Reversible loss of CO occurred on heating solutions of the dpam species only to form $M(CO)_2(dpam)_2X_2$ containing one bidentate and one monodentate dpam group. The analogous bis-(diphenylarsino)ethane (dpae) complex $M(CO)_2(dpae)_2X_2$ is far more stable towards addition of CO [78], suggesting that it is the chelate ring size which determines this behaviour.

1.7 THE STRUCTURE OF SIX COORDINATE Mo AND W CARBONYL COMPLEXES

Optimising the distance between six electron pairs using the 'points on a sphere' model of Gillespie and others [40-42], results in two stable geometries for six coordinate complexes. These are the octahedron (O_h) and the trigonal prism (TP) shown in Fig. 1.18. With the exception of a restricted number of tris-thiolate complexes [44], the vast majority of 6-coordinate molecules have been found to adopt octahedral geometry. As illustrated in Fig. 1.18, this form can be notionally generated from the three stable 7-coordinate geometries PB, COC and CTP, by vertex removal from the equatorial plane of the PB form accompanied by minor movements of the remaining four co-planar vertices or by removal of one vertex from either the COC or CTP forms and motion of an adjacant vertex. Table 1.7 contains

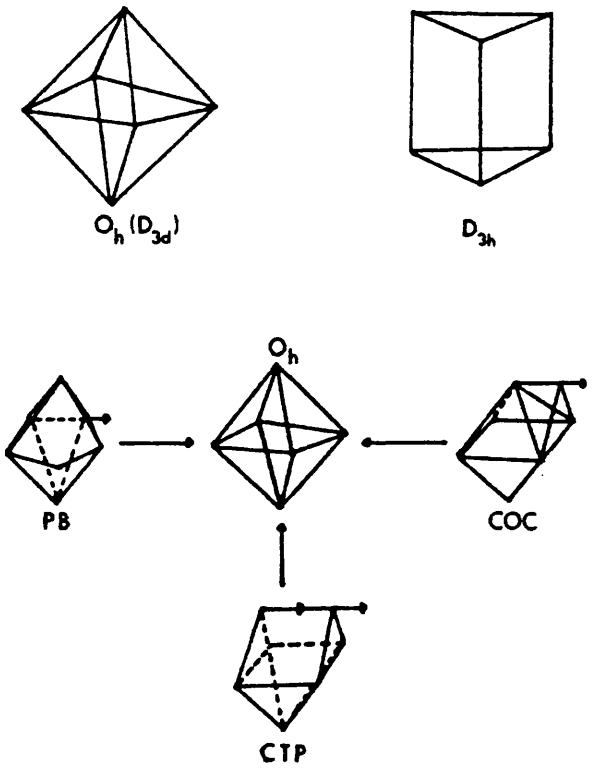

Fig. 1.18 Predicted geometries for six coordinate complexes.

examplee of 6-coordinate dicarbonyl d^4 metal complexes which adopt octahedral or trigonal prismatic geometries. Distortion from the

regular forms can be calculated from either dihedral angles or the r.m.s. separation in a similar manner to that used for 7-coordinate complexes.

Table 1.7 Examples of 6-Coordinate Mo and W Carbonyl Complexes.

Complex	Structure	OC-M-CO angle(°)	Ref.
$Mo(CO)_2(PPh_3)_2Br_2$	O_h	119.0	85
$Mo(CO)_2(py)_2(OBu^t)_2$	O_h	72.0	90
$Mo(CO)_2(S_2CNPr^i_2)_2$	TP	74.3	91
$W(CO)_2(PPh_3)_2Br_2$	O_h	110.0	14
$W(CO)_2(C_7H_8)Br_2$	O_h	172.9	92

A theoretical explanation for distortion from O_h geometry can be achieved by consideration of the molecular orbitals of the d^4 metal and the donor or acceptor ability of the ligands.

1.8 DISTORTION IN Mo AND W COMPLEXES $M(CO)_2(PR_3)_2X_2$

Kubáček and Hoffmann [93] analysed the molecular distortions within diamagnetic d^4 six coordinate Mo(II) and W(II) carbonyl complexes using as a model system $ML_2L'_2L''_2$ ($L \neq L' \neq L''$) in an ideal octahedral configuration, since this accommodated spatial changes whilst retaining C_{2v} symmetry. This molecule was referenced to a three dimensional coordinate system x,y,z and inter-bond angles α,β,γ defined (Fig. 1.19). The metal t_{2g} orbitals xz,yz and x^2-y^2 may become involved with π-bonding or π-anti-bonding to ligands and in low spin d^4 complexes two orbitals will be full and one empty. The π-donor or acceptor abilities of the ligands L, L' and L'' will influence the order of orbitals in terms of their energy, and the molecular geometry will be determined by which orbital remains empty.

Alteration of angles α, β and γ will occur to produce maximum overlap of metal d and ligand σ orbitals and the resultant hybrid orbitals will become distorted towards other ligands. The subunits ML_2, ML'_2 and ML''_2 may be considered independently and after considering the effect of α, β and γ variation on the orbital level pattern, the whole molecule may be reassembled.

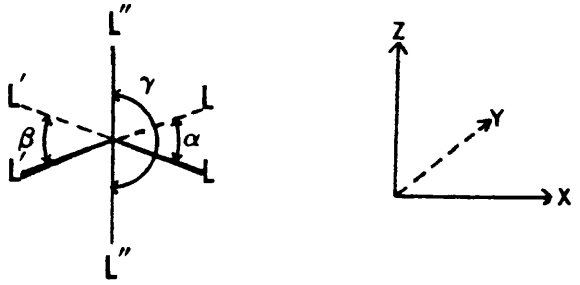

Fig. 1.19 Coordinate system and inter-bond angles for $ML_2L'_2L''_2$.

The model π-acceptor and σ-donor systems used were the two hypothetical species cis-$Mo(CO)_2H_4^{2-}$ and cis-$MoCl_2H_4^{4-}$, and extended Hückel computations produced the relative energies for the t_{2g} orbitals of each model as the α angle between the CO or Cl ligands was varied from 90°. The effect of the π-acceptor or σ-donor ligands upon the t_{2g} orbitals was to stabilise or destabilise them respectively, the greatest effect being felt by x^2-y^2 as seen in Fig. 1.20.

The electronic state of $M(CO)_2(PR_3)_2X_2$ (X=halogen) will be most affected by the good π-acceptor CO ligands. Increasing OC-M-CO angles α leads to greater yz, but less xz overlap with ligand z orbitals, the reverse effect occurring with decreasing α. Increasing overlap is stabilising for π-acceptor ligands and this explains the changes observed in Fig. 1.20. In principle the four metal d electrons may occupy either $(x^2-y^2)^2(yz)^2$ or $(x^2-y^2)^2(xz)^2$ configurations and this leads to energy minima for $\alpha<90°$ and $\alpha>90°$.

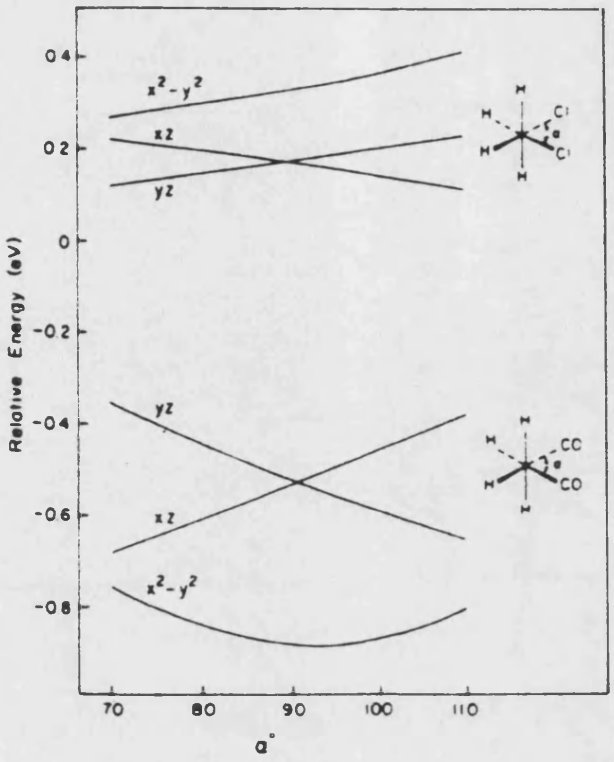

Fig. 1.20 Changes in orbital energy with L-M-L angles.

Consideration of the energy changes shown in Fig. 1.20 for cis-$MoCl_2H_4^{4-}$ suggests that for the β angle X-M-X in $M(CO)_2(PR_3)_2X_2$ values below 90° are favoured by $(x^2-y^2)^2(yz)^2$, whilst the effects of (x^2-y^2) and xz are opposite and result in β angles near 90°. Thus the two electronic configurations favour angular arrangements of α<90°, β<90° and α>90°, β near 90° as shown in Fig. 1.21.

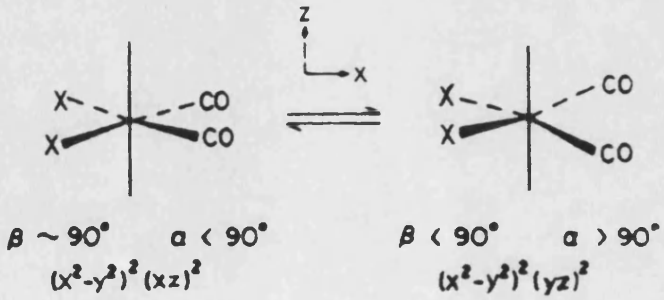

Fig. 1.21 Preferred angular arrangement in $M(CO)_2(PR_3)_2X_2$.

The axial phosphines have little π-bonding abilities and as γ changes above or below 180° less yz overlap, but greater xz interaction occurs which destabilises the latter orbital. The stability of the $(x^2-y^2)^2(yz)^2$ configuration is dependent upon the energy difference between these filled and the empty xz orbital. As shown in Fig. 1.22, mixing of the xz orbital with the metal z orbital

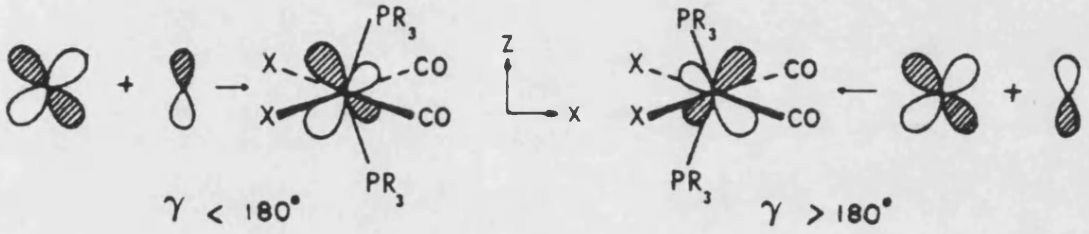

Fig. 1.22 Effects of varying the PR_3-M-PR_3 angle in $M(CO)_2(PR_3)_2X_2$.

results in hybridisation which for γ>180° is directed towards the carbonyls. This might appear to lead to greater stabilisation due to greater interaction with them, however σ-antibonding is generated by this distortion which dominates π-bonding effects and results in destabilisation of this configuration.

Thus the most stable configuration of $M(CO)_2(PR_3)_2X_2$ is theoretically $(x^2-y^2)^2(yz)^2$, with a preferred angular form of α>90°, β<90° and γ<180°. Although PPh_3 ligands are relatively large, experimental structures show that their bulk does not affect this predicted form (Table 1.9).

Table 1.9 Observed α, β and γ angles in $M(CO)_2(PPh_3)_2Br_2$.

observed (°)		angle^
M=Mo[85]	M=W[14]	
119	110	α
83	82	β
128	128	γ

^-defined in the text

The following chapter reports an examination of the steric and electronic factors influencing the decarbonylation of $M(CO)_3(PR_3)_2X_2$ (M=Mo, X=Br, PR_3=$PEtPh_2$, PEt_2Ph or PMe_2Ph, X=Cl, Br or I, PR_3=$PMePh_2$; M=W, X=Br, PR_3=$PMePh_2$ or PMe_2Ph), their effect upon the nature of the resultant new products $[M(CO)_2(PR_3)_2X_2]_n$ (n=1 or 2) and the product formed from analogous reactions in acetonitrile.

CHAPTER 2

DECARBONYLATION OF THE Mo AND W PHOSPHINE HALOCARBONYLS $M(CO)_3(PR_3)_2X_2$

2.1 INTRODUCTION

Interest in the seven coordinate tertiary phosphine Mo(II) and W(II) halocarbonyls $M(CO)_3(PR_3)_2X_2$ has been continuous since their first discovery in 1966 [11,12]. In addition to undergoing an extensive range of stoichiometric reactions, they have also been shown recently to exhibit catalytic activity [94,95], and as discussed in Chapter 1, some complexes (R=Ph or Et) act as carbon monoxide carriers [84,16]. As only a limited amount of work has been carried out on the relationship between ease of CO loss and the electronic and steric effects of ligands in $M(CO)_3(PR_3)_2X_2$ complexes [96], a more systematic study of the decarbonylation of a series of complexes $M(CO)_3(PR_3)_2X_2$ (M=Mo or W, PR_3=$PMePh_2$ or PMe_2Ph, X=Br, M=Mo, PR_3=$PEtPh_2$, PEt_2Ph or PMe_2Ph, X=Br, PR_3=$PMePh_2$, X=Cl or I) in the presence and absence of coordinating solvents has been undertaken, and is reported in this chapter. In the course of these studies further six-coordinate monomeric and seven-coordinate dimeric Mo(II) and W(II) halocarbonyl complexes $[M(CO)_2(PR_3)_2X_2]_n$ (n=1 or 2) have been generated and the new seven-coordinate complexes $M(CO)_2(PR_3)_2X_2(MeCN)$ have been isolated and characterised.

2.2 EXPERIMENTAL

The physical techniques and solvents used in this chapter appear in Appendix 1 and the starting materials $M(CO)_3(PR_3)_2X_2$ (M=Mo, PR_3=$PEtPh_2$, PEt_2Ph or $PMePh_2$, X=Br, M=Mo, PR_3=$PMePh_2$, X=Cl or I, M=W, PR_3=$PMePh_2$ or PMe_2Ph, X=Br) were prepared from either cis-$M(CO)_4(PR_3)_2$ (X=I) or $[M(CO)_4X_2]_2$ (X=Cl or Br) using standard literature methods [11,16,14,96].

PREPARATION OF $M(CO)_2(PR_3)_2X_2(MeCN)$ (M=Mo, PR_3=$PEtPh_2$, PEt_2Ph or $PMePh_2$, X=Br, M=Mo, PR_3=$PMePh_2$, X=Cl or I, M=W, PR_3=$PMePh_2$ or PMe_2Ph, X=Br).

A slow stream of nitrogen gas was passed through a stirred suspension of $M(CO)_3(PR_3)_2X_2$ (0.5mmol) in acetonitrile (15cm^3). All reactions were carried out at room temperature except those involving tungsten which were heated under gentle reflux. The yellow or orange suspensions produced clear solutions and the course of the reaction was followed by monitoring the infra-red solution spectra. The reaction was terminated when the three ν(CO) bands of the tricarbonyl had been replaced by two new CO bands of almost equal intensity. The solvent was evaporated to low bulk in vacuo and refrigeration yielded the analytically pure products as yellow, microcrystalline powders.

The solid samples of $M(CO)_2(PR_3)_2X_2(MeCN)$ used in Chapter 3 to examine the reactions of these complexes with alkynes or anions were generated in quantitative yield by evaporating the acetonitrile solutions to dryness in vacuo.

Table 2.1 Yields and analytical data for $M(CO)_2(PR_3)_2X_2(MeCN)$.

Complex			Yield	Analysis found(calculated)		
M	PR_3	X	%	%C	%H	%N
Mo	$PEtPh_2$	Br	68	48.6(49.2)	4.4(4.2)	1.9(1.8)
Mo	PEt_2Ph	Br	68	42.1(42.0)	4.8(4.8)	2.1(2.0)
Mo	$PMePh_2$	Cl	67	52.2(54.2)	4.5(4.4)	2.5(2.1)
Mo	$PMePh_2$	Br	77	47.7(47.8)	3.9(3.8)	2.0(1.9)
Mo	$PMePh_2$	I	53	42.5(42.5)	3.6(3.4)	1.8(1.7)
Mo	PMe_2Ph	Br	64	38.1(38.2)	3.9(3.9)	2.2(2.2)
W	$PMePh_2$	Br	63	42.8(42.8)	3.4(3.5)	1.6(1.7)
W	PMe_2Ph	Br	59	33.2(33.5)	3.5(3.6)	2.1(2.0)

PREPARATION OF $Mo(CO)_2(PR_3)_2X_2$ (PR_3=$PEtPh_2$ or PEt_2Ph, X=Br, PR_3 =$PMePh_2$, X=I)

A vigorous stream of nitrogen was passed through a solution of either $Mo(CO)_3(PR_3)_2X_2$ or $Mo(CO)_2(PR_3)_2X_2(MeCN)$ (0.5mmol) in dichloromethane, acetone or 3-pentanone (15cm^3). Reaction of the iodo tricarbonyl complex was carried out under reflux, but all other reactions occurred at ambient temperature. The yellow solutions slowly darkened until a deep blue or purple colouration was observed. The course of the reaction was again monitored by infra-red spectroscopy. The products were isolated by dropwise addition of n-hexane (10cm^3) to the solution, followed by slow partial evaporation at room temperature. The products were filtered, washed with n-hexane and dried in vacuo.

PREPARATION OF $Mo(CO)_2(PMePh_2)_2Br_2$

A slow stream of nitrogen was bubbled through a suspension of $Mo(CO)_3(PMePh_2)_2Br_2$ (0.15g, 0.2mmol) in dichloromethane, acetone

or 3-pentanone ($5cm^3$). The yellow solution darkened and after 5min the purple product was isolated as a powder following dropwise addition of n-hexane ($10cm^3$) and partial evaporation. The product was filtered, washed with hexane and dried.

The length of reaction time was critical, since extended times (10-30min) resulted in formation of increasing amounts of $[Mo(CO)_2(PMePh_2)_2Br_2]_2$.

PREPARATION OF $W(CO)_2(PMePh_2)_2Br_2$

Nitrogen gas was bubbled through a boiling solution of $W(CO)_2(PMePh_2)_2Br_2(MeCN)$ (0.17g,0.2mmol) in chloroform ($10cm^3$). The orange solution darkened and after 10min became purple. After cooling to room temperature, n-hexane ($10cm^3$.) was added dropwise. The purple microcrystalline product was isolated following partial evaporation, and was filtered, washed with hexane and dried *in vacuo*.

Extended reaction times resulted in mixtures of the product with $[W(CO)_2(PMePh_2)_2Br_2]_2$.

PREPARATION OF $[M(CO)_2(PR_3)_2Br_2]_2$ (M=Mo or W, PR_3=$PMePh_2$ or PMe_2Ph)

Method 1.

A suspension of $M(CO)_2(PR_3)_2Br_2(MeCN)$ or $M(CO)_n(PR_3)_2Br_2$ (PR_3=$PMePh_2$, n=2 or 3, PR_3=PMe_2Ph, n=3) (0.5mmol) in dichloromethane ($10cm^3$) was vigorously bubbled with nitrogen for 1hr at ambient temperature (M=Mo) or under gentle reflux (M=W). The orange product precipitated as an insoluble powder which was collected by filtration, washed with n-hexane and dried *in vacuo*.

Method 2.

A sample of $M(CO)_3(PR_3)_2Br_2$ (0.5mmol) was heated under reflux in ethanol ($10cm^3$) for 2hr. The yellow solution became orange and the insoluble product precipitated as a powder. The filtered product was washed with hexane and dried in vacuo.

Yields and analytical data for $[M(CO)_2(PR_3)_2X_2]_n$ (n=1 or 2) are given in Table 2.2. The complex $[Mo(CO)_2(PMe_2Ph)_2Br_2]_2$ was spectroscopically identical to that obtained by Moss and Shaw via decarbonylation of $Mo(CO)_3(PMe_2Ph)_2Br_2$ in methanol [16].

Table 2.2 Yields and analytical data for $[M(CO)_2(PR_3)_2X_2]_n$

Complex			Yield	Analysis found(calculated)		
M	PR_3	X	%	%C	%H	%X
n=1						
Mo	$PEtPh_2$	Br	59	48.5(48.7)	4.0(4.1)	21.0(21.6)
Mo	PEt_2Ph	Br	85	40.7(41.0)	4.7(4.6)	25.0(24.9)
Mo	$PMePh_2$	Br	56	47.2(47.2)	3.6(3.7)	21.3(22.5)
Mo	$PMePh_2$	I	45	41.0(41.7)	3.1(3.3)	29.5(31.5)
W	$PMePh_2$	Br	51	41.9(42.0)	3.2(3.3)	20.0(20.0)
n=2						
Mo	$PMePh_2$	Cl	82	53.6(53.9)	4.0(4.2)	11.2(11.4)
Mo	$PMePh_2$	Br	77	47.3(47.2)	3.8(3.6)	22.2(22.5)
W	$PMePh_2$	Br	74	42.0(42.0)	3.8(3.2)	19.2(20.0)
W	PMe_2Ph	Br	59	32.3(32.0)	3.4(3.2)	23.1(23.7)

2.3 RESULTS AND DISCUSSION

2.3.1 FORMATION AND CHARACTERISATION OF $M(CO)_2(PR_3)_2X_2(MeCN)$

These complexes were formed by the passage of nitrogen gas through a stirred suspension of $M(CO)_3(PR_3)_2X_2$ in acetonitrile at ambient (M=Mo) or elevated (M=W) temperature. The yellow powdered products were stable in a nitrogen atmosphere and as solutions in acetonitrile, but in chlorinated or ketonic solvents gradual loss of MeCN resulted in formation of $[M(CO)_2(PR_3)_2X_2]_n$ (n=1 or 2).

INFRA-RED AND CONDUCTIVITY DATA

Significant infra-red bands for these complexes are tabulated in Table 2.3. In addition to the bands associated with the ligated phosphine, all the spectra showed two important features. Firstly, two intense carbonyl stretching frequencies of approximately equal intensity were found in the range 1945-1830cm^{-1}, being separated by approximately 90cm^{-1}. These are typical of a cis-dicarbonyl species and values of OC-M-CO angles (2ϕ) obtained using equation 2.1 compare well with those quoted for a large number of seven coordinate Mo(II) and W(II) carbonyl complexes [97], being in the range 70-80°. Secondly, a weaker band approximately 30cm^{-1} above

$$2\phi = 2\sqrt{\text{arccotan(band intensity ratio)}} \qquad (2.1)$$

the value for free acetonitrile (ν(CN) MeCN liquid = 2250cm^{-1} [98]) observed in the range 2285-2275cm^{-1} can be assigned to ν(CN) of coordinated nitrile. The presence of only a terminal metal-chlorine stretching frequency at 266cm^{-1} in the far infra-red spectrum of solid $Mo(CO)_2(PMePh_2)_2Cl_2(MeCN)$ is consistent with the expected monomeric formulation, and the low conductivity values for $M(CO)_2(PR_3)_2X_2(MeCN)$ in MeCN (Table 2.3) are typical of non-ionic

species in these solvents [99]. In addition reaction with $NaBPh_4$ failed to yield an ionic product. Thus all data indicate that displacement of CO and coordination of MeCN results in formation of the seven coordinate, neutral complexes $M(CO)_2(PR_3)_2X_2(MeCN)$.

Table 2.3 Infra-red and conductivity data for $M(CO)_2(PR_3)_2X_2(MeCN)$.

Complex			Colour	Λ_M[a]	ν(CO)cm^{-1}[b]		ν(CN)cm^{-1}[b]
M	PR_3	X		(MeCN)			
Mo	$PEtPh_2$	Br	Yellow	5.91	1942s	1839s	2275w
Mo	PEt_2Ph	Br	Yellow	6.53	1945s	1835s	2283w
Mo	$PMePh_2$	Cl[d]	Yellow	7.04	1935s	1853s	2275w
Mo	$PMePh_2$	Br	Yellow	6.99	1945s	1843s	2273w
Mo	$PMePh_2$	I	Yellow	7.61	1935s	1853s	2278w
Mo	PMe_2Ph	Br	Yellow	7.69	1939s	1838s	2285w
W	$PMePh_2$	Br	Yellow-green	[c]	1923s	1839s	2275w
W	PMe_2Ph	Br	Yellow-green	[c]	1919s	1834s	2283w

[a]=Molar conductivity of 10^{-3}M solutions in units of $Scm^{-1}mole^2$

[b]=As Nujol mulls [c]=Too insoluble for measurement [d]=ν(Mo-Cl)=266cm^{-1}

NMR SPECTA

On dissolving the most soluble complex $Mo(CO)_2(PEtPh_2)_2Br_2(MeCN)$ in CD_2Cl_2, the solution slowly darkened and became dark blue, whilst in CD_3CN a yellow solution was formed whose colour did not change on storage. The ^1H NMR data for this complex and for $Mo(CO)_2(PEtPh_2)_2Br_2$, whose preparation and properties are discussed in the next section, in these solvents are presented in Table 2.4. A comparison of these two sets of results shows that in CD_2Cl_2 the acetonitrile complex loses MeCN (δ 1.93ppm) to form the six coordinate derivative, indeed spectra of the analogous $PMePh_2$ or PMe_2Ph complexes in this solvent could not be obtained due to the

formation of mixtures of the acetonitrile complexes and either $[Mo(CO)_2(PMePh_2)_2Br_2]_n$ (n=1 or 2) or $[Mo(CO)_2(PMe_2Ph)_2Br_2]_2$. In CD_2CN, $Mo(CO)_2(PEtPh_2)_2Br_2$ and $Mo(CO)_2(PEtPh_2)_2Br_2(MeCN)$ gave

Table 2.4 ^1H NMR data for $Mo(CO)_2(PEtPh_2)_2Br_2(MeCN)$ and $Mo(CO)_2(PEtPh_2)_2Br_2$.

	Chemical shift, δ(ppm)		
Solvent	Aliphatic	Aromatic	Other
$Mo(CO)_2(PEtPh_2)_2Br_2(MeCN)$			
CD_2Cl_2	0.94 m,6H	7.47-7.72 m,20H	1.94 s,3H
CD_3CN	0.76 m,6H	7.35-7.52 m,20H	1.98 s
$Mo(CO)_2(PEtPh_2)_2Br_2$			
CD_2Cl_2	0.99 m,6H	7.35-7.48 m,20H	
CD_3CN	0.76 m,6H	7.35-7.52 m,20H	1.93 s

identical resonance positions at 0.76, 2.75 and 7.35-7.52ppm attributable to the methyl, methylene and aromatic protons of the ligated phosphine respectively. The intense peak at 1.98ppm in the spectrum of the acetonitrile complex compares with the free CD_3CN position of 1.93ppm in the spectrum of $Mo(CO)_2(PEtPh_2)_2Br_2$ in the same solvent, suggesting that exchange of CD_3CN and CH_3CN occurs for $Mo(CO)_2(PEtPh_2)_2Br_2(MeCN)$.

2.3.2 THE COMPLEXES $M(CO)_2(PR_3)_2X_2$

Passing a vigorous stream of nitrogen gas through a suspension of either $M(CO)_3(PR_3)_2X_2$ or $M(CO)_2(PR_3)_2X_2(MeCN)$ in chlorinated or ketonic solvents at ambient (M=Mo) or elevated (M=W) temperatures, resulted in loss of carbon monoxide or acetonitrile respectively to form $[M(CO)_2(PR_3)_2X_2]_n$. The complexes $PR_3=PEtPh_2$ or PEt_2Ph, X=Br and $PR_3=PMePh_2$, X=I formed monomeric (n=1) dark blue or mauve products which were stable in air as solids, but which gradually decomposed in solution on prolonged exposure to air, resulting in absorption of CO and reformation of $M(CO)_3(PR_3)_2X_2$. For both $PEtPh_2$ and PEt_2Ph bromo complexes, complete loss of one-third of the CO content from the tricarbonyl required extended reaction times (>3hrs), whilst complete conversion of $Mo(CO)_3(PMePh_2)_2I_2$ to the dicarbonyl required elevated temperatures. In contrast both the preparation of $Mo(CO)_2(PR_3)_2X_2(MeCN)$ (X=Br, $PR_3=PEtPh_2$ or PEt_2Ph, X=I, $PR_3=PMePh_2$) via the tricarbonyl and subsequent displacement of MeCN occurred more rapidly (ca 30min), and the acetonitrile complexes therefore provide an improved, rapid route to mononuclear $M(CO)_2(PR_3)_2X_2$ derivatives.

Ease of CO loss from $Mo(CO)_3(PMePh_2)_2X_2$ was in the order Cl>Br>I in agreement with previous decarbonylation studies of $M(CO)_3(PPh_3)_2X_2$ [10-12], which cited the differing π-electron donation of the halogens X as the main factor in determining the rate of CO loss from these halocarbonyl complexes. The bromo complexes of $PMePh_2$ showed anomalous behaviour and reaction conditions were critical to obtain the six-coordinate product. Thus the passage of nitrogen through solutions of $Mo(CO)_3(PMePh_2)_2Br_2$ at room temperature resulted in rapid (5min) loss of CO and analytically pure samples of purple $Mo(CO)_2(PMePh_2)_2Br_2$ were obtained. However extended reaction

times resulted in formation of an insoluble, orange product which was identified as $[Mo(CO)_2(PMePh_2)_2Br_2]_2$ and will be discussed later in section 2.3.3 in this chapter. Solutions of $Mo(CO)_2(PMePh_2)_2Br_2(MeCN)$ or $W(CO)_3(PMePh_2)_2Br_2$ in chlorinated solvents at ambient (M=Mo) or elevated (M=W) temperatures darkened when bubbled with N_2, but rapid precipitation of insoluble, orange $[M(CO)_2(PMePh_2)_2Br_2]_2$ prevented isolation of pure $M(CO)_2(PMePh_2)_2Br_2$. The monomeric product $W(CO)_2(PMePh_2)_2Br_2$ could however be obtained by passing N_2 through a boiling solution of $W(CO)_2(PMePh_2)_2Br_2(MeCN)$ in chloroform for ten minutes, although again prolonged reaction times produced admixtures of monomeric and dimeric complexes $[W(CO)_2(PMePh_2)_2Br_2]_n$ (n=1 or 2). Loss of CO or MeCN respectively from solutions of $Mo(CO)_3(PMePh_2)_2Cl_2$ or $Mo(CO)_2(PMePh_2)_2Cl_2(MeCN)$ in chlorinated solvents yielded $[Mo(CO)_2(PMePh_2)_2Cl_2]_2$ only, and a deep blue or purple colouration expected for $Mo(CO)_2(PMePh_2)_2Cl_2$ was not observed.

INFRA-RED SPECTRA

Selected infra-red data for these complexes are given in Table 2.5. Two intense bands typical of cis-$M(CO)_2$ moieties were

Table 2.5 Selected IR data and force constants for $M(CO)_2(PR_3)_2X_2$.

Complex	ν(CO)[a]		Force constant[b]	
			k_i	k
$MoBr_2(CO)_2(PEtPh_2)_2$	1955	1845	0.85	14.78
$MoBr_2(CO)_2(PEt_2Ph)_2$	1949	1868	0.63	14.73
$MoBr_2(CO)_2(PMePh_2)_2$	1955	1865	0.69	14.75
$MoI_2(CO)_2(PMePh_2)_2$	1943	1861	0.63	14.63
$WBr_2(CO)_2(PMePh_2)_2$	1944	1850	0.72	14.55

[a]-as Nujol mulls in cm^{-1}.

[b]-k_i CO-CO interaction, k C-O stretching force constant, in mdyne$Å^{-1}$.

found for these complexes between ca. 1955 and 1845cm^{-1} respectively. The Cotton-Kraihanzel [100] CO stretching force constants have been calculated for these complexes and are listed in Table 2.5. Force constants (k) for tungsten compounds are approximately 2% lower than for the corresponding molybdenum compounds and show little variation with phosphine or halogen type.

The OC-M-CO angles for these distorted octahedral complexes were calculated from intensity measurements and are summarised in Table 2.6 below.

Table 2.6 Values of the cis-$M(CO)_2$ angle in $M(CO)_2(PR_3)_2X_2$.

Complex	OC-M-CO[a] 2ϕ(°)	cone angle θ(°)
$MoBr_2(CO)_2(PEtPh_2)_2$	105	140
$MoBr_2(CO)_2(PEt_2Ph)_2$	101	137
$MoBr_2(CO)_2(PMePh_2)_2$	103	136
$MoI_2(CO)_2(PMePh_2)_2$	98	136
$WBr_2(CO)_2(PMePh_2)_2$	107	136

[a]–from eqn. 2.1

ULTRA-VIOLET SPECTRA

The intense colourations of the $M(CO)_2(PR_3)_2X_2$ complexes are related to broad absorbances in the 500-600nm region of their ultra-violet spectra, and the wavelengths at which these absorbances were observed and the associated molar extinction coefficients in order of phosphine cone angle are listed in Table 2.7. As discussed in the previous chapter, distortion from regular octahedral form can be linked to a splitting of the t_{2g} orbitals into two sets, and the absorbance bands may be attributed to d_π-d_π HOMO-LUMO transitions between these orbitals. In Chapter 1 the relative stabilities of the $(x^2-y^2)^2(yz)^2$ configuration and the xz orbital was shown in theory to be related to the interbond angle (γ) between the trans-phosphine groups in $M(CO)_2(PR_3)_2X_2$. Thus for small phosphines, smaller γ values lead to greater overlap and destabilisation of xz compared to the lower energy $(x^2-y^2)^2(yz)^2$ configuration and this increases the energy transition between them. Conversely, increasing the size of the phosphine group should result in less interaction with the xz orbital and thus greater stability of this empty higher energy orbital compared to the filled $(x^2-y^2)^2(yz)^2$ orbitals. Since energy

is inversely proportional to wavelength ($E=h\nu$), the increased energy separation for smaller phosphines should be accompanied by a decrease in the wavelength at which transition occurs.

A plot of wavelength against θ (Fig. 2.1) is in agreement with this observation showing a steady rise in λ_{max} as the larger phosphine groups lead to less destabilisation of the empty higher energy orbital and consequently lower transition energies.

Table 2.7 Ultra-violet data for $M(CO)_2(PR_3)_2X_2$.

Complex	Colour	λ_{max}[a]	ϵ[b]	θ[c]
$MoBr_2(CO)_2(PEtPh_2)_2$	blue	584	592.5	140
$MoBr_2(CO)_2(PEt_2Ph)_2$	blue	568	487.2	137
$MoBr_2(CO)_2(PMePh_2)_2$	purple	557	542.8	136
$MoI_2(CO)_2(PMePh_2)_2$	blue	536	536.7	136
$WBr_2(CO)_2(PMePh_2)_2$	purple	501	539.6	136

[a]-wavelength at maximum absorbance, in CH_2Cl_2

[b]-molar extinction coefficient, in units of $Lmol^{-1}cm^{-1}$

[c]-Tolman angle in degrees

Fig. 2.1 Plot of cone angle, θ against UV value λ_{max} for $M(CO)_2(PR_3)_2X_2$.

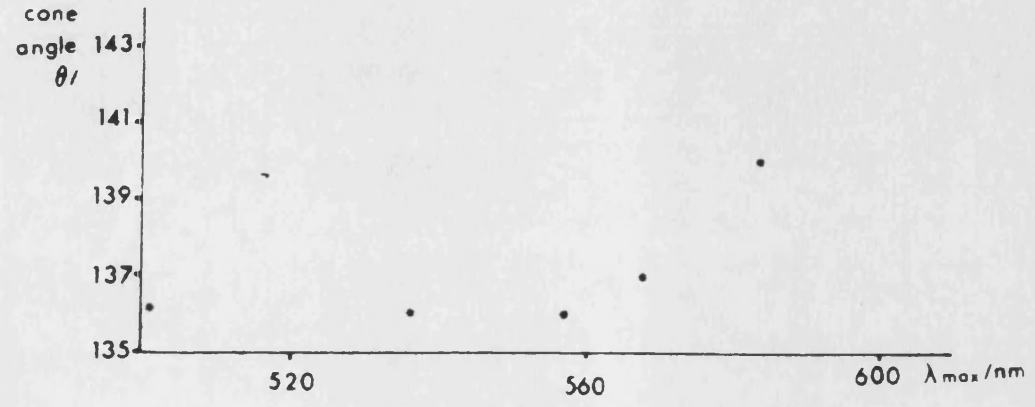

2.3.3 THE COMPLEXES $[M(CO)_2(PR_3)_2X_2]_2$

These orange, diamagnetic compounds are precipitated upon rapid passage of N_2 through solutions of $M(CO)_2(PR_3)_2X_2(MeCN)$ (M=Mo or W, PR_3=$PMePh_2$ or PMe_2Ph, X=Br, M=Mo, PR_3=$PMePh_2$, X=Cl) or $M(CO)_2(PR_3)_2X_2$ (M=Mo or W, PR_3=$PMePh_2$ or PMe_2Ph, X=Br) in chlorinated solvents at room temperature (M=Mo) or under reflux (M=W), or by heating $M(CO)_3(PR_3)_2X_2$ under reflux in ethanol. Full characterisation of these complexes was prevented by their low solubility in all common solvents.

INFRA-RED SPECTRA

The solid state infra-red data for $[M(CO)_2(PR_3)_2X_2]_2$ are given in Table 2.8. The presence of far infra-red absorptions for the chloro complex attributable to both terminal and bridging halogens is in keeping with the dimeric formulation. The related complexes $[Mo(CO)_2(PMe_2Ph)_2X_2]_2$ and $[M(CO)_2(EMe_3)_2X_2]_2$ (E=P, As or Sb) [16,86] have both been identified as dimeric on this basis, but the insolubility of all these complexes has prevented direct experimental confirmation of this.

Table 2.7 Infra-red data for $[M(CO)_2(PR_3)_2X_2]_2$

Complex			Colour	ν(CO)cm^{-1}	
M	PR_3	X		Nujol	mull
Mo	$PMePh_2$	Cl[a]	orange	1942s	1860s
Mo	$PMePh_2$	Br	orange	1943s	1868s
W	$PMePh_2$	Br	orange	1927s	1830s
W	PMe_2Ph	Br	orange	1910s	1810s

[a]-ν(Mo-Cl) terminal=289cm^{-1}, ν(Mo-Cl) bridging=240cm^{-1}

MASS SPECTRA

The most intense metal-containing peaks in the FAB mass spectrum of $[MoBr_2(CO)_2(PR_3)_2]_2$ (PR_3=$PMePh_2$ or PMe_2Ph) are listed in Table 2.9. The highest metal-containing ion corresponding to $[Mo(CO)_2(PR_3)_2(glycerol)]^+$, fragmentated by initial loss of glycerol followed by step-wise elimination of CO ligands and PR_3. No peaks corresponding to halogen-containing species were observed and thus no evidence for a dimeric formulation was obtained from these studies.

Table 2.9 Metal-containing ions in the mass spectra of $[Mo(CO)_2(PMePh_2)_2Br_2]_2$ and $[Mo(CO)_2(PMe_2Ph)_2Br_2]_2$

Assignment	PR_3=$PMePh_2$ m/z	PR_3=PMe_2Ph m/z
$[Mo(CO)_2(PR_3)_2(glycerol)]^+$	643	520
$[Mo(CO)(PR_3)_2(glycerol)]^+$	615	492
$[Mo(CO)(PR_3)_2]^+$	524	400
$[Mo(PR_3)_2]^+$	495	372
$[Mo(PR_3)(glycerol)]^+$	387	326
$[Mo(PR_3)]^+$	296	234
$[Mo(PR_2)]^+$	219	156

2.3.4 RELATIONSHIPS BETWEEN COMPLEXES $M(CO)_3(PR_3)_2X_2$, $[M(CO)_2(PR_3)_2X_2]_n$ (n=1 or 2) AND $M(CO)_2(PR_3)_2X_2(MeCN)$

All the Mo(II) and W(II) six coordinate monomers $M(CO)_2(PR_3)_2X_2$ reported in this thesis reacted quantitatively with CO to reform the tricarbonyl and interconversion between six and seven coordination occurred readily in chlorinated or ketonic solvents (equation 2.2).

$$M(CO)_3(PR_3)_2X_2 \underset{CO}{\overset{N_2}{\rightleftharpoons}} M(CO)_2(PR_3)_2X_2 \qquad (2.2)$$

M=Mo, PR_3=$PEtPh_2$, PEt_2Ph or $PMePh_2$, X=Br; PR_3=$PMePh_2$, X=I,
M=W, PR_3=$PMePh_2$, X=Br

Similarly a suspension of $[M(CO)_2(PR_3)_2X_2]_2$ in CH_2Cl_2 reacted with CO resulting in conversion of the insoluble solid into a clear solution of the tricarbonyl, showing that these systems are also reversible CO carriers. Although this conversion presumably occurs by initial breakage of the halogen bridges to form a monomer, blue or purple colourations characteristic of such six coordinate species were not observed, indicating that addition of CO is rapid and therefore bridge breaking is the rate-determining step (r.d.s) (equation 2.3).

$$[M(CO)_2(PR_3)_2X_2]_2 \xrightarrow{\text{r.d.s}} M(CO)_2(PR_3)_2X_2$$

$$M(CO)_2(PR_3)_2X_2 \xrightarrow{+CO,\ \text{fast}} M(CO)_3(PR_3)_2X_2 \qquad (2.3)$$

Attempts to carry out decarbonylations of the tricarbonyl in MeCN yielded complexes $M(CO)_2(PR_3)_2X_2(MeCN)$ in all cases. The rate of CO loss during their preparation showed no appreciable halogen or phosphine dependence, in contrast to loss of CO from the tricarbonyl analogues, where ease and rate of CO loss decreased in the order Cl>Br>I. Freshly prepared solutions of $M(CO)_2(PR_3)_2X_2(MeCN)$ in

solvents other than MeCN gradually lost MeCN on standing and this process could be accelerated by rapid passage of N_2 through the solutions, producing analytically pure samples of complexes $[M(CO)_2(PR_3)_2X_2]_n$ (n=1 or 2) (equation 2.4). Loss of MeCN from solutions of $Mo(CO)_2(PMe_2Ph)_2Br_2(MeCN)$ in chlorinated or ketonic solvents resulted in the observation of a transient blue colouration prior to precipitation of the dimer, suggesting that an unstable six coordinate monomer formed before dimerisation occurred.

$$M(CO)_3(PR_3)_2X_2 \xrightarrow[N_2]{MeCN} M(CO)_2(PR_3)_2X_2(MeCN) + CO\uparrow$$

$$M(CO)_2(PR_3)_2X_2(MeCN) \xrightarrow[CH_2Cl_2 \text{ or acetone}]{N_2} M(CO)_2(PR_3)_2X_2 \qquad (2.4)$$

$$M(CO)_2(PR_3)_2X_2 \longrightarrow [M(CO)_2(PR_3)_2X_2]_2$$

Previous routes to monomeric and dimeric dicarbonyl complexes of this type involved elevated temperatures or low pressures, with typical reaction times of several hours [14,16,26] and thus the rapid formation of $M(CO)_2(PR_3)_2X_2(MeCN)$ and its conversion to $[M(CO)_2(PR_3)_2X_2]_n$ (n=1 or 2) provides an improved, facile route to this type of complex, which for the molybdenum species may be used at room temperature.

Attempts to prepare the analogous complexes $M(CO)_2(PPh_3)_2X_2(MeCN)$ by either decarbonylation of the tricarbonyl in acetonitrile or by recrystallisation of $M(CO)_2(PPh_3)_2X_2$ from acetonitrile were unsuccessful, and may result from the larger steric bulk of the two PPh_3 groups (θ=145°).

Repeated attempts at both ambient and elevated temperatures to prepare acetone complexes analogous to the acetonitrile series failed, suggesting that the linearity of the nitrile facilitates reaction, whilst the larger steric size of acetone and the lower affinity of Mo and W(II) species for oxygen donor ligands prevents strong coordination at room temperature or above.

In keeping with Colton's observation that it was the steric bulk of the ligated phosphine which caused one CO group in $Mo(CO)_3(PPh_3)_2X_2$ to become labile leading to $Mo(CO)_2(PPh_3)_2X_2$ formation [10-12], the more sterically congested $PEtPh_2$ and PEt_2Ph tricarbonyls readily formed blue, diamagnetic monomers $Mo(CO)_2(PR_3)_2Br_2$, which are presumably too crowded to allow dimer formation. In contrast, the analogous PMe_2Ph tricarbonyl complex formed dimeric $[Mo(CO)_2(PMe_2Ph)_2Br_2]_2$ on decarbonylation, presumably via an unstable monomer species which has a less sterically strained metal centre, whilst $Mo(CO)_3(PMePh_2)_2Br_2$ behaves in an intermediate manner to yield a monomer which was sufficiently stable to be isolated, but with a metal centre uncongested enough to permit dimerisation. The ease of CO loss from the complexes $Mo(CO)_3(PMePh_2)_2X_2$ (X=Cl, Br or I) decreased in the order Cl>Br>I, producing the series of complexes $[Mo(CO)_2(PMePh_2)_2Cl_2]_2$, $[Mo(CO)_2(PMePh_2)_2Br_2]_2$, $Mo(CO)_2(PMePh_2)_2Br_2$ and $Mo(CO)_2(PMePh_2)_2I_2$. The degree of π-bonding between halogen and metal increases in the order Cl<Br<I, resulting in less charge transfer from the metal into the carbonyl anti-bonding orbitals and thus the carbonyl groups of $Mo(CO)_n(PMePh_2)_2X_2$ (n=2 or 3) are most stable for X=I and thus require elevated temperatures to effect decarbonylation. The inability of $Mo(CO)_2(PMePh_2)_2I_2$ to dimerise presumably results from a combination of steric crowding around the metal centre and the general instability of iodo-bridged complexes. Thus, the type of product formed on CO loss from $M(CO)_3(PR_3)_2X_2$ is dependent upon both the halogen type and the phosphine cone angle, θ and this relationship can be seen in Table 2.10.

Table 2.10 Correlation between the cone angle of PR_3, the halide X and the decarbonylation product of $M(CO)_3(PR_3)_2X_2$.

Phosphine	Cone angle, θ (°)	Halide, X	Product[a]
$PEtPh_2$	140	Br	A
PEt_2Ph	137	Br	A
$PMePh_2$	136	I	A
$PMePh_2$	136	Br	A, B
$PMePh_2$	136	Cl	B
PMe_2Ph	122	Br	B

[a] A=$M(CO)_2(PR_3)_2X_2$, B=$[M(CO)_2(PR_3)_2X_2]_2$

Decarbonylation of $W(CO)_3(PR_3)_2X_2$ in chloroform or ethanol at elevated temperatures produced a series of monomeric and dimeric complexes $W(CO)_2(PMePh_2)_2Br_2$ and $[W(CO)_2(PR_3)_2Br_2]_2$ (PR_3=$PMePh_2$ or PMe_2Ph), whilst loss of CO from the tricarbonyl in acetonitrile under similar reaction conditions yielded $W(CO)_2(PR_3)_2Br_2(MeCN)$ (PR_3=$PMePh_2$ or PMe_2Ph). The influence of halogen and phosphine type upon the ease of CO loss from the tricarbonyl and the nature of the product formed closely paralleled that of the molybdenum tricarbonyl complexes.

In order to establish the reactivity of the new complexes $M(CO)_2(PR_3)_2X_2(MeCN)$, reactions with neutral and ionic ligands have been carried out and the results are reported in Chapter 3.

CHAPTER 3

THE REACTIVITY OF $M(CO)_3(PR_3)_2X_2(MeCN)$ WITH ALKYNES AND MONO- OR BIDENTATE S, C OR O LIGANDS

3.1 INTRODUCTION

In addition to the CO carrier phosphine halocarbonyl Mo(II) and W(II) complexes described in the previous chapter, there exists another series of complexes based upon the sulphur chelating anionic dialkyldithiocarbamate ligands, which behave in a similar manner. Although the reactivity of $M(CO)_3(PR_3)_2X_2$ and $M(CO)_3(S_2CNR_2)_2$ complexes show several close similarities [11-13,16,17,101], differences in relative reactivities and reaction rates frequently arise. Thus for the latter series delocalisation of charge between N and S_2C in the dialkyldithiocarbamate ligands $S_2CNR_2^-$ results in less electron density at the metal centre, and hence increased lability of CO in $M(CO)_3(S_2CNR_2)_2$ in the presence or absence of other donor groups. Reactions of $M(CO)_n(S_2CNR_2)_2$ (n=2 or 3) with a range of P- or N-donor ligands L (L=PPh_3, PEt_3, amine, $P(OR)_3$), halides X^- or alkynes R'C≡CR" have generated complexes with general formulae $M(CO)_2(S_2CNR_2)_2L$ [65,102-105], $[M(CO)_2(S_2CNR_2)_2X]^-$ [102,106] and $M(CO)(S_2CNR_2)_2(R'C{\equiv}CR")$ [107,108]. In contrast reactions of the seven coordinate monomeric phosphine complexes may be restricted by the formation of insoluble $[M(CO)_2(PR_3)_2X_2]_2$ as an unwanted product and by the limited number of previously known stable electrophilic six coordinate complexes $M(CO)_2(PR_3)_2X_2$. Isolation of the new complexes $M(CO)_2(PR_3)_2X_2(MeCN)$ has now provided an opportunity to expand this area of research by providing a facile route to d^4 metal dicarbonyl species, which avoids dimer formation. Thus reactions of $M(CO)_2(PR_3)_2X_2(MeCN)$ with various mixed C-, S- and O-donor ligands which are capable of adopting more than one coordination mode in bonding to metal centres have been investigated and are reported in this chapter. The structures of the products

have been inferred where possible by a combination of spectroscopic methods.

Interest in alkyne complexes of Mo and W arises from their possible involvement in the catalytic polymerisation and oligomerisation of alkynes [109] and from the ability of these unsaturated ligands to coordinate to metal centres as 2, 3 or 4 electron donors [110]. In order to extend the range of such complexes and to further define the reactivities of the new acetonitrile complexes, reactions with 2-butyne and diphenylacetylene have been carried out and the crystal structure of one of the derivatives, $Mo(CO)(PMePh_2)_2Br_2(MeC{\equiv}CMe)$, determined.

3.2 EXPERIMENTAL

The starting materials $M(CO)_2(PR_3)_2X_2(MeCN)$ were prepared using the method given in Chapter 2. Details of physical techniques and solvent purification appear in Appendix 1. Yields and analytical data are given in Tables 3.1-3.6.

PREPARATION OF $M(CO)(PR_3)_2X_2(R'C{\equiv}CR')$ (M=Mo, R'=Me, X=Br, $PR_3=PEtPh_2$, PEt_2Ph, $PMePh_2$, PMe_2Ph, X=Cl or I, $PR_3=PMePh_2$, R'=Ph, X=Br, $PR_3=PMePh_2$, M=W, R'=Me or Ph, X=Br, $PR_3=PMePh_2$).

An excess of 2-butyne or diphenylacetylene (10mmol) in dichloromethane ($15cm^3$) was added to freshly prepared solid $M(CO)_2(PR_3)_2X_2(MeCN)$ (0.5mmol) and the mixture was stirred at room temperature for 12hr (M=Mo) or at 40°C for 8hr (M=W). The yellow solutions darkened and became deep green (Mo) or purple (W). The filtered solutions were concentrated *in vacuo* and n-hexane ($5cm^3$) added. Refrigeration yielded the products as fine green or purple needles, which were recrystallised from dichloromethane-hexane mixtures. Reaction times for the complexes $Mo(CO)(PR_3)_2X_2(R'C{\equiv}CR')$ could be reduced to 0.5hr by heating the reactants to 40°C.

Table 3.1 Yields and analytical data for $M(CO)(PR_3)_2X_2(R'C{\equiv}CR')$.

Complex		Yield	Analysis found(calculated)		
PR_3	X	%	%C	%H	%X
$Mo(CO)(PR_3)_2X_2(MeC{\equiv}CMe)$					
$PEtPh_2$	Br	51	51.3(51.7)	4.7(4.7)	21.2(20.9)
PEt_2Ph	Br	44	44.4(44.8)	5.4(5.4)	23.9(23.9)
$PMePh_2$	I	49	43.4(44.7)	3.8(3.8)	
$PMePh_2$	Br	55	50.2(50.4)	4.5(4.3)	21.5(21.7)
$PMePh_2$	Cl	37	57.4(57.3)	4.9(4.9)	10.4(10.9)
PMe_2Ph	Br	39	41.2(41.0)	4.7(4.6)	26.2(26.1)
$Mo(CO)(PR_3)_2X_2(PhC{\equiv}CPh)$					
$PMePh_2$	Br	41	52.8(57.1)	4.1(4.2)	
$W(CO)(PR_3)_2X_2(MeC{\equiv}CMe)$					
$PMePh_2$	Br	53	44.3(45.0)	4.0(3.9)	19.5(19.4)
$W(CO)(PR_3)_2X_2(PhC{\equiv}CPh)$					
$PMePh_2$	Br	50	51.7(51.8)	3.7(3.8)	

PREPARATION OF $M(CO)_2(PMePh_2)_2(SCN)_2$ (M=Mo or W).

A solution of potassium thiocyanate (9 7mg,1.0mmol) in acetone ($20cm^3$) was added dropwise to freshly prepared solid $M(CO)_2(PMePh_2)_2Br_2(MeCN)$ (M=Mo or W) (0.5mmol). The mixture was stirred for 18hr and the orange mixture was filtered to remove KBr. Solvent was removed *in vacuo* and the residue was extracted with ether ($10cm^3$). The solution was cooled to -10°C to afford the product as yellow microcrystalline powders, which were collected and recrystallised from methanol-hexane mixtures.

Table 3.2 Yields and analytical data for $M(CO)_2(PR_3)_2(SCN)_2$.

Complex		Yield	Analysis found(calculated)		
M	PR_3	%	%C	%H	%N
Mo	$PMePh_2$	51	53.3(53.9)	3.3(3.9)	3.9(4.2)
W	$PMePh_2$	55	47.2(47.6)	3.0(3.4)	3.3(3.7)

PREPARATION OF $M(CO)_2(PR_3)(S_2CNEt_2)_2$ (M=Mo or W, $PR_3=PMePh_2$, M=W, $PR_3=PMe_2Ph$) AND $W(CO)(PMe_2Ph)_2(S_2CNEt_2)_2$.

A freshly prepared sample of solid $M(CO)_2(PR_3)_2Br_2(MeCN)$ (M=Mo or W, $PR_3=PMePh_2$, M=W, $PR_3=PMe_2Ph$) (0.5mmol) was stirred for 18hr at ambient temperature with a solution of sodium diethyldithiocarbamate trihydrate (225mg,1.0mmol) in acetone ($20cm^3$). A dark red solution formed which was filtered to remove NaBr and evaporated to dryness *in vacuo*. The residue was dissolved in CH_2Cl_2 ($5cm^3$) and the solution filtered. Addition of hexane ($3cm^3$) and cooling (-10°C) yielded the $PMePh_2$ products as dark red crystals, or a mixture of the mono- and dicarbonyl PMe_2Ph products as dark red and

orange-red crystals respectively. The latter mixture was separated by hand.

Table 3.3 Yields and analytical data for $M(CO)_2(PR_3)(S_2CNEt_2)_2$ and $M(CO)(PMe_2Ph)_2(S_2CNEt_2)_2$.

M	PR_3	Yields %	Analysis found(calculated) %C	%H	%N
Complex $M(CO)_2(PR_3)(S_2CNEt_2)_2$					
Mo	$PMePh_2$	69	46.1(46.3)	5.2(5.1)	4.1(4.3)
W	$PMePh_2$	73	40.7(40.8)	4.4(4.5)	3.7(3.8)
W	PMe_2Ph	44	35.6(35.6)	4.5(4.6)	4.1(4.2)
Complex $M(CO)(PR_3)_2(S_2CNEt_2)_2$					
W	PMe_2Ph	41	42.3(41.3)	5.6(5.4)	3.6(3.6)

PREPARATION OF $[MBr(CO)_2(PR_3)_2]_2-(\mu-C_2O_4)$ (M=Mo, PR_3= $PEtPh_2$, PEt_2Ph or $PMePh_2$, M=W, PR_3=$PMePh_2$ or PMe_2Ph).

A slurry of an excess of finely ground sodium oxalate (0.5g) in acetone (50cm^3) was added to fresh solid $M(CO)_2(PR_3)_2Br_2(MeCN)$ (M=Mo, PR_3=$PEtPh_2$, PEt_2Ph or $PMePh_2$, M=W, PR_3=$PMePh_2$ or PMe_2Ph) (1.0mmol) and stirred for 15hr. The resulting orange suspension was evaporated to dryness in vacuo and the residue repeatedly extracted with dichloromethane. The combined, filtered extracts were reduced in volume and the orange microcrystalline products were isolated by addition of hexane and storage at low temperature (-10°C). The more soluble products were recrystallised from saturated CH_2Cl_2 solutions. The tungsten dimethylphenylphosphine complex only was isolated as a mixture of two crystalline forms which were hand picked to separate the minor product of yellow cubic

crystals from the major orange product. The former constituted less than 5% of the total yield. An isomeric relationship between the orange (I) and yellow (II) products was indicated by their analytical data which are given in Table 3.4

Table 3.4 Yields and analytical data for $\{MBr(CO)_2(PR_3)_2\}_2-(\mu-C_2O_4)$.

M	PR_3	Yield %	Analysis found(calculated) %C	%H	
Mo	$PEtPh_2$	64	49.8(52.8)	4.1(4.2)	
Mo	PEt_2Ph	59	43.4(45.3)	4.9(4.9)	
Mo	$PMePh_2$	66	45.7(51.4)	3.6(3.8)	
W	$PMePh_2$	67	45.2(45.5)	3.4(3.4)	
W	PMe_2Ph	51	34.3(35.6)	3.4(3.4)	(I)
			35.6(35.6)	3.3(3.4)	(II)

PREPARATION OF $M(CO)_2(PR_3)_2(O_2CCF_3)_2$ (M=Mo or W, PR_3=$PMePh_2$ or PMe_2Ph).

A solution of sodium trifluoroacetate (272mg,2.0mmol) in acetone (30cm^3) was added to freshly prepared $M(CO)_2(PR_3)_2Br_2(MeCN)$ (M=Mo or W, PR_3=$PMePh_2$ or PMe_2Ph) (1.0mmol) and stirred for 1hr. The suspension was filtered, evaporated to low volume in vacuo and 40-60° petroleum ether (10cm^3) added. Storage at low temperature (-10°C) precipitated the yellow crystalline products which were recrystallised from CH_2Cl_2-hexane mixtures.

Reactions of $M(CO)_3(PMePh_2)_2Br_2$ with NaO_2CCF_3 under the reaction conditions described above yielded products which possessed identical spectroscopic properties to those obtained from $M(CO)_2(PMePh_2)_2Br_2(MeCN)$, and the analogous triphenylphosphine

complexes $M(CO)_2(PPh_3)_2(O_2CCF_3)_2$ were similarly obtained by reaction of $M(CO)_3(PPh_3)_2Br_2$ with NaO_2CCF_3.

Table 3.5 Yields and analytical data for $M(CO)_2(PR_3)_2(O_2CCF_3)_2$.

	Yield (%)	Analysis found(calculated) %C	%H
$Mo(CO)_2(PPh_3)_2(O_2CCF_3)_2$	47	53.0(55.9)	3.4(3.3)
$Mo(CO)_2(PMePh_2)_2(O_2CCF_3)_2$	51	48.9(49.3)	3.2(3.3)
$Mo(CO)_2(PMe_2Ph)_2(O_2CCF_3)_2$	39	39.9(40.4)	3.1(3.4)
$W(CO)_2(PPh_3)_2(O_2CCF_3)_2$	48	47.6(50.9)	3.0(3.0)
$W(CO)_2(PMePh_2)_2(O_2CCF_3)_2$	46	43.8(44.3)	3.1(3.0)
$W(CO)_2(PMe_2Ph)_2(O_2CCF_3)_2$	35	34.8(35.6)	2.7(2.9)

PREPARATION OF $MBr(CO)_2(PR_3)_2(O_2CCF_3)$ (M=Mo, PR_3=$PMePh_2$, M=W, PR_3=PPh_3.

A solution of sodium trifluoroacetate (136mg,1.0mmol) in acetone (10cm^3) was stirred with either $W(CO)_2(PPh_3)_2Br_2$ or freshly prepared $Mo(CO)_2(PMePh_2)_2Br_2(MeCN)$ (1.0mmol) for 12hrs. For M=Mo, PR_3=$PMePh_2$ the filtered orange solution was reduced to dryness *in vacuo* and redissolved in CH_2Cl_2 (5cm^3). Addition of 40-60°C petroleum ether (10cm^3) to the filtered solution and cooling (-10°C) yielded the dark orange crystalline products, which were recrystallised from CH_2Cl_2-hexane mixtures. For M=W, PR_3=PPh_3 the product precipitated from solution as a yellow-orange powder which was washed first with a little aqueous MeOH to remove NaBr, and then with diethyl ether before being dried in air.

Table 3.6 Yields and analyses for $MBr(CO)_2(PR_3)_2(O_2CCF_3)$.

M	PR_3	Yield	Analysis found(calculated)	
		%	%C	%H
Mo	$PMePh_2$	50	48.0(48.3)	3.5(3.5)
W	PPh_3	49	49.8(50.2)	3.0(3.1)

3.3 REACTIONS OF $M(CO)_2(PR_3)_2X_2(MeCN)$

3.3.1. WITH ALKYNES R'C≡CR' (R'=Me or Ph)

Reaction of $M(CO)_2(PR_3)_2X_2(MeCN)$ with excess 2-butyne or diphenylacetylene (R'C≡CR') in dichloromethane at room temperature (M=Mo) or 40°C (M=W) yielded air-stable green (Mo) or purple (W) products $M(CO)(PR_3)_2X_2(R'C{\equiv}CR')$ which were characterised by their analytical data and IR, ^1H and ^{13}C NMR spectra. The products formed from reactions involving complexes with $PR_3=PMe_2Ph$, X=Br or $PR_3=PMePh_2$, X=Cl were contaminated with small quantities of $[Mo(CO)_2(PR_3)_2X_2]_2$, which were removed by recrystallisation of the crude products from dichloromethane-hexane mixtures. Direct reaction between the alkynes and dimers did not yield $M(CO)(PR_3)_2X_2(R'C{\equiv}CR')$.

INFRA-RED SPECTRA

Selected infra-red data for these complexes are given in Table 3.7. A strong, single carbonyl stretching frequency in the

Table 3.7 Selected infra-red data[a] for $M(CO)(PR_3)_2X_2(R'C{\equiv}CR')$.

Complex	Colour	$\nu(CO)cm^{-1}$	$\nu(C{\equiv}C)cm^{-1}$
$Mo(CO)(PEtPh_2)_2Br_2(MeC{\equiv}CMe)$	green	1955s	1666vw
$Mo(CO)(PEt_2Ph)_2Br_2(MeC{\equiv}CMe)$	green	1947s	1670vw
$Mo(CO)(PMePh_2)_2Cl_2(MeC{\equiv}CMe)$	green	1939s	1678vw
$Mo(CO)(PMePh_2)_2Br_2(MeC{\equiv}CMe)$	green	1951s	1650vw
$Mo(CO)(PMePh_2)_2I_2(MeC{\equiv}CMe)$	green	1921s	1673vw
$Mo(CO)(PMe_2Ph)_2Br_2(MeC{\equiv}CMe)$	green	1936s	1677vw
$W(CO)(PMePh_2)_2Br_2(MeC{\equiv}CMe)$	purple	1901s	1652vw
$Mo(CO)(PMePh_2)_2Br_2(PhC{\equiv}CPh)$	green	1980s	1622vw
$W(CO)(PMePh_2)_2Br_2(PhC{\equiv}CPh)$	purple	1953s	1620vw

[a]—as Nujol mulls

range 1901-1955cm^{-1} characterised these monocarbonyls and a very weak absorption between 1620-1678cm^{-1} was attributed to the ν(C≡C) stretching mode. The related complex Mo(CO)(PEt$_3$)$_2$Br$_2$(MeC≡CMe) (obtained from Mo(CO)$_2$(PEt$_3$)$_2$Br$_2$ [111]), showed a similar weak band at 1645cm^{-1}. Donation of charge from the triple bond to the metal may occur through a combination of σ- and π-bonding. The alkyne ligand is capable of utilising both parallel ($\pi_\parallel$) and perpendicular ($\pi_\perp$) π-orbitals as shown in Fig. 3.1, and weakening of the multiple bonds may therefore occur by donation of charge from $\pi_\parallel$ and $\pi_\perp$ to the metal or by charge acceptance via the vacant π^* orbital of the alkyne. Variation of ν(C≡C) for an alkyne-metal complex from the free alkyne value will therefore reflect to some degree the metal-alkyne interaction.

Fig. 3.1 Orbitals involved in metal-alkyne bonding.

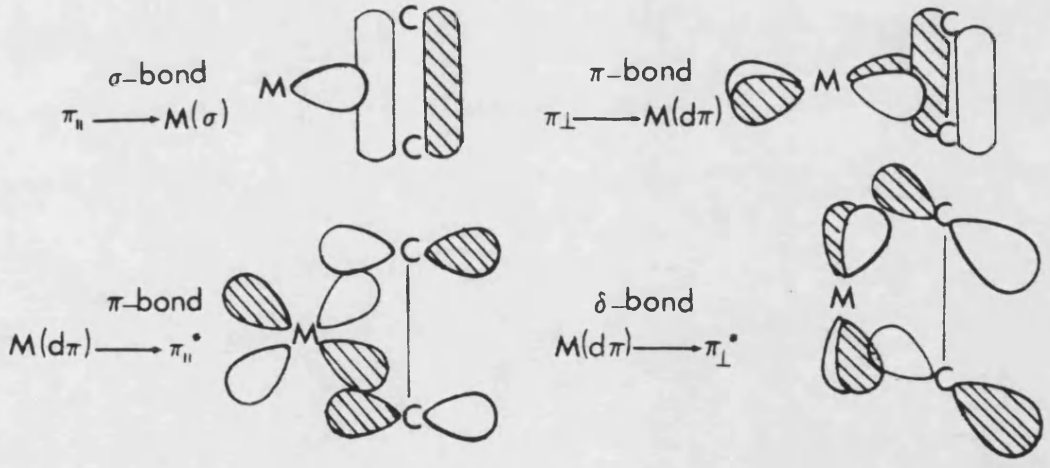

The range of ν(C≡C) values for the butyne complexes in Table 3.7 (1645-1678cm^{-1}) shows an average decrease of 677cm^{-1} from uncoordinated 2-butyne (2333cm^{-1}) indicating considerable reduction of the carbon-carbon triple bond order. Herrick and Templeton [112] examined a series of dimethylacetylenedicarboxylate (DMAC) complexes

and showed that high ν(C≡C) frequencies are observed where the alkyne and another ligand compete for the same empty metal dπ orbital e.g. Mo(O)(DMAC)(dedtc)$_2$ ν(C≡C) 1850cm^{-1}. The lowest ν(C≡C) frequencies were observed for coordinatively unsaturated complexes in which the alkyne acted as a four-electron donor. Examination of Table 3.7 shows no discernible correlation between these frequencies and the nature of PR_3 or X, and a review of these data in known complexes given in Table 3.8 supports this observation and confirms that the alkynes in the complexes reported here are acting as four electron donors.

Table 3.8 Values of ν(C≡C) in known alkyne complexes.

Complex		ν(C≡C)/cm^{-1}	Ref.
Mo(CO)(PEt$_3$)$_2$X$_2$(MeC≡CMe)	X=Cl	1645	111
	X=Br	1645	111
W(CO)(P(OR)$_3$)$_2$I$_2$(MeC≡CMe)	R=Me	1715	113
	R=Et	1658	113
	R=Pr^i	1718	113
	R=Bu^t	1658	113
Mo(CO)(dppe)X$_2$(EtC≡CEt)	X=Cl	1671	114
	X=Br	1625	114

It has previously been observed that a correlation exists between the colour of alkyne complexes and the number of electrons donated to the metal by the unsaturated ligand [115]. Thus bis-alkyne molybdenum derivatives containing 3-electron donor ligands e.g. Mo(RC≡CR')$_2$(dedtc)$_2$ are commonly yellow, whilst mono-alkynes with 4-electron donors, such as M(CO)(alkyne)(dedtc)$_2$ may be deep purple, blue or green [116]. The molybdenum and tungsten alkyne complexes in this work showed dark green or purple colouration respectively in

agreement with 4-electron donation from 2-butyne or diphenylacetylene. Such colourations in the related complexes $M(CO)(PR_3)_2X_2(R'C{\equiv}CR')$ (R=Ph or Et) have been shown to be associated with broad absorptions in their ultra-violet spectra which arise from HOMO-LUMO transitions, and since these results are well documented [111,114] the UV spectra of the complexes reported here were not examined.

NMR SPECTROSCOPY

Tables 3.9 and 3.10 summarise respectively the room temperature ^1H and ^{13}C NMR data for $M(CO)(PR_3)_2X_2(R'C{\equiv}CR')$. Resonances due to aromatic protons appeared as multiplets between 7.0 and 7.6ppm for the phosphine groups and at 6.97ppm for diphenylacetylene. Phosphorus coupling to the methyl and ethyl phosphine protons resulted in J_{P-H} values of ca 4.4 and 7.5Hz respectively. Most of the 2-butyne complexes exhibited resonances at ca 2.3-2.4ppm due to the alkyne methyl protons which were split into triplets by phosphorus coupling with $^4J_{H-P}$ values of 1.5Hz. The analogous resonances in the spectra of the $PEtPh_2$ and PEt_2Ph complexes were unresolved singlets at ca 2.3ppm.

The ^{13}C NMR spectra exhibit multiplets for the phosphine and alkyne aromatic carbon nuclei between 128 and 138ppm. The complexes containing $PMePh_2$ produce an apparent triplet due to the P-Me group with $^1J_{P-C}$ coupling of 15.5Hz, whereas in the spectra of the $PEtPh_2$ complex, the phosphine methyl species resonate as two singlets at 7.80 and 7.85ppm and the methylene groups as a single triplet with $^1J_{P-C}$ =12.1Hz. The two methyl and methylene groups in the PEt_2Ph complex produce respectively, singlets at 6.96 and 7.40ppm and triplets centred at 15.93 and 17.62ppm with $^1J_{P-C}$ equal to 12.2Hz. Similarly, the PMe_2Ph complex produces two triplet P-Me carbon resonances at 13.73 and 14.49ppm, having phosphorus coupling constants of 14.4Hz.

The alkyne carbon atoms appeared as triplets with $^2J_{P-C}$ coupling constants (5.5-9.5Hz) typical of a cis-P-M-C geometry. The ability of alkynes to utilise both $\pi_{\parallel}$ and $\pi_{\perp}$ orbitals leads to high frequency shifts in ^{13}C NMR resonances, and a correlation between the number of electrons formally donated by each alkyne to achieve coordinative saturation and the ^{13}C chemical shift of the alkyne

Table 3.9 'H NMR data^ for $M(CO)(PR_3)_2X_2(R'C{\equiv}CR')$ in CD_2Cl_2.

Complex				Chemical shift δ (ppm) (multiplicity, assignment, coupling constant in Hz)		
				$\delta(R'C{\equiv}CR')$	$\delta(PR_3)$	
M	PR_3	X	R'		Aliphatic	Aromatic
Mo	$PEtPh_2$	Br	Me	2.24 (s,6H)	0.68 (t,6H,7.51)	7.25 (m),7.41 (m),
					2.52 (m,2H,7.51), 2.92 (m,2H,7.51)	7.62 (m) (20H)
Mo	PEt_2Ph	Br	Me	2.39 (s,6H)	0.89 (dt,6H,7.51)	7.11 (m),7.26 (m),
					1.09 (dt,6H,7.51), 2.19 (m,8H,7.33)	7.28 (m) (10H)
Mo	$PMePh_2$	Cl	Me	2.35 (t,6H,1.5)	2.15 (t,6H,4.40)	7.25 (m), 7.41 (m),
						7.58 (m) (20H)
Mo	$PMePh_2$	Br	Me	2.38 (t,6H,1.5)	2.18 (t,6H,4.40)	7.25 (m), 7.40 (m),
						7.56 (m) (20H)
Mo	$PMePh_2$	I	Me	2.40 (t,6H,1.5)	2.28 (t,6H,4.41)	7.24 (m), 7.41 (m),
						7.58 (m) (20H)
Mo	PMe_2Ph	Br	Me	2.52 (t,6H,1.5)	1.64 (t,6H,4.49)	7.10 - 7.29 (m) (10H)
					1.78 (t,6H,4.30)	

Table 3.9 continued.

Complex				Chemical shift δ (ppm) (multiplicity, assignment, coupling constant in Hz)		
				δ(R'C≡CR')	δ(PR_3)	
M	PR_3	X	R'		Aliphatic	Aromatic
Mo	$PMePh_2$	Br	Ph	6.96 (m, 10H)	2.25 (t, 6H, 4.22)	7.01 - 7.52 (m) (20H)
W	$PMePh_2$	Br	Me	2.35 (s, 6H)	2.18 (t, 6H, 4.40)	7.23 (m), 7.40 (m), 7.54 (m) (20H)
W	$PMePh_2$	Br	Ph	6.98 (m, 10H)	2.31 (t, 6H, 4.26)	7.01 - 7.49 (m) (20H)

[a]-Measured at 20°C, δ relative to TMS in ppm.

(multiplicity, relative intensity, coupling constant J in Hz.).

Table 3.10 ^{13}C NMR data[a] for $M(CO)(PR_3)_2X_2(R'C{\equiv}CR')$ in CH_2Cl_2.

Complex				Chemical shift δ (ppm)			
				$\delta(R'C{\equiv}CR')$	$\delta(CO)$	$\delta(PR_3)$	
M	PR_3	X	R'			Aliphatic	Aromatic
Mo	$PEtPh_2$	Br	Me	22.67 (s,Me) 229.41 (t,C≡C,8.8)	238.51 (brs)	20.90 (t,CH_2,12.1) 7.80 ((s,CH_3), 7.85 (s,CH_3)	128.04 - 133.73 (m)
Mo	PEt_2Ph	Br	Me	22.01 (s,Me) 229.99(t,C≡C,9.5)	236.88 (brs)	17.62 (t,CH_2,12.2), 15.93 (t,CH_2,12.1) 7.40 (s,CH_3), 6.96 (s,CH_3)	128.22 - 136.17 (m)
Mo	$PMePh_2$	Cl	Me	22.43 (s,Me) 229.95 (s,C≡C)	238.64 (brs)	12.49 (t,CH_3,15.5)	128.10 - 136.17 (m)
Mo	$PMePh_2$	Br	Me	22.65 (s,Me) 229.90 (s,C≡C)	237.77 (brs)	15.73 (t,CH_3,15.5)	128.07 - 136.15 (m)
Mo	$PMePh_2$	I	Me	24.15 (s,Me) 228.82 (t,C≡C,7.4)	234.10 (brs)	20.16 (t,CH_3,15.6)	127.97 - 133.13 (m)
Mo	PMe_2Ph	Br	Me	22.16 (s,Me) 229.48 (s,C≡C)	235.24 (brs)	13.73 (t,CH_3,14.3) 14.49 (t,CH_3,14.4)	128.17 - 138.27 (m)

Table 3.10 continued.

Complex				Chemical shift δ (ppm)		
			δ(R'C≡CR')	δ(CO)	δ(PR_3)	
M	PR_3	X	R'		Aliphatic	Aromatic
Mo	$PMePh_2$	Br	Ph	232.98 (t,9.5)	16.25 (t,CH_3,15.4)	128.02 - 134.69 (m)
			230.27 (t,C≡C,6.4)			
W	$PMePh_2$	Br	Me	228.86 (brs)	15.68 (t,CH_3,15.5)	127.97 - 136.40 (m)
			21.94 (s,Me)			
			225.63 (t,C≡C,5.5)			
W	$PMePh_2$	Br	Ph	226.82 (t,4.6)	16.36 (t,CH_3,15.5)	127.90 - 139.90 (m)
			225.94 (t,C≡C,5.4)			

^-Measured at 20°C, δ relative to TMS in ppm.
(multiplicity,assignment,coupling constant J in Hz.).

carbon nuclei has been established [110]. Table 3.10 shows δ(MeC≡CMe) and δ(PhC≡CPh) resonances between 225-230ppm, suggesting substantial donation from $\pi_{\perp}$ into the vacant metal dπ orbitals and consequently these alkynes can be considered as 4-electron donors in $M(CO)(PR_3)_2X_2(R'C{\equiv}CR')$.

DISCUSSION

Alkyne complexes of general formula $M(CO)(PR_3)_2X_2(R'C{\equiv}CR')$ (M=Mo or W, X=halogen) have previously been prepared from $M(CO)_n(PR_3)_2X_2$ (n=2 or 3, PR_3=PPh_3, PEt_3 or py, $(PR_3)_2$=dppe) [114] by direct reaction with excess alkyne at elevated temperatures and reaction times varying from 0.5hr to 6d, and this method has to date only been employed where loss of CO from the parent halo-tricarbonyl leads to a relatively stable 6-coordinate dicarbonyl monomer. Thus this author found that reaction of $[M(CO)_2(PMe_2Ph)_2Br_2]_2$ (M=Mo or W) or $[Mo(CO)_2(PMePh_2)_2Cl_2]_2$ with $MeC{\equiv}CMe$ under identical reaction conditions failed to produce the required alkyne-monocarbonyl and only the insoluble dimeric complexes $[M(CO)_2(PMe_2Ph)_2Br_2]_2$ or $[Mo(CO)_2(PMePh_2)_2Cl_2]_2$ could be isolated. Although the bis-alkyne dimers $[W(CO)Br_2(RC{\equiv}CR)_2]_2$ are known to react with nucleophiles such as PPh_3 to form $W(CO)(PPh_3)_2Br_2(RC{\equiv}CR)$ [117], reaction of $[M(CO)_2(PR_3)_2X_2]_2$ with alkynes fails to break the halogen bridges and no reaction occurs. However reaction of 2-butyne or diphenylacetylene with $M(CO)_2(PR_3)_2X_2(MeCN)$ generates the green or purple products $M(CO)(PR_3)_2X_2(R'C{\equiv}CR')$ by a simple displacement reaction, the relative rate of alkyne complex formation from $M(CO)_2(PR_3)_2X_2(MeCN)$ showing no significant differences between the different halogen or phosphine complexes of the same metal. Thus the acetonitrile complexes provide a preparative route to the previously unobtainable $PMePh_2$ (X=Br or Cl) and PMe_2Ph (X=Br) complexes, and an alternative facile route to stable iodo-alkyne complexes of general formula $M(CO)(PR_3)_2I_2(R'C{\equiv}CR')$. Attempts by Winston et al. [114] to generate such species by reaction of alkyne $R'C{\equiv}CR'$ with $M(CO)_n(PR_3)_2I_2$ (M=Mo or W, n=2 or 3, R=Ph or Et, R'=Me or Ph) were unsuccessful and led to decomposition products only. The only previously known member of this iodo-alkyne class is

$M(CO)(PPh_3)_2I_2(R'C{\equiv}CR')$ [118], which was obtained by a complicated route involving initial reaction of the alkyne and $M(CO)_3(MeCN)_2I_2$ to form the unstable intermediate $M(CO)(MeCN)_2I_2(R'C{\equiv}CR')$, which rapidly dimerised to unstable $[M(\mu\text{-}I)I(CO)(MeCN)(R'C{\equiv}CR')]_2$, and was then finally cleaved by PPh_3 to yield the required product.

Structural predictions for alkyne complexes of general formula $M(CO)(PR_3)_2X_2(R'C{\equiv}CR')$ have been based upon bonding considerations [119], and it has been suggested that greatest stability can be achieved by a cis-coplanar arrangement of CO and the C≡C axis, which allows maximum back donation from the two π metal orbitals into the ligand π* orbitals. The four possible isomers expected for $M(CO)(PR_3)_2X_2(R'C{\equiv}CR')$ containing a cis-$M(CO)(R'C{\equiv}CR')$ group are shown in Fig. 3.2

Fig. 3.2 Possible isomers of $M(CO)(PR_3)_2X_2(R'C{\equiv}CR')$.

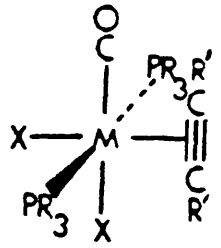

A

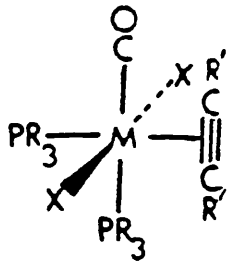

B

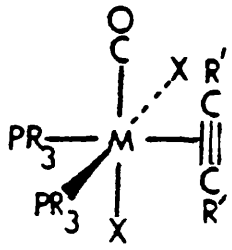

C

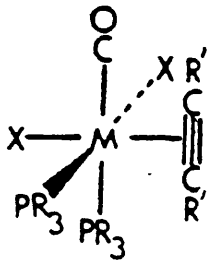

D

In order to confirm the molecular configuration of these complexes a single crystal X-ray determination of a representative member, namely $Mo(CO)(PMePh_2)_2Br_2(MeC{\equiv}CMe)$, has been undertaken and is reported below.

THE SOLID STATE STRUCTURE OF $Mo(CO)(PMePh_2)_2Br_2(MeC{\equiv}CMe)$

The solid state molecular structure of the title complex was determined in collaboration with Drs. M.F.Mahon and K.C.Molloy of the University of Bath.

A sample of $Mo(CO)(PMePh_2)_2Br_2(MeC{\equiv}CMe)$ was recrystallised twice from CH_2Cl_2-hexane mixtures at -10°C to produce crystals suitable for an X-ray single crystal structure determination. A green cubic crystal of approximate dimensions 0.2x0.2x0.2mm. was selected, mounted on a glass fibre and coated with epoxy resin. This was mounted at random on a Hilger-Watts Y290 four-circle automatic diffractometer which was used to measure diffraction intensities and unit cell dimensions. Graphite filtered molybdenum X-radiation was used and 3,098 independent reflections with $2\theta<44°$ were measured. Of these 1,790 reflections with $I>3\sigma(I)$ were used for subsequent refinement calculations. No significant changes were observed in intensities from standard reflections monitored during the experiment. Neither an extinction nor an absorption correction were applied.

CRYSTAL DATA: $Br_2C_{31}H_{22}MoOP_2$, M=728.2, Orthorhombic, a=31.569(7)Å, b=12.701(3)Å, c=15.477(7)Å, α=90°, β=90°, γ=90°, U(unit cell volume)=6,205.36Å^3, D_c(calculated density)=1.56gcm^{-3}, Z(number of molecules in the unit cell)=8, F(000) (number of electrons in the unit cell)=2928, μ(Mo-K_α absorption factor)=30.10cm^{-1}, λ(Mo-K_α)=0.7107Å, space group Pbca from the successful structure determination.

SOLUTION AND REFINEMENT

The position of the molybdenum, phosphorus and bromine atoms were obtained by a Patterson search using Shelx 86 [120] and subsequent Fourier analyses gave the positions of the remaining non-hydrogen atoms. The hydrogen atoms were not located. The structure was refined by full-matrix least squares using Shelx 76 [121] to R=6.35% and R_w=6.39% with a weighting scheme of $W=3.0065/[(\sigma^2(F_o)+0.0010(F_o)^2]$. Scattering factors and dispersion corrections were obtained from the International Tables for X-Ray Crystallography [122]. The resulting list of atom positions, structural factors and thermal parameters are given in Appendix 2 and bond lengths and angles appear in Table 3.11.

Fig. 3.3 shows an ORTEP view of the molecule and the atomic numbering scheme used. The central molybdenum atom can be described as heptacoordinate being bonded to two bromines [Mo-Br(1) 2.641(2), Mo-Br(2) 2.705(3)Å], one carbonyl carbon [Mo-C(27) 1.925(25)Å], two phosphine groups [Mo-P(1) 2.558(5), Mo-P(2) 2.556(5)Å] and a bidentate 2-butyne ligand [Mo-C(28) 2.037(17), Mo-C(29) 2.005(17)]. The two bromides occupy cis-sites in the girdle plane of the pentagonal bipyramidal arrangement, with the phosphine ligands mutually trans in axial positions. The alkyne and carbonyl groups are cis and parallel and complete the girdle plane. Although there is no crystallographic symmetry imposed on the molecule, the structure has virtual C_s symmetry with the mirror plane defined by Mo, Br(1), Br(2), C(27) and the entire alkyne unit.

Bond lengths between the metal atom and the phosphine groups and bromides are not significantly different from those observed for other Mo(II) phosphine halocarbonyls [39]. The alkyne carbon-carbon bond length [C(28)-C(29) 1.362(25)Å] has been shown in

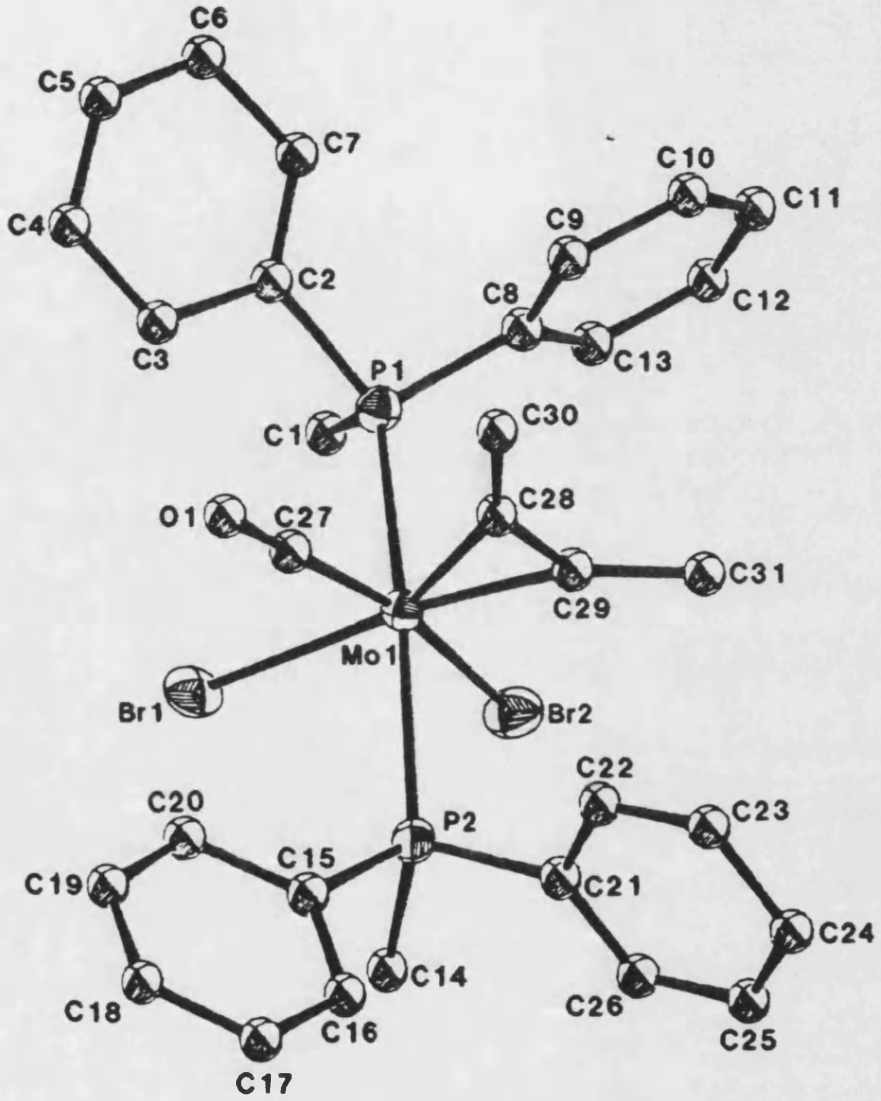

Fig. 3.3 An ORTEP view of $Mo(CO)(PMePh_2)_2Br_2(MeC{\equiv}CMe)$ with hydrogen atoms omitted for clarity, and the atomic numbering scheme used.

Table 3.11 Interatomic Distances and Angles with Standard Deviations in Parentheses for $Mo(CO)(PMePh_2)_2Br_2(MeC{\equiv}CMe)$.

Coordination Sphere:

Distances (Å):

Mo-Br(1)	2.641(2)	Mo-C(27)	1.925(25)
Mo-Br(2)	2.705(3)	Mo-C(28)	2.037(17)
Mo-P(1)	2.558(5)	Mo-C(29)	2.005(17)
Mo-P(2)	2.556(5)		

Angles (°):

Br(1)-Mo-Br(2)	86.4(0.1)	P(1)-Mo-C(28)	93.9(0.5)
P(1)-Mo-Br(1)	86.1(0.1)	P(2)-Mo-C(28)	99.9(0.5)
P(1)-Mo-Br(2)	84.5(0.1)	C(27)-Mo-C(28)	71.5(0.8)
P(2)-Mo-Br(1)	83.7(0.1)	Br(1)-Mo-C(29)	168.5(0.6)
P(2)-Mo-Br(2)	84.6(0.1)	Br(2)-Mo-C(29)	82.2(0.7)
P(2)-Mo-P(1)	165.5(0.2)	P(1)-Mo-C(29)	94.5(0.5)
Br(1)-Mo-C(27)	80.7(0.5)	P(2)-Mo-C(29)	93.5(0.5)
Br(2)-Mo-C(27)	167.1(0.5)	C(27)-Mo-C(29)	110.7(0.8)
P(1)-Mo-C(27)	94.3(0.6)	C(28)-Mo-C(29)	39.4(0.7)
P(2)-Mo-C(27)	94.2(0.5)	Br(2)-Mo-C(28)	121.4(0.6)
Br(1)-Mo-C(28)	152.1(0.6)		

Carbonyl group:

Distances (Å):

C(27)-O(1)	1.191(22)

Angles (°):

Mo-C(27)-O(1)	176.0(1.7)

Alkyne ligand:

Distances (Å):

C(28)-C(30)	1.498(27)	C(29)-C(30)	1.448(26)
C(28)-C(29)	1.362(25)		

Angles (°):

C(29)-C(28)-Mo	69.0(1.1)	C(28)-C(29)-Mo	71.6(1.1)
C(30)-C(28)-Mo	149.1(1.5)	C(31)-C(29)-Mo	148.0(1.8)
C(30)-C(28)-C(29)	141.9(1.6)	C(31)-C(29)-C(28)	140.1(1.9)

Table 3.11 continued

Methyldiphenylphosphine ligand:

Distances (Å):

P(1)-C(1)	1.840(21)	P(2)-C(14)	1.830(20)
P(1)-C(2)	1.808(19)	P(2)-C(14)	1.844(17)
C(2)-C(3)	1.417(24)	C(15)-C(16)	1.425(22)
C(3)-C(4)	1.419(27)	C(16)-C(17)	1.406(27)
C(4)-C(5)	1.388(27)	C(17)-C(18)	1.426(27)
C(5)-C(6)	1.378(28)	C(18)-C(19)	1.372(24)
C(6)-C(7)	1.431(29)	C(19)-C(20)	1.391(24)
C(7)-C(2)	1.400(24)	C(20)-C(15)	1.422(23)
P(1)-C(8)	1.843(17)	P(2)-C(21)	1.832(16)
C(8)-C(9)	1.398(25)	C(21)-C(22)	1.424(22)
C(9)-C(10)	1.458(25)	C(22)-C(23)	1.394(22)
C(10)-C(11)	1.354(28)	C(23)-C(24)	1.426(25)
C(11)-C(12)	1.430(29)	C(24)-C(25)	1.334(25)
C(12)-C(13)	1.411(27)	C(25)-C(26)	1.387(24)
C(13)-C(8)	1.451(26)	C(26)-C(21)	1.367(24)

Angles (°):

C(1)-P(1)-Mo	116.7(0.6)	C(13)-C(8)-C(9)	123.0(1.6)
C(2)-P(1)-Mo	118.3(0.6)	C(1)-C(9)-C(8)	118.6(1.9)
C(2)-P(1)-C(1)	101.2(0.8)	C(11)-C(10)-C(9)	117.5(2.0)
C(8)-P(1)-Mo	109.4(0.5)	C(12)-C(11(-C(10)	125.4(2.0)
C(8)-P(1)-C(2)	104.8(0.9)	C(13)-C(12)-C(11)	118.4(2.0)
C(8)-P(1)-C(2)	105.1(0.8)	C(12)-C(13)-C(8)	117.1(1.8)
C(14)-P(2)-Mo	114.1(0.6)	C(16)-c(15)-P(2)	118.0(1.3)
C(15)-P(2)-C(14)	100.3(0.8)	C(20)-C(15)-P(2)	119.2(1.3)
C(21)-P(2)-Mo	112.1(0.5)	C(20)-C(15)-C(16)	122.7(1.6)
C(21)-P(2)-C(14)	104.6(0.8)	C(17)-C(16)-C(15)	116.0(1.7)
C(21)-P(2)-C(15)	103.0(0.7)	C(18)-C(17)-C(16)	122.7(1.9)
C(3)-C(2)-P(1)	117.9(1.4)	C(19)-C(18)-C(17)	117.8(1.9)
C(7)-C(2)-P(1)	121.1(1.5)	C(20)-C(19)-C(18)	123.6(1.8)
C(7)-C(2)-C(3)	121.1(1.8)	C(19)-C(20)-C(15)	117.2(1.7)
C(4)-C(3)-C(2)	118.9(1.9)	C(22)-C(21)-P(2)	115.9(1.2)
C(5)-C(4)-C(3)	118.4(2.1)	C(26)-C(22)-P(2)	125.2(1.4)
C(6)-C(5()-C(4)	123.9(2.3)	C(23)-C(22)-C(21)	119.5(1.6)
C(7)-C(6)-C(5)	117.8(2.0)	C(24)-C(23)-C(22)	119.4(1.7)
C(6)-C(7)-C(2)	119.7(1.9)	C(25)-C(24)-C(23)	119.2(1.7)
C(9)-C(8)-P(1)	118.2(1.5)	C(26)-C(25)-C(24)	122.2(1.9)
C(13)-C(8)-P(1)	118.7(1.4)	C(25)-C(26)-C(21)	120.7(1.8)

general not to be much affected by the nature of the substituents or degree of electron donation of $\pi_{\perp}$ to the metal [123-125]. The bent cis alkyne geometry has been observed before in 2-butyne complexes [108,126] and the metal-alkyne carbon distances have been shown to reflect the extent of electron donation to the metal [124,125]. For molybdenum or tungsten d^4 monocarbonyl alkynes derivatives 2, 3 or 4-electron donation has been accommpanied by typical average M-C bond lengths of respectively 2.10, 2.06 and 2.00Å, and thus the average Mo-C(alkyne) distance of 2.021Å in $Mo(CO)(PMePh_2)_2Br_2(MeC{\equiv}CMe)$ is in keeping with four-electron donation from the butyne group.

The parallel configuration of the carbonyl and alkyne groups in the cis-Mo(CO)(alkyne) unit has been previously observed in the related complexes $Mo(CO)(PEt_3)_2Br_2(PhC{\equiv}CH)$ [114] and $V(CO)(HC{\equiv}CH)(S_2CNEt_2)_2$ [123] and arises from optimisation of the π-donor and π-acceptor capabilites of the alkyne. The relatively short carbonyl-alkyne carbon-carbon distance (C(27)-C(28)) of 2.316(4)Å in $Mo(CO)(PMePh_2)_2Br_2(MeC{\equiv}CMe)$ is consistant with a weak 3-centre, 2-electron interaction in which the metal d_{xz} orbital is stabilised by mixing of the CO π* and alkyne π* orbitals, and compares with an even shorter analogous carbon-carbon distance of 2.29(1)Å in $MoBr_2(CO)(PEt_3)_2(PhC{\equiv}CH)$.

As discussed in Chapter 1, a pentagonal bipyramidal structure is predicted for molecules of the type M(unidentate)$_5$(bidentate) which contain chelates with bites less than 1.1. In $Mo(CO)(PMePh_2)_2Br_2(MeC{\equiv}CMe)$ the bite of the 2-butyne unit falls well below this value at 0.72 and as predicted occupies adjacent sites in the girdle. Distortion within the PB is evident from the bond distances around the girdle and from the position of the axial phosphorus atoms, which are at an angle of 165.5° and bent towards the two bromine atoms. However calculation of the dihedral

angles between L_{EQ}-L_{AX}-L_{EQ} planes and the L_{AX}-M-L_{EQ} angles (L_{AX}=axial ligand, L_{EQ}=equatorial ligand) gives average values of 57.24° and 91° respectively, not dissimilar from the values of 54.4° and 90° for the ideal PB geometry.

In their discussion and prediction of electronic site preferences of donor and acceptor ligands in 7-coordinate d^4 species, Hoffmann et al. [81] considered only those combinations of ligands whose π-donating or π-accepting abilities were clearly distinguished, and predicted an order of site preferrence of axial>equitorial for d^4 acceptor ligands in complexes with PB geometry. However for $Mo(CO)(PMePh_2)_2Br_2(MeC{\equiv}CMe)$ the strongest π-acceptor is the carbonyl ligand, which is found in the girdle plane and not in a predicted axial site. Consequently in this molecule the steric effects of the phosphines and the M-alkyne chelate ring size appear to determine both the overall geometry and the specific location of substituent atoms.

3.3.2. REACTIONS WITH SODIUM THIOCYANATE

The thiocyanate ligand is ambidentate and capable of acting as either a monodentate or a bridging bidentate group. As a monodentate species two metal-ligand arrangements are possible, S-thiocyanato (thiocyanate) or N-thiocyanato (isothiocyanate) (Fig. 3.4) and both steric and electronic factors will influence which mode is

Fig. 3.4 Coordination modes of the thiocyanate ligand.

isothiocyanate thiocyanate bridging bidentate

adopted. Borderline cases such as $Mo(CO)_3(NCS)Cp$ [127] are known in which isomerisation between S- and N- bonded forms occurs in solution and assignments can often be made on the basis of changes in the CN and CS stretching frequency regions of their infra-red spectra, of which the latter is of most diagnostic value [128,129]. However the general applicability of this method is limited and diagnostic bands are often obscured by absorptions due to other ligands.

Examination of the solid state IR data for $M(CO)_2(PMePh_2)_2(SCN)_2$ (Table 3.12) shows the presence of two intense carbonyl frequencies, in keeping with a cis-dicarbonyl arrangement, and two ν(CN) stretching frequencies between 2100 and 2060cm^{-1} are observed, together with a weak, broad absorption due to the ν(CS) stretching mode at ca. 815cm^{-1}. A strong band at about 487cm^{-1} can be attributed to the δ(M-NSC) bending frequency. Both of these air-stable complexes were slightly soluble in alcohols, chlorinated and

Table 3.12 The solid state infra-red data for $M(CO)_2(PMePh_2)_2(SCN)_2$.

Assignment	$M(CO)_2(PMePh_2)_2(SCN)_2$		
	M=Mo	Nujol mull	M=W
	cm^{-1}		cm^{-1}
ν(C-N)str	2065vs		2090vs
	2090s		2100s
ν(CO)str	1947s		1947s
	1856s		1856s
ν(C-S)str	815br,w		813br,w
δ(M-NCS)bend	486m		487m

ketonic solvents, but insufficiently so for useful NMR measurements to be carried out.

In previous studies [130] of the phosphine containing thiocyanato-carbonyl complexes $M(CO)_2(PPh_3)_2(SCN)_2$ (M=Mo,W) (prepared by reaction of PPh_3, NH_4SCN and $[M(CO)_4Cl_2]_2$), IR evidence was used to support monodentate coordination of the thiocyanate groups and hence the complexes were described as six coordinate. However this description is not consistent with their yellow colouration, and indicates that coordinative saturation may be achieved by formation of a dimeric or polymeric complex $[M(CO)_2(PR_3)_2(SCN)_2]_n$, in which each metal is bonded to two bridging thiocyanate groups and one N-bonded terminal thiocyanate ligand. A similar polymeric formulation based upon the absence of IR bridging carbonyl bands, has been proposed for $Mo(CO)_4(SCN)_2$ which can be prepared by direct reaction of $Mo(CO)_6$ and thiocyanogen [131]. Thus the complexes reported here may be tentatively formulated as $[M(CO)_2(PMePh_2)_2(SCN)_2]_n$ (M=Mo or W), with n probably greater than one.

3.3.3. REACTION WITH SODIUM DIETHYLDITHIOCARBAMATE

The complexes $M(CO)_2(PR_3)_2X_2(MeCN)$ reacted with NaS_2CNEt_2 in acetone at room temperature to produce $M(CO)_2(PR_3)(S_2CNEt_2)_2$ (M=Mo or W, PR_3=$PMePh_2$ or M=W, PR_3=PMe_2Ph) or $W(CO)(PMe_2Ph)_2(S_2CNEt_2)_2$ as dark red crystalline solids which were sensitive to air in both the solid state and in solution, producing purple oxidation products $M_2O_3(S_2CNEt_2)_4$ [11]. Complexes of the type $M(CO)_2(PR_3)(S_2CNEt_2)_2$ (R=Ph, Bu^n or Et) have been previously prepared by direct reaction of $W(CO)_3(S_2CNEt_2)_2$ with phosphines PR_3 and an X-ray analysis of the PPh_3 derivative revealed an unusual 4:3 geometry with the quadrilateral face comprising one carbonyl, a diethyldithiocarbamate group and the phosphine [65]. Carmona et al. prepared complexes of general formula $M(CO)_{3-n}(PMe_3)_n(S_2CNR'_2)_2$ (n=1 or 2, R'=alkyl) by reaction of $M(CO)_2(PMe_3)_2X_2$ and NaS_2CNR_2 and showed that conversion between these mono and dicarbonyl complexes could be achieved by reaction with excess phosphine or CO respectively [132]. The reaction conditions suggested that substitution of the second carbonyl is more difficult than displacement of PR_3 by CO and for R=Ph, Bu^n or Et only the dicarbonyl species have been isolated.

Table 3.13 shows that for the reactions described above a direct correlation can be observed between the phosphine cone angle and the nature of the product. A comparison of the OC-M-CO angles calculated from ν(CO) intensity measurements for the $PMePh_2$, PMe_2Ph and PMe_3 dicarbonyl complexes with a value of 71.6° found by X-ray analysis for the analogous PPh_3 derivative, suggests that a similar 4:3 geometry cannot be assumed. Thus for larger phosphines PPh_3 (θ=145°) and $PMePh_2$ (θ=136°) the steric strain of two of these phosphine groups cannot be accommodated in addition to two bidentate S_2CNEt_2 groups and hence a dicarbonyl product only is formed. In

Table 3.13 Correlation between OC-M-CO angle[A], phosphine cone angle θ and product type in $M(CO)_{3-n}(PR_3)_n(S_2CNEt_2)_2$ (n=1 or 2).

PR_3	θ(°)	OC-M-CO[A](°)		Product[D]
		Mo	W	
PPh_3	145	-	71.6°[B]	A
$PMePh_2$	136	88°	87°	A
PMe_2Ph	122	-	89°	A,B
PMe_3	118	85°[C]	85°[C]	A,B

[A]-Calculated cis-$M(CO)_2$ angle in $M(CO)_2(PR_3)(S_2CNEt_2)_2$, [B]-ref. 65, [C]-ref. 132, [D]-A=$M(CO)_2(PR_3)(S_2CNEt_2)_2$, B=$M(CO)(PR_3)_2(S_2CNEt_2)_2$.

contrast the smaller PMe_2Ph (θ=122°) and PMe_3 (θ=118°) species can displace a CO group from the dicarbonyl mono-phosphine complex to form a monocarbonyl bis-phosphine complex.

Selected infra-red data for the $PMePh_2$ and PMe_2Ph complexes are given in Table 3.14. All the complexes exhibited a

Table 3.14 Infra-red data for $M(CO)_2(PR_3)(S_2CNEt_2)_2$ and $M(CO)(PR_3)_2(S_2CNEt_2)_2$.

M	PR_3	ν(CO)[A]	ν(CO)[B]	ν(CN)[A]	$\nu(NC_2)$[A]	ν(C=S)[A]
Complex $M(CO)_2(PR_3)(S_2CNEt_2)_2$						
Mo	$PMePh_2$	1915s,1830s	1929s,1843s	1486m	1143m	1070w
W	$PMePh_2$	1912s,1815s	1917s,1813s	1491m	1143m	1068w
W	PMe_2Ph	1917s,1822s	1916s,1820s	1496m	1145m	1071w
Complex $M(CO)(PR_3)_2(S_2CNEt_2)_2$						
W	PMe_2Ph	1749msh,1739s	1735m,br	1485m	1145m	1076w

[A]-As Nujol mulls, units of cm^{-1}, [B]-In CH_2Cl_2, units of cm^{-1}.

band of medium intensity at ca. 1490cm^{-1} which can be attributed to the ν(C-N) stretching frequency. The dicarbonyl products $M(CO)_2(PR_3)(S_2CNEt_2)_2$ were identified by the two intense ν(CO) stretching frequencies found between 1917-1815cm^{-1}. For the monocarbonyl $W(CO)(PMePh_2)_2(S_2CNEt_2)_2$, two overlapping intense bands between ca. 1739 and 1749cm^{-1} were observed which resolved into a broad singlet in CH_2Cl_2 at 1735cm^{-1}. The latter results may initially appear to indicate the presence of isomeric products, however variable temperature ^{1}H and ^{31}P NMR studies of the related complexes $M(CO)(PMe_3)_2(S_2CNEt_2)_2$ [132], has shown that only one isomer is present in solution at room temperature. The dynamic ^{13}C and ^{31}P NMR solution spectra of $M(CO)_2(PPh_3)(S_2CNEt_2)_2$ [65] has been attributed to movement of the phosphine between the two faces of a 4:3 structure of a single isomer as shown in a and b in Fig. 3.5.

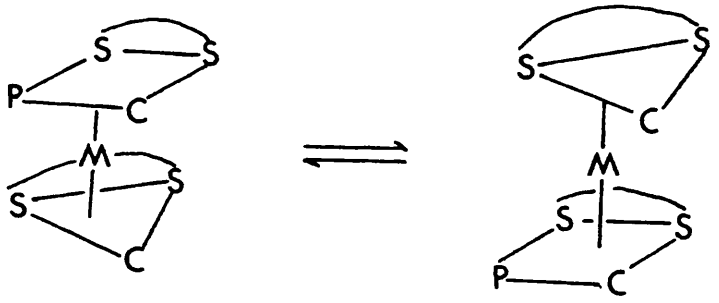

a b

Fig. 3.5 Possible dynamic behaviour of $M(CO)_2(PPh_3)(S_2CNEt_2)_2$.

Cotton-Kraihanzel force constants [100] calculated from the IR spectra are given in Table 3.15 and show that the extent of π-electron density provided to the CO ligands by the d^4 metal ions is nearly independent of the type of phosphine involved.

Table 3.15 Force constants for $M(CO)_2(PR_3)(S_2CNEt_2)_2$

M	PR_3	k_{CO}	k_i	θ	Ref.
W	PPh_3	14.20	0.69	145	65
Mo	$PMePh_2$	14.18	0.64	136	this work
W	$PMePh_2$	14.16	0.62	136	this work
W	PBu^n_3	14.13	0.68	132	65
W	PEt_3	14.23	0.70	132	65
W	PMe_2Ph	14.14	0.71	122	this work

3.3.4. REACTIONS WITH SODIUM OXALATE

Reactions of $M(CO)_2(PR_3)_2Br_2(MeCN)$ (M=Mo, PR_3=$PEtPh_2$, PEt_2Ph or $PMePh_2$, M=W, PR_3=$PMePh_2$ or PMe_2Ph) with excess sodium oxalate in acetone at ambient temperature yielded yellow or orange air-stable complexes. Chemical tests with silver nitrate confirmed that bromide was still present in all of the complexes, and their yellow or orange colouration indicated that the metal centres were probably 7-coordinate. In general the complexes were too insoluble in chlorinated solvents or acetone to be recrystallised, however the tungsten dimethylphenylphosphine complex only could be recrystallised from a saturated CH_2Cl_2 solution to yield a mixture of a major orange product and a minor yellow product. The analytical data for all the complexes given in Table 3.4 are in reasonable agreement with the general formula $(MBr(CO)_2(PR_3)_2)_2-(\mu-C_2O_4)$.

In theory the oxalate ligand may coordinate to one metal centre as a bidentate ligand (I,Fig.3.6) or may bridge several metal centres (II to V,Fig.3.6).

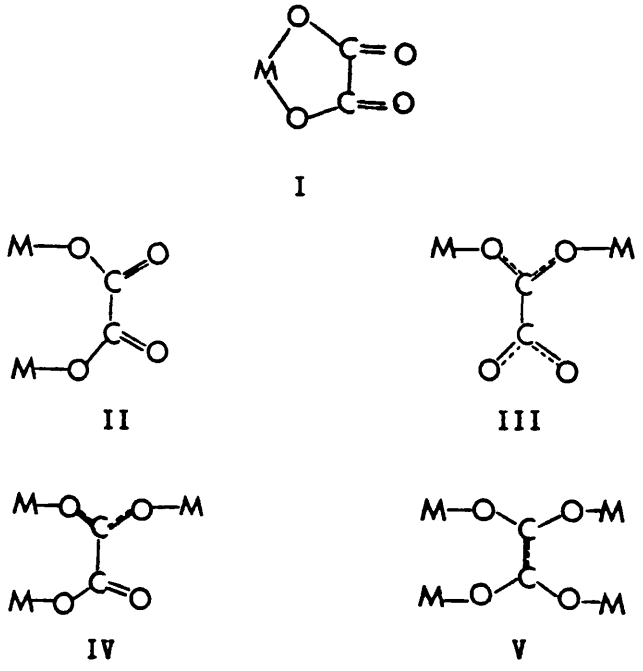

Fig.3.6 Bonding modes of the oxalate ligand.

In the absence of direct structural evidence from X-ray diffraction studies, infra-red data can be used as a less reliable tool to identify the coordination mode of oxalate ligands in complexes such as $Fe_2(acac)_4(\mu\text{-}C_2O_4)$ [133] and $[Ph_4B][Cu_2(1,1,4,7,7\text{-}Et_5\text{-dien})_2(\mu\text{-}C_2O_4)]$ [134].

For the oxalate ligand the presence of both a ν_{As}(CO) (oxalate) stretching vibration in the region 1640 to 1680cm^{-1} and a δ(O-C-O) bending vibration ca. 800cm^{-1} is taken as indicative of a bridging mode. Normal coordinate analyses of the metal-chelate rings in model bidentate oxalate complexes were carried out by Fujita et al. [135,136] and tentative assignments of the observed IR absorptions for the oxalato complexes reported here, based upon these predictions, are given in Table 3.16. (The data given for the tungsten dimethylphenylphosphine complex are for the major product only, the minor product exhibiting IR absorptions for ν_s(CO) and ν_{As}(CO) (carbonyl) at 1931 and 1832cm^{-1} respectively and for ν_{As}(CO) (oxalate) at 1632cm^{-1}.) Two absorptions observed in the range 1825-1950cm^{-1} can be attributed to ν_s(CO) and ν_{As}(CO) carbonyl stretching modes and bridging oxalate groups are indicated by the presence of both ν_{As}(CO) (oxalate) absorptions at ca. 1630-1640cm^{-1} and weak δ(O-C-O) bending vibrations at ca. 790cm^{-1}. Thus their spectroscopic and chemical properties and orange colouration, support a general molecular formula involving the presence of a bridging oxalate ligand in a bromine-containing seven coordinate metal species.

All of the oxalate complexes were of low solubility in common solvents and their solution NMR spectra could not therefore be measured, however two types of crystal of the tungsten dimethylphenylphosphine complex suitable for an X-ray diffraction analysis were isolated from a saturated solution of the complex in dichloromethane. The two crystalline products were examined by X-ray

Table 3.16 Selected infra-red data^ for the oxalate complexes.

M=Mo	M=Mo	M=Mo	M=W	W	Band
PR_3=$PEtPh_2$	PR_3=PEt_2Ph	PR_3=$PMePh_2$	PR_3=$PMePh_2$	PR_3=PMe_2Ph	assignment
1941m	1923m	1946m	1931m	1920m	ν_s(CO) carbonyl
1858s	1841s	1856s	1840s	1825s	ν_{as}(CO) carbonyl
1637s	1628s	1631s	1640s	1640s	ν_{as}(C-O) oxalate
1299	1290	1284	1284	1285	ν_s(C-O)+δ(O-C=O)
-	-	966	920vw	948vw	ν_s(C-O)+δ(O-C=O)
790	787	784	788	795	δ(O-C=O)+ν(M-O)
565	591	570	567	581	ν(M-O)+ν(C-C)
490	496	490	460	490	ring def.+δ(O-C=O)

^-As Nujol mulls, all bands weak unless stated otherwise.

-not observed

crystal structure determinations to identify the molecular formulae of these new complexes, to determine the coordination mode of the oxalato group, and to examine the stereochemical differences in the two crystalline forms.

The crystal structure determinations were completed whilst this thesis was being written, and hence full details will appear elsewhere. The solid state structures of the major isomer (I) and the minor isomer (II) are shown in Fig. 3.7 together with the atomic numbering scheme used (the hydrogen atoms were not located). The two crystalline forms proved to be isomers with the molecular formula $\{WBr(CO)_2(PMe_2Ph)_2\}_2-(\mu-C_2O_4)$. In each isomer the tungsten atoms are seven coordinate with the oxalate anion bridging the two tungsten atoms to form two five-membered chelate rings. Each metal centre contains trans-phosphine groups with the cis-dicarbonyl unit adjacent to one bromine atom, and these ligands together with the two oxygen atoms of the oxalate group complete the coordination sphere.

The bond lengths and angles associated with the phosphine and carbonyl groups are unexceptional. In both isomers the bromine-metal-oxygen angles and metal-oxygen distances are very similar, however a comparison of the angles between these atoms and the atoms of the carbonyl and phosphine groups for the two isomers shows several differences. Thus for example the angles Br(1)-W-P(1) and Br(1)-W-P(2) in isomers (I) and (II) are respectively 129.3° and 87.2° for (I) and 78.4° and 156.1° for (II), whilst angles Br(1)-W-C(17) and Br(1)-W-C(18) are 157.5° and 86.7° for (I) and 104.1° and 128.1° for (II).

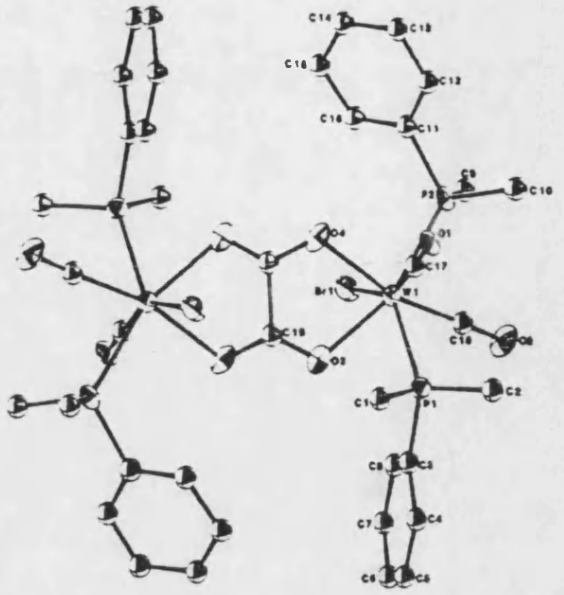

Isomer (I)

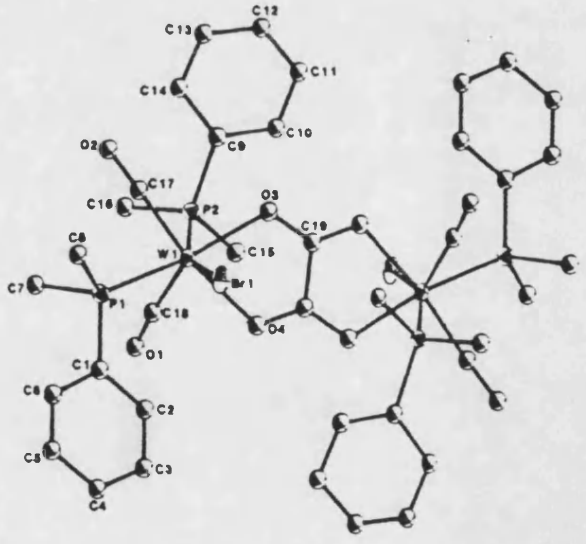

Isomer (II)

Fig. 3.7 The atomic numbering scheme used and the structures of isomers (I) and (II) of $\{WBr(CO)_2(PMe_2Ph)_2\}_2$-($\mu$-$C_2O_4$).

The centres of the bridging oxalate groups in both isomers are centres of inversion. This type of structure is not very common, but has been found for complexes $[Me_2Ga]_2(\mu\text{-}C_2O_4)$ [137] and $[Bu_4N][WO(O_2)_2(\mu\text{-}C_2O_4)WO(O_2)_2]$ [138]. The latter is the only previously known tungsten oxalate complex of this type, and to date no isomeric forms of such systems have been reported.

3.3.5 REACTIONS WITH SODIUM TRIFLUOROACETATE

The trifluoroacetate ligand is capable of adopting three basic modes of coordination as shown in Fig.3.10. Structurally characterised examples of each type are known and have been reviewed [139,140]. In the absence of direct structural evidence however, the

Fig. 3.10 Bonding modes of the trifluoroacetate ligand.

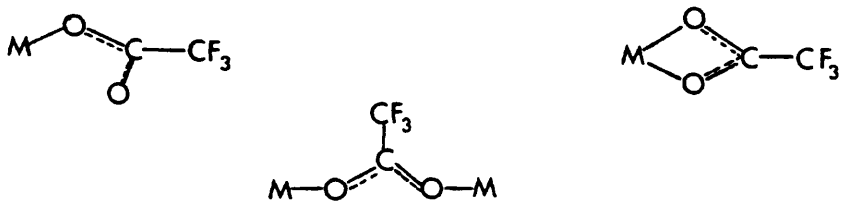

mode of bonding in transition metal-trifluoroacetate complexes is normally inferred from infra-red data. Although bridging and chelating bidentate forms are not easily distinguished by this method, monodentate versus bidentate coordination can usually be predicted with reasonable confidence. Deacon and Phillips [139] argued that upon monodentate coordination, the carboxylate group assumes a pseudo-ester configuration, M-O-CO-R and changes in the CO bond orders results in an increased separation (Δ) between the $\nu_{as}(CO_2)$ and $\nu_s(CO_2)$ modes relative to the value for the free carboxylate ion. In general trifluoroacetate complexes with Δ greater than the free ion value (NaO_2CCF_3 Δ=223cm^{-1}) are expected to contain monodentate O_2CCF_3 ligands, whilst significantly lower Δ values are indicative of chelating or bridging groups (3.1).

$$\nu_{as}(CO_2) - \nu_s(CO_2) = \Delta \qquad (3.1)$$

$$\Delta(\text{mono}) > \Delta(\text{ionic}) > \Delta(\text{bridging}) \text{ or } \Delta(\text{chelate})$$

Reactions of sodium trifluoroacetate with $M(CO)_2(PR_3)_2Br_2(MeCN)$ or $M(CO)_3(PR_3)_2Br_2$ in 2:1 molar ratios yielded the air-stable crystalline products $M(CO)_2(PR_3)_2(O_2CCF_3)_2$, whilst analogous reactions involving $Mo(CO)_2(PMePh_2)_2Br_2(MeCN)$ or $W(CO)_2(PPh_3)_2Br_2$ with sodium trifluoroacetate in 1:1 molar ratios yielded complexes of general formula $MBr(CO)_2(PR_3)_2(O_2CCF_3)$. Selected infra-red data for these complexes are given in Table 3.18. All the complexes contained frequencies in the range 1965-1837cm^{-1}, typical of cis-dicarbonyl groups. The trifluoroacetate ligands in $M(CO)_2(PR_3)_2(O_2CCF_3)_2$ gave rise to two asymmetric $\nu_{AS}(CO_2)$ stretching fequencies at ca. 1714 and 1600cm^{-1} with a single symmetric $\nu_S(CO_2)$

Table 3.18 Selected infra-red data[a] for $M(CO)_2(PR_3)_2(O_2CCF_3)_2$ and $MBr(CO)_2(PR_3)_2(O_2CCF_3)$.

M	PR_3	ν(CO)	$\nu_{AS}(CO_2)$	$\nu_S(CO_2)$	Δ	$\nu(CF_3)$	
Complex $M(CO)_2(PR_3)_2(O_2CCF_3)_2$							
Mo	PPh_3	1962m	1691m	1410wsh	281	1201vs	1158m
		1880vs	1605m		195	1134m	
Mo	$PMePh_2$	1955m	1693m	1410wsh	283	1201vs	1160m
		1860vs	1611m		201	1137m	
Mo	PMe_2Ph	1961m	1714m	1412wsh	302	1202vs	1164m
		1837vs	1610m		198	1136m	
W	PPh_3	1940m	1695m	1405w	290	1190vs	1158m
		1846vs	1596m		191		
W	$PMePh_2$	1935m	1700m	1412w	288	1190vs	1170s
		1842vs	1602m		190	1134s	
W	PMe_2Ph	1940m	1712m	1414wsh	298	1191vs	1173s
		1847vs	1608m		194	1137s	

Table 3.18 continued

M	PR_3	ν(CO)	$\nu_{as}(CO_2)$	$\nu_s(CO_2)$	Δ	$\nu(CF_3)$	
Complex $MBr(CO)_2(PR_3)_2(O_2CCF_3)$							
Mo	$PMePh_2$	1954s	1608m	1413w	199	1201s	1164m
		1866vs				1154m	
W	PPh_3	1942s	1603m	1419w	183	1168s	1155m
		1857vs					

^-Measured as Nujol mulls in units of cm^{-1}

frequency at ca. 1410cm^{-1}. Thus two possible values of Δ of ca. 290 and 190cm^{-1} are obtained, which suggest that one trifluoroacetate ligand acts as a bidentate and the other as a monodentate ligand resulting in seven coordination of the metal. In contrast for $MBr(CO)_2(PR_3)_2(O_2CCF_3)$ only one absorbance for $\nu_{as}(CO_2)$ was observed at ca. 1600cm^{-1} and a value of Δ<223 indicated bidentate coordination of the trifluoroacetate ligand.

In keeping with these results similar reactions of $Mo(CO)_2(PPh_3)_2Br_2$ with carboxylate and thiocarboxylate ligands L (L=O_2CR' or SOCR',R'=Me or Ph) in 2:1 and 1:1 ratios have subsequently been shown [141] to yield complexes $Mo(CO)_2(PPh_3)_2L_2$ and $MoBr(CO)_2(PPh_3)_2L$ respectively, whose IR spectra support the presence of both mono- and bidentate forms of L in the former complexes and bidentate bonding only of L in the latter. To date complexes of general formula $MBr(CO)_2(PR_3)_2(O_2CCF_3)$ have not been examined by X-ray diffraction analysis, and the arrangement of the two phosphines, bidentate trifluoroacetate group and halogen atom have yet to be identified.

Shortly after the complexes $M(CO)_2(PR_3)_2(O_2CCF_3)_2$ and $MBr(CO)_2(PR_3)_2(O_2CCF_3)_2$ reported above had been synthesised and identified as 7-coordinate, Arabi and coworkers published a new route to the related complexes $Mo(CO)_2(PEt_3)_2(O_2CCF_3)_2$ and $Mo(CO)_2(PMe_3)_3(O_2CCF_3)_2$. This involved the reaction shown in 3.2 below, in which reaction of trifluoroacetic acid and fac-$Mo(CO)_3(PR_3)_3$ (PR_3=PMe_3 or PEt_3) formed a protonated product $[HMo(CO)_3(PR_3)_3]^+(O_2CCF_3)^-$, which reacted with a further molecule of CF_3CO_2H to produce either $Mo(CO)_2(PMe_3)_3(O_2CCF_3)_2$ [60] or $Mo(CO)_2(PEt_3)_2(O_2CCF_3)_2$ [142]. Both neutral complexes have been

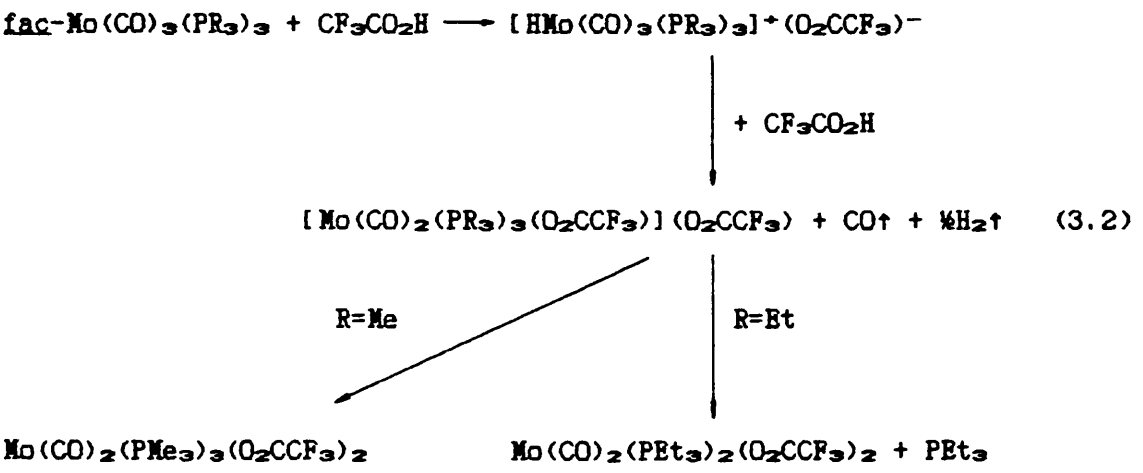

(3.2)

structurally characterised by X-ray analysis and shown to be 7-coordinate, with the bonding mode of the two O_2CCF_3 ligands being dependent upon the number of coordinated phosphine ligands as shown in Fig. 3.9. Thus two larger phosphine groups in $Mo(CO)_2(PEt_3)_2(O_2CCF_3)_2$ (cone angle,θ=132°) result in the presence of both mono- and bidentate $CF_3CO_2^-$ groups, whilst the three smaller phosphines present in $Mo(CO)_2(PMe_3)_3(O_2CCF_3)_2$ (θ=118°) lead to two monodentate trifluoroacetate groups.

Fig. 3.11 P-Mo-P angles in the complexes $Mo(CO)_2(PEt_3)_2(O_2CCF_3)_2$ and $Mo(CO)_2(PMe_3)_3(O_2CCF_3)_2$.

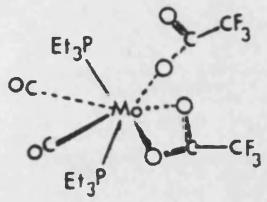

P-Mo-P=131.4°

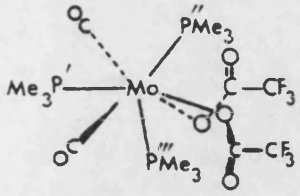

P'-Mo-P"=119.4°, P"-Mo-P"'=107.1°, P"'-Mo-P'=108.5°

Thus reactions of sodium trifluoroacetate with $M(CO)_2(PR_3)_3X_2$ (X=halide) in 1:1 molar ratios should prove interesting, and should yield complexes of the type $M(CO)_2(PR_3)_3(O_2CCF_3)X$ containing monodentate trifluoroacetate groups.

3.4 SUMMARY

A reaction scheme summarising the results of reacting $M(CO)_2(PR_3)_2X_2(MeCN)$ with various neutral and ionic species is given in Fig. 3.10. The reactivity pattern of these complexes shows close parallels to reactions of $M(CO)_2(PR_3)_2X_2$ (PR_3=PPh_3 or PEt_3), and thus the acetonitrile complexes provide an easy access to analogous reactions involving phosphine and halocarbonyl derivatives which do not form isolable monomeric $M(CO)_2(PR_3)_2X_2$ complexes.

Fig. 3.10 Reaction scheme for $M(CO)_2(PR_3)_2X_2(MeCN)$.

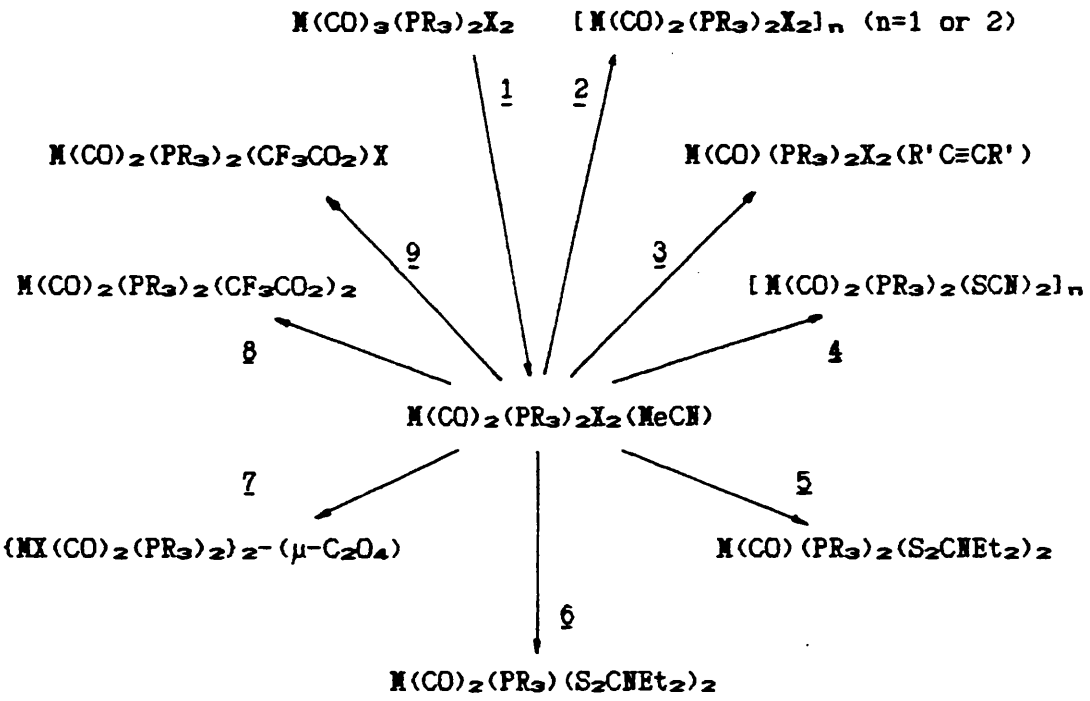

1 N_2 in MeCN at r.t. (Mo) or 82°C (W), 2 N_2 in CH_2Cl_2 at r.t. (Mo) or $CHCl_3$ at 61°C (W), 3 with R'C≡CR' in CH_2Cl_2 at r.t. (M=Mo) or 40°C (M=W), 4 with NaSCN in acetone at r.t., 5 and 6 with NaS_2CNEt_2 in CH_2Cl_2 at r.t., 7 with $Na_2C_2O_4$ in acetone at r.t., 8 and 9 with NaO_2CCF_3 in acetone at r.t.

Investigations into the reactivity of $M(CO)_2(PR_3)_2I_2(MeCN)$ complexes completes the first half of this thesis. The next section concerns complexes of general formulae $M(CO)_2(\eta^3\text{-allyl})L_2X$ and $[M(CO)_2(\eta^3\text{-allyl})L_3]X$ containing bi- (L_2) and tridentate (L_3) nitrogen donor ligands, and examines the nature and reactivity of complexes of general formula $MCl(CO)_2(\eta^3\text{-allyl})(MeCN)_2$ in hydroxylic solvents and describes the synthesis and reactions of the closely related species $MCl(CO)_2(\eta^3\text{-butadienyl})L_2$ containing the unusual (η^3-CH_2=C(COXR)=C=CH_2) ligand (X=O,N,S). This section commences with a review of the methods of preparation, bonding, spectroscopic properties and reactions of η^3-allyl transition metal complexes.

CHAPTER 4

AN INTRODUCTION TO η^3-ALLYL TRANSITION METAL COMPLEXES

4.1 INTRODUCTION

The current interest in transition metal allyl complexes can undoubtedly be traced to their unusual structural and chemical properties. In addition to theoretical bonding studies [143-145] and the interpretation of often complicated spectra [146] generated by isomerism and dynamic behaviour, recent research has revealed the importance of these complexes as catalysts for stereospecific polymerisations and oligomerisations of alkenes, alkynes and dienes [147-152], and their involvement in isomerisation, oxidation, hydrogenation and carbonylation reactions of various unsaturated organic compounds [153-158]. Of particular importance in this context is the ability of the allyl ligand to bond to metal centres in several possible ways, and to easily change between two or more of the modes described below.

4.2 CLASSIFICATION OF ALLYL SYSTEMS

4.2.1 η^1-ALLYLS Formation of a conventional single σ-bond between a metal and the terminal sp^3 hybridised carbon atom of an isolated allyl group leads to the formation of an η^1-allyl complex. As the M-C link is a normal covalent bond there is free rotation about this axis. The low stability of η^1-allyl metal complexes compared to their η^3-allyl analogues has resulted in only a limited number of examples which have been fully characterised by crystallographic studies. The example shown in Fig. 4.1 confirms that major features of the uncoordinated allyl group do not significantly alter upon bonding to the metal centre [159].

Fig. 4.1 Crystal structure of $Nb(\eta^1\text{-}C_3H_5)(Cp)_2(CS_2)$.

Bond length	Bond angle
C(2)-C(3) =1.52Å	C(2)-C(3)-C(4) =121.9°
C(3)-C(4) =1.14Å	

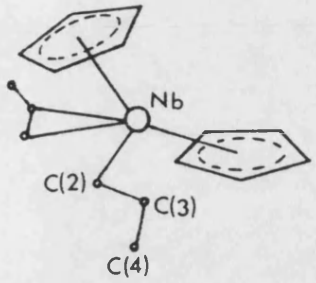

4.2.2 BRIDGING (μ)-ALLYLS An allyl group may also adopt a bridging mode between two metal centres. The bonding in complexes such as $[Pt(\mu\text{-}C_3H_5)Cl]_4$ [160] may be described as a combination of π-bonding via the carbon-carbon double bond to one metal and a σ-bond from the terminal C to the other metal, however in other complexes such as $[Ru_3(\mu\text{-}\eta^3\text{-}C_3H_5)(\mu\text{-}Ph_2PCH_2PPh_2)(CO)_8]$ [161] the approximately equal C-C bond lengths of the allyl ligand (1.39 and 1.42Å) indicate symmetrical bonding of the ligand. In the binuclear molybdenum complexes $[Mo_2(\mu\text{-}(\sigma,\eta^3,\eta^3,\sigma\text{-}C_6Me_6))(\eta^5\text{-}C_9H_7)_2]$ [162] and $[Mo_2(\mu\text{-}\sigma,\eta^3\text{-}CHCHMe_2)(CO)_4(\eta^5\text{-}C_5H_5)_2]$ [184] shown in Fig. 4.2, one terminal carbon atom of the bridging ligand is σ-bonded to one metal and three carbon atoms are η^3-bonded to the other metal atom.

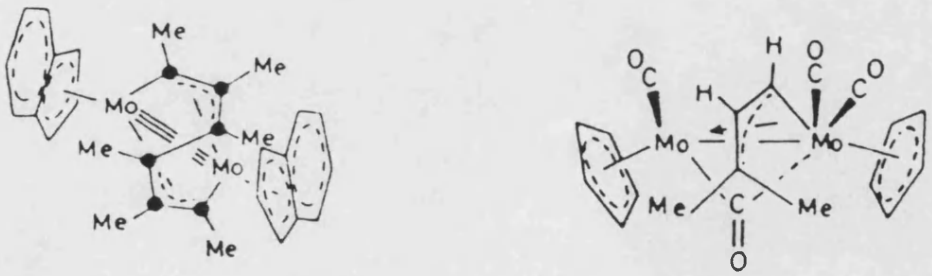

Fig. 4.2 Examples of complexes with bridging allyl groups.

4.2.3 η^3-ALLYLS Numerous examples of η^3-allyl transition metal complexes are now known, many of which are formed via η^1-allyl intermediates. The electronic demands of a low valent metal centre in attempting to achieve an 18-electron configuration will strongly

influence which mode of bonding (η^1 or η^3) will finally be adopted. In η^3-allyl complexes interaction between the metal and all three carbon atoms of the allyl results in delocalised, multicentric bonding. X-ray diffraction and NMR spectroscopy have identified many different types of η^3-allyl-metal species and shown that both substituents on the allyl unit and the steric and electronic properties of other ligands in the metal coordination sphere strongly influence the molecular structure and conformation of the coordinated allyl moiety. The commonest types of η^3-allyl-metal complexes which are relevant to the work in this thesis are acyclic unsubstituted or substituted η^3-allyl complexes or those in which the η^3-allyl either forms part of a larger hydrocarbon system or is part of a carbo-cyclic three to eight-membered ring as shown by the examples shown below.

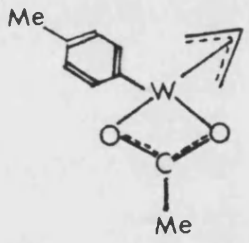

[ref. 164]

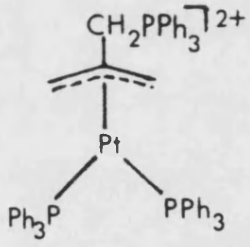

[ref. 165]

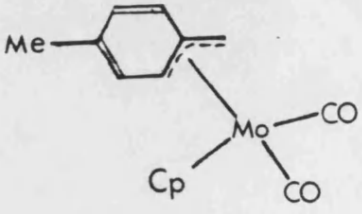

[ref. 166]

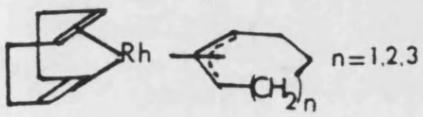

[ref. 167]

4.3 SYNTHETIC METHODS FOR η^3-ALLYL COMPLEXES

The last twenty years have seen a large growth in the range of known η^3-allyl transition metal complexes and these have been prepared by a wide variety of routes. The most frequently used methods of synthesis involve either the direct reaction of an allyl-containing moiety with a metal complex, or conversion (frequently via nucleophilic attack) of an organic ligand already attached to the metal. These methods, together with some less common routes leading to specific complexes, are illustrated below.

4.3.1 ALLYL GRIGNARD REAGENTS AND RELATED COMPOUNDS

Allyl Grignard reagents react with many anhydrous metal halides to produce η^1-intermediates which may rapidly convert to an η^3-allyl complex, e.g. [168-170].

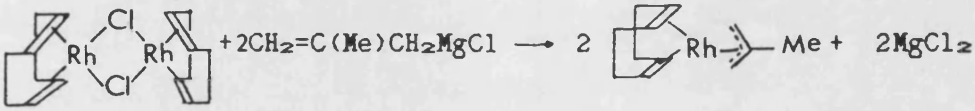

$$\tfrac{1}{2}[Mo(\eta^3\text{-}C_3H_5)(\eta^6\text{-}C_6H_6)Cl]_2 + C_3H_5MgCl \longrightarrow MgCl_2 + Mo(\eta^3\text{-}C_3H_5)_2(\eta^6\text{-}C_6H_6)$$

$$TiClCp_2 + CH_2{=}CH(CH_2)_2MgCl \xrightarrow[-MgCl_2]{} Ti(CH_2)_2CH{=}CH_2Cp_2 \longrightarrow Ti(\eta^3\text{-}1\text{-}C_3H_4Me)Cp_2$$

Homoleptic allyl complexes such as $Ni(\eta^3\text{-}C_3H_5)_2$ [171] are frequently prepared by this method. Although the analogous allyl-lithium reagents are less commonly employed, they, and other main group metal allyl species have been shown to be equally effective in many such reactions [172-174].

4.3.2 OXIDATIVE ADDITION OF ALLYL HALIDES TO TRANSITION METAL COMPOUNDS

Reaction of allyl halides with low valent transition metal complexes may result in displacement of a coordinated ligand and formation of an η^3-allyl complex, in which the metal oxidation state has increased by two units. This reaction is often accompanied by an increase in the metal coordination number, since the η^3-allyl group formally occupies two coordination sites. Of all the synthetic routes to η^3-allyl transition metal complexes, this route has probably been the most commonly used and was employed in the preparation of some of the earliest η^3-allyl complexes, starting from carbonyl derivatives. A few examples from the extensive number of published reactions are illustrated below [175-180].

$$W(CO)_4(bipy) + C_3H_5X \longrightarrow W(CO)_2(\eta^3\text{-}C_3H_5)bipyX + 2CO, \quad X=\text{halide}$$

$$Fe_2(CO)_9 + 2C_3H_5I \longrightarrow 2Fe(CO)_3(\eta^3\text{-}C_3H_5)I + 3CO$$

$$2Ni(CO)_4 + 2C_3H_5X \longrightarrow [Ni(\eta^3\text{-}C_3H_5)(\mu\text{-}X)]_2 + 8CO, \quad X=\text{halide}$$

$$[Ir(CO)(\eta^2\text{-}C_2H_4)_2(PMe_2Ph)_2]BPh_4 + CH_2=C(Me)CH_2Cl \longrightarrow 2C_2H_4 + [IrCl(CO)(\eta^3\text{-}2\text{-}C_3H_4Me)(PMe_2Ph)_2]BPh_4$$

$$Mo(CO)_3(MeCN)_3 + CH_2=CHCH_2Cl \longrightarrow MoCl(CO)_2(\eta^3\text{-}C_3H_5)(MeCN)_2 + MeCN$$

Sodium cleavage of dimeric metal carbonyls or displacement of CO by quaternary ammonium halides yields metal carbonyl anionic complexes which are more nucleophilic than their neutral analogues and attack allyl halides to yield η^3-allyl derivatives which may not be readily available by other routes, e.g.[181-183]

$[Mo(CO)_3Cp]^- + \text{crotyl bromide} \longrightarrow Mo(CO)_2(\eta^3\text{-crotyl})Cp + CO + Br^-$

$[Co(CO)_4]^- + C_3F_5I \longrightarrow Co(CO)_3(\eta^3\text{-}C_3F_5) + I^- + CO$

$[CrCl(CO)_3(bipy)]^- + C_4H_7Cl \longrightarrow CrCl(CO)_2(bipy)(\eta^3\text{-}C_4H_7) + CO$

Various mechanisms are known for the oxidative-addition of organic halides to low oxidation state transition metals and these have been the subject of several reviews and discussions in the literature [184,185]. These mechanisms include nucleophilic attack of the metal at a carbon atom bearing a halogen [186], a concerted insertion reaction of the metal into the C-halogen bond [187] and a radical chain process [188]. In some reactions involving allyl halides, such as that of $Mo(CO)_4(phen)$ with a Lewis base L (L=phosphine or phosphite) [189], the initial breaking of a metal-carbonyl bond, induced by the Lewis base, is thought to precede coordination of the carbon-carbon olefinic bond of the allyl bromide to the metal and to be the rate determining step [190]. Subsequent oxidative-addition and expulsion of a carbonyl generates the product $MoBr(CO)_2(\eta^3\text{-allyl})phen$.

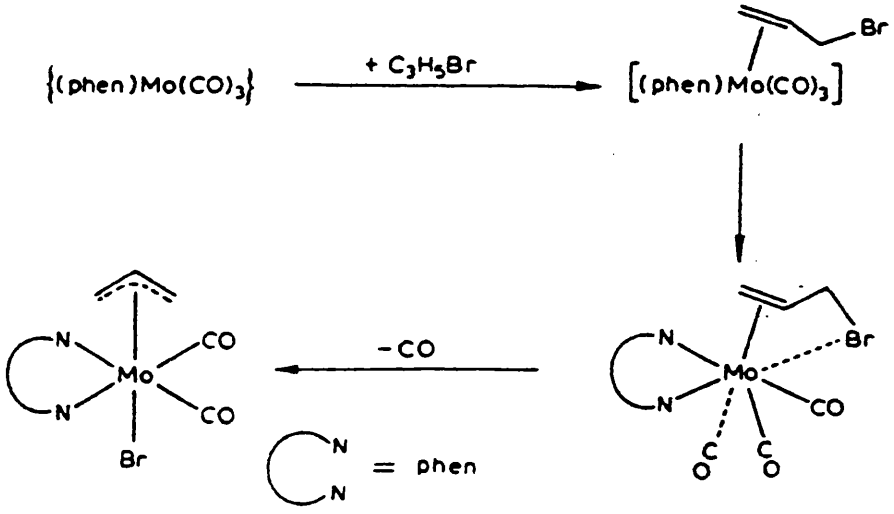

Direct reactions between transition metals and allyl halides under normal conditions are often thermodynamically

unfavourable and thermal kinetic barriers to interaction necessitate temperatures at which the required products would decompose. However hot atom synthesis can be used in some instances and several halogen-bridged η^3-allyl complexes have been prepared by this route, e.g. [191,192]

$$4Pt(atoms) + 4allylCl \longrightarrow [Pt(\eta^3\text{-allyl})Cl]_4$$

$$Pd(gas) + PhCH_2Cl \longrightarrow [Pd(\eta^3\text{-}CH_2Ph)Cl]_2$$

Transfer of allyl groups from one transition metal to another is known for a limited number of examples, mainly between metal carbonyls and palladium complexes, e.g. [193].

$$Fe_2(CO)_9 + [Pd(\eta^3\text{-}C_3H_5)halide]_2 \longrightarrow Fe + Fe(CO)_5 + Pd + Fe(CO)_3(\eta^3\text{-}C_3H_5)halide$$

4.3.3 REACTIONS INVOLVING ATTACK ON DIENES OR ALKYNES

(i) Coordinated to transition metals.

A range of novel substituted η^3-allyl complexes have been produced by reactions of alcohols or thiols (RXH=ROH or RSH) with η^1-propargylic transition metal complexes, e.g. [194-197].

$$[M]L(CO)(\eta^1\text{-}CH_2C{\equiv}CR') + RXH \longrightarrow [M]L(\eta^3\text{-}1\text{-}R'CH{=}C(COXR){=}CH_2)$$

[M]=M(CO)Cp, M=Mo or W, L=CO, PPh_3, $P(OPh_3)$, R,R'=alkyl or aryl

Coordinated conjugated 1,3-diene groups may be protonated by a variety of acids to form η^3-allyl derivatives in which the anion associated with the protonating agent may become coordinated to the metal, e.g. [198,199].

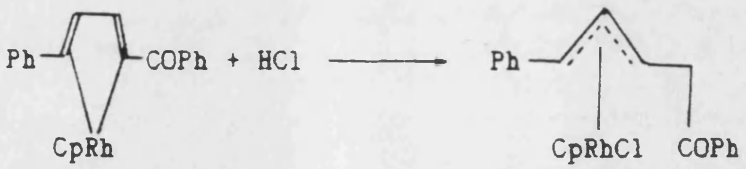

These reactions are may be stereospecific, resulting in only one geometrical isomer. Deuterium exchange studies on the reaction of trifluoroacetic acid with (η^4-cyclohexadiene)cyclopentadienylrhodium [200] suggested that protonation occurs initially at the metal to produce a transient metal hydride cation. Transfer of the proton to one end of the 1,3-diene produces an anti-methyl substituent on the η^3-allyl group and exchange then occurs between this proton and the terminal CH_2 group, as shown for the analogous iridium complex below.

$Rh(\eta^4\text{-}C_4H_6)Cp + CF_3CO_2H \qquad [Rh(\eta^3\text{-anti-1-}C_3H_4Me)Cp][O_2CCF_3]$

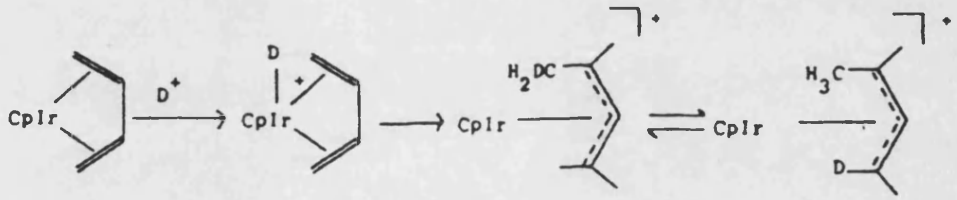

Attack by nucleophiles such as H^-, OR^- or OAc^- on a coordinated diene may also produce an η^3-allyl species as illustrated below by the reaction of a tetraphenylcyclobutadiene Pd complex with basic alcohol ROH to yield an exo-substituted η^3-cyclobutenyl derivative, and the addition of H^- to coordinated 1,3-dienes to yield crotyl-containing products, e.g.[201-203]

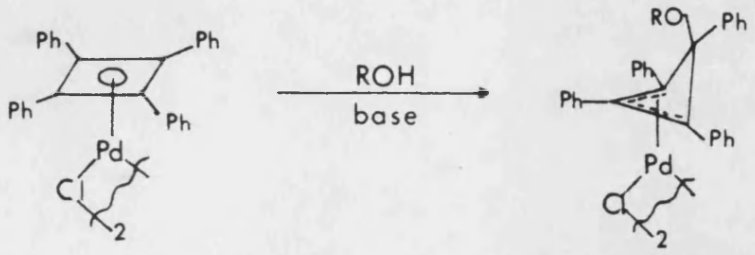

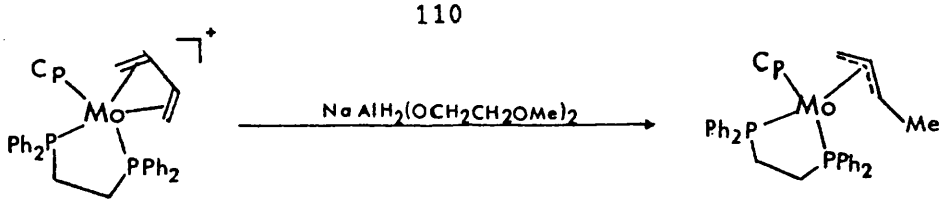

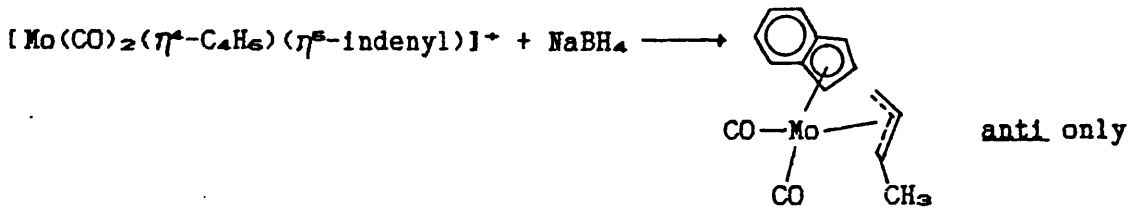

(ii) on dienes or alkynes

Many substituted η^3-allyl complexes have been prepared by insertion of a 1,3-diene into transition-metal hydride or -alkyl complexes or by attack of a metal anion upon either an uncoordinated diene or alkyne, e.g. [204-207].

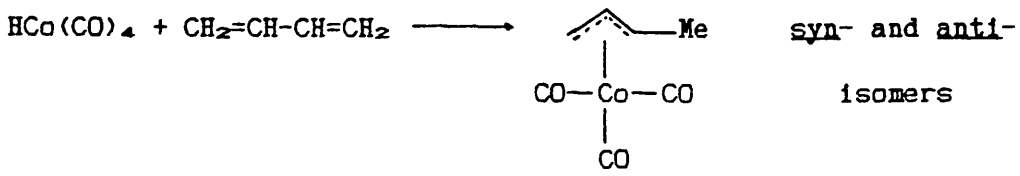

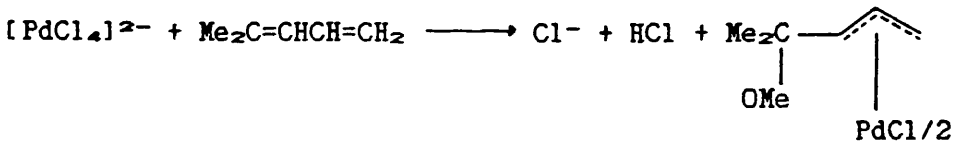

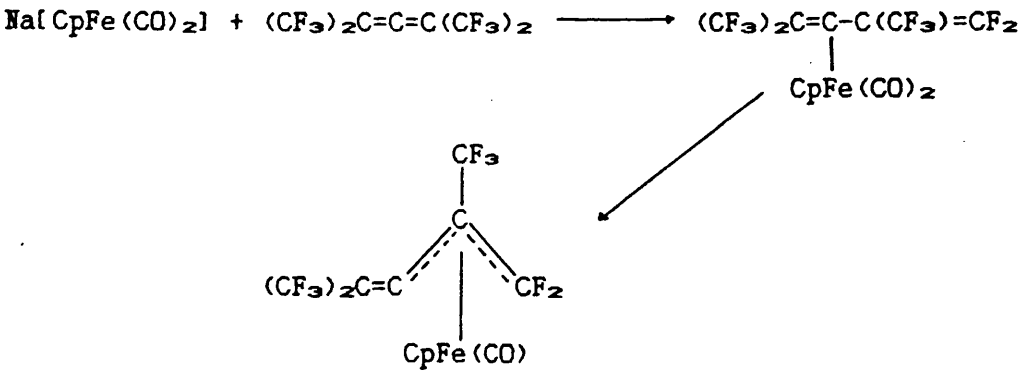

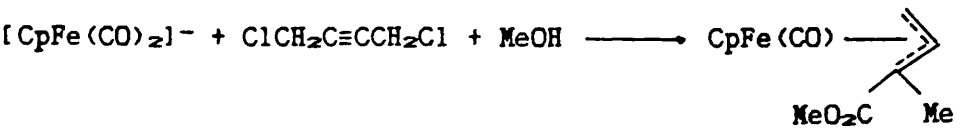

Conditions are often crucial to achieve these reactions, and low reaction temperatures are often required. Use of deutero-labelled butadiene in the reaction below revealed that the observed stereochemistry of the product resulted not from reaction via a 1-4 hydrogen shift, but by formation of an η^3-allyl intermediate which facilitated adoption of a transoid conformation [204,208].

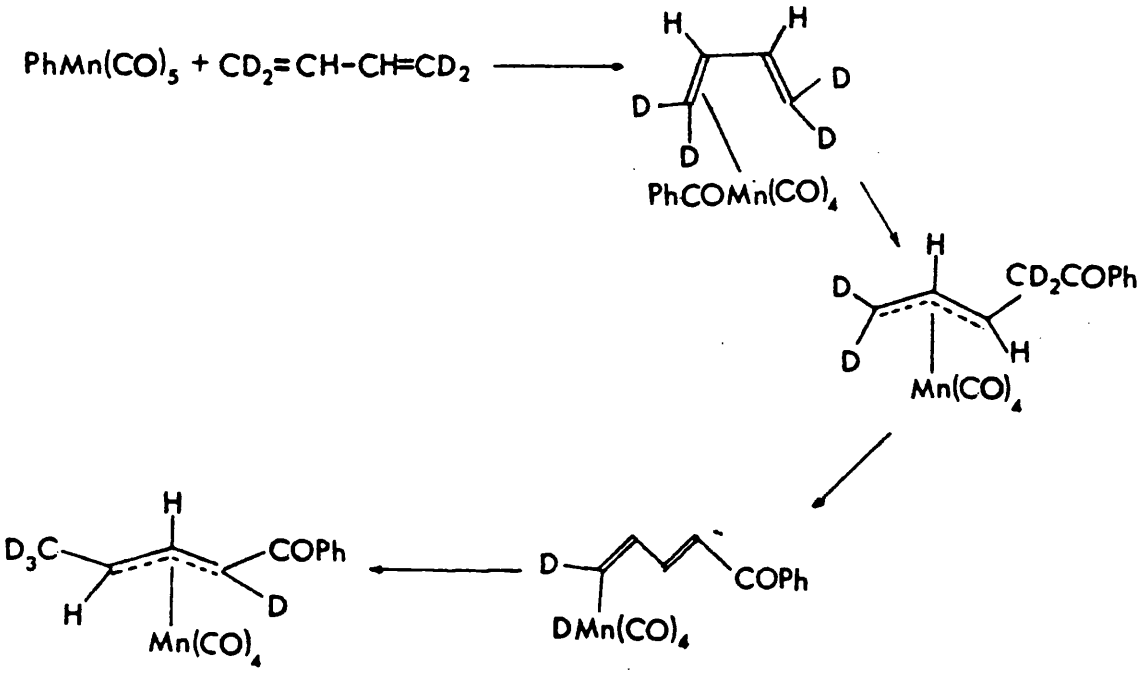

4.3.4 CONVERSION FROM η^1- TO η^3-ALLYL

Conversion of a coordinated η^1-allyl ligand to an η^3-allyl species is accompanied by the loss of two electrons from the metal coordination sphere, and may be brought about using chemical, thermal or photochemical methods, e.g. [209-211].

(i) by halide extraction

$$Pt(cod)_2 + CH_2{=}CHCH_2Cl \longrightarrow PtCl(cod)(\eta^1\text{-}C_3H_5)$$

$$\downarrow +AgBF_4$$

$$[Pt(cod)(\eta^3\text{-}C_3H_5)]^+BF_4^- + AgCl$$

(ii) by thermolysis

$$Mn(CO)_5(\eta^1\text{-}C_3H_5) \xrightarrow[-CO]{T>80^\circ} Mn(CO)_4(\eta^3\text{-}C_3H_5)$$

(iii) by photolysis

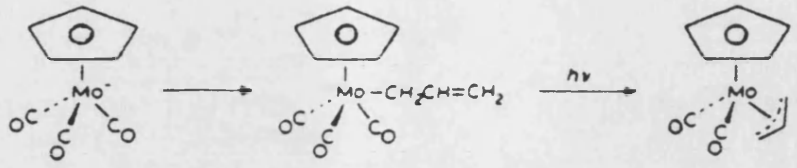

4.3.5 PHASE TRANSFER CATALYSIS

Phase transfer catalysis has been successfully employed in the preparation of allyl derivatives and this technique offers the advantages of a rapid, simple method requiring mild reaction conditions and providing exceptionally good yields. Early studies by Alper [212] utilised the two phase system of aqueous NaOH-benzene using $PhCH_2NEt_3^+Cl^-$ as the phase transfer catalyst to prepare $Co(CO)_3(\eta^3\text{-}CHRCR'CH_2)$ and led to a proposed mechanism in which the catalyst is converted to the hydroxide in the aqueous phase and transfers as an ion-pair to the organic phase, where $Co_2(CO)_8$ is attacked to generate $[Co(CO)_4]^-$ [213]. The allyl halide then reacts with this anion via an η^1-allyl intermediate to finally yield $Co(CO)_3(\eta^3\text{-allyl})$ and the regenerated catalyst reverts to the aqueous phase.

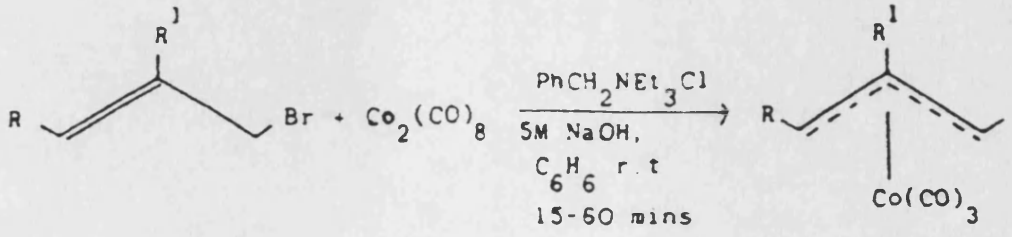

This method has since been extended by Gibson and co-workers to synthesise other η^3-allyl complexes, including $Mo(CO)_2(\eta^3\text{-}C_3H_5)Cp$ and $Fe(CO)(\eta^3\text{-}C_3H_5)Cp$ [214].

4.4 SPECTROSCOPIC CHARACTERISATION OF η^3-ALLYL TRANSITION METAL COMPLEXES

The major techniques which have been used in the study and characterisation of η^3-allyl organometallics are vibrational and different forms of NMR spectroscopy. Since many η^3-allyl species are dynamic, variable temperature ^1H and ^{13}C NMR measurements can be usefully employed in the investigation of rearrangement mechanisms and the determination of their activation energies.

4.4.1 PROTON NUCLEAR MAGNETIC RESONANCE SPECTROSCOPY

In theory, a static, symmetrically bonded η^3-C_3H_5 group possesses up to five magnetically distinct protons as shown below.

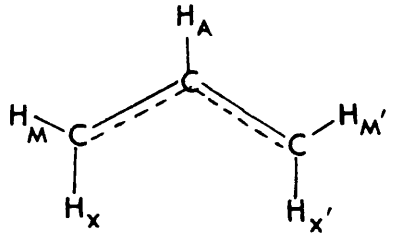

H_M and $H_{M'}$ = H_{syn}

H_X and $H_{X'}$ = H_{anti}

First order rules apply to this system and predict an AMM'XX' pattern. However since J_{MX}, $J_{M'X'}$ and $J_{MX'}$, $J_{M'X}$ coupling is small, this pattern is only observed in high resolution studies and the majority of symmetrical η^3-allyl complexes produce spectra which can be explained in terms of an AM_2X_2 spin system, a diagram of which, together with typical values of ^1H NMR parameters for transition metal complexes are shown below.

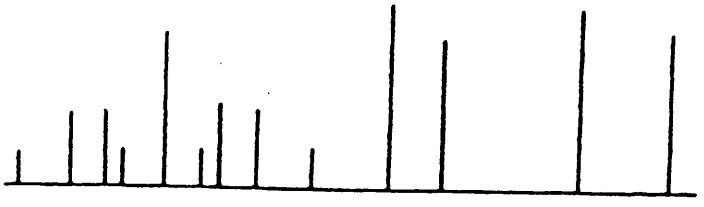

Typical values	H_A	H_M	H_X
Chemical shift (δ)	6.5-4ppm	5-2.5ppm	4-1ppm
Coupling constants (J)		5-10Hz	9-14Hz

Assignment of syn- and anti- protons can be made by comparison of their coupling constants, which for η^3-allyl complexes are typically 9-14Hz (anti), 5-10Hz (syn) and 0.2Hz (gem). Thus, since trans-vic protons couple more strongly than cis-vic protons, the doublet at higher field can be assigned to the H_X protons. H_A should, in theory, give rise to sixteen resonance lines, of which a maximum of fifteen lines have been successfully resolved [215]. Although small, both $J_{MX}, J_{M'X'}$ and $J_{MX'}, J_{M'X}$ coupling constants are not zero and under suitable high resolution conditions these second order splittings can be observed. Karplus [216] attributed these small coupling constants to the attachment of both protons to the same carbon atom with the H_XCH_M angle near 125° for J_{MX} and $J_{M'X'}$ and to a long range coupling for $J_{MX'}$ and $J_{M'X}$. The apparent equivalence of $J_{MX}, J_{M'X'}$ and $J_{MX'}, J_{M'X}$ results in each of the bands for the M and X protons appearing as a doublet of triplets, with both coupling constants in the order of 1Hz. Values of $J_{MM'}$ and $J_{XX'}$ are small due to the large separation between protons H_M and $H_{M'}$ and H_X and $H_{X'}$ and have only been obtained from high resolution ^1H and ^{13}C NMR spectra of substituted η^3-allyls such as Pd(η^3-2-C_3H_4Cl)acac [215], for which $J_{MM'}$=2.7Hz and $J_{XX'}$=0.5Hz. Symmetrical, substituted η^3-allyl complexes yield simplified spectra, however 1-substitution results in possible syn and anti isomerism as shown and hence yields more complex spectra.

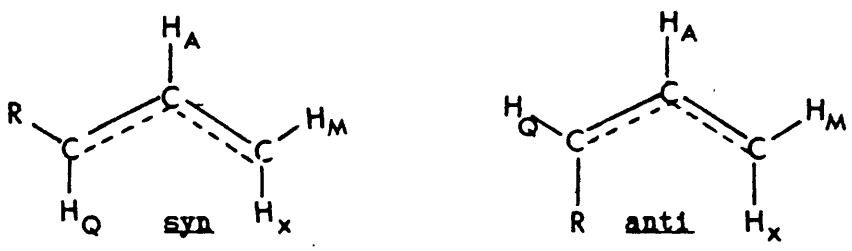

Resonances due to these two isomeric forms may be assigned on the basis of their relative coupling constants, J_{AQ}. Coupling between

trans-vic protons H_A and H_Q in the syn-isomer produces larger J values (ca. 10.5Hz) than those attributed to cis-vic proton coupling of H_A and H_Q in the anti-isomer (ca. 6.8Hz).

Dynamic η^3-allyl complexes often exhibit deceptively simple spectra at room temperature or above due to fluxional behaviour. In general such rearrangements may be due to the movement of the η^3-allyl group relative to the rest of the molecule or to the dynamic behaviour of other ligands around the metal centre. The exact mechanisms involved in such processes are in dispute, but the following three types of rearrangement have been recognised [217]; (1) syn-anti exchange, (2) syn,syn-anti,anti-exchange and (3) conformational changes.

(1) Syn,anti exchange.

This process, illustrated diagrammatically below, results in rapid interchange of the syn and anti- protons of the allyl group. Exchange at both terminal carbon atoms in complexes such as the homoleptic

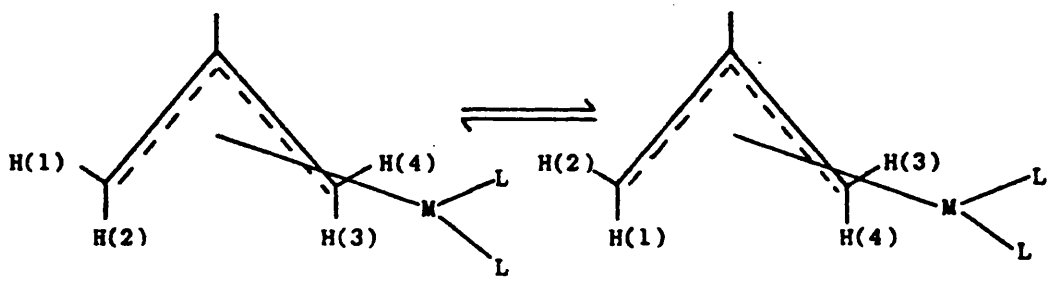

allyls $Th(\eta^3\text{-}C_3H_5)_4$ [148] results in simplified ^1H NMR spectra typical of AX_4 spin systems, which, at low temperature, resolve into an AM_2X_2 spin pattern. Exchange at one carbon atom only may also be observed e.g. $RhCl_2(\eta^3\text{-}2\text{-}C_3H_4Me)(PPh_3)_2$ [218] which is thought to occur via an η^3-η^1-η^3 interchange as shown in (C) below. Several mechanisms have been suggested to explain the equivalence of the terminal allylic protons at ambient temperature in all these systems, including;

(A) formation of a planar 1,3-η^2-allyl-metal complex, as an intermediate which returns to an η^3-allyl bonding mode.

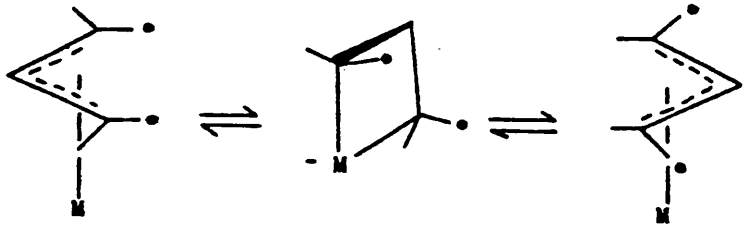

(B) formation of an η^2-allyl intermediate which undergoes internal rotation of a $-CH_2-$ group about a carbon-carbon single bond.

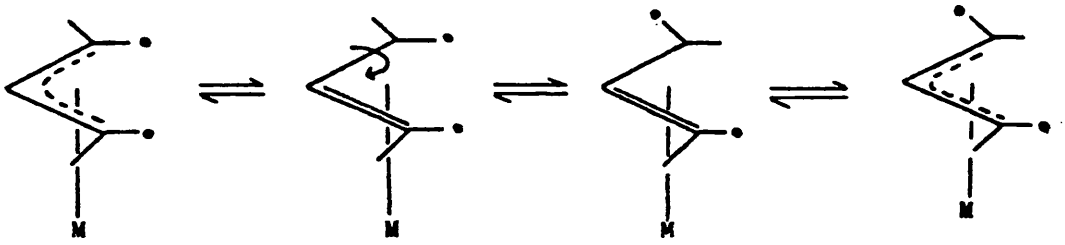

(C) rotation of a short-lived η^1-allyl intermediate about a metal-carbon single bond, which reverts to an η^3-allyl complex.

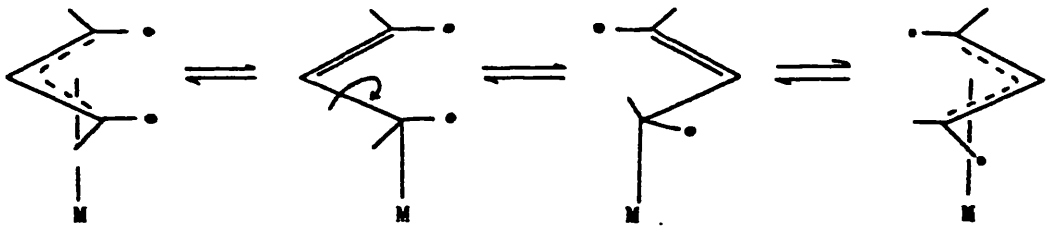

The last mechanism, involving an η^3-η^1-η^3 interconversion is perhaps the most commonly used to explain fluxional behaviour.

(2) <u>syn,syn-anti,anti exchange</u>.

This rearrangement can be envisaged as an exchange of <u>syn,syn</u> and <u>anti,anti</u> protons, as shown below, by either rotation of the allyl about the allyl-metal axis or by pseudo-rotation of other ligands about the metal centre resulting in observation of an average environment for the terminal allylic protons. This interchange can be

detected by ^1H NMR spectroscopy in complexes which contain substituted, asymmetric η^3-allyl groups or where the arrangement of

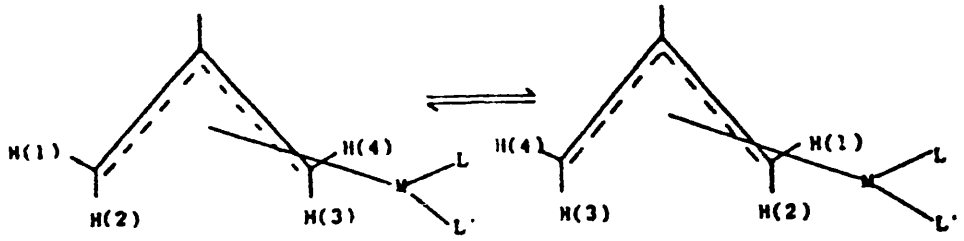

other ligands about the metal centre results in an asymmetric complex.

The apparent syn,syn-anti,anti exchange observed in the ^1H NMR spectra of the low symmetry complexes $Mo(CO)_2(\eta^3\text{-}C_3H_5)L_2X$ (L_2=dppe, X=halogen [219], L_2=acac, X=py [220]) at ambient temperature, has been shown by variable temperature ^1H, ^{13}C and ^{31}P NMR studies and by X-ray analysis to arise from pseudo-rotation of the triangular face composed of the bidentate and halogen or pyridine with respect to the face formed by the allyl and cis-dicarbonyl groups. The limited number of stable configurations resulting from this 'trigonal twist' process lead to enantiomerisation of the metal centre. Thus the diagram shown below represents a proposed trigonal twist between S and R configurations in these complexes [221].

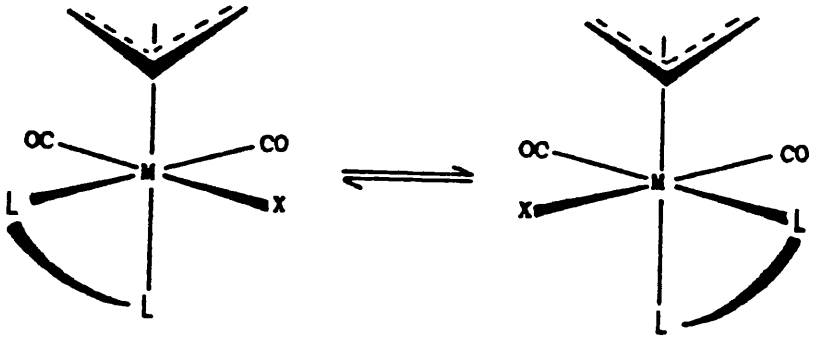

(3) Conformational isomerism.

Restricted rotation of the η^3-allyl ligand about the metal-allyl axis in complexes such as $Mo(CO)_2(\eta^3\text{-}2\text{-}C_3H_4R)Cp$, results in the

formation of conformational isomers as illustrated below. The ^1H NMR spectra of these complexes below 5°C exhibit two overlapping AM_2X_2 spin patterns which collapse to a single AM_2X_2 profile at higher temperatures [222] as rotation of the allyl ligand becomes fast on the NMR time-scale. Barriers to interconversion between these conformers are found to be controlled by steric interactions between the allyl and the cyclopentadienyl ring; thus when R=H, the exo/endo conformer ratio K(exo/endo)=4.7, whereas when R=Me, K(exo/endo)=0.38 [223].

EXO ENDO

Many complexes, particularly those containing substituted allyls, exhibit this type of isomerism, but a more unusual example is $Rh(\eta^3\text{-}C_3H_5)_3$ [224,225] which at -74°C contains three inequivalent, but symmetrically bonded allyl groups. At 34°C, two of the allyls appear to be magnetically equivalent, presumably due to the rotation of the third allyl in its own plane as shown below.

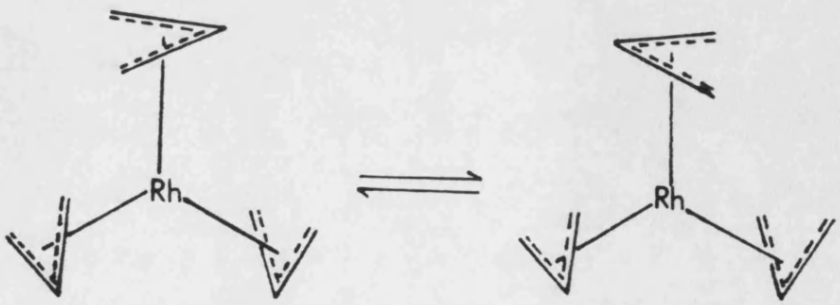

4.4.2 ^{13}C NUCLEAR MAGNETIC RESONANCE SPECTROSCOPY

The ^{13}C NMR shift values of η^3-allyl ligands are generally found within characteristic ranges as shown in Table 4.1. The terminal carbon atoms of the allyl group, C(1) and C(3), have been found in the chemical shift range δ 35-80ppm, with the central carbon C(2) resonance observed at lower field (90-140ppm.) The deshielding effect of a methyl substituent on C(2) results in a shift to lower field of the C(2)-Me resonance relative to that of C(2)-H. The chemical shift value appears to be fairly insensitive to the formal charge on the complex [226], however shielding of the crotyl carbon signals in $[Ni(\eta^3\text{-}1\text{-}MeC_3H_4)X]_2$ increases with the electronegativity of the halide X in the order I<Br<Cl (Table 4.1). Variable temperature ^{13}C NMR spectra have been used to examine dynamic systems. Thus the process postulated above for $[Rh(\eta^3\text{-}C_3H_5)_3]$ on the basis of ^1H NMR studies is supported by the observation at -75°C of three signals for both the terminal and central carbons of the allyl groups, which on warming resulted in two sharp signals and four broad resonances, the latter finally coalescing into two sharp peaks at room temperature [224].

Examples of typical J(H-C) or J(P-C) coupling constants are given in Table 4.1. Values of J(H-C) have been used to reflect the degree of hybridisation of carbon atoms [233] with typical ranges being ca. 125Hz for sp^3 carbon atoms in alkanes, 155-165Hz for sp^2 hybridised carbon atoms in alkenes and arenes and ca. 250Hz for alkynes. Coupling constants J(P-C) are characteristically 21-28Hz and 30-40Hz for phosphine and phosphite ligands trans to C(1) and C(3) and 3-6Hz. for cis coupling, whilst coupling constants to C(2) are typically 1 and 4-7Hz for phosphines and phosphites respectively.

Table 4.1 Selected ^{13}C NMR data and coupling constants for η^3-allyl complexes.

Complex[a]		Chemical shift, δ (ppm) C(1)	C(2)	C(3)	Coupling constant, J(Hz)	Ref.
$[Mo(CO)_2(\eta^3\text{-}2\text{-}C_3H_4Me)(bipy)(P(OPh)_3)]^+$		64.1	94.9	64.1	J[P-C(2)]=7	227
$[Mo(CO)_2(\eta^3\text{-}2\text{-}C_3H_4Me)(bipy)(py)]^+$		58.8	86.2	58.8		227
$Mn(CO)_4(\eta^3\text{-}C_3H_5)$[b]		43.2	93.8	43.8	J[H-C(1)]=J[H-C(3)]=161, J[H-C(2)]=157	228
$[Fe(CO)_4(\eta^3\text{-}1\text{-}C_3H_4Me)]^+$	syn isomer	83.6	98.2	49.1	J[H-C(1)]=J[H-C(2)]=160.3, J[H-C(3)]=165.5	229
	anti isomer	82.4	94.3	56.5	J[H-C(1)]=J[H-C(2)]=164.7, J[H-C(3)]=165.9	
$[Pt(\eta^3\text{-}1\text{-}C_3H_4Me)(PEt_3)_2]^+$		80.0	111.5	54.8	J[P-C(1)]=27.6, J[P-C(2)]=6, J[P-C(3)]=25.8	230
$V(CO)_3(\eta^3\text{-}C_3H_5)(Ph_2AsCH_2CH_2PPh_2)$		53.1	88.0	53.1		231
$MCl(CO)_2(\eta^3\text{-}C_3H_5)$dppe	M=Mo	60.4	83.7	60.4		219
	M=W	52.2	73.0	52.2		
$Pd(\eta^3\text{-}1\text{-}C_3H_4R)$acac	R=H	55.8	113.5	55.8		215
	R=Me	73.6	113.3	51.6		
	R=CH_2Ph	77.6	112.0	52.6		
$[Ni(\eta^3\text{-}1\text{-}C_3H_4Me)X]_2$	X=Cl	48.0	106.9	70.0	J[H-C(1)]=159, J[H-C(2)]=163, J[H-C(3)]=161	232
	X=Br	49.6	105.6	71.2	J[H-C(1)]=161, J[H-C(2)]=165, J[H-C(3)]=161	232
	X=I	52.4	105.5	76.3	J[H-C(1)]=162, J[H-C(2)]=161, J[H-C(3)]=161	232

[a]-measured at room temperature [b]-determined at -95°C

4.4.3 INFRA-RED SPECTROSCOPY

Most features observed in the IR spectra of η^3-allyl complexes can be satisfactorily assigned to internal vibrations of the η^3-allyl group based upon C_s local symmetry. Group theory predicts that a total of 18 normal modes of vibration should occur. The additional modes shown below, associated with allyl-metal skeletal vibrations, are often difficult to assign due to vibrations of other ligands, and although the complete vibrational

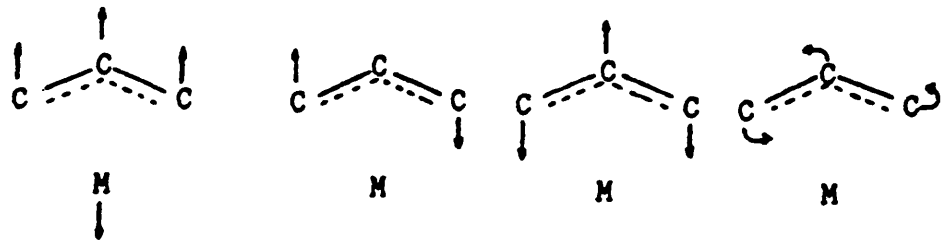

A'sym. stretching mode | A'sym. tilt (A'≠A") | A"sym. tilt | A" torsional

spectra of several η^3-allyl complexes have been studied in depth [234-238], in general such detailed assignments are not possible for highly substituted complexes where extensive coupling modes and absorptions due to other ligands obscure bands arising from the allyl group. In such cases the absence of a band at ca. 1650cm^{-1} attributable to the ν(C=C) stretching frequency of a carbon-carbon double bond and two bands at ca. 1400 and 530cm^{-1} arising from ν_{As}(CCC) and δ(CCC) respectively can be reliably used to identify η^3-allyl complexes.

4.5 BONDING IN η^3-ALLYL COMPLEXES

The palladium dimer $[PdCl(\eta^3\text{-}C_3H_5)]_2$ was one of the first η^3-allyl complexes to be examined crystallographically [239]. The allyl group was found to be bonded symmetrically, with C-C bond distances averaging 1.376Å and the plane containing the three carbon allyl skeleton tilted at 115±0.9° to the $PdCl_2Pd$ plane. X-ray structural data for a variety of other η^3-allyl complexes are listed in Table 4.2 and reveals a similar non-perpendicular arangement of the allyl group with respect to the plane passing through the allyl centre, the metal and the trans-ligand (dihedral angle $\chi \neq 90°$). The reason for this arrangement can be understood by considering the bonding between the metal and allyl ligand, and the differing values of χ are the result of maximising the orbital overlap between the

Table 4.2 Selected structural data for the M-(η^3-allyl) unit in transition metal complexes.

Complex	Dihedral angle[a]	Bond lengths(Å)			Ref.
	$\chi°$	MC(1)	MC(2)	MC(3)	
$[Mo(CO)_2(\eta^3\text{-}C_3H_5)(bipy)(py)]^+$	107.9	2.31	2.28	2.29	240
$[Fe(CO)_3(\eta^3\text{-}C_3H_5)]_2$	98.8	2.21	2.10	2.20	241
$[NiBr(\eta^3\text{-}2\text{-}C_2H_5CO_2C_3H_4)]_2$	106.2	2.05	1.90	2.06	242
$[PdCl(\eta^3\text{-}C_3H_5)]_2$	108.0	2.14	2.02	2.17	243
$MoCl(CO)_2(\eta^3\text{-}C_3H_5)(P(OMe)_3)_2$	112.2	2.40	2.36	2.40	244
$[IrCl(CO)(\eta^3\text{-}C_3H_5)(PMe_2Ph)_2]^+$	126.0	2.28	2.24	2.25	245
$RhCl_2(\eta^3\text{-}2\text{-}C_3H_4Me)AsPh_3$	126.6	2.25	2.27	2.23	246
$NiBr(\eta^3\text{-}2\text{-}C_3H_4Me)$dppe	106.5	2.06	2.02	2.05	247
$Ti(\eta^3\text{-}1\text{-}2\text{-}C_3H_3Me_2)(Cp)_2$	124.1	2.24	2.43	2.35	248

[a]-The dihedral angle χ is the angle between the allyl plane and the plane passing through the centre of the allyl, metal and trans ligand.

ligand and metal centre.

Simple Hückel calculations [249] show that the $2p_x$ orbitals of the allyl carbon atoms can form three molecular orbitals which are shown in Fig. 4.3. The electron population of these orbitals depends upon whether the allyl ligand is considered to be a cation (2 electron), a radical (3 electron) or an anion (4 electron) species. The number of electrons supplied by the allyl group can be formally compensated for by changes in valency of the metal atom, but convention dictates that the allyl group normally be considered as an anion so contributing one unit to the oxidation

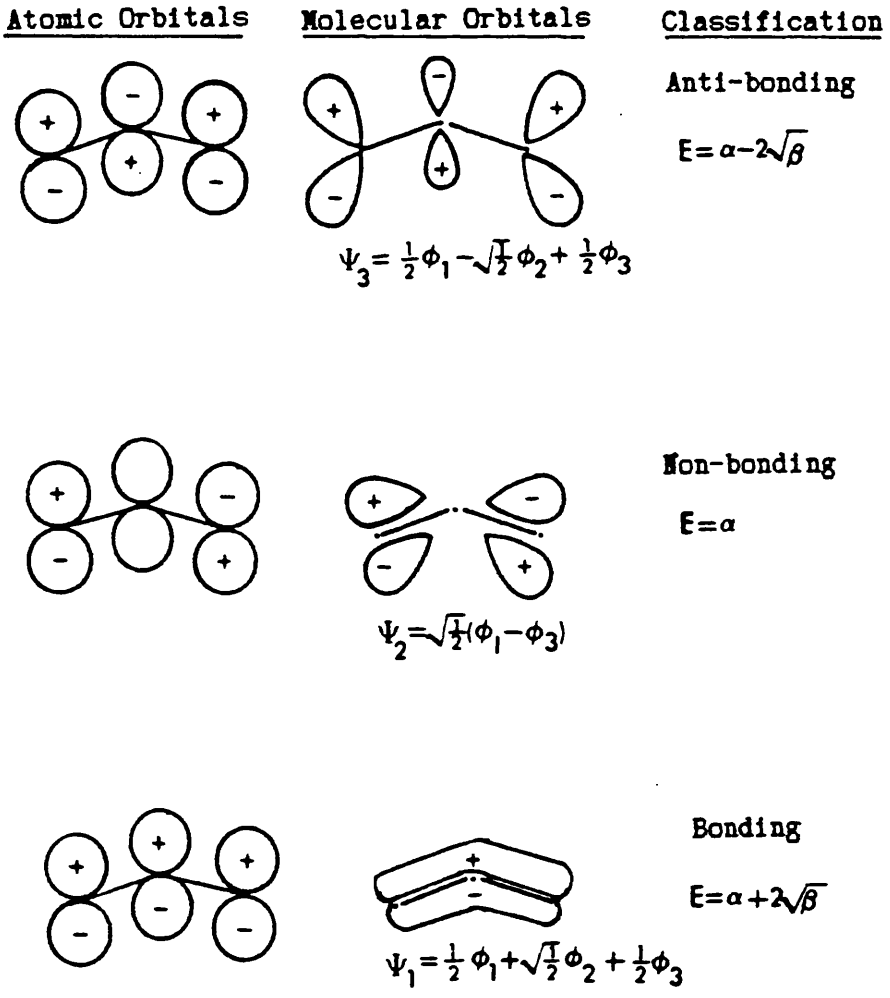

Fig. 4.3 The molecular bonding orbitals for the allyl anion.

number of the metal. The vacant anti-bonding orbital ψ_3 is in theory available for back-bonding from the metal, but to what extent it is utilised is still unclear.

In order to explain the observed tilt of the allyl plane ($\chi>90°$), Mason and Kettle [143] proposed a bonding scheme which results in two possible overlap mechanisms between the allyl and metal with $\chi=90°$ or $\chi=180°$ as shown in Fig. 4.4. Experimentally observed values of χ showed that bonding interactions between these extremes results in $90°<\chi<180°$ values and thus accounts for the observed tilt common to most allyl systems. Kettle predicted the maximum ψ_1-metal and ψ_2-metal orbital overlap and hence greatest total bonding energy for χ in $[Pd(\eta^3\text{-}C_3H_5)Cl]_2$ at 114° and 102° respectively, which compares well with observed values as seen in Table 4.2.

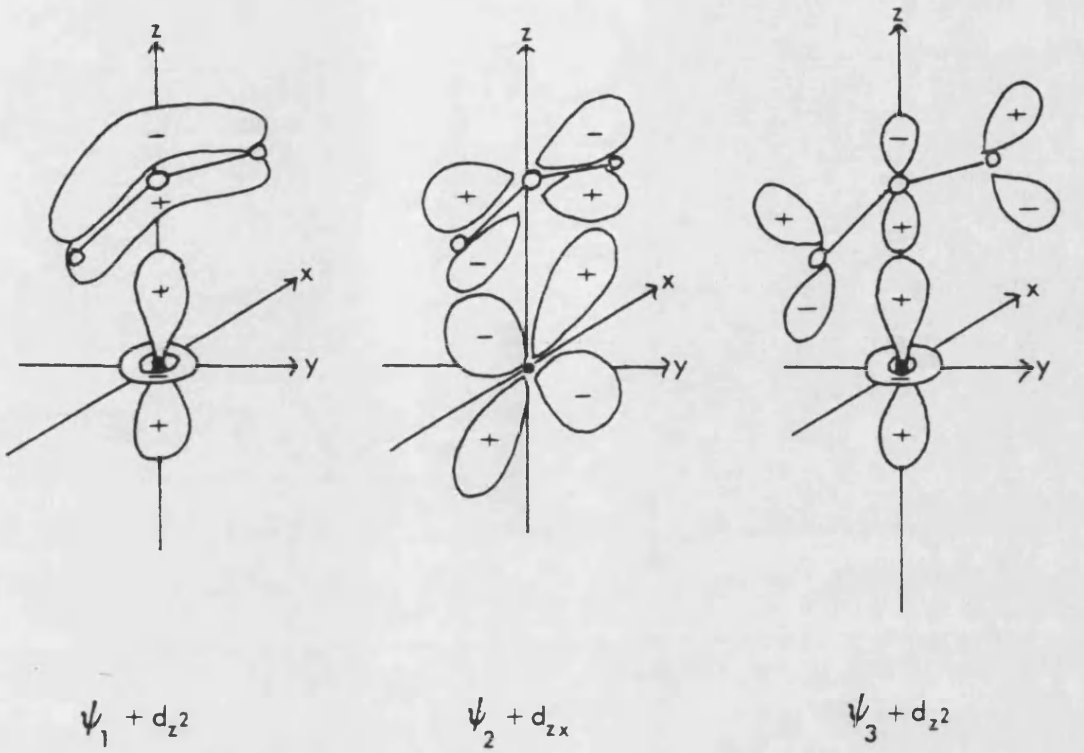

$\psi_1 + d_{z^2}$ $\psi_2 + d_{zx}$ $\psi_3 + d_{z^2}$

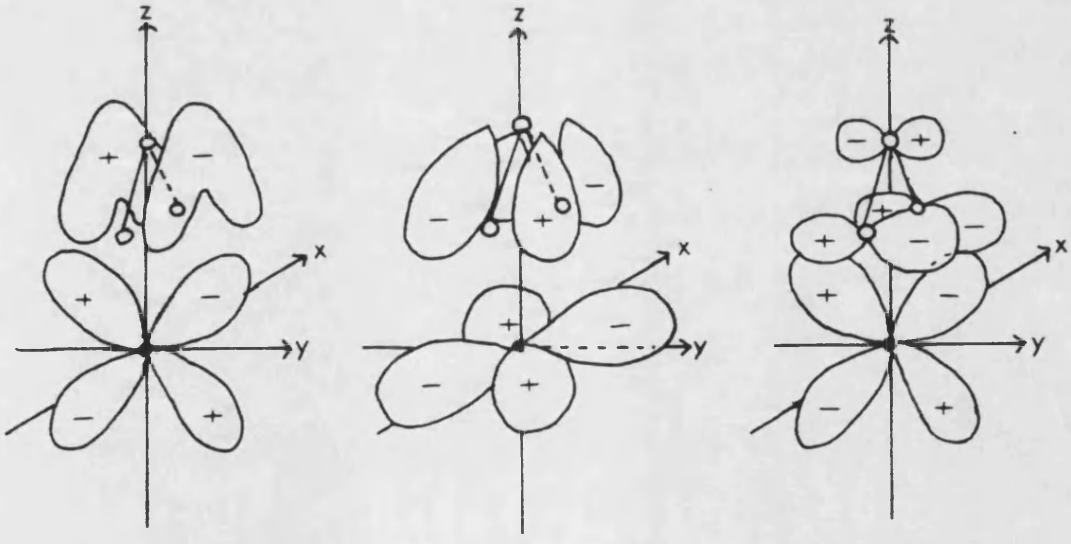

$\psi_1 + d_{yz}$ $\psi_2 + d_{xy}$ $\psi_3 + d_{yz}$

Fig. 4.4 Bonding interactions between η^3-allyls and transition metals.

4.6 CONFORMATION OF THE η^3-ALLYL LIGAND IN $[M(CO)_2(\eta^3\text{-}C_3H_5)L_3]^{n+,0}$.

Almost all the d^4 $[M(CO)_2(\eta^3\text{-}C_3H_5)L_3]^{n+,0}$ complexes whose structures have been confirmed by X-ray diffraction studies, adopt a pseudo-octahedral configuration containing a fac-$M(CO)_2(\eta^3\text{-}C_3H_5)$ unit in which the open face of the allyl points towards the two carbonyl groups. The preference for this orientation of the allyl group has been recently explained in terms of the electronic requirements of the molecule. Curtis and Eisenstein [252] calculated the rotational energy barriers for three orientations of the allyl fragment in the model compounds $[Mo(CO)_2(\eta^3\text{-}C_3H_5)(HCN)_3]^+$ and $[Mo(CO)_2(\eta^3\text{-}C_3H_5)Cl_3]^-$ and found that if the energies for the three orientations of the allyl (θ=0.0°,90° or 180°) were referenced to the energy at θ=0.0° as shown in Fig. 4.5, then this value was the lowest by 40-55kJ mol^{-1}, correctly predicting the observed preference for this low energy conformer. Since θ=0.0° and θ=180° are respectively the lowest and highest energy conformations, only these two rotameters will be discussed further.

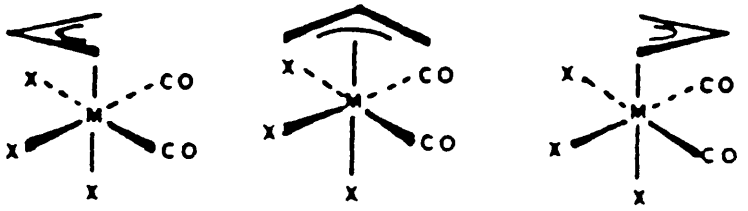

	θ=0.0°	θ=90°	θ=180°	X
ΔE=	0.0	25.6	61.7	HCN
ΔE=	0.0	31.9	42.4	Cl

Fig. 4.5 Rotational energy barriers for η^3-C_3H_5 in $[Mo(CO)_2(\eta^3\text{-}C_3H_5)X_3]^{n+}$.

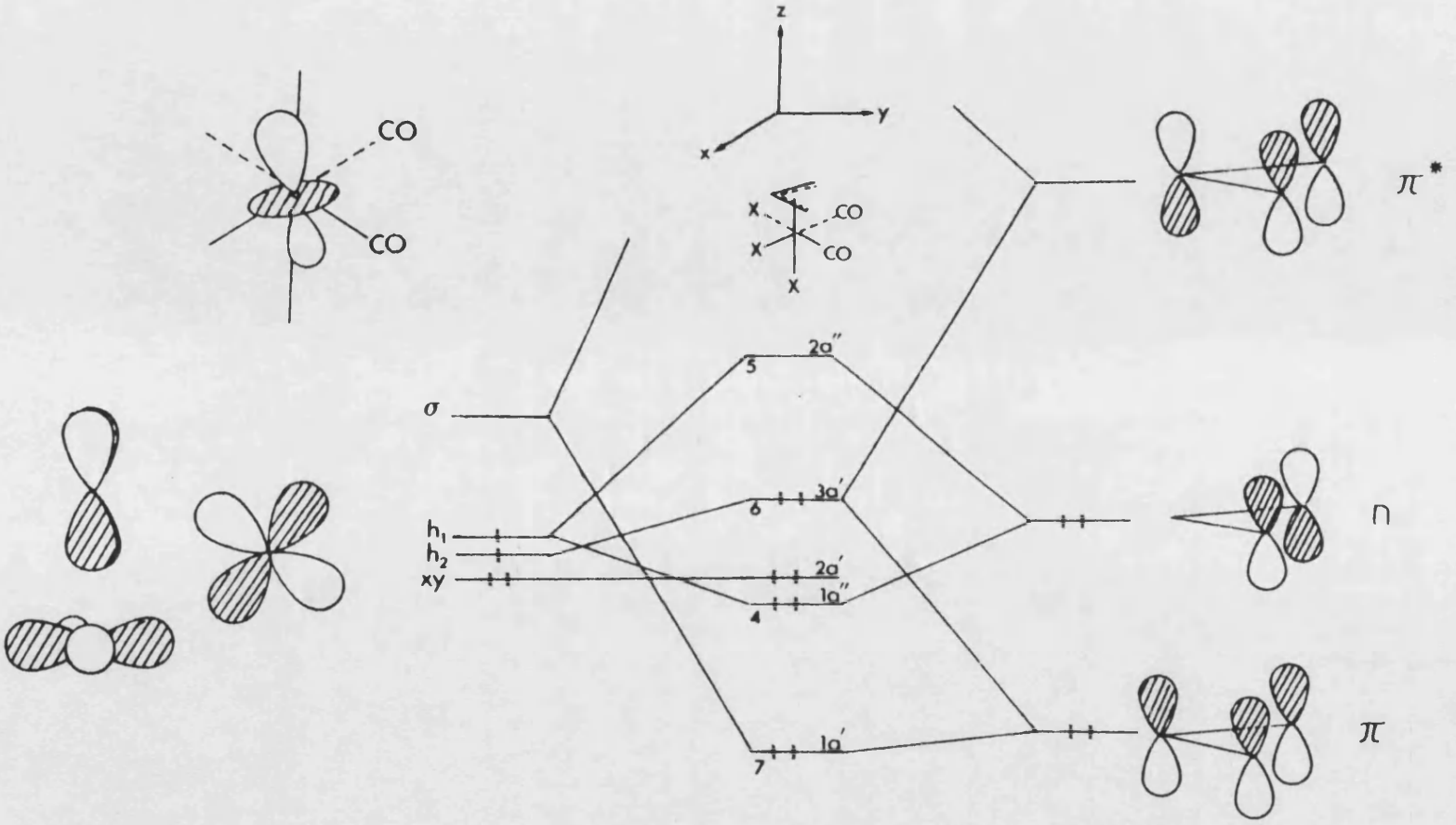

Fig. 4.6 Molecular orbitals of the allyl group and $M(CO)_2X_3$ fragment for θ=0.0°.

The interactions between the frontier orbitals of the d^4 $Mo(CO)_2X_3$ fragment and the occupied π, n and empty π^* orbitals of the allyl group for $\theta=0.0°$ are depicted in Fig. 4.6. The $Mo(CO)_2X_3$ moiety contains a σ-type hybrid orbital mainly due to z^2 at higher energy, a δ-type xy orbital at lower energy which only weakly interacts with the allyl orbitals and need not concern us here, and two nearly degenerate π-type hybrids h_1 (=xz-yz) and h_2 (=xz+yz). At $\theta=0.0°$ bonding (4,Fig. 4.6) and anti-bonding (5,Fig. 4.6) combinations are obtained by interaction of the h_1 hybrid with the non-bonding allyl orbital n, whilst both symmetric π and anti-symmetric π^* orbitals interact with the h_2 and σ orbitals of the $Mo(CO)_2X_3$ fragment to give bonding orbitals (6 and 7,Figs. 4.6 and 4.7). The interaction which forms the bonding (4) and anti-bonding (5) combinations is essentially the same for both $\theta=0.0°$ and $\theta=180°$, however rotation of the allyl group through 180° (Fig.4.7) results in destabilisation of the $\theta=0.0°$ orbital (6) relative to the $\theta=180°$ orbital (8) by 25kJ mol^{-1}. Closer examination of the $Mo(CO)_2X_3$ fragment, in particular of the σ and h_2 orbitals, reveals the source of this destabilisation.

Fig. 4.7 Bonding orbitals arising from interaction of π and π^* with σ and h_2 hybrid orbitals.

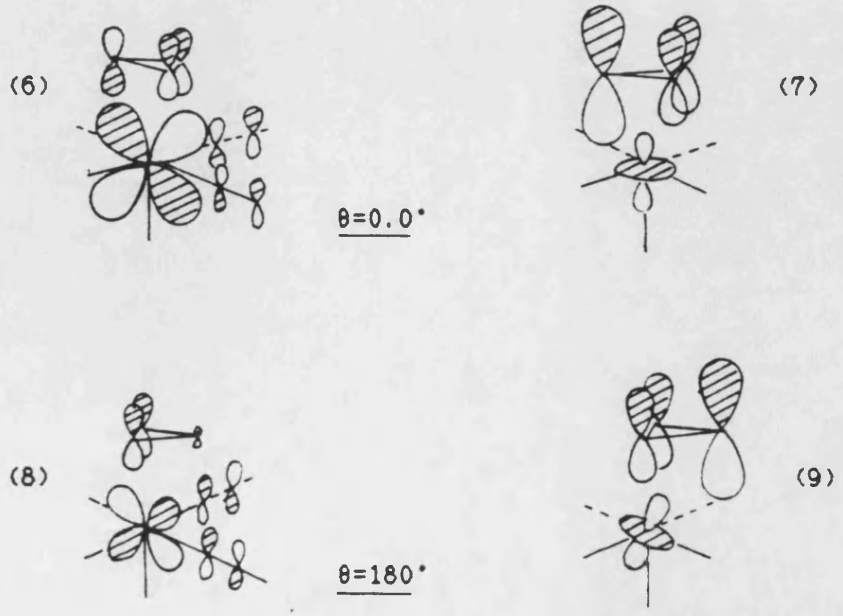

The σ-orbital ((10),Fig.4.8) is a hybrid consisting of a mixture of z^2 with 5s, $5p_x$ and (xz+yz) orbitals, whilst the hybrid h_2 ((11),Fig.4.8) is a combination of z^2 and (xz+yz) orbitals. Mixing of $(s+p_x+z^2)$ and (xz+yz) hybrid orbitals, which have σ and π symmetries respectively, is achieved by their interaction with the carbonyl π^* orbitals, and tilts the (xz+yz) orbitals to produce h_2 which has greatest overlap with the allyl π orbital for the θ=180° orientation. Since h_2 is of higher energy than the allyl π orbital this results in destabilisation, and thus the better overlap of h_2 and π for the 180° orientation produces a greater destabilisation compared to the θ=0.0° orientation.

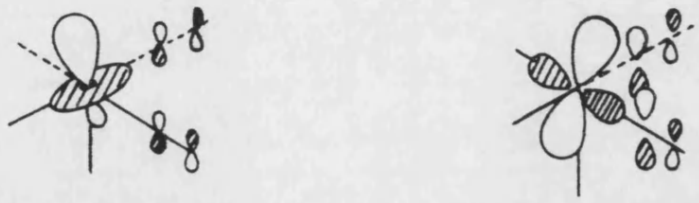

(10) (11)

Fig. 4.8 Hybrid orbitals σ and h_2.

Although this arrangement of the fac-$M(CO)_2(\eta^3-C_3H_5)$ unit is extremely common in d^4 $M(CO)_2(\eta^3-C_3H_5)X_3$ complexes, examples of alternative structures are known and will be described in the following section.

4.7 Mo(II) AND W(II) COMPLEXES OF GENERAL FORMULAE $[M(CO)_2(\eta^3\text{-allyl})L_2X]^{n+,0}$ AND $[M(CO)_2(\eta^3\text{-allyl})L_3]^{n+,0}$

4.7.1 STRUCTURE

X-ray analyses have revealed that if the allyl group is regarded as occupying one coordination site, the majority of d^4 $[M(CO)_2(\eta^3\text{-allyl})L_2X]^{n+,0}$ complexes can be described as possessing a pseudo-octahedral environment for the metal and a fac-arrangement of the $M(CO)_2(\eta^3\text{-allyl})$ unit. Two orientations of the L_2X group with respect to the η^3-allyl group and cis-dicarbonyl groups have been found. The majority of reported structures reveal a trans-arrangement of the η^3-allyl and X as shown by (A) in Fig. 4.9 and this form is found for complexes such as $Mo(CO)_2(\eta^3\text{-}C_3H_5)Cp$ [253] (a special case of L_2X) and for complexes with substituted η^3-allyl groups such as $Mo(CO)_2(phen)(NCS)(\eta^3\text{-1-}C_3H_4Ph)$ [254]. Few examples of structural

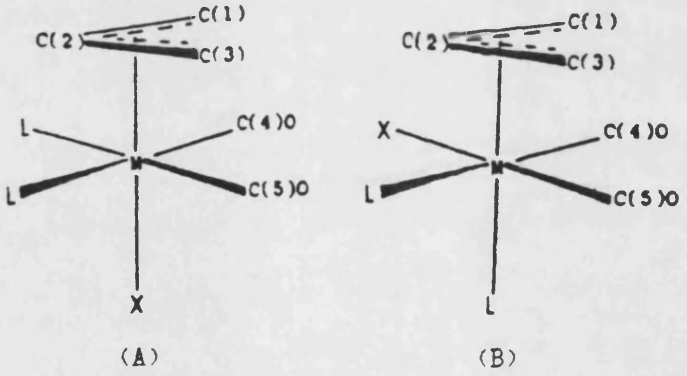

Fig. 4.9 Structures adopted by $M(CO)_2(\eta^3\text{-}C_3H_5)L_2X$.

type (B) are known for this type of complex, but this form has been confirmed for L_2X=(dppe)Cl [219] and (acac)(py) [220] in the solid state.

Table 4.3 shows that in general the geometry of the fac-$M(CO)_2(\eta^3\text{-allyl})$ unit in $M(CO)_2(\eta^3\text{-}C_3H_5)L_2X$ complexes is little affected by the type and position of other ligands. However in some substituted allyl complexes which contain other bulky ligands

Table 4.3 Bond lengths and angles in the $M(CO)_2(\eta^3\text{-allyl})$ unit of $M(CO)_2(\eta^3\text{-allyl})L_2X$ and $M(CO)_2(\eta^3\text{-allyl})L_3$.

Complex[b]	Structure[a]	Ref.	C(1)-C(2)[a]	C(2)-C(3)[a]	C(1)-C(2)-C(3)[c]	M-C(1)[a]	M-C(2)[a]	M-C(3)[a]	C(4)-M-C(5)[c]	Average M-C(4) & M-C(5)
$M(CO)_2(\eta^3\text{-allyl})L_2X$										
$Mo(CO)_2(\eta^3\text{-}C_3H_5)(bipy)(NCS)$	A	255	1.46	1.42	116	2.29	2.20	2.35	78	1.93
$Mo(CO)_2(\eta^3\text{-}C_4H_7)(phen)(NCS)$	A	256	1.45	1.40	117	2.32	2.27	2.35	83	1.97
$[Mo(CO)_2(\eta^3\text{-}C_3H_5)(bipy)(py)]BF_4$	A	240	1.37	1.47	111	2.31	2.28	2.29	78	1.99
$Mo(CO)_2(\eta^3\text{-}C_3H_5)(dme)(O_2CCF_3)_2$	A	257	1.45	1.45	114	2.34	2.16	2.34	79	1.90
$W(CO)_2(\eta^3\text{-}C_3H_5)(dme)(O_2CCF_3)_2$	A	257	1.36	1.36	123	2.29	2.07	2.29	75	1.84
$MoCl(CO)_2(\eta^3\text{-}C_3H_5)(dppe)$	B	219	1.40	1.40	116	2.34	2.22	2.35	78	1.96
$Mo(CO)_2(\eta^3\text{-}C_3H_5)(acac)(py)$	B	220	1.40	1.37	115	2.30	2.20	2.31	80	1.95
$Mo(CO)_2(\eta^3\text{-}C_3H_5)(salal)(py)$	B	258	1.37	1.42	115	2.32	2.24	2.34	79	1.91
$WCl(CO)_2(\eta^3\text{-}C_3H_5)(C_6H_{11}NCHCHNC_6H_{11})$	A	259	1.43	1.43	114	2.33	2.20	2.33	80	1.99
$MoBr(CO)_2(\eta^3\text{-}C_3H_5)(C_6H_{11}NCHCHNC_6H_{11})$	A	260	1.42	1.42	112	2.33	2.27	2.33	81	1.98
$Et_4N[WCl_2(CO)_2(\eta^3\text{-}C_3H_5)PPh_3]$	A	261	1.47	1.41	114	2.33	2.20	2.35	76	1.94
$Mo(CO)_2(\eta^3\text{-}C_3H_5)(Et_2B(pz)_2)(Hpz)$	A	262	1.39	1.41	117	2.34	2.26	2.35	82	1.95

Table 4.3 continued.

Complex[D]	Structure[A]	Ref.	C(1)-C(2)[B]	C(2)-C(3)[B]	C(1)-C(2)-C(3)[C]	M-C(1)[B]	M-C(2)[B]	M-C(3)[B]	C(4)-M-C(5)[C]	Average M-C(4) & M-C(5)
$Mo(CO)_2(\eta^3\text{-}C_3H_5)(PhBpz_3)$	A	263	1.42	1.42	116	2.37	2.22	2.34	79	1.92
$Mo(CO)_2(\eta^3\text{-}C_4H_7)(HBpz_3)$	A	264	1.42	1.42	113	2.34	2.26	2.36	82	1.96
$Mo(CO)_2(\eta^3\text{-}C_3H_5)(MeGapz_3)$	A	265	1.38	1.37	116	2.36	2.23	2.34	81	1.94
$Mo(CO)_2(\eta^3\text{-}C_4H_7)(MeGa(3,5\text{-}Me_2pz)_2OH)$	B	266	1.40	1.41	121	2.36	2.24	2.36	83	1.95
$Mo(CO)_2(\eta^3\text{-}C_3H_5)(Me_2Ga(3,5\text{-}Me_2pz)(OCH_2CH_2NH_2))$	B	267	1.39	1.40	116	2.33	2.37	2.32	79	1.93
$Mo(CO)_2(\eta^3\text{-}C_4H_7)(Ph_2Bpz_2)$[E]		268	1.43	1.40	114	2.33	2.26	2.36	76	1.92
$Mo(CO)_2(\eta^3\text{-}C_3H_5)Cp$		253	1.38	1.38	117	2.36	2.25	2.35	82	1.95
$[Mo(CO)_2(\eta^3\text{-}C_3H_5)(MeCN)_3]^+$	A	269	1.47	1.47	118	2.38	2.23	2.30	82	1.94
$[Mo_2(CO)_4(\eta^3\text{-}C_3H_5)_2Cl_3]^-$	A	269	1.38	1.46	113	2.32	2.18	2.35	78	1.93
			1.41	1.45	113	2.32	2.18	2.35	78	1.93
Average values										
$M(CO)_2(\eta^3\text{-allyl})L_2X$			1.4114	1.4114	115.29	2.3207	2.2286	2.3329	78.857	1.9400
$M(CO)_2(\eta^3\text{-allyl})L_3$			1.4111	1.4177	116.87	2.3575	2.2300	2.3525	81.125	1.9412

[A]-A=symmetrical structure, B=unsymmetrical structure, [B]-measured in Å, [E]-no sixth coordination atom
[C]-degrees, [D]-numbering system for carbon atoms given in Fig. 4.9

attached to the metal such as examples 1 and 2 below [176,166], the central carbon of the η^3-allyl group is found between the two cis-carbonyl groups (i.e.θ=180°) due to the electronically preferred θ=0.0 orientation of the η^3-allyl being overruled by the steric demands of other ligands.

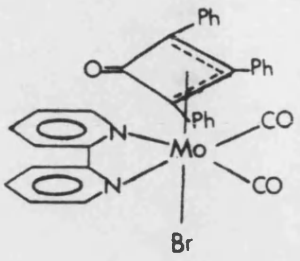

(1)

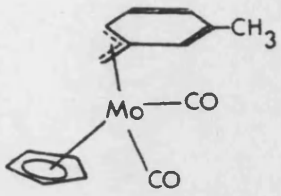

(2)

From a structural viewpoint the allyl can also be described as a bidentate group with a small normalised bite. For complexes of general formula M(bidentate)(monodentate)$_3$ where the bite of the bidentate is small, the predicted geometries are the pentagonal bipyramid (PB) or capped trigonal prism (CTP) [37]. Thus many d^4 M(CO)$_2$(η^3-allyl) complexes can be equally accurately described as being of CTP form with the allyl and carbonyl groups occupying the unique edge and adjacent sites in the quadrilateral plane respectively. Such an arrangement for MoCl(CO)$_2$(η^3-C_3H_5)(P(OMe)$_3$)$_2$ would however create a sterically strained molecule due to a cis-arrangement of the two bulky phosphite ligands, and one phosphite ligand being sited trans to a carbonyl group would be in a position to compete as a π-acceptor. The complex therefore adopts the unusual distorted PB structure shown in Fig. 4.10, in which the chloride and one carbonyl group are in axial positions and the η^3-allyl ligand occupies two adjacent sites in the distorted equatorial girdle [244].

In the Mo and W complexes M(CO)$_2$(η^3-allyl)(RR'Bpz$_2$)X of symmetrical structure type (A), the anionic bis-(pyrazolyl)borato ligands RR'Bpz$_2$ [262] adopt a conventional bidentate bonding mode.

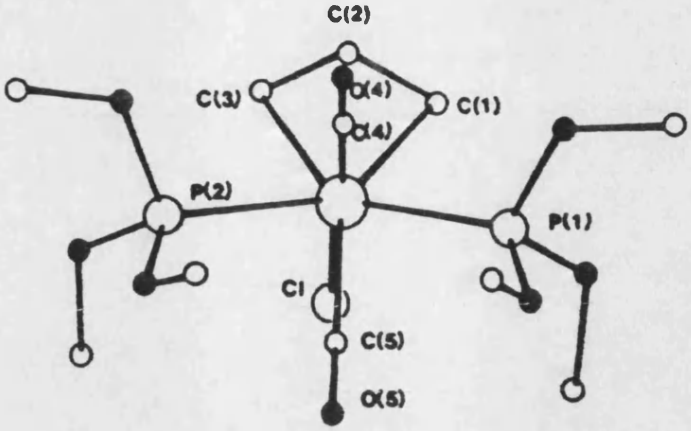

Fig. 4.10 Molecular structure of $MoCl(CO)_2(\eta^3-C_3H_5)(P(OMe)_3)_2$.

However X-ray analyses of related $M(CO)_2(\eta^3$-allyl$)(RR'Bpz_2)$ complexes have shown that for R=R'=Ph [267] bidentate coordination of the anion occurs in a 16 electron species, whilst for R=H or alkyl effective tridentate coordination is achieved via C(B)-H-M bridges and the formation of 3 centre-2 electron bonds [270] as illustrated below. Low symmetry structures predominate in the latter tridentate

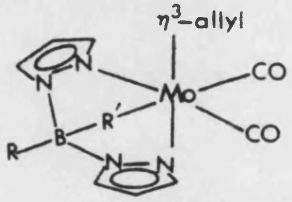

tridentate

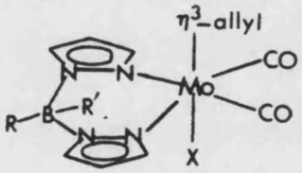

bidentate

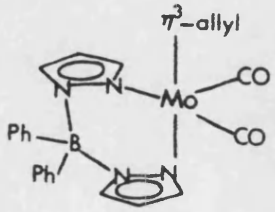

16-electron

complexes and their gallato analogues ((B),Table 4.3), presumably because the allyl group has greater steric freedom when sited trans to a pyrazoyl ring, whilst the related tris-(pyrazolyl)borato ($RBpz_3^-$) and gallato ($RGapz_3^-$) complexes adopt symmetrical structures ((A), Table 4.3), with the anions in a fac arrangement [263-265].

B. PREPARATION AND REACTIVITY

The major synthetic routes to the complexes $[M(CO)_2(\eta^3\text{-allyl})L_2X]$ (M=Mo or W) are summarised below, and exemplified in Table 4.4.

1. Oxidative-addition of allylX to cis-$M(CO)_4L_2$ or $M(CO)_3L_2Y$.
2. Direct reaction of $M(CO)_6$, allylX and donor ligand e.g. MeCN, diamine.
3. Bridge-splitting e.g. cleavage of $[Et_4N][Mo_2(CO)_4(\eta^3\text{-}C_3H_4Me)_2Cl_3]$ by py, bipy, 1,2-diaminoethane.
4. Reactions of anions $[M(CO)_3L_2X]^-$ (M=Cr, Mo or W) with allyl compounds.
5. Exchange of MeCN by L or L_2.
6. Replacement of X by pseudo-halide or monodentate Lewis base.

The fourth route is especially important since it provides the only known access to the chromium analogues and yields a facile route to tungsten complexes. Displacement of acetonitrile from the complexes $Mo(CO)_2(\eta^3\text{-allyl})(MeCN)_2X$ (M=Mo or W, allyl=C_3H_5, C_4H_7, C_3H_4Cl, C_4H_9 or C_3Ph_3, X=Cl or Br) [284] provides an important route to a very wide range of substituted derivatives of general formula $M(CO)_2(\eta^3\text{-allyl})L_2X$ containing monodentate (N,P) or bidentate (N,O,P,As) donor ligands (L or L_2 respectively), since the parent tetracarbonyls $M(CO)_4(\eta^3\text{-}C_3H_5)X$ have proved extremely difficult to synthesise [285,277]. The nature of X in the dicarbonyl complexes may be altered by anion exchange, and Lewis bases such as amines, phosphines or arsines (L') may be coordinated to the metal to yield $[M(CO)_2(\eta^3\text{-allyl})L_2L']BF_4$ by halide extraction in coordinating solvents using silver(I) salts [227]. X-ray analysis [286] revealed that attempts to form sixteen electron species by removal of halide from $MoCl(CO)_2(\eta^3\text{-allyl})$bipy in the absence of coordinating ligands or solvents resulted in a novel dimeric halogen-bridged complex

Table 4.4 Synthetic routes to $[M(CO)_2(\pi^3\text{-allyl})L_2X]^{n\pm,0}$ (M=Mo or W).

L_2	X	Method[^]	Ref.	n±,0[■]
Nitrogen donors				
bipy or phen	halide, SCN,	1,2,3,4,5 or 6	175	N
bipy or phen	xanthate, $HS_2CNR_2^-$	6	272	N
bipy or phen	$MeCO_2$, CF_3CO_2,	6	271	N
bipy or phen	$PhSO_2$, SC_6F_5	6	273	N
bipy or phen	PPh_3, $AsPh_3$, $P(OPh)_3$	6	227	A
bipy or phen	py, NH_3	6	227	A
en, 2(py)	halide, SCN	3,5,6	274,275	N
Et_2Bpz_2	Hpz	2	262	N
R'N=CHCH=NR'	halide, SCN	6	276	N
Phosphorus donors				
PPh_3	halide	1	277	N
dppe, dppm, dae	halide	6	278	N
dam, arphos, diars				
Oxygen donors				
acac	halide	1	279	C
acac	py	5,6	200	N
$CH_3O(CH_2)_2OCH_3$	CF_3CO_2	2	257	N
Other donors				
CNR'	halide	5	280	N
2-picolinate	halide	1	281	A
$R_2CN{=}NNHCONH_2$	halide	5	282	N
$R_2CN{=}NNHCSNH_2$	halide	5	283	N

[^]-see text
[■]-N=neutral, A=anion, C=cation

$[\{Mo(CO)_2(\eta^3\text{-allyl})(bipy)\}_2\text{-}\mu\text{-}Cl]^+BF_4^-$ due to rapid reaction between an unstable, unsaturated intermediate and the unreacted halo-complex.

Two different reactions occur in the attempted preparation of phosphine substituted allyl complexes under mild conditions. Thus the monodentate phosphines PPh_3 and PBu^n_3 react with $M(CO)_2(\eta^3\text{-allyl})(MeCN)_2X$ with elimination of the allyl as allylphosphonium halide and the formation of M(0) products $M(CO)_2(MeCN)LL'_2$ (L=MeCN, L'=PR_3 or L=L'=PR_3) [287-290]. For these phosphines no evidence of the expected intermediate $M(CO)_2(\eta^3\text{-allyl})L'_2X$ was observed, however with methyldiphenylphosphine, diphenylphosphine, or the bidentate phosphines dppe or dppm, displacement of MeCN initially forms $Mo(CO)_2(\eta^3\text{-allyl})L_2X$ which under more forcing conditions is reduced to cis-$Mo(CO)_2(L_2)_2$ (L_2=dppe or dppm) [278,291]. Reaction of $M(CO)_2(\eta^3\text{-allyl})(MeCN)_2X$ with isocyanides (RNC) (R=alkyl or aryl) also leads to reductive elimination of allyl-X and the formation of substituted Mo(0) complexes such as $Mo(CO)_2(CNR)_4$ and $[MoCl(CNBu^t)_4]_2$ [292] via the isolable intermediates $M(CO)_2(\eta^3\text{-allyl})(CNR)_2X$ [280].

The η^3-allyl ligand in $M(CO)_2(\eta^3\text{-allyl})L_2X$ is susceptible to nucleophilic attack, particularly if the metal complex is cationic. NMR studies have shown that the nucleophilic attack on the chiral complexes $[Mo(CO)(NO)(\eta^3\text{-allyl})Cp]^+$ [293,294] is complicated by an intra-molecular rearrangement process shown below, which interconverts the exo and endo conformers and is dependent upon the rates of exo-endo interconversion of (A) and (B) compared to reaction of (A) with NO^+. Nucleophilic attack was found to occur cis to NO in both the exo and endo conformers [295] and the exo isomer shown to

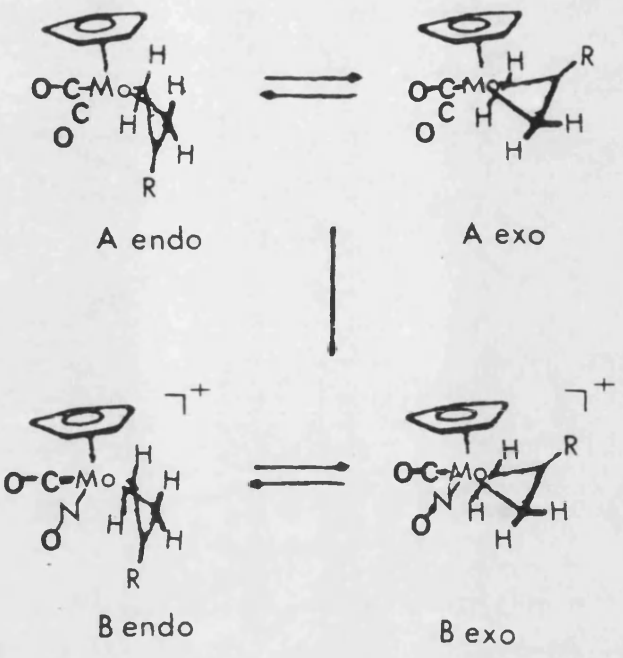

react faster than the endo form. Reagent assisted exo-endo equilibration was reached faster than product formation and thus the exo species was the major product.

In contrast to these acyclic systems, the products of nucleophilic addition to the endo and exo complexes [Mo(CO)(NO)(η^3-cyclooctenyl)Cp]$^+$ have been found [296] to be highly dependent upon the conformation of the reactant cation. Reagent assisted conversion between exo and endo cations occurred more slowly than nucleophilic attack due to the steric interactions of the Cp and cyclooctenyl moieties and thus at low temperature addition of D^-, OH^- or $Me_2NCS_2^-$ (deuteride, hydroxide or dimethyldithiocarbamate) to the exo complex cation resulted in a regioselectivity of >95% in each case, whilst addition to the endo isomer at room temperature showed variable regioselectivity, with ratios of 99:1 to 1:99, depending upon the nucleophile and reaction conditions. Nucleophilic attack upon the

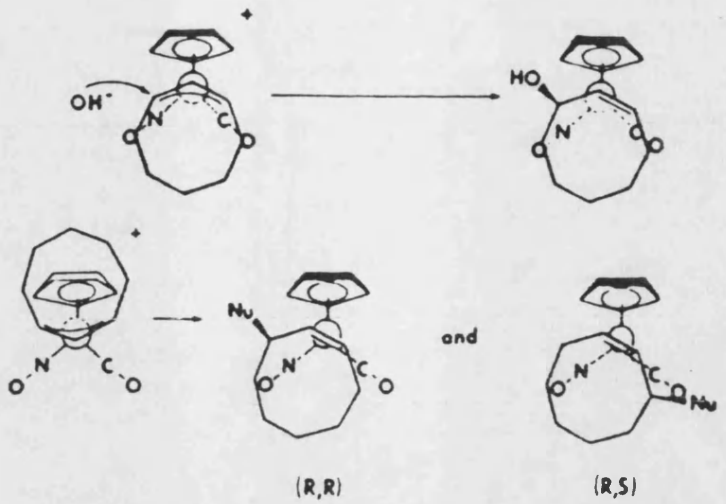

complexes $MoCl(CO)_2(\eta^3\text{-allyl})L_2$ (L_2=bipy or dppe) [297] shows a similar dependence upon the arrangement of ligands about the metal centre with the bipy and dppe complexes showing different regioselectivities, presumably due to their differing influence upon the allyl frontier orbitals.

In contrast to the many Mo and W complexes containing bidentate ligands bipy and phen discussed above, related allylic complexes containing symmetrical tridentate N-donor ligands have been relatively neglected. Thus to date only the tris-(pyrazolyl)borato (L_3=$RBpz_3^-$) and gallato (L_3=$RGapz_3^-$) complexes $M(CO)_2(\eta^3\text{-allyl})L_3$ have been reported [264-266], which are prepared by reactions of $M(CO)_2(\eta^3\text{-allyl})(MeCN)_2X$ and NaL_3 or allyl halide with $Na[M(CO)_3L_3]$. In order to extend this limited range of allylic complexes containing symmetrical tridentate N-donor ligands, the solution behaviour of $MCl(CO)_2(\eta^3\text{-2-}C_3H_4R)(MeCN)_2$ (M=Mo or W, R=H or Me) in neutral or basic hydroxylic solvents has been studied, together with the reactivity of the neutral aqueous solutions with 2,2'-dipyridyl, 2,2'-dipyridylamine, diethylenetriamine and bis-(pyridylmethyl)amine, and these results are reported in Chapter 5.

CHAPTER 5

THE BEHAVIOUR OF $M(CO)_2(\eta^3\text{-}C_3H_4R)(MeCN)_2X$ IN HYDROXYLIC SOLVENTS AND REACTIONS WITH BIDENTATE AND TRIDENTATE NITROGEN DONOR LIGANDS

5.1 INTRODUCTION

In 1979 Brisdon and Cartwright [298] investigated the solution properties of $Mo(CO)_2(\eta^3-C_3H_5)(MeCN)_2X$ (X=Cl, Br or I) in CD_3CN, CD_2Cl_2 and $(CD_3)_2CO$ and obtained complex ^1H NMR spectra which they attributed to the presence of three allyl species generated by an equilibrium process as indicated by equation (5.1) below. This

$$3\ Mo(CO)_2(\eta^3-C_3H_5)(MeCN)_2X \longrightarrow 3MeCN + [Mo(CO)_2(\eta^3-C_3H_5)(MeCN)_3]^+ + [Mo_2(CO)_4(\eta^3-C_3H_5)_2X_3]^- \quad (5.1)$$

postulate was confirmed when recrystallisation of $MoCl(CO)_2(\eta^3-C_3H_5)(MeCN)_2$ from hot benzene led to the isolation of the benzene solvate of $[Mo(CO)_2(\eta^3-C_3H_5)(MeCN)_3][Mo_2(CO)_4(\eta^3-C_3H_5)_2Cl_3]$, whose structure was established by a single crystal X-ray diffraction study [269].

The degree of ionisation of the halo complexes in solution was shown to decrease in the order Cl>Br>I and reflected the relative stabilities of the halogen-bridged ions. The iodo-complexes failed to undergo this autoionisation but solvolysis in MeCN yielded the cationic species $[Mo(CO)_2(\eta^3-C_3H_5)(MeCN)_3]^+$. Subsequent studies by Hill [299] of the analogous tungsten complexes revealed a similar halide dependency for the extent of autoionisation and also showed that $[W_2(CO)_4(\eta^3-C_3H_5)_2Cl_3]^-$ was stable in CD_2Cl_2, but was solvolysed in CD_3CN with the formation of $WCl(CO)_2(\eta^3-C_3H_5)(MeCN)_2$. Thus the stability, number and nature of the species present in the solutions of $M(CO)_2(\eta^3-C_3H_5)(MeCN)_2X$ (M=Mo or W) are highly halide and solvent dependent.

The reactivity of $MoCl(CO)_2(\eta^3-C_3H_5)(MeCN)_2$ in methanol has been shown to differ in some respects from that in other solvents [300,301] and under alcoholic conditions these bis-acetonitrile

complexes have been used to effectively catalyse Diels-Alder cycloadditions [302] and to promote alkyne polymerisation reactions [109]. Interest in the nature of the species involved in these reactions and the possibility of examining some related aqueous allyl-Mo(II) and W(II) chemistry has led to an investigation of the solution properties of $MCl(CO)_2(\eta^3\text{-}C_3H_4R)(MeCN)_2$ (M=Mo or W, R=H or Me) in the hydroxylic solvents R'OH (R'=H, Me or Et). The results of this study and the reactivity of the aqueous species towards bidentate (L_2=2,2'-bipyridyl or 2,2'-dipyridylamine) and tridentate (L_3=diethylenetriamine or bis-(2-pyridylmethyl)amine) nitrogen donor ligands are reported in this chapter.

5.2 EXPERIMENTAL

Details of physical techniques and solvents appear in Appendix 1. The starting materials $M(CO)_2(\eta^3\text{-}C_3H_4R)(MeCN)_2X$ and $[M(CO)_2(\eta^3\text{-}C_3H_4R)(MeCN)_3]BF_4$ (M=Mo, R=H, X=Br or I, M=Mo or W, R=H or Me, X=Cl) were synthesised according to literature methods [284,301]. Diethylenetriamine was obtained from commercial sources and used without further purification. Bis-(2-pyridylmethyl)amine was prepared in ca. 75% yield by reaction of chloromethylpyridine and 2-aminomethylpyridine using the method outlined in ref. 303.

PREPARATION OF $Ph_4As[M_2(CO)_4(\eta^3\text{-}2\text{-}C_3H_4R)_2(\mu\text{-}OR')_3]$ (M=Mo or W, R=H or Me, R'=Me or Et, M=Mo, R=H, R'=H).

A stirred solution of $MCl(CO)_2(\eta^3\text{-}2\text{-}C_3H_4R)(MeCN)_2$ (1.0mmol) in R'OH ($10cm^3$) was treated dropwise with Ph_4AsCl (0.21g, 0.5mmol) dissolved in 2M NaOH solution ($20cm^3$). After 0.5hr the yellow product was filtered, washed with cold water, dried and recrystallised from R'OH containing a few drops of aqueous NaOH solution.

Yields and analytical data for these complexes are given in Table 5.1.

Table 5.1 Yields and analytical data for complexes of general formula $Ph_4As[M_2(CO)_4(\eta^3\text{-}2\text{-}C_3H_4R)_2(\mu\text{-}OR')_3]$.

M	R	R'	Yield %	Analysis found(calculated) %C	%H
Mo	H	Et	37	52.9(53.1)	5.2(5.0)
Mo	H	Me	53	50.6(51.5)	4.6(4.5)
Mo	H	H	43	48.9(49.8)	3.8(4.0)
Mo	Me	Et	48	53.9(54.1)	5.2(5.3)
Mo	Me	Me	58	52.4(52.6)	4.8(4.8)
W	H	Et	77	43.2(44.4)	4.0(4.2)
W	H	Me	41	41.6(42.7)	3.8(3.8)
W	Me	Et	85	43.8(45.5)	4.2(4.4)
W	Me	Me	30	42.7(43.9)	4.1(4.0)

PREPARATION OF $MCl(CO)_2(\eta^3\text{-}2\text{-}C_3H_4R)L_2$ (M=Mo or W, R=H or Me, L_2=2,2'-bipyridyl (bipy) or 2,2'-dipyridylamine (dpa)).

A hot (40°C) solution of bipy or dpa (2.0mmol) dissolved in the minimum volume of 10% aqueous acetone was added dropwise to a solution of $MCl(CO)_2(\eta^3\text{-}2\text{-}C_3H_4R)(MeCN)_2$ (2.0mmol) in hot (40°C) deoxygenated water (20cm^3). The mixture was stirred for 0.5hr while cooling to room temperature and the product was filtered, washed with hot water and dried *in vacuo*. Yields 40-50%.

The physical and spectroscopic properties of these complexes were identical to those of $MCl(CO)_2(\eta^3\text{-}2\text{-}C_3H_4R)L_2$ prepared from the appropriate allyl halide and $M(CO)_4L_2$ [175,273].

PREPARATION OF $M(CO)_2(\eta^3\text{-}2\text{-}C_3H_4R)L_3X$ (M=Mo or W, R=H or Me, L_3=diethylenetriamine (dien) or bis-(2-pyridylmethyl)amine (bpma), X=Cl, M=Mo, R=H, L_3=dien, X=Br or I).

Three methods were employed in the preparation of $M(CO)_2(\eta^3\text{-}2\text{-}C_3H_4R)L_3X$ as outlined below. The products possessed identical physical and spectroscopic properties irrespective of the method employed and were isolated in 55-80% yields.

Method 1.

A solution of $M(CO)_2(\eta^3\text{-}2\text{-}C_3H_4R)(MeCN)_2X$ (1.0mmol) in acetonitrile ($25cm^3$) was heated under reflux with excess dien or bpma ($5cm^3$) for 1hr. Partial reduction of solvent *in vacuo* to *ca*. $10cm^3$ precipitated the yellow product which was filtered, washed with MeCN, and dried *in vacuo*.

Method 2.

A solution of $M(CO)_3L_3$ (1.0mmol) in THF ($25cm^3$) was heated under reflux with excess of the appropriate allyl halide ($3cm^3$) for 4hr (R=H) or 22hr ($R=CH_3$). Addition of diethylether to the cooled mixture and storage at low temperature (-10°C) precipitated the product as a yellow microcrystalline powder which was filtered, washed with diethylether and dried *in vacuo*.

Method 3.

Excess dien ($2.0cm^3$) or bpma (0.02g, 1.0mmol) was stirred with $M(CO)_2(\eta^3\text{-}C_3H_4R)(MeCN)_2X$ (1.0mmol) in hot (40°C) deoxygenated water ($50cm^3$) for 0.5hr. Methanol ($20cm^3$) was added to the yellow solution which was then extracted with diethyl ether ($20cm^3$) and the aqueous layer discarded. Cooling (-10°C) precipitated the crystalline product which was washed with diethyl ether and dried *in vacuo*.

Analytical data for these complexes are given in Table 5.2.

Table 5.2 Analytical data for complexes of general formula $M(CO)_2(\eta^3\text{-}2\text{-}C_3H_4R)L_3X$.

M	R	L_3	X	Analysis found(calculated)		
				%C	%H	%N
Mo	H	dien	Cl	31.7(32.6)	5.4(5.4)	13.3(12.7)
Mo	H	dien	Br	29.2(28.7)	5.0(4.8)	11.5(11.2)
Mo	H	dien	I	26.2(25.5)	4.4(4.3)	10.4(9.9)
Mo	Me	dien	Cl	33.5(34.7)	6.0(5.8)	14.1(12.2)
Mo	H	bpma	Cl	47.2(47.7)	4.4(4.2)	10.1(9.8)
Mo	Me	bpma	Cl	48.3(48.9)	4.7(4.5)	9.7(9.5)
W	H	dien	Cl	26.0(25.8)	4.4(4.3)	10.6(10.1)
W	Me	dien	Cl	27.7(27.7)	4.7(4.6)	10.5(9.7)
W	H	bpma	Cl	38.7(39.5)	3.9(3.5)	8.1(8.1)
W	Me	bpma	Cl	40.4(40.7)	4.1(3.8)	7.9(7.9)

PREPARATION OF $[M(CO)_2(\eta^3\text{-}2\text{-}C_3H_4R)L_3]PF_6$ (M=Mo or W, R=H or Me, L_3=dien or bpma).

A solution of $MCl(CO)_2(\eta^3\text{-}2\text{-}C_3H_4R)(MeCN)_2$ (1.0mmol) in hot (40°C) deoxygenated water (50cm^3) was stirred with excess dien (2cm^3) or bpma (0.02g, 1.0mmol) for 0.5hr. Excess aqueous NH_4PF_6 was added dropwise to the solution and the mixture stirred at 40°C for 0.5hr prior to filtration. The yellow product was washed with water, dried in vacuo and recrystallised from aqueous acetone.

The spectroscopic properties of these complexes were identical to those obtained by reaction of aqueous solutions of $MCl(CO)_2(\eta^3\text{-}2\text{-}C_3H_4R)L_3$ with NH_4PF_6. Table 5.3 contains yields and analytical data for these complexes.

Table 5.3 Yields and analytical data for complexes of general formula $[M(CO)_2(\eta^3\text{-}2\text{-}C_3H_4R)L_3]PF_6$.

M	R	L_3	Yield %	Analysis found(calculated) %C	%H	%N
Mo	H	dien	75	24.1(24.3)	3.7(4.1)	9.7(9.5)
Mo	Me	dien	82	26.8(26.2)	4.2(4.5)	9.6(9.2)
Mo	H	bpma	77	38.0(38.0)	3.4(3.4)	7.7(7.8)
Mo	Me	bpma	75	39.8(39.2)	3.6(3.6)	7.2(7.6)
W	H	dien	86	19.8(20.4)	3.4(3.4)	7.7(7.9)
W	Me	dien	83	22.1(22.1)	3.8(3.7)	7.9(7.7)
W	H	bpma	88	32.8(32.7)	2.9(2.9)	6.9(6.7)
W	Me	bpma	79	33.5(33.8)	3.0(3.1)	6.5(6.6)

The complex $[W(CO)_2(\eta^3\text{-}C_3H_5)bpma]PF_6$ only was isolated as a mixture of two crystalline forms. This mixture was hand-picked to separate the minor product of yellow needles from the major product of orange cubic crystals. The latter constituted approximately 95% of the total yields. The elemental analyses and room temperature ^1H NMR solution spectra of the two types of crystal were identical. The FAB positive ion mass spectrum of the major product only is reported in section 5.3.3.3.

5.3 RESULTS AND DISCUSSION

5.3.1 THE BEHAVIOUR OF $MCl(CO)_2(\eta^3\text{-}C_3H_4R)(MeCN)_2$ (M=Mo or W, R=H or Me) IN HYDROXYLIC SOLVENTS R'OH (R'=H, Me or Et)

Dissolution of $MCl(CO)_2(\eta^3\text{-}C_3H_4R)(MeCN)_2$ (M=Mo or W, R=H or Me) in water, methanol or ethanol produced yellow, conducting solutions which were stable in air for several hours before slowly decolourising. The ^1H and ^{13}C NMR data obtained for these complexes in CD_3OD and warm D_2O are summarised in Tables 5.4 and 5.5. Unlike non-hydroxylic solvents, no evidence of autoionisation was observed and only one main set of resonances for each of the η^3-allyl entities was present in each spectrum. Facile exchange of the coordinated MeCN with the solvent was indicated by the average resonance position of the acetonitrile signal, which at ca. 2.00ppm is very close to that of free nitrile. Although removal of excess solvent *in vacuo* from the aqueous solution yielded only decomposition products, tan-coloured, nitrogen-free, hygroscopic solids were recovered from methanol. These proved to contain a variable methanol content and were not fully identified. However the allyl region of the ^1H NMR spectra of $[Mo(CO)_2(\eta^3\text{-}C_3H_4R)(MeCN)_3]BF_4$ in CD_3OD (Table 5.4) proved to be very similar to that of $MoCl(CO)_2(\eta^3\text{-}C_3H_4R)(MeCN)_2$ dissolved in this solvent, suggesting that the cationic species $[Mo(CO)_2(\eta^3\text{-}C_3H_4R)(CD_3OD)_3]^+$ was probably present in both cases.

Methanolic solutions of $MCl(CO)_2(\eta^3\text{-}C_3H_4R)(MeCN)_2$ produced infra-red spectra containing two intense absorptions separated by ca. $100cm^{-1}$ between 1835 and 1950 cm^{-1} (Table 5.6). The positions of these bands were very similar to those of $[M(CO)_2(\eta^3\text{-}C_3H_4R)(MeCN)_3]BF_4$ in methanol and these values together with the molar conductivities of $MCl(CO)_2(\eta^3\text{-}C_3H_4R)(MeCN)_2$ and $[M(CO)_2(\eta^3\text{-}C_3H_4R)(MeCN)_3]BF_4$ in methanol and water (Table 5.6) confirmed the

Table 5.4 ^{1}H NMR data[a] for $MCl(CO)_2(\eta^3\text{-}C_3H_4R)(MeCN)_2$ and $[Mo(CO)_2(\eta^3\text{-}C_3H_4R)X_3]BF_4$

Complex			Solvent	Chemical shifts δ(ppm), (coupling constant in Hz)			
				Aliphatics	Allyl		
M	R				H_{anti}	H_{syn}	$H_{central}$ or Me
$MCl(CO)_2(\eta^3\text{-}C_3H_4R)(MeCN)_2$							
Mo	H		CD_3OD	2.09s	1.06d(9.5)	3.40d(6.4)	3.47m
			D_2O	2.07s	1.22d(9.5)	3.47d(6.4)	3.64m
Mo	Me		CD_3OD	2.10s	0.91s	3.13s	2.16s
			D_2O	2.08s	1.05s	3.21s	2.08s
W	H		CD_3OD	2.06s	1.26d(9.6)	3.17d(6.4)	3.32m
			D_2O[b]	2.08s	1.39d(9.6)	3.22d(6.4)	3.26m
W	Me		CD_3OD	2.07s	1.12s	2.93s	2.23s
			D_2O[b]	2.08s	1.25s	3.01s	2.12s
$[Mo(CO)_2(\eta^3\text{-}C_3H_4R)X_3]BF_4$							
M	R	X					
Mo	H	MeCN	CD_3OD	2.04s	1.19d(9.9)	3.41d(6.7)	3.47m
Mo	Me	MeCN	CD_3OD	2.04s	1.04s	3.23s	2.05s

[a]=Measured at ambient temperature unless stated otherwise, [b]=Measured at 56°C.

Table 5.5 ^{13}C NMR data[a] for $MCl(CO)_2(\eta^3\text{-}C_3H_4R)(MeCN)_2$

Complex		Solvent	Aliphatics	Chemical shift δ(ppm) Allyl			
M	R						
$MCl(CO)_2(\eta^3\text{-}C_3H_4R)(MeCN)_2$				CO	$C_{terminal}$	$C_{central}$	Me
Mo	H	CD_3OD	1.15s	227.25	59.07	73.25	
Mo	H	D_2O[b]	1.62s	227.51	57.89	73.94	
Mo	Me	CD_3OD	1.14s	227.92	57.34	83.86	18.43
Mo	Me	D_2O[b]	1.39s	227.75	57.16	84.21	20.00
W	H	CD_3OD	1.17s	220.11	52.82	65.63	
W	H	D_2O[c]					
W	Me	CD_3OD	1.32s	219.94	52.07	74.21	20.05
W	Me	D_2O[c]					

[a]=Measured at ambient temperature unless stated otherwise
[b]=At 90°C, [c]=Too insoluble for ^{13}C NMR measurements

presence of 1:1 ionic species containing cis-$M(CO)_2$ moieties in all these solutions.

Table 5.6 CO stretching frequencies and molar conductivity values for $MCl(CO)_2(\eta^3-C_3H_4R)(MeCN)_2$ and $[M(CO)_2(\eta^3-C_3H_4R)(MeCN)_3]BF_4$ in ROH (R=H, R=Me).

		$\nu(CO)^a$	Λ_M^a	Λ_M^b
		cm^{-1}	Scm^2mole^{-1}.	
$MCl(CO)_2(\eta^3-C_3H_4R)(MeCN)_2$				
M	R			
Mo	H	1848,1942	72.1	96.2
Mo	Me	1844,1937	72.0	99.6
W	H	1816,1924	85.6	101.1
W	Me	1824,1926	85.4	106.4
$[M(CO)_2(\eta^3-C_3H_4R)(MeCN)_3]BF_4$				
M	R			
Mo	H	1848,1946	75.7	95.7
Mo	Me	1846,1939	77.5	91.2
W	H	1825,1931	c	c
W	Me	1825,1928	c	c

a=in MeOH, b=in H_2O, c=too unstable for measurement.

The close similarities of both NMR and infra-red spectra and conductivity data for the neutral and cationic complexes suggested that dissolving $MCl(CO)_2(\eta^3-C_3H_4R)(MeCN)_2$ in CD_3OD produced $[M(CO)_2(\eta^3-C_3H_4R)(CD_3OD)_3]^+Cl^-$ as the major metal-containing product. Attempts to isolate analogous ionic aqua species by reaction of aqueous solutions of the bis-acetonitrile complexes with various non-coordinating anions were unsuccessful, but on the basis of the above conductrimetric and spectroscopic data it appears likely that

dissolution of $MCl(CO)_2(\eta^3\text{-}C_3H_4R)(MeCN)_2$ in water results in formation of cationic $[M(CO)_2(\eta^3\text{-}C_3H_4R)(H_2O)_3]^+$ as a major species.

All these solution studies were carried out in neutral hydroxylic solvents and there was no evidence of halogeno- or alkoxy-bridged anions $[M_2(CO)_4(\eta^3\text{-}C_3H_4R)_2X_3]^-$ being formed under these conditions. However addition of Ph_4AsCl to basic R'OH (R'=H, Me or Et) solutions of $MCl(CO)_2(\eta^3\text{-}C_3H_4R)(MeCN)_2$ yielded yellow, microcrystalline products which were stable in air for short periods, were readily soluble in chlorinated and ketonic solvents and were identified as the dimeric alkoxy-bridged complexes $Ph_4As[M_2(CO)_4(\eta^3\text{-}C_3H_4R)_2(\mu\text{-}OR')_3]$.

5.3.2 THE COMPLEXES $Ph_4As[M_2(CO)_4(\eta^3\text{-}C_3H_4R)_2(\mu\text{-}OR')_3]$ (M=Mo or W, R=H or Me, R'=H, Me or Et)

INFRA-RED SPECTROSCOPY

Selected infra-red data for these complexes are presented in Table 5.7. The presence of four strong bands in the ν(CO) infra-red region of their solid state spectra is consistent with a confacial bi-octahedral structure for the anions, analogous to that reported for $[Mo_2(CO)_4(\eta^3\text{-}C_3H_5)_2Cl_3]^-$ [269] and shown in Fig. 5.1.

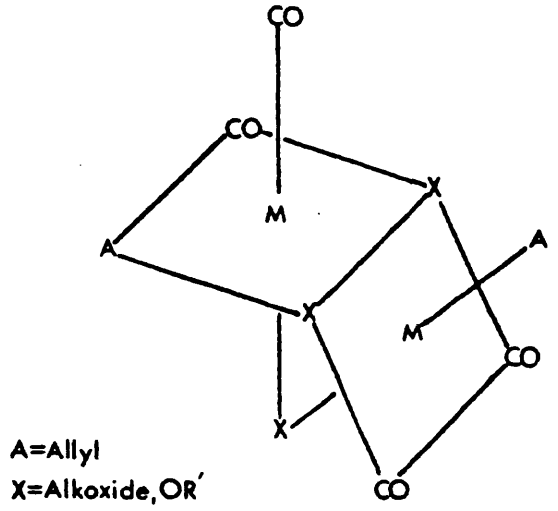

Fig. 5.1 A model of $[M_2(CO)_4(\eta^3\text{-}C_3H_4R)_2(\mu\text{-}OR')_3]^-$.

In CH_2Cl_2 however these bands were unresolved and only two broad absorptions of approximately equal intensity were observed in this region. All these ν(CO) frequencies occur as expected at lower wavenumbers relative to the halo analogues. The region 1600-300cm^{-1} in the infra-red spectra of $Ph_4As[M_2(CO)_4(\eta^3\text{-}C_3H_4R)_2(\mu\text{-}OR')_3]$ where many of the absorptions due to the $[M_2(CO)_4(\eta^3\text{-allyl})_2X_3]^-$ anion might be expected to occur was dominated by bands associated with the tetraphenylarsonium cation, and only a single band of medium intensity between 1050 and 1100cm^{-1} could be positively assigned to the C-O stretching vibrations of the alkoxy groups -OR'. A weak band

at 3650cm^{-1} was associated with -OH stretching vibrations of the tris-hydroxy complex.

Table 5.7 Selected infra-red data for $Ph_4As[M_2(CO)_4(\eta^3\text{-}C_3H_4R)_2(\mu\text{-}OR')_3]$.

Complex			ν(CO)/cm^{-1}		ν(OR')/cm^{-1}	ν(CO)/cm^{-1}
M	R	R'	Nujol mull		Nujol mull	in CH_2Cl_2
Mo	H	H	1911,1894	1801,1775	3650	1900,1795
Mo	H	Me	1890,1878	1788,1772	1055	1902,1790
Mo	H	Et	1906,1890	1790,1778	1106	1906,1890
Mo	Me	Me	1910,1891	1800,1778	1058	1904,1792
Mo	Me	Et	1917,1896	1806,1778	1100	1899,1790
W	H	Me	1896,1878	1789,1768	1051	1880,1782
W	H	Et	1896,1882	1787,1767	1102	1894,1781
W	Me	Me	1898,1879	1795,1774	1052	1897,1782
W	Me	Et	1893,1871	1782,1762	1100	1894,1781

^{1}H AND ^{13}C NMR SPECTROSCOPY

The ^{1}H and ^{13}C NMR chemical shift values for these alkoxy-bridged complexes are given in Tables 5.8 and 5.9, and examples of typical proton NMR spectra are given in Fig. 5.2. In the proton NMR spectra signals of the appropriate intensity associated with the protons of the tetraphenylarsonium cation were observed near 7.9ppm. The two η^3-allyl groups of the anion produced only one set of resonances, however two sets of resonances in the intensity ratio 2:1, attributable to the three bridging alkoxy groups were observed. The related trichloro bridged complexes also produced only one set of resonances due to the two allyl groups over the temperature range +55 to -120°C [298], suggesting that the species either adopts a more

Table 5.8 ^{1}H NMR data[a] for $Ph_4As[M_2(CO)_4(\eta^3\text{-}C_3H_4R)_2(\mu\text{-}OR')_3]$.

Complex			Chemical shift δ(ppm)				
M	R	R'	H_{anti}	Allyl H_{syn}	$H_{central}$	Aliphatic OR'	Aromatic Ph
Mo	H	Et	2.83d	0.52d	2.15m	1.34t,1.48t, 4.54q,4.88q	7.89m
Mo	Me	Et	2.62s	0.27s	1.82s	1.17t,1.73t, 3.63q,4.88q	7.86m
Mo	H	Me	2.90d (6.3)	0.36d (9.0)	2.92m	4.07s,4.62s	7.88brm
Mo	Me	Me	2.70s	0.34s	1.79s	3.81s,4.96s	7.88brm
Mo	H	H	2.99d	0.42d	3.04m	-	7.93m
W	H	Et	2.76d	0.74d	2.54m	1.30t,1.42t, 4.56q,4.71q	7.83m
W	Me	Et	2.51s	0.75s	1.97s	1.22t,1.58t, 3.64q,3.96q	7.82
W	H	Me	2.83d	0.56d	3.18m	3.94s,4.62s	7.90m
W	Me	Me	2.62s	0.64s	1.96s	3.91s,5.01s	7.80brm

[a]=Measured in $(CD_3)_2CO$ at room temperature,
-=Not observed.

Table 5.9 ^{13}C NMR data[a] for $Ph_4As[M_2(CO)_4(\eta^3\text{-}C_3H_4R)_2(\mu\text{-}OR')_3]$.

Complex			Chemical shift δ(ppm)[b]						
M	R	R'	CO	C_t	C_c	Me	Aliphatic (OR')		Aromatic (Ph)
Mo	H	Et	234.7	55.11	75.64		20.99	57.40	131.93-135.37
Mo	Me	Et	234.2	55.43	75.06	18.26	20.80	57.52	131.86-135.43
Mo	H	Me	234.1	55.00	74.93		49.40		131.80-135.40
Mo	Me	Me	233.6	55.90	74.40	19.60	49.40		131.90-135.40
Mo	H	H	234.3	55.24	74.87		[c]		131.86-135.37
W	H	Et	239.8	57.45	67.33		20.27	47.96	131.86-135.37
W	Me	Et	235.7	57.58	67.30	21.93	20.32	47.84	131.85-135.39
W	H	Me	229.6	49.39	67.26		47.70		131.70-135.38
W	Me	Me	230.8	49.70	67.20	22.60	47.20		131.50-135.10

[a]=Measured in $(CD_3)_2CO$ at room temperature, [b]=C_t and C_c represent terminal and central allylic carbon nuclei respectively, [c]=OH resonance not detected

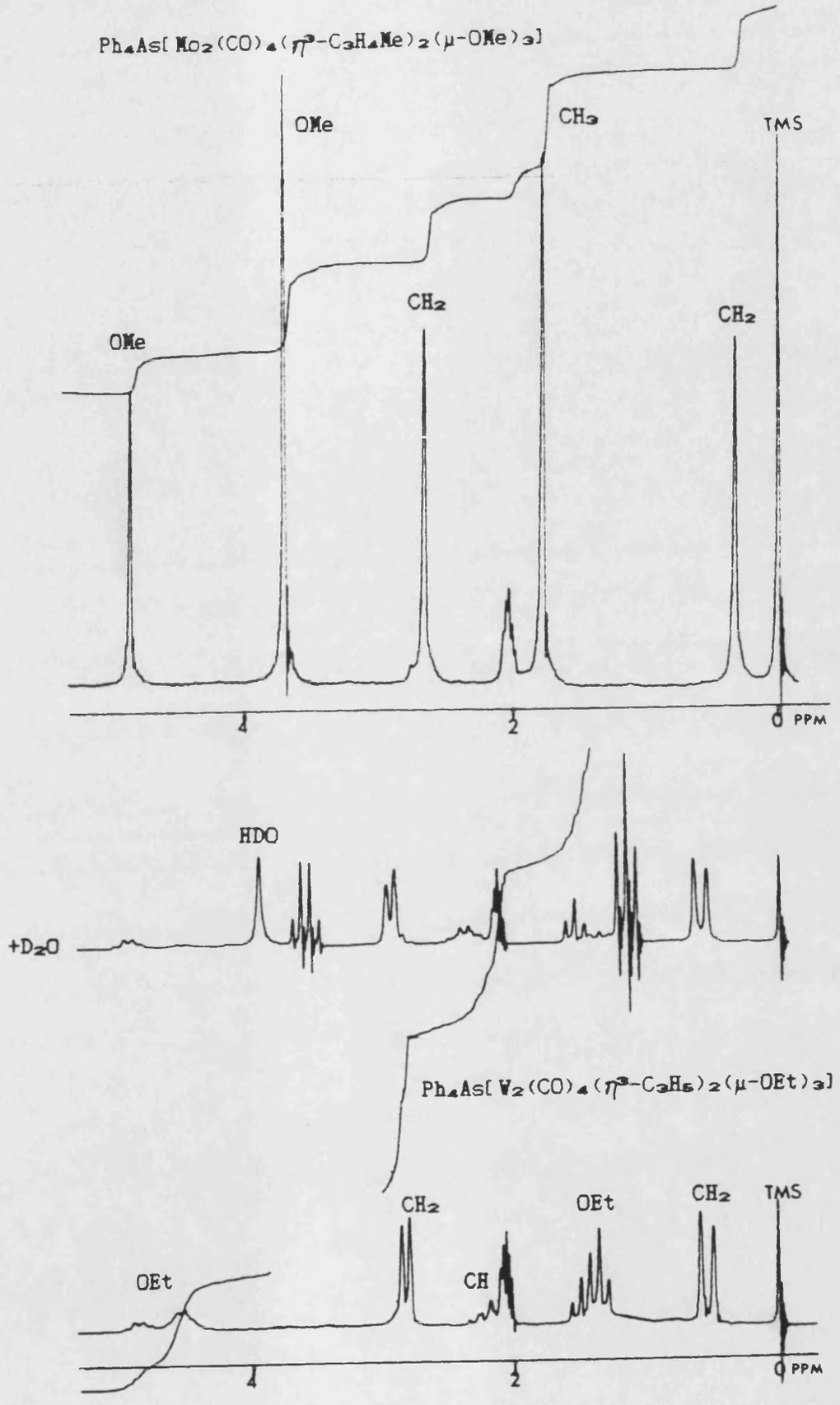

Fig. 5.2 Part of the ^{1}H NMR spectra of $Ph_4As[M_2(CO)_4(\eta^3\text{-}C_3H_4R)_2(\mu\text{-}OR')_3]$ (M=W, R=H, R'=Et and M=Mo, R=Me, R'=Me) in $(CD_3)_2CO$ at 25°C.

symmetrical structure than that observed for the solid [269], or that any dynamic rearrangement process has a very low activation energy. Molecular models of the alkoxy complexes suggest that the resonance patterns may be attributed to a species in which two of the bridging groups are in identical magnetic environments which differ from that of the third, and in which the two allyl groups are either in equivalent magnetic environments or dynamic about the metal-allyl bond. Thus the more intense peak in the spectra of the methoxy complexes can be assigned to the two equivalent -OMe groups and the weaker peak at lower field to the unique -OMe. This explanation also accounts for the observed proton NMR spectra of the tris-μ-ethoxy complexes, which contain two distinct sets of triplet and quartet resonances in the ratio 2:1. ^{1}H NMR signals for the -OH resonances of the tris-μ-hydroxy complex were not observed however, possibly due to rapid proton exchange with the solvent.

Thus it has been shown that the behaviour of $MCl(CO)_2(\eta^3-C_3H_4R)(MeCN)_2$ in neutral hydroxylic solvents differs from that in chlorinated and ketonic solvents with no evidence of autoionisation in CD_3OD or D_2O. Solvation of the bis-acetonitrile complexes in neutral or basic methanol or water (R'OH) results in the formation of $[M(CO)_2(\eta^3-C_3H_4R)(HOR')_3]^+$ and $[M_2(CO)_4(\eta^3-RC_3H_4)_2(\mu-OR')_3]^-$ respectively as the major solution species. Reactions of the neutral solutions of $MCl(CO)_2(\eta^3-RC_3H_4)(MeCN)_2$ with bidentate and tridentate nitrogen-donor ligands are described in the following section.

5.3.3 REACTIONS OF $M(CO)_2(\eta^3\text{-}C_3H_4R)(MeCN)_2X$ (X=HALIDE) WITH BIDENTATE AND TRIDENTATE NITROGEN LIGANDS IN AQUEOUS SOLUTIONS

Addition of bidentate (L_2) ligands 2,2'-bipyridyl (bipy) or 2,2'-dipyridylamine (dpa) to hot aqueous solutions of $MCl(CO)_2(\eta^3\text{-}C_3H_4R)(MeCN)_2$ (M=Mo or W, R=H or Me) yielded precipitates of the neutral complexes $MCl(CO)_2(\eta^3\text{-}C_3H_4R)L_2$ which were spectroscopically identical to the products previously obtained by reaction of $M(CO)_4L_2$ with the appropriate allyl halide [175,273]. Similar aqueous reactions with the potentially tridentate (L_3) ligands diethylenetriamine (dien) and bis-(2-pyridylmethyl)amine (bpma) produced a new series of yellow or orange air-stable complexes $M(CO)_2(\eta^3\text{-}C_3H_4R)L_3X$ (X=halide) in which the dien or bpma either behave as bidentates and the halide remains coordinated or L_3 acts as a tridentate with the halide present as an uncoordinated anion. Structurally constrained L_3 ligands such as terpyridyl frequently adopt a bidentate mode of bonding [304], but both dien and bpma possess less rigid carbon skeletons and are known to bond to transition metals in either a bidentate, or more commonly a tridentate manner [305]. In order to determine the correct formulation for these new dien and bpma complexes, and to explore the possibility that different structures may be adopted in solid and solution states the complexes were examined by a range of physical and spectroscopic techniques.

5.3.3.1 COMPLEXES WITH GENERAL FORMULA $M(CO)_2(\eta^3\text{-}C_3H_4R)L_3X$ OR $[M(CO)_2(\eta^3\text{-}C_3H_4R)L_3]X$

INFRA-RED AND CONDUCTIVITY MEASUREMENTS

Selected solid state and solution infra-red data are presented in Table 5.10. The complexes were of low solubility in chlorinated solvents, but were soluble in methanol. The $\nu(CO)$ region of their infra-red spectra both in this solvent and in the solid state showed two bands of almost equal intensity between 1800 and

Table 5.10 Selected infra-red data[a] for $M(CO)_2(\eta^3\text{-}C_3H_4R)L_3X$ or $[M(CO)_2(\eta^3\text{-}C_3H_4R)L_3]X$

M	R	X	L_3	$\nu(CO)cm^{-1}$ in MeOH	$\nu(CO)cm^{-1}$ as Nujol mulls	$\nu(NH)cm^{-1}$ as Nujol mulls	$R^b cm^{-1}$
Mo	H	Cl	dien	1831,1926	1827,1924	3122,3170,3201	
Mo	H	Br	dien	1829,1929	1824,1924	3135,3173,3218	
Mo	H	I	dien	1833,1931	1829,1931	3128,3210,3420	
Mo	Me	Cl	dien	1831,1934	1832,1930	3105,3216,3346	
Mo	H	Cl	bpma	1835,1936	1832sh,1856 1930	3218,3318, 3460	1631m,1608s, 1568w
Mo	Me	Cl	bpma	1837,1934	1837sh,1861 1938	3220,3315, 3465	1630m,1606s, 1569w
W	H	Cl	dien	1824,1922	1819,1919	3100,3157,3185	
W	Me	Cl	dien	1820,1925	1818,1924	3065,3170,3320	
W	H	Cl	bpma	1825,1927	1829sh,1852 1928	3195,3300, 3356	1633m,1607s, 1569w
W	Me	Cl	bpma	1828,1931	1815sh,1844 1925	3200,3290, 3490	1635m,1608s, 1569w

[a] all bands strong unless otherwise stated

[b] ring deformations

1940cm^{-1}, typical of cis-dicarbonyl groups. No metal-chlorine absorptions were observed in the far infra-red spectra of these solid compounds between 300 and 200cm^{-1} and ν(CO) values for Mo(CO)$_2$(η^3-C_3H_5)dienX showed no apparent dependence upon the nature of the halogen, X.

For both dien and bpma complexes, bands associated with the ν(N-H) stretching vibrations of the ligand L_3 were found in the range 3470 to 3065cm^{-1}, at lower frequencies than ν(N-H) in the uncomplexed ligands. The ν(N-H) stretching frequencies of the dien ligand were different for the allyl and 2-methylallyl chloro complexes, presumably as a result of interaction between L_3 and the central allylic proton or methyl substituent. The central aliphatic nitrogen in these ligands is the most basic donor of the three N-groups and is unlikely to remain uncoordinated in these complexes and thus bidentate coordination of L_3 should result in a terminal uncoordinated N-donor group. Absorptions resulting from ring deformations of the pyridine groups in the bpma complexes were found between 1635 and 1568cm^{-1}. It has been shown [305] that changes in frequency arising from these ring deformations reflect the degree of coordination of bpma to metal centres, the highest energy pyridine ring deformation at 1590cm^{-1} (8a) increasing in frequency upon coordination (+15-20cm^{-1}), whilst the second highest frequency (8b) remains virtually unchanged at 1570cm.$^{-1}$. Thus complexes in which bpma is coordinated through both pyridine rings (tridentate) exhibit two bands in their infra-red spectra, one at ca. 1600 to 1610cm^{-1} and the other at ca. 1570cm^{-1}, whilst complexes with only one coordinated pyridine ring (bidentate) show three bands between 1610 and 1565cm^{-1}, with the central one at ca. 1590cm^{-1} being at almost the same frequency as 8a of the free ligand. All the complexes with an overall formula of MCl(CO)$_2$(η^3-C_3H_4R)bpma exhibit two deformation

bands in this region, with δb within ±1cm^{-1} of the free ligand and δa showing an increase of 18±1cm^{-1} compared to free bpma. A third absorption of medium intensity is present at ca. 1630cm^{-1}, however this is approximately 40cm^{-1} higher than the band at ca. 1590cm^{-1} normally observed for species containing a bidentate bpma ligand and therefore cannot be used with confidence to identify bidentate coordination of bpma in $MCl(CO)_2(\eta^3\text{-}C_3H_4R)$bpma.

Conductivity measurements for both dien and bpma complexes as 10^{-3}M solutions in methanol resulted in the molar conductivity values given in Table 5.11, being in the range 80 to 115 Scm^{2}mole^{-1} which Geary [99] suggested was typical of 1:1 ionic complexes.

Table 5.11 Molar conductivity values for $M(CO)_2(\eta^3\text{-}C_3H_4R)L_3X$ or $[M(CO)_2(\eta^3\text{-}C_3H_4R)L_3]X$.

Complex	Mo,dien		Mo,bpma		W,dien		W,bpma	
	R=H	R=Me	R=H	R=Me	R=H	R=Me	R=H	R=Me
Λ^a_M	94.4	89.9	90.3	87.8	89.4	91.0	84.5	92.6

Λ^a_M=Molar conductivity values in MeOH, units of Scm^{2}mole^{-2}

^{1}H NMR DATA

The Mo and W complexes were insufficiently soluble in D_2O at room temperature to obtain good quality proton NMR spectra, however this was resolved for the former by warming solutions of the samples to +85°C, whilst spectra for the tungsten complexes could be obtained at room temperature using CD_3OD solutions. These conditions were insufficient however to allow ^{13}C NMR data to be obtained. Selected ^{1}H NMR data for the Mo and W complexes in D_2O and CD_3OD respectively are presented in Table 5.12 and examples of typical spectra are shown in Fig. 5.3.

Table 5.12 ^{1}H NMR data for $M(CO)_2(\eta^3\text{-}C_3H_4R)L_3X$ in CD_3OD^a or D_2O^c.

Complex			Solvent	Chemical shift δ(ppm), (coupling constant J in Hz)					
				Allyl			L_3		N-H
M	R	L_3		H_{syn}	H_{anti}	$H_{central}$ or Me	Aliphatic	Aromatic	
Mo	H	dien	D_2O	3.14d(6.5)	1.14d(9.3)	3.79tt	2.78m,3.2*m		
Mo	Me	dien	D_2O	2.82s	1.11s	2.05s	2.8*m,3.18m,3.24m		
Mo	H	bpma	D_2O	3.54d(6.4)	1.61d(9.5)	4.06tt	4.45[b]	7.38m,7.81m,8.88m	
Mo	Me	bpma	D_2O	3.45s	1.59s	1.95s	4.51[b]	7.41m,7.86m,8.87m	
W	H	dien	CD_3OD	3.3br	1.08d(9.2)	3.7*	2.78m,3.17m,4.3br		7.65br
W	Me	dien	CD_3OD	2.68s	1.10s	2.18s	2.8*m, 3.35*m,4.22br		7.60br
W	H	bpma	CD_3OD	3.2*br(6.4)	1.66d(9.4)	4.3*	4.52[b]	7.38m,7.84m,8.98m	
W	Me	bpma	CD_3OD	3.14s	1.74s	2.00s	4.52[b]	7.43m,7.89m,8.94m	

[a]=Measured at 28°C, [b]=Centre of AB quartet, [c]=Measured at 85°C.
*=partially or wholly obscured by solvent or ligand peaks,

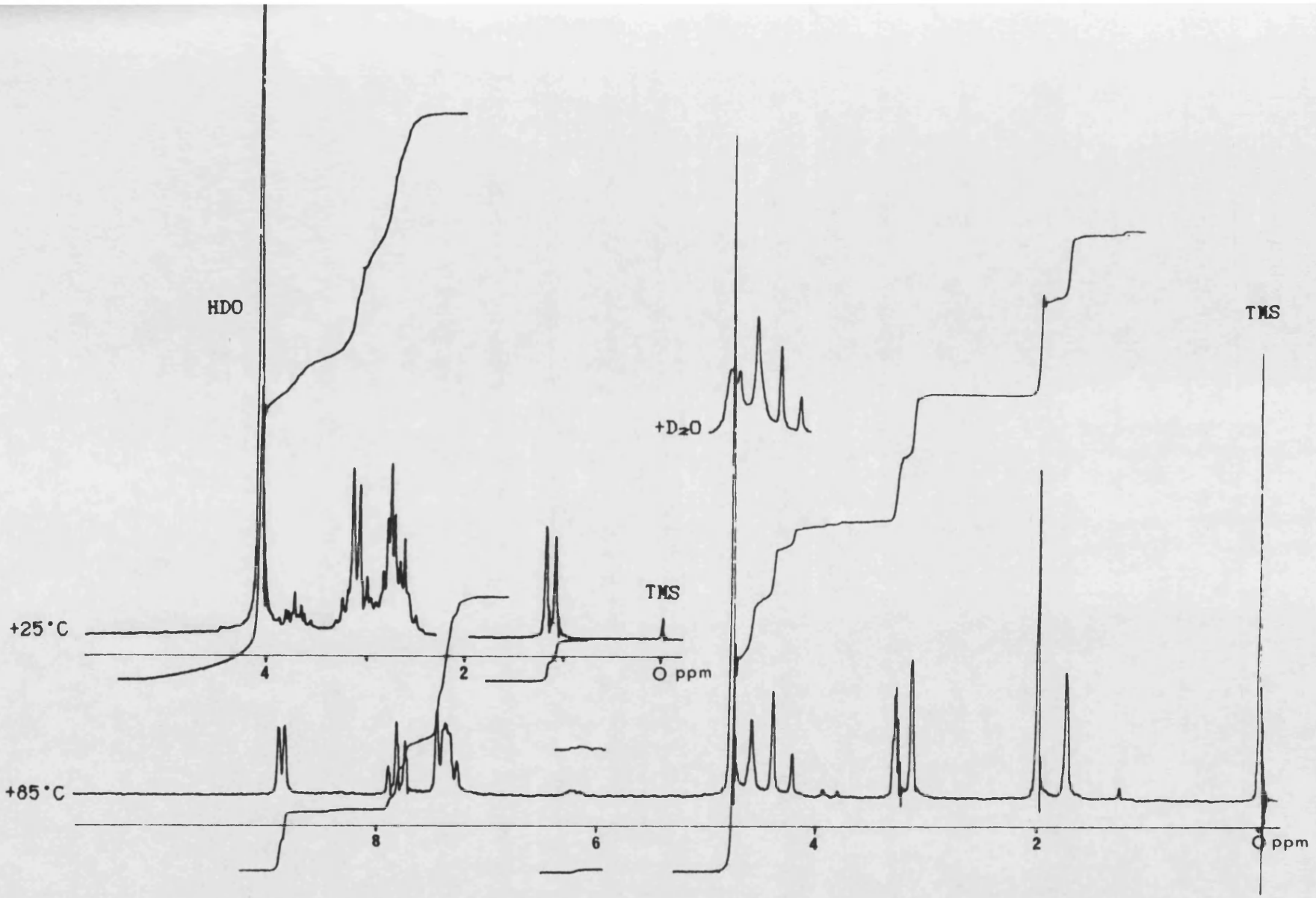

Fig. 5.3 ^{1}H NMR spectra of $MoCl(CO)_2(\eta^3\text{-}C_3H_5)$dien in D_2O (25°C) and $WCl(CO)_2(\eta^3\text{-}C_3H_4Me)$bpma in CD_3OD (85°C).

The $H_{central}$, H_{syn} and H_{anti} allylic protons of $MCl(CO)_2(\eta^3\text{-}C_3H_5)L_3$ in either solvent appeared as a triplet of triplets and two doublets (J_{syn} 6.5Hz, J_{anti} 9.3Hz) respectively, however in several instances the lower field resonances were either wholly or partially obscured by solvent peaks, the multiplet resonances associated with the methylene and NH_2 protons of dien (2.8-4.2ppm) or by the AB quartet arising from the methylene protons of bpma (4.3-4.7ppm). Some overlapping also occurred between these peaks and the H_{syn} singlet of $MCl(CO)_2(\eta^3\text{-}C_3H_4Me)L_3$, however the H_{anti} and C-Me singlets were clearly resolved at ca. 1.1 and 2.1ppm (dien) or 1.6 and 2.0ppm (bpma) respectively. Peaks due to N-H and NH_2 in dien and N-H in bpma were absent in D_2O, and in CD_3OD the weak broad signals for the NH_2 of dien near 7.6ppm and the absence of coupling of N-H to the AB quartet of bpma indicated deuteration was occurring.

DISCUSSION

Tridentate coordination of L_3 in an ionic complex of the type $[M(CO)_2(\eta^3\text{-}C_3H_4R)L_3]^+Cl^-$ is indicated by the conductivity data, by the absence of ν(M-Cl) IR absorptions, and is consistent with similarities between the solid state ν(CO) values and ^{1}H NMR data for the chloro complexes and their PF_6^- derivatives which are reported in the next section. The presence of three ν(N-H) absorptions for the halo complexes (L_3=dien or bpma) in contrast to the one (bpma) or two (dien) bands observed for the PF_6^- derivatives, may arise from hydrogen bonding between the central N-H groups and the halo anions as indicated by a successive increase in ν(N-H) values of Cl<Br<I for the series $Mo(CO)_2(\eta^3\text{-}C_3H_5)dienX$. Only the ambiguous IR evidence may be interpreted in terms of anything other than tridentate coordination of the ligand L_3.

Reaction of mixtures of aqueous $MCl(CO)_2(\eta^3\text{-}C_3H_4R)(MeCN)_2$ and L_3 with NH_4PF_6 yielded the new complexes $[M(CO)_2(\eta^3\text{-}C_3H_4R)L_3]PF_6$ which have been fully identified by spectroscopic methods and the structure of the major crystalline form of $[W(CO)_2(\eta^3\text{-}C_3H_5)bpma]PF_6$ has been established by X-ray diffraction analysis.

5.3.3.2 THE COMPLEXES $[M(CO)_2(\eta^3\text{-}C_3H_4R)L_3]PF_6$ (L_3=dien or bpma)

These air-stable, orange crystalline complexes were readily soluble in chlorinated and ketonic solvents and as $10^{-3}M$ solutions in methanol gave molar conductivity values of between 103 and 114 Scm^2mole^{-1} typical of 1:1 ionic species in this solvent [99]. These values together with selected solid state infra-red data for $[M(CO)_2(\eta^3\text{-}C_3H_4R)L_3]PF_6$ are given in Table 5.13 and all data confirm that the L_3 ligands behave as tridentates.

Table 5.13 Selected infra-red data[a,b] and molar conductivities[c] (Λ_M) for $[M(CO)_2(\eta^3\text{-}C_3H_4R)L_3]PF_6$.

M	R	L_3	ν(CO)	ν(NH)	R 8a	R 8b	PF_6^-	Λ_M
Mo	H	dien	1830,1926	3346,3298			830	113.1
Mo	Me	dien	1833,1922	3340,3295			838	110.8
Mo	H	bpma	1850,1935	3322	1610,1570		839	103.6
Mo	Me	bpma	1847,1936	3322	1610,1569		835	105.9
W	H	dien	1820,1920	3328,3293			838	114.3
W	Me	dien	1820,1925	3331,3296			837	112.5
W	H	bpma	1840,1933	3318	1611,1568		835	102.7
W	Me	bpma	1842,1933	3315	1612,1571		838	104.4

[a]=as Nujol mulls, units of cm^{-1} [b]=ring deformations, R

[c]=in MeOH, units of Scm^2mole^{-1}

5.3.3.3 THE MASS SPECTRA OF COMPLEXES $MCl(CO)_2(\eta^3\text{-}RC_3H_4)L_3$ AND $[M(CO)_2(\eta^3\text{-}RC_3H_4)L_3]PF_6$

Following this study of the solution behaviour of $MCl(CO)_2(\eta^3\text{-}C_3H_4R)(MeCN)_2$ and the preparation of the complexes $MCl(CO)_2(\eta^3\text{-}C_3H_4R)L_2$, $[M(CO)_2(\eta^3\text{-}C_3H_4R)L_3]^+Cl^-$ and $[M(CO)_2(\eta^3\text{-}C_3H_4R)L_3]PF_6$, the author supplied samples of the hexafluorophosphate species to Brisdon and Floyd [306] who carried out an examination of the FAB positive ion mass spectra of these complexes and of $MoCl(CO)_2(\eta^3\text{-}C_3H_4R)L_2$ (L_2=bipy or $(py)_2$) in glycerol. These spectra were compared to those generated by $MCl(CO)_2(\eta^3\text{-}C_3H_4R)(MeCN)_2$ (M=Mo, R=H, M=W, R=Me) in a glycerol matrix doped with ligands L_2, dien or bpma. The neutral acetonitrile complexes produced spectra in which $[M(CO)_2(\eta^3\text{-}C_3H_4R)(glycerol)]^+$ were the major metal-containing ions and no evidence of metal-MeCN or metal-Cl containing ions was observed. Attempts to obtain negative ion spectra for the acetonitrile complexes in glycerol were unsuccessful, confirming the observations based on NMR data in section 5.3.1 that in neutral hydroxylic solvents metal-cation rather than metal-anion formation is favoured. Addition of methanol to these mixtures produced ion peaks due to binuclear species $[M_2(CO)_4(\eta^3\text{-}C_3H_4R)_2(glycerol\text{-}H)]^+$. FAB positive ion spectra for $MoCl(CO)_2(\eta^3\text{-}C_3H_5)L_2$ and for $MoCl(CO)_2(\eta^3\text{-}C_3H_5)(MeCN)_2$ in glycerol doped with L_2 were found to be identical, containing both $[M\text{-}Cl]^+$ and related fragments and ions due to replacement of L_2 or chloride ligands by glycerol. Similarly the complexes $[M(CO)_2(\eta^3\text{-allyl})L_3]PF_6$ and $MCl(CO)_2(\eta^3\text{-}C_3H_4R)(MeCN)_2$ (M=Mo, R=H, M=W, R=Me) in L_3 doped glycerol produced identical spectra, but here no replacement of L_3 by glycerol was observed. The behaviour of the neutral and cationic complexes were shown to closely parallel that observed earlier in hydroxylic solvents R'OH and indicated that

this technique can provide a valuable aid in studying solution reactions under appropriate conditions.

Following these initial results, this author subsequently examined the FAB positive ion spectra for those complexes not previously studied, i.e. $MCl(CO)_2(\eta^3-C_3H_4R)L_3$ (M=Mo or W, R=H or Me), $[Mo(CO)_2(\eta^3-C_3H_4R)L_3]PF_6$ and $[W(CO)_2(\eta^3-C_3H_5)L_3]PF_6$ (L_3=dien or bpma). These results are presented in Tables 5.14 and 5.15, and examples of typical FAB mass spectra for the chloro and hexafluorophosphate complexes in glycerol are given in Fig. 5.4. In agreement with the observations made by Brisdon and Floyd, the hexafluorophosphate salts produced the ions $[M(CO)_2(\eta^3-C_3H_4R)L_3(glycerol)_n]^+$ and $[M(CO)_2(\eta^3-C_3H_4R)L_3]^+$ showing that the tridentate was not replaced by glycerol. Comparison of the major m/z values and assignments in Tables 5.14 and 5.15 for $MCl(CO)_2(\eta^3-C_3H_4R)L_3$ and the hexafluorophosphate salts shows the close similarity of spectra for these two types of complex. Thus the highest m/z values for mono-nuclear metal-containing ions in the spectra of $MCl(CO)_2(\eta^3-C_3H_4R)L_3$ were also those for $[M(CO)_2(\eta^3-C_3H_4R)L_3(glycerol)_n)]^+$ (n=0 to 2). Ion peaks with m/z values corresponding to ([M] +[M-Cl]) where [M] = $M(CO)_2(\eta^3-C_3H_4R)L_3Cl$ are of interest and probably reflect the formation within the mass spectrometer of either a chloro-bridged dimer of the type $[(M(CO)_2(\eta^3-C_3H_4R)L_3)_2-\mu-Cl]^+$ or a dimer in which L_3 is a bridging ligand, being coordinated to one metal atom as a bidentate with the third N-donor atom bonded to the second metal. The former has a precedent in the related dimer $[(Mo(CO)_2(\eta^3-C_3H_5)bipy)_2-\mu-Cl]BF_4$ [286], and this fact together with the absence of ion peaks above [M]+[M-Cl] values due to other polymeric species of the latter type favours the chloro-bridged formulation.

Table 5.14 FAB mass spectral data for $MCl(CO)_2(\eta^3\text{-}C_3H_4R)L_2$ in glycerol.

Complex			m/z values, relative abundance and assignments^
M	R	L_2	
Mo	H	dien	632.5,15,([M]+[M-Cl]);482,18,([M-Cl]+glycerol);425.5,22,([M]+2glycerol); 390,85,([M-Cl]+glycerol);333.5,42,[M];298,100,[M-Cl]; 270,18,([M-Cl]-CO);242,12,([M-Cl]-2CO)
Mo	Me	dien	659.5,38,([M]+[M-Cl]);496,13,([M-Cl]+glycerol);404,58,([M-Cl]+glycerol); 347.5,25,[M];312,100,[M-Cl],284,10,([M-Cl]-CO);256,23,([M-Cl]-2CO)
Mo	H	bpma	823.5,46,([M]+[M-Cl]);519,13,([M]+glycerol);429.5,51,[M]; 394,100,[M-Cl];366,13,([M-Cl]-CO);338,23,([M-Cl]-2CO)
Mo	Me	bpma	851.5,57,([M]+[M-Cl]);535.5,28,([M]+glycerol);500,33,[M-Cl]; 408,100,[M];380,12,([M-Cl]-CO);352,22,([M-Cl]-2CO)
W	H	dien	568,45,([M-Cl]+2glycerol);511.5,100,([M]+glycerol); 476,88,([M-Cl]+glycerol);419.5,45,[M];384,76,[M-Cl]; 356,12,([M-Cl]-CO);328,26,([M-Cl]-2CO)
W	Me	dien	582,21,([M-Cl]-2glycerol);525.5,77,([M]+glycerol); 490,85,([M-Cl]+glycerol);433.5,36,[M];398,100,[M-Cl]
W	H	bpma	494,21,[M];480,100,[M-Cl];452,25,([M-Cl]-CO); 424,43,([M-Cl]-2CO)
W	Me	bpma	1023.5,47,([M]+[M-Cl);586,45,([M-Cl]+glycerol);529.5,82,[M]; 494,100,[M-Cl];465,8,([M-Cl]-CO);437,33,([M-Cl]-2CO)

^=Based on mol.wt. Mo=98 and W=184 with [M] representing m/z of the neutral molecule.

Table 5.15 FAB mass spectral data for $[M(CO)_2(\eta^3\text{-}C_3H_4R)L_3]PF_6$ in glycerol.

Complex			m/z values, relative abundance and assignments[a]
M	R	L_3	
Mo	H	dien	390, 6.7, ([M]+glycerol); 298, 100, [M]; 270, 17.3, ([M]-CO); 242, 10.6, ([M]-2CO)
Mo	Me	dien	404, 82, ([M]+glycerol); 312, 100, [M]; 284, 12, ([M]-CO); 256, 18, ([M]-2CO)
Mo	H	bpma	492, 10.7, ([M]+glycerol); 394, 100, [M]; 366, 10.0, ([M]-CO); 338, 13.0, ([M]-2CO); 296, 14.7, ([M]-2CO-C_3H_6)[b]
Mo	Me	bpma	500, 8.3, ([M]+glycerol); 408, 100, [M]; 380, 11.1, ([M]-CO); 352, 15.2, ([M]-2CO)
W	H	dien	476, 9.4, ([M]+glycerol); 384, 100, [M]; 356, 12.5, ([M]-CO); 328, 13, ([M]-2CO)
W	Me	dien	582, 5.4, ([M]+2glycerol); 490, 16.1, ([M]+glycerol); 398, 100, [M]; 342, 18.0, ([M]+glycerol-2CO)[b]
W	H	bpma	572, 10.0, ([M]+glycerol); 480, 100, [M]; 452, 12, ([M]-CO); 424, 31, ([M]-2CO); 383, 37, ([M]-2CO-C_3H_6)
W	Me	bpma	494, 5.7, [M]; 438, 1.7, ([M]-2CO)

[a]=Based on mol.wt. Mo=98 and W=184, [M] representing m/z of the cation
[b]=Reference 306

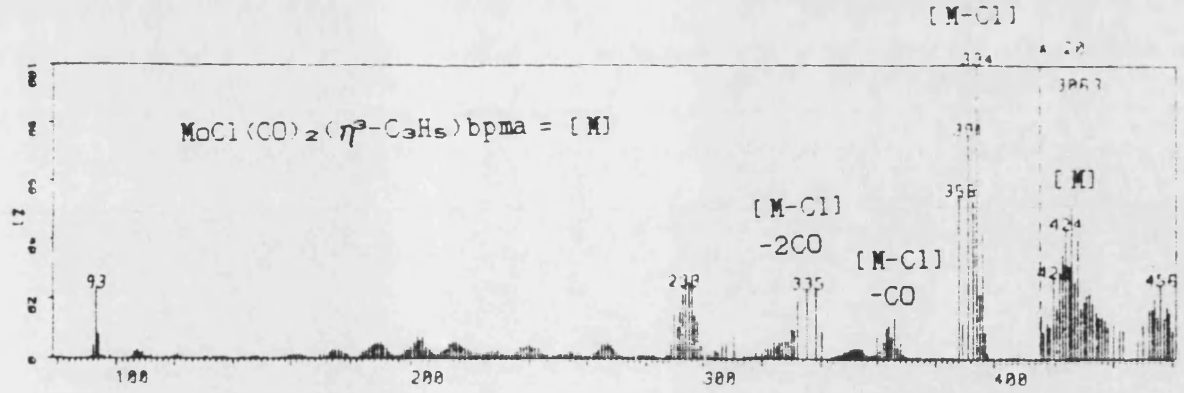

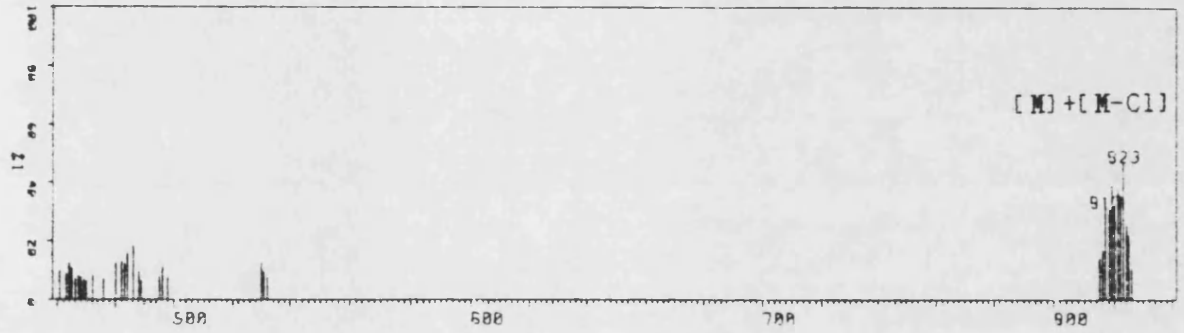

G=glycerol

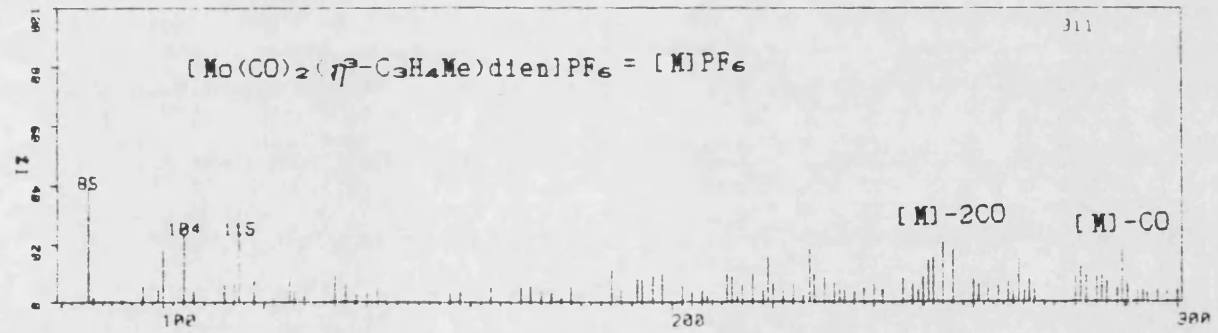

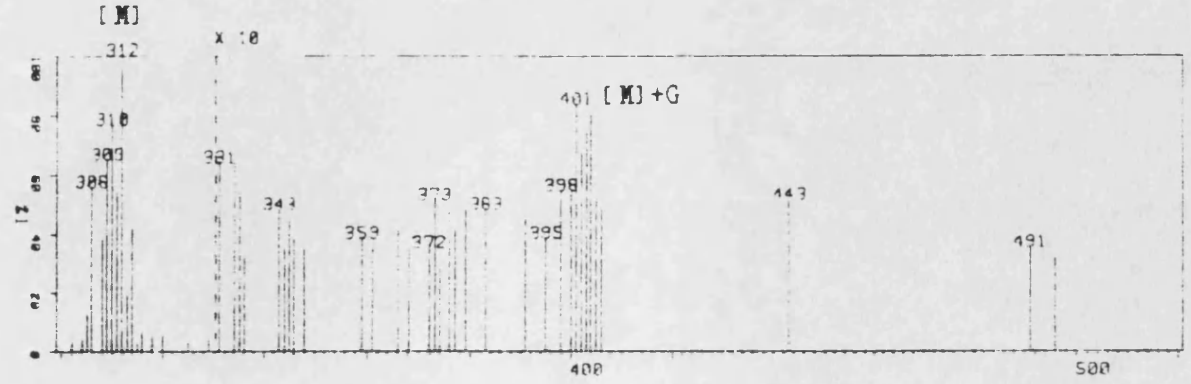

Fig. 5.4 FAB mass spectra of $MoCl(CO)_2(\eta^3\text{-}C_3H_5)bpma$ and $[Mo(CO)_2(\eta^3\text{-}C_3H_4Me)dien]PF_6$ in glycerol.

NMR SPECTRA OF $[M(CO)_2(\eta^3\text{-}C_3H_4R)L_3]PF_6$

The ^1H and ^{13}C NMR spectra of $[M(CO)_2(\eta^3\text{-}C_3H_4R)L_3]PF_6$ in $(CD_3)_2CO$ were obtained at ambient temperature and these data are presented in Tables 5.16 and 5.17. The chemical shifts of the allylic protons were found to be sensitive to the nature of the tridentate and variable temperature studies showed that these systems were dynamic. On cooling to -102°C, the proton NMR spectrum of the dien complexes lost fine structure and the allyl resonances, the two AA'BB' multiplets of the methylene protons of the dien and the NH and NH_2 signals of the coordinated amine overlapped and appeared as broad signals. However at -80°C proton signals for the allyl and amine ligands in the corresponding bpma complexes did not overlap and clearly resolved spectra were obtained. Fig. 5.5 shows the proton NMR spectra of $[Mo(CO)_2(\eta^3\text{-}C_3H_5)bpma]PF_6$ between +28°C and -80°C.

At -80°C the allyl group in $[Mo(CO)_2(\eta^3\text{-}C_3H_5)bpma]PF_6$ produced an ABMNX spin pattern and the two pyridine rings of the bpma ligand were shown to be in different environments by the splitting of each of the three aromatic signals into two components of equal intensity. The decoupled spectrum at this temperature showed two overlapping AB quartets indicating the non-equivalence of the bpma methylene groups. At room temperature and above N-H coupling (ca. 6Hz) to two of the bpma methylene protons was observed which was lost on addition of D_2O, resulting in the formation of a single AB quartet.

Table 5.16 ^{1}H NMR data[^] for $[M(CO)_2(\eta^3\text{-}C_3H_4R)L_3]PF_6$.

Complex			Chemical shift δ(ppm), (coupling constant J in Hz)					
			Allyl			L_3		N-H
M	R	L_3	H_{syn}	H_{anti}	$H_{central}$ or Me	Aliphatic	Aromatic	
Mo	H	dien	3.21d(6.5)	1.02d(9.3)	3.81tt	2.94m, 3.25*m		7.28br
Mo	Me	dien	2.88s	0.93s	2.06s	2.9*m, 3.06m, 3.3m		7.15br
Mo	H	bpma	3.59d(6.3)	1.59d(9.5)	4.09tt	4.64■	7.48m, 7.90m, 9.00m	5.79br
Mo	Me	bpma	3.48s	1.56s	1.92s	4.60■	7.52m, 7.96m, 9.02m	5.42br
W	H	dien	3.0*(6.4)	1.10d(9.6)	*	3.0brm, 3.4brm, 4.1brm		7.35br
W	Me	dien	2.82s	1.12s	2.25s	3.0brm, 3.4brm, 4.1brm		7.36br
W	H	bpma	3.34br	1.72d(9.4)	*	4.76■	7.49m, 7.96m, 9.02m	5.51br
W	Me	bpma	3.21s	1.78s	2.06s	4.70■	7.53m, 8.00m, 9.03m	5.68br

[^]=Measured in $(CD_3)_2CO$ at r.t.
■=Centre of AB quartet
*=wholly or partially obscured by solvent or ligand peaks

Table 5.17 ^{13}C NMR data[a] of $[M(CO)_2(\eta^3\text{-}C_3H_4R)L_3]PF_6$.

Complex			Chemical shift δ(ppm)[b]					
M	R	L_3	CO	C_t	C_c	Me	Aliphatic	Aromatic
Mo	H	dien	226.1	55.4	68.2		42.0,52.3	
Mo	Me	dien	226.4	55.2	80.5	20.0	41.8,51.2	
Mo	H	bpma	226.5	58.2	71.5		61.1	124.0-159.0
Mo	Me	bpma	226.7	60.8	84.8	20.3	60.8	124.1-159.0
W	H	dien	218.9	47.3	59.1		42.4,52.8	
W	Me	dien	219.4	47.0	69.7	19.1	42.4,51.5	
W	H	bpma	219.8	50.3	62.1		61.6	124.0-159.0
W	Me	bpma	219.5	49.5	75.5	19.0	61.0	124.0-159.0

[a]=Measured in $(CD_3)_2CO$ at room temperature, [b]=C_t and C_c represent terminal and central allylic carbon nuclei respectively.

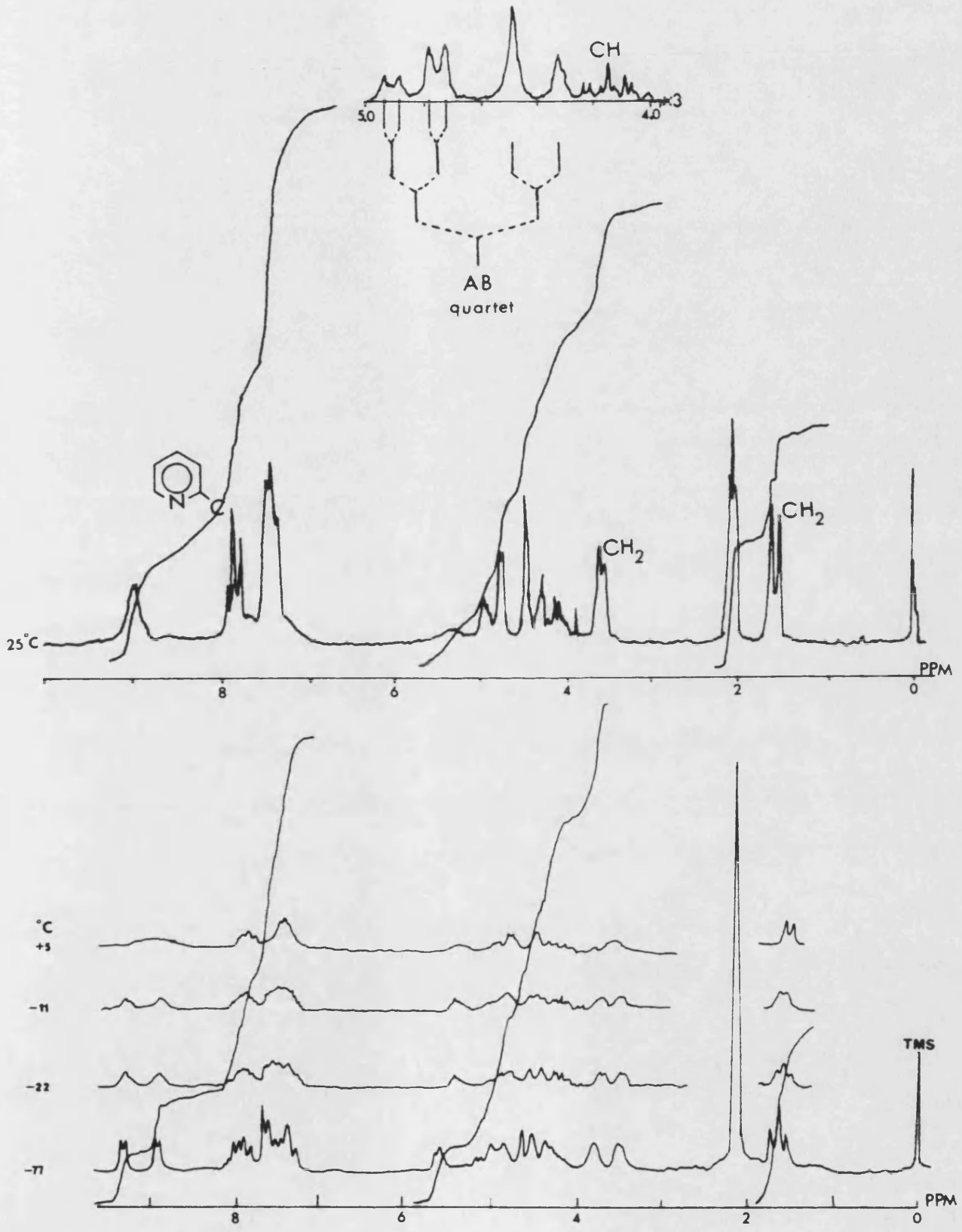

Fig. 5.5 Variable temperature ^1H NMR spectra of

[Mo(CO)$_2$(π^3-C$_3$H$_5$)bpma]PF$_6$ in (CD$_3$)$_2$CO.

These results are consistent with a restricted trigonal twist rearrangement about an enantiomeric metal centre at room temperature in which the molecule interconverts between S and R configurations as shown in Fig. 5.6. This process is also consistent

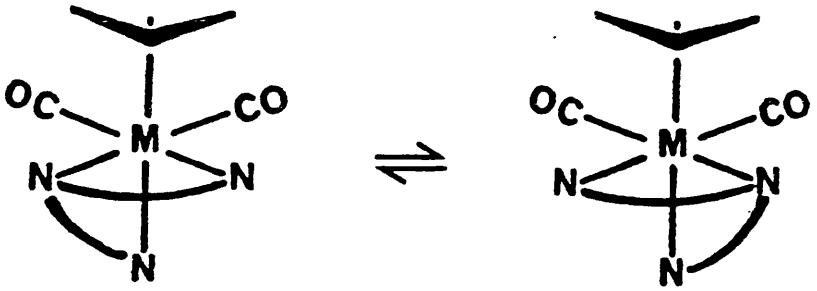

Fig. 5.6 R and S configurations of $[M(CO)_2(\pi^3\text{-allyl})L_3]PF_6$.

with the observation that over the range +80°C to -80°C only two of the four methylene protons are strongly coupled to the NH group. Construction of molecular models of $[M(CO)_2(\pi^3\text{-}C_3H_4R)L_3]^+$ in which L_3 occupies one face of a pseudo-octahedral structure, reveals dihedral angles ω between planes H-N-C and N-C-H of ca. 20° for two of the methylene protons adjacent to NH and ca. 90° for the other two (Fig. 5.7). It has been shown previously in conformational studies of

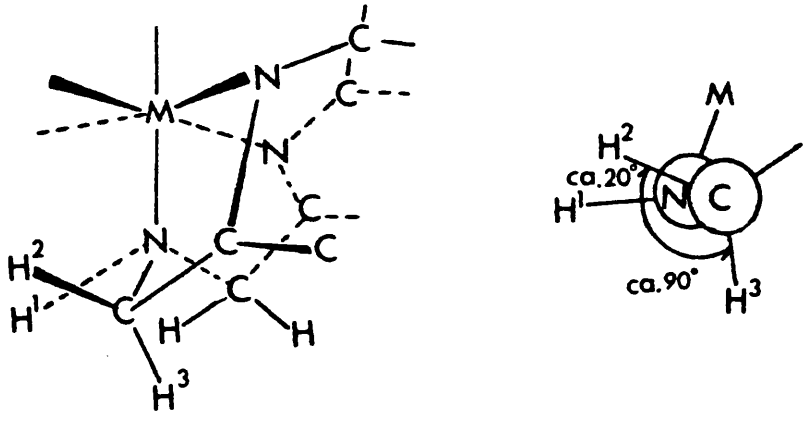

Fig. 5.7 Dihedral angles within the L_3 unit in $[M(CO)_2(\pi^3\text{-allyl})L_3]PF_6$.

alanine dipeptides of general formula R'CONHCH(Me)CON(R")CH(Me)CO_2Me [307] that the vicinal proton coupling constants ^3J(NH-CH) can be correlated with the dihedral values ω between planes H-N-C and N-C-H as shown in Fig. 5.8. For ω angles of approximately 90° values of ^3J(NH-CH) are small, in agreement with coupling of N-H to two of the methylene protons in [$M(CO)_2(\eta^3$-$C_3H_4R)$bpma]PF_6 not being observed. However coupling of the other two methylene protons to N-H gave constants of 6.5-7Hz, in agreement with ω values of 20-30°.

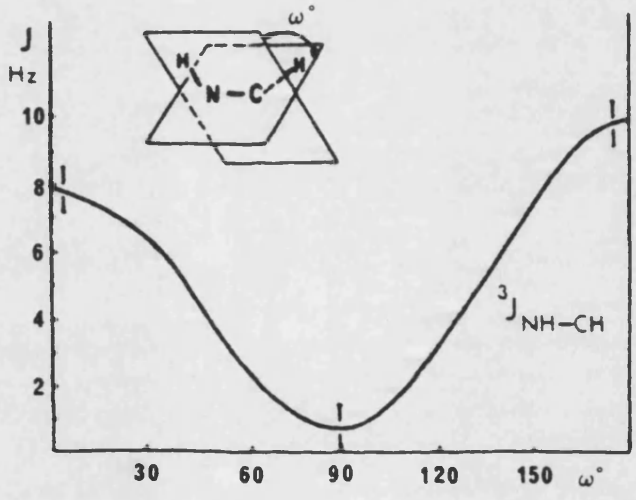

Fig. 5.8 Correlation of ^3J(NH-CH) coupling constants with dihedral angles, ω

DISCUSSION

Trofimenko and coworkers [5,308] examined the temperature dependent proton NMR spectra of the related tridentate complexes $M(CO)_2(\eta^3\text{-}CH_2{=}C(R){=}CH_2)(R_1Bpz_3)$ (M=Mo or W, pz=pyrazolyl, R_1=H or pz, R=H, Me or Ph) (Fig. 5.9) and proposed a rearrangement process involving rotation of the tridentate. For R_1=H, R=Me three resonances

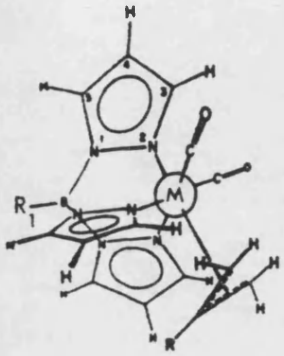

Fig. 5.9 The complexes $M(CO)_2(\eta^3\text{-}CH_2{=}C(R){=}CH_2)(R_1Bpz_3)$

due to the pyrazolylborato anion appeared at low temperature, each split into two components in the ratio 2:1, indicating two identical and one unique magnetic environment for the pyrazolyl groups. The high temperature limiting spectra (Fig. 5.10) indicated three equivalent pyrazolyl groups, suggesting that the tridentate ligand was rotating about the B-M axis [5,308].

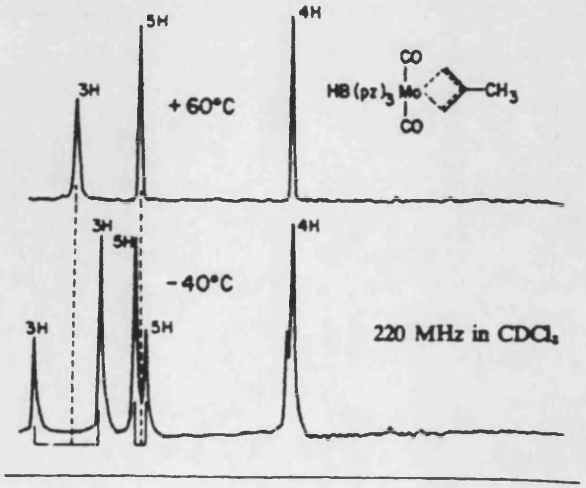

Fig. 5.10 The ^1H NMR spectra of $Mo(CO)_2(\eta^3\text{-}CH_2{=}C\,Me{=}CH_2)(\,H\,Bpz_3)$.

The dynamic proton NMR spectra of $Mo(CO)_2Cp(R_1R_2Bpz_2)$ (R_1=H, R_2=pz or R_1=R_2=Et), in which the pyrazolylborato ligand is in a bidentate bonding mode, were explained by the existence of two conformational isomers (A and B, Fig. 5.11), which interconvert by rotation of the Cp and dicarbonyl groups about the B-M axis [309].

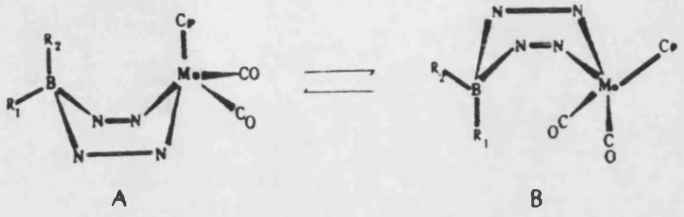

Fig. 5.11 Models of two possible ring isomers of $Mo(CO)_2Cp(R_1R_2Bpz_2)$.

Variable temperature ^1H, ^{13}C and ^{31}P NMR spectra of related complexes such as $M(CO)_2(\eta^3\text{-}C_3H_4R)L_2X$ (L_2=dppe, dppm, diphos or diars, X=halide) have been interpreted in terms of a rotation process in which the triangular face containing the allyl and two carbonyl groups in a pseudo-octahedral structure rotate against the face containing the bidentate L_2 and anion X. For unsymmetrical bidentates such as arphos this leads to two enantiomeric pairs (R and S, Fig. 5.12) which do not interconvert [2].

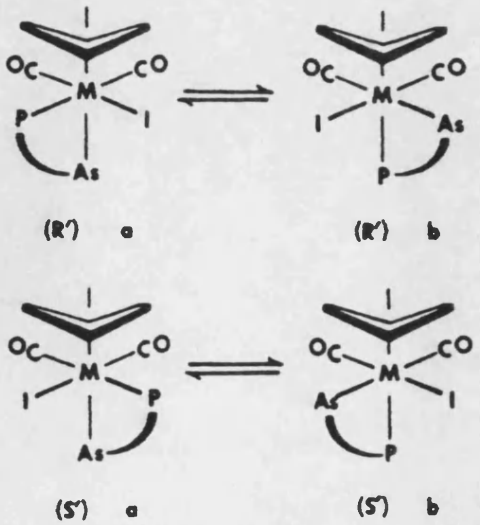

Fig. 5.12 Possible interconversions between enantiomers of $Mo(CO)_2(\eta^3\text{-}C_3H_5)$(arphos)I.

Recent investigations [109] of other $M(CO)_2(\eta^3\text{-}C_3H_4R)L_2X$ complexes in which L_2=E-paphy, E-Øaphy or E-paØhy (depicted below), have shown that these ligands all fail to fully utilise the three or

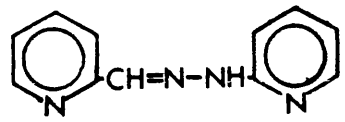

E-paphy

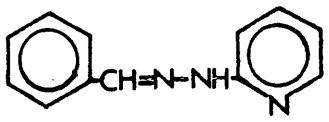

E-Øaphy

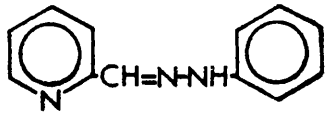

E-paØhy

four N-groups present and involve bidentate chelation only. Thus the dynamic behaviour of $[Mo(CO)_2(\eta^3\text{-}C_3H_5)bpma]PF_6$ reported here is the first example of a complex containing a neutral tridentate nitrogen donor ligand which undergoes a trigonal twist rearrangement in solution at room temperature.

5.3.4 THE STRUCTURE OF $[M(CO)_2(\eta^3\text{-}C_3H_4R)L_3]PF_6$

Three potential orientations of the tridentate group L_3 with respect to the fac-$M(CO)_2(\eta^3\text{-}C_3H_4R)$ unit in $[M(CO)_2(\eta^3\text{-}C_3H_4R)L_3]PF_6$ are theoretically possible as shown by A, B and C below. For the complex M=W, R=H, L_3=bpma two crystalline products were isolated which possessed identical elemental analyses, IR and room temperature ^1H NMR spectra. Variable temperature ^1H NMR studies of the complex $[Mo(CO)_2(\eta^3\text{-}C_3H_5)L_3]PF_6$ have shown that in solution at room temperature a trigonal twist rearrangement of the M-L_3 group occurs, which may be associated with the enantiomeric structural types A and B, and this gives rise to the supposition that the major product of the tungsten complex may be of a mixture of types A and B, whilst the minor product is of type C.

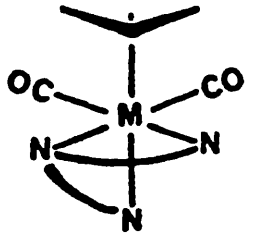

A

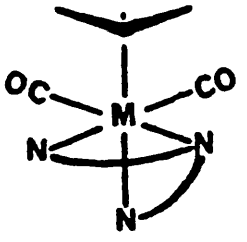

B

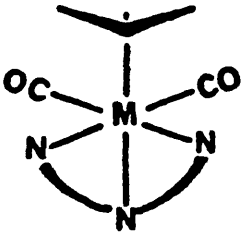

C

To examine the postulate that the major product of the complex $[W(CO)_2(\eta^3\text{-}C_3H_5)bpma]PF_6$ consists of a racemic mixture of types A and B, an X-ray diffraction analysis of the major crystalline form of this complex has been carried out and is reported in the following section.

5.3.4.1 THE SOLID STATE STRUCTURE OF $[W(CO)_2(\eta^3\text{-}C_3H_5)bpma]PF_6$

The crystal and molecular structures of the title compound were determined in collaboration with Drs. M.F.Mahon and K.C.Molloy at the University of Bath.

Crystals of $[W(CO)_2(\eta^3\text{-}C_3H_5)bpma]PF_6$ for X-ray analysis were recrystallised twice from aqueous methanol at -10°C. An orange crystal of approximate dimensions 0.15x0.2x0.2mm. was selected, mounted on a glass fibre, coated with epoxy resin and finally mounted at random on a Hilger-Watts Y290 four-circle automatic diffractometer, which was used to measure diffraction intensities and unit cell dimensions. Graphite filtered molybdenum X-radiation was used and 4,578 independent reflections with $2<\theta<44°$ were measured. Of these 3,607 reflections with $I>3\sigma(I)$ were used for subsequent refinement calculations. Backgrounds were measured from plots of background as a function of 2θ and no significant changes were observed in intensities from standard reflections monitored during the experiment. Neither an extinction nor an absorption correction were applied.

Crystal data: $C_{17}F_6H_{20}N_3PO_2W$, M=627.17, Monoclinic, a=12.489(5)Å, b=19.780(4)Å, c=16.698(4)Å, α=90.0(-)°, β=98.98(2)°, γ=90.0(-)°, U(unit cell volume)=4074.2Å^3, D_c(calculated density)=2.05gcm^{-3}, Z(number of molecules in the unit cell)=8, F(000)(number of electrons in the unit cell)=2,464, λ(Mo-K_α)=0.7107Å, μ(Mo-K_α absorption factor)=56.09cm^{-1}, space group $P2_1/c$ from the successful structure determination.

SOLUTION AND REFINEMENT

The position of the tungsten and non-hydrogen atoms were obtained by a Patterson search. The hydrogen atoms were not located, but were included in the final refinements at calculated positions. The structure was refined by full-matrix least squares to R=4.47% and R_w=4.61% with a weighting scheme of $W=3.0065/[(\sigma^2(F_o)+0.0010(F_o)^2]$. Calculations were made using the Shelx 86 [120] system of programs at the University of Bath and scattering factors and dispersion corrections were obtained from the International Tables for X-Ray Crystallography [122]. The asymmetric unit consisted of two molecules of the complex and the resulting list of atom positions for molecules 1 and 2 is given in Appendix 3. Bond lengths and angles for the two molecules were not significantly different and consequently only parameters for molecule 1 are given in Table 5.18 and discussed below. Appendix 3 contains a list of structural factors and thermal parameters.

An ORTEP view of the cation of molecule 1 and the atomic numbering scheme used are shown in Fig. 5.13. The central tungsten atom is bonded to the three nitrogen atoms of bis-(pyridylmethyl)amine [W(1)-N(1) 2.203(10)Å, W(1)-N(2) 2.266(10)Å, W(1)-N(3) 2.238(10)Å], two carbonyl groups [W(1)-C(1) 1.953(15)Å, W(1)-C(2) 1.900(16)Å] and a bidentate η^3-allyl unit [W(1)-C(3) 2.308(16), W(1)-C(5) 2.203(16), W(1)-C(4) 2.327(17)]. The mutually cis carbonyl groups have a C(1)-W(1)-C(2) bond angle of 83.9(0.6)° which compares well with the value of 87.4° predicted from solution infra-red ν(CO) intensity measurements and the two metal-carbonyl groups are essentially linear [W(1)-C(1)-O(1) 178.3(1.3)°, W(1)-C(2)-O(2) 178.0(1.4)°]. The metal-carbon and C-O carbonyl bond lengths for C(1) and C(2) are dissimilar. The shorter W(1)-C(2) [1.900(15)Å] and longer C(2)-O(2) [1.218(18)Å] carbonyl bond lengths [W(1)-C(1)

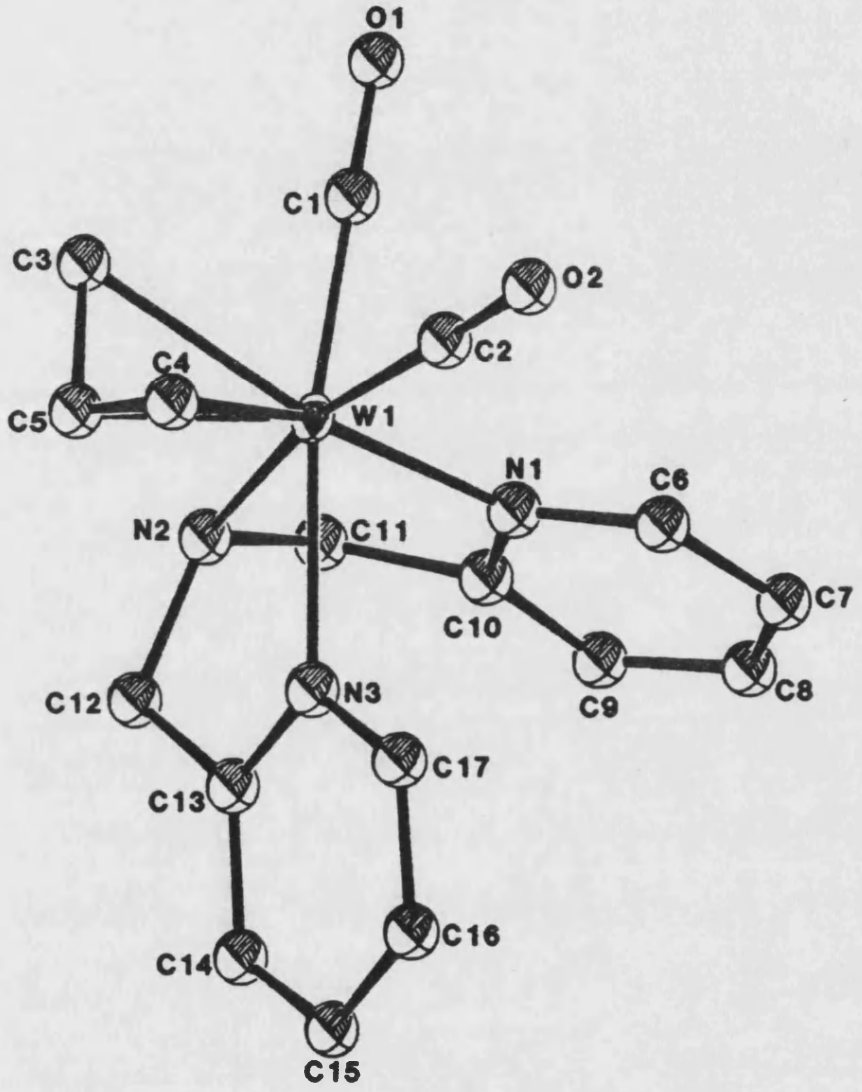

Fig. 5.13 An ORTEP view of $[W(CO)_2(\pi^5\text{-}C_5H_5)bpma]PF_6$ with hydrogen atoms omitted for clarity, and the atomic numbering scheme used.

Table 5.18 Interatomic distances and angles for [W(CO)$_2$(η^3-C$_3$H$_5$)bpma]PF$_6$ with standard deviations in parentheses.

Coordination Sphere:

Distances (Å):

W(1)-N(1)	2.203(10)
W(1)-N(2)	2.266(10)
W(1)-N(3)	2.238(10)
W(1)-C(1)	1.953(15)
W(1)-C(2)	1.900(16)
W(1)-C(3)	2.308(16)
W(1)-C(4)	2.327(17)
W(1)-C(5)	2.203(16)

Angles (°):

N(1)-W(1)-N(3)	76.4(0.4)	C(2)-W(1)-N(1)	93.6(0.5)
N(1)-W(1)-N(2)	74.5(0.4)	C(2)-W(1)-N(2)	167.8(0.5)
N(2)-W(1)-N(3)	74.9(0.4)	C(2)-W(1)-N(3)	100.2(0.6)
C(1)-W(1)-N(1)	88.9(0.5)	C(2)-W(1)-C(3)	107.8(0.6)
C(1)-W(1)-N(2)	98.1(0.5)	C(2)-W(1)-C(4)	69.0(0.6)
C(1)-W(1)-N(3)	164.9(0.5)	C(2)-W(1)-C(5)	102.7(0.6)
C(1)-W(1)-C(3)	70.1(0.6)		
C(1)-W(1)-C(4)	111.5(0.6)		
C(1)-W(1)-C(5)	106.4(0.6)		

Carbonyl groups:

Distances (Å):

C(1)-O(1)	1.180(17)
C(2)-O(2)	1.218(18)

Angles (°):

C(1)-W-C(2)	83.9(0.6)
W-C(1)-O(1)	178.3(1.3)
W-C(2)-O(2)	178.0(1.4)

Allyl ligand:

Distances (Å):

C(3)-C(5)	1.455(22)
C(5)-C(4)	1.374(22)

Angles (°):

C(3)-W(1)-C(4)	61.7(0.6)	C(3)-C(5)-C(4)	114.4(1.4)
C(4)-W(1)-C(5)	35.2(0.6)		
C(3)-W(1)-C(5)	37.5(0.5)		

Table 5.18 continued.

Bis-(pyridylmethyl)amine ligand:

Distances (Å):

N(1)-C(6)	1.362(18)	N(3)-C(13)	1.378(18)
C(6)-C(7)	1.387(20)	C(13)-C(14)	1.405(20)
C(7)-C(8)	1.388(21)	C(14)-C(15)	1.373(22)
C(8)-C(9)	1.393(20)	C(15)-C(16)	1.391(22)
C(9)-C(10)	1.389(18)	C(16)-C(17)	1.412(21)
C(10)-N(1)	1.341(16)	C(16)-C(17)	1.412(21)
C(10)-C(11)	1.525(18)	C(12)-C(13)	1.505(19)
C(11)-N(2)	1.483(17)	C(12)-N(2)	1.480(17)

Angles (°):

W(1)-N(1)-C(6)	121.2(0.9)	W(1)-N(3)-C(17)	123.9(0.9)
N(1)-C(6)-C(7)	120.9(1.4)	N(3)-C(17)-C(16)	121.4(1.4)
C(6)-C(7)-C(8)	118.5(1.5)	C(17)-C(16)-C(15)	118.9(1.6)
C(7)-C(8)-C(9)	120.9(1.4)	C(16)-C(15)-C(14)	119.5(1.6)
C(9)-C(10)-N(1)	122.2(1.20	C(14)-C(13)-N(3)	120.1(1.3)
W(1)-N(1)-C(10)	118.2(0.8)	W(1)-N(3)-C(13)	115.6(0.8)
N(1)-C(10)-C(11)	122.2(1.2)	N(3)-C(13)-C(12)	117.5(1.1)
C(9)-C(10)-C(11)	122.2(1.2)	C(14)-C(13)-C(12)	122.4(1.2)
C(11)-N(2)-C(12)	113.7(1.0)		

Hexafluorophosphate anion:

Distances (Å):

P(1)-F(1)	1.594(8)	P(1)-F(4)	1.589(8)
P(1)-F(2)	1.603(8)	P(1)-F(5)	1.590(9)
P(1)-F(3)	1.591(8)	P(1)-F(6)	1.577(8)

Angles (°):

F(1)-P(1)-F(2)	89.3(0.5)	F(2)-P(1)-F(3)	98.9(0.5)
F(1)-P(1)-F(3)	88.4(0.5)	F(2)-P(1)-F(4)	90.3(0.5)
F(1)-P(1)-F(4)	179.6(0.3)	F(2)-P(1)-F(5)	180.0(0.1)
F(1)-P(1)-F(5)	90.7(0.5)	F(2)-P(1)-F(6)	88.3(0.5)
F(1)-P(1)-F(6)	90.3(0.5)	F(3)-P(1)-F(4)	91.3(0.5)
F(3)-P(1)-F(5)	90.2(0.5)	F(4)-P(1)-F(6)	90.0(0.5)
F(3)-P(1)-F(6)	177.8(0.5)	F(5)-P(1)-F(6)	91.5(0.5)
F(4)-P(1)-F(5)	89.6(0.5)		

1.953(15)Å, C(1)-O(1) 1.180(17)Å] may arise from the differing σ-donor abilities of the pyridyl N(3) ring and the aliphatic N(2) group trans to C(1) and C(2) respectively. Bond lengths and angles associated with the η^3-allyl unit compare well with values found for related Mo and W $M(CO)_2(\eta^3\text{-allyl})L_2X$ and $[M(CO)_2(\eta^3\text{-allyl})L_3]^{n+}$ structures listed in Table 4.3.

Within the bpma ligand the three metal-nitrogen bond lengths are noticably different. Thus the aliphatic and pyridyl ring moieties are both trans to CO groups with W(1)-N(2) and W(1)-N(3) distances of 2.266(10)Å and 2.238(10)Å respectively, whilst the pyridyl ring sited trans to the allyl has a W(1)-N(1) bond length of 2.203(10)Å. Two 5-membered rings sharing the W(1)-N(2) bond as a common edge can be identified, each comprising the metal, two nitrogens, a methylene carbon and one pyridyl ring carbon. Bond lengths and angles within the two 5-membered rings are very similar, with an average N-W-N angle of 75.3°. The two pyridyl rings are approximately planar within experimental error and the N(1) pyridyl plane is skewed at an angle of 72.2° relative to the plane C(5)-W(1)-N(1) which bisects the angle C(1)-W(1)-C(2).

Fig. 5.14 shows an ORTEP view of the asymmetric unit containing two molecules of $[W(CO)_2(\eta^3\text{-}C_3H_5)bpma]PF_6$ and the complete numbering system used. Both hexafluorophosphate groups approximate to octahedra and the P-F bond lengths and F-P-F angles are unexceptional Although only one orientation of bpma with respect to the fac-$W(CO)_2(\eta^3\text{-}C_3H_5)$ unit is shown in Fig. 5.14, the space group for this crystal does not allow any distinction between S and R forms of this complex and thus the racemic character of this crystal can only be assumed from the asymmetric bonding mode of bpma and the NMR evidence.

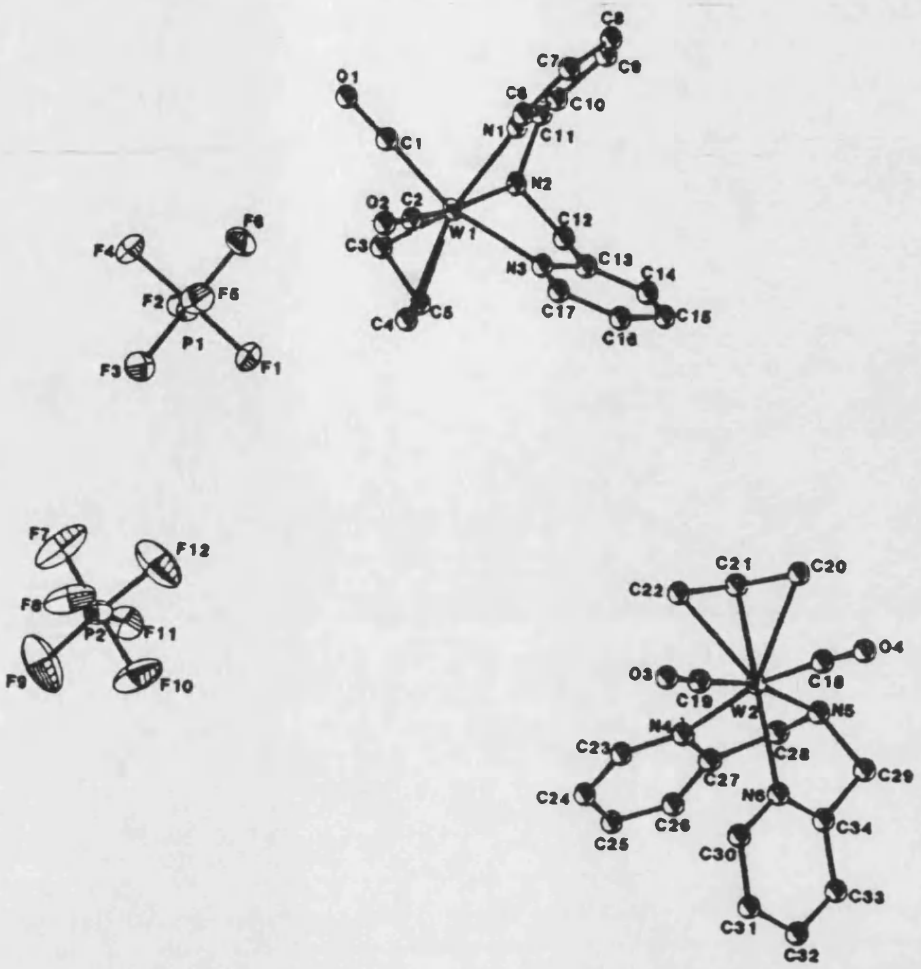

Fig. 5.14 The asymmetric unit of $[W(CO)_2(\eta^3\text{-}C_3H_5)bpma]PF_6$.

This structure may be compared with those adopted by the related tris-pyrazolyl borato and gallato complexes $Mo(CO)_2(\eta^3\text{-}C_3H_4R)(R'Epz_3)$ (R=H,Me, R'=H,Me,Ph, E=B,Ga) [263-265], in which the tridentates assume a symmetrical arrangement with respect to the fac-$M(CO)_2(\eta^3$-allyl) unit with the line through E and M forming an approximate three-fold axis. The metal, two pyrazolyl rings and the B or Ga atom constitute 6-membered rings, and the allyl central carbon, metal and trans pyrazolyl nitrogen subtend an average angle of 165.5°, which compares with an angle of 158.6(0.5)° for C(5)-W(1)-N(1) in the bpma ligand. A similar symmetric bonding mode has recently been found [310] for the potentially quadridentate ligand

tpma (tris-(2-pyridylmethyl)amine) in the complex [Mo(CO)$_2$(η^3-C$_3$H$_5$)tpma]PF$_6$, which is illustrated in Fig. 5.15. Bond lengths and angles of the allyl and carbonyls are similar to those of the bpma complex, however the shorter W(1)-C(2) [1.900(16)Å] and longer C(2)-O(2) [1.218(18)Å] distances compared to the Mo-C(2) [2.044(18)Å] and C(2)-O(2) [1.078(16)Å] lengths indicate greater electron density on the tungsten centre, resulting from the greater σ-donor ability of the aliphatic group over the pyridyl ring. All the M-N bond lengths

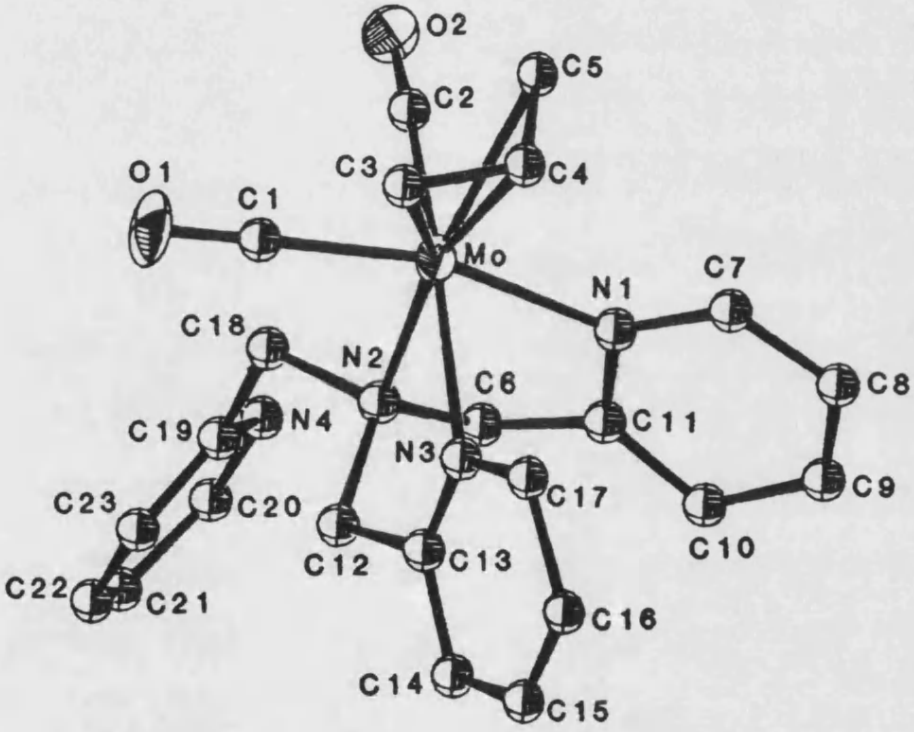

Fig. 5.15 The structure of [Mo(CO)$_2$(η^3-C$_3$H$_5$)tpma]PF$_6$.

are noticably longer for the Mo complex [Mo-N(1) 2.275(12)Å, Mo-N(2) 2.296(15)Å, Mo-N(3) 2.284(11)Å] than for the W complex [W(1)-N(1) 2.203(10)Å, W(1)-N(2) 2.266(10)Å, W-N(3) 2.238(10)Å] due to less donation of electron density from the third pyridyl ring of tpma, than from the aliphatic nitrogen ligand in the bpma complex.

The complex $Mo(CO)_2(\eta^3\text{-}C_3H_4Me)(MeGa(3,5\text{-}Me_2pz)_2OH)$ [266] which contains an asymmetrically bonded mixed tridentate is shown in Fig. 5.16 and has several structural features in common with the bpma complex. Thus the gallato unit contains two linked 5-membered rings [O(1)-Mo-N average 80.0°, C(9)-Mo-N(2) angle 161.1(2)°], with the metal-pyrazolyl bond <u>trans</u> to the allyl being the shorter of the two metal-nitrogen bond lengths [Mo-N(2) 2.237(4)Å, Mo-N(4) 2.276(4)Å]. In both the gallato and bpma complexes the rings of the tridentate are twisted to avoid strain about the congested metal centre.

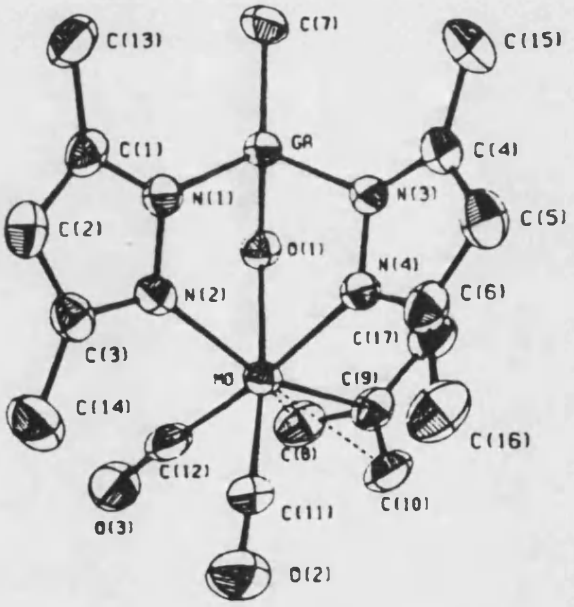

Fig. 5.16 The structure of $Mo(CO)_2(\eta^3\text{-}C_3H_4Me)(MeGa(3,5\text{-}Me_2pz)_2OH)$.

The importance of the allyl substituents and tridentate ring sizes to the structures of these types of complexes can be illustrated by the complex $Mo(CO)_2(\eta^3\text{-}C_3H_4Me)(Me_2Ga(3,5\text{-}Me_2pz)(OCH_2CH_2NH_2))$ [267], in which the unusual orientation of the methylallyl substituent towards the two carbonyl groups arises from the steric requirements of the allyl and tridentate gallato ligands. The structure and dynamic behaviour of complexes containing bulky or mixed nitrogen donor tridentate ligands or substituted allyl groups should therefore prove interesting.

In summary therefore, spectroscopic evidence has shown that in neutral or basic hydroxylic solvents R'OH, the major species formed from $MCl(CO)_2(\eta^3\text{-}C_3H_4R)(MeCN)_2$ are $[M(CO)_2(\eta^3\text{-}C_3H_4R)(HOR')_3]^+$ or $[M_2(CO)_4(\eta^3\text{-}C_3H_4R)_2(\mu\text{-}OR')_3]^-$ respectively. The former react with bidentate and tridentate N-donor ligands to form pseudo-octahedral neutral and cationic complexes $M(CO)_2(\eta^3\text{-}C_3H_4R)L_2X$ and $[M(CO)_2(\eta^3\text{-}C_3H_4R)L_3]^+$ respectively, the latter species having been isolated as their PF_6^- salts. The cation has been shown by NMR methods to undergo a trigonal twist rearrangement in solution at ambient temperature, and an X-ray analysis of $[W(CO)_2(\eta^3\text{-}C_3H_5)bpma]PF_6$ has shown that the tridentate bpma ligand is coordinated to an asymmetric metal centre.

CHAPTER 6

COMPLEXES OF GENERAL FORMULA

$M(CO)_2(\eta^3\text{-}CH_2{=}C(COB){-}C{=}CH_2)L_2X$ (B=OR, NRR', SR)

6.1 INTRODUCTION

Extensive research over the past decade has shown the utility of transition metal templates as catalysts in reactions involving allylic compounds. Early studies centred upon allylic alkylation reactions involving palladium phosphine complexes, as illustrated by the scheme below [311-314], and until recently

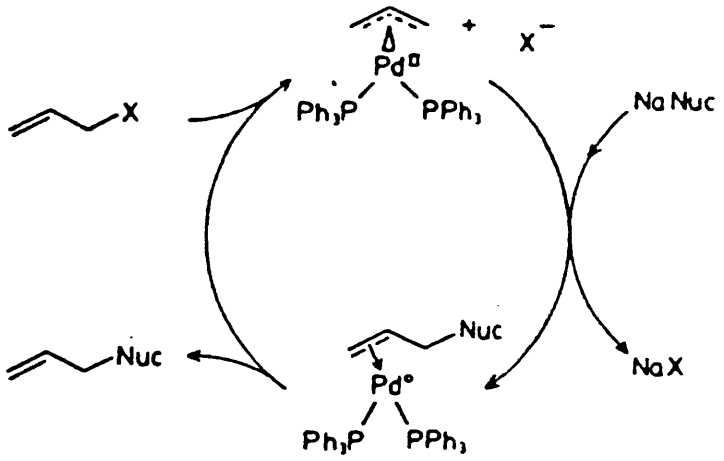

reactions involving other transition metal templates have been relatively neglected. However in the last few years work by groups led by Trost [315] and Tsuji [316] has centred upon the use of less expensive, air-stable Mo and W templates in allylic alkylations and these studies have shown that regioselectivity in these reactions may be highly dependent upon the reaction conditions, the nature of the metal and the nucleophile and upon the steric and electronic requirements of the reactants, products and postulated π-allyl intermediates.

In contrast to palladium templates, which have been shown to react at the less hindered terminus of the allyl fragment [252,311-314,318], tungsten templates show a bias for reaction at the more hindered position regardless of the nucleophile employed [319], whilst molybdenum complexes have been found to behave in an

intermediate manner, showing a regioselectivity which is highly nucleophile dependent [297,320,321]. Reactions involving a range of cyclic and acyclic allylic acetates with nucleophiles of varying sizes in the presence of Mo catalysts such as $Mo(CO)_6$, $Mo(CO)_3(MeCN)_3$ or $Mo(CO)_4(bipy)$ [146,297,320] have been used to illustrate the steric constraints imposed by larger nucleophiles upon the site of nucleophilic attack and to reveal the role of solvent on both the rate and regioselectivity of the reaction. A comparison of the reactivity of the preformed bipy and dppe (L_2) complexes $MoCl(CO)_2(\eta^3\text{-allyl})L_2$ with the anion of 2-carbomethoxycyclopentanone showed a marked difference in regioselectivity as shown below and it was suggested that this may in part be connected with the differing geometries adopted by these complexes and the stronger σ-donating ability of bipy over dppe [2,175,271,322]. The differing control of regioselectivity found with tungsten templates is thought to reflect the reactivity of the proposed η^3-allyl intermediate [315], which may be the limiting factor in the viability of such catalytic systems [323].

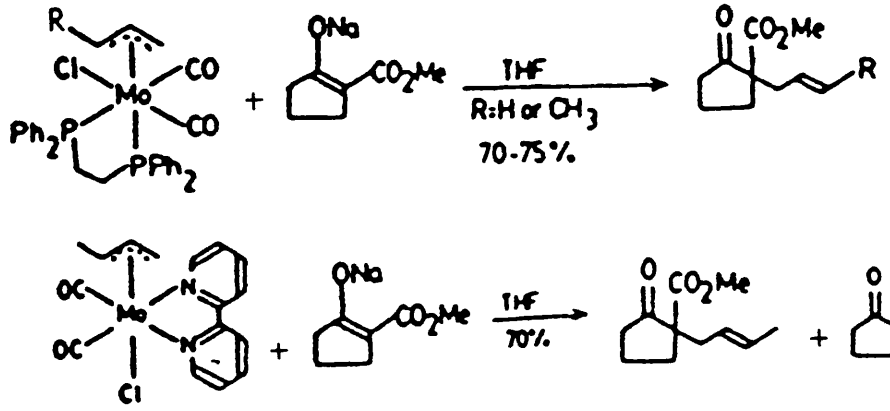

In order to better understand the nature and role of the metallo intermediates in these processes and to explore possible new

routes to C-C formation, the reactivity of $Mo(CO)_4(bipy)$ towards various unsaturated organic species has been examined [324]. Initial attempts to generate new C-C bonds by propargyl alkylation or coupling reactions using the tetracarbonyl and an anion were unsuccessful, however the more nucleophilic anion $[MoCl(CO)_3(bipy)]^-$ reacted with propargyl chloride in methanol to yield $MoCl(CO)_2(C_5H_7O_2)bipy$ which was thought from a consideration of IR and NMR data to contain a η^3-2-methoxy-4-methyl-1-oxacyclobutenyl group as shown below. In the presence of base, ring opening of the organic moiety was achieved to yield a metal bonded σ-vinyl entity whose structure was determined by X-ray crystallography [324].

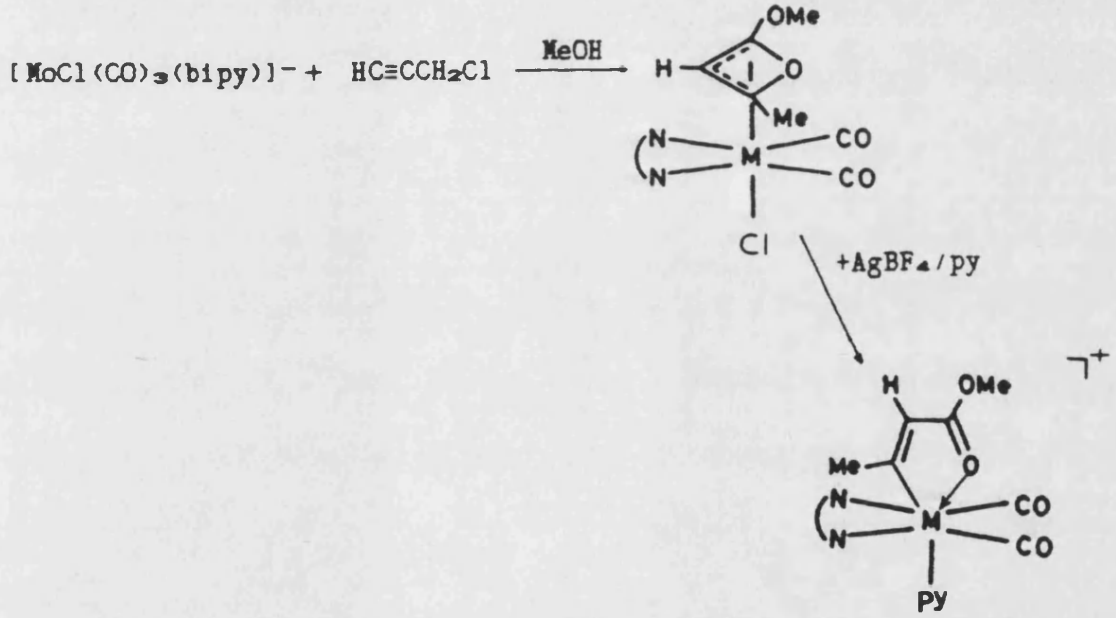

Extension of this reaction to the difunctional alkyne, 1,4-dichloro-2-butyne led to the isolation of two different products from methanolic solutions. Single crystal X-ray diffraction studies [325] of these two derivatives showed that in aqueous methanol the complex $MoCl(CO)_2(\eta^3\text{-}CH_2{=}C(CO_2Me){-}C{=}CH_2)bipy$ was formed, whilst in anhydrous methanol the hydroxymethylated derivative $MoCl(CO)_2(\eta^3\text{-}CH_2{=}C(CO_2Me){-}C(OMe)(Me))bipy$ was the major product. Analogous procedures using ethanol as solvent led to the corresponding ethoxy products and confirmed that the reaction conditions in either alcohol were very

critical with traces of moisture leading to mixtures of both types of complex.

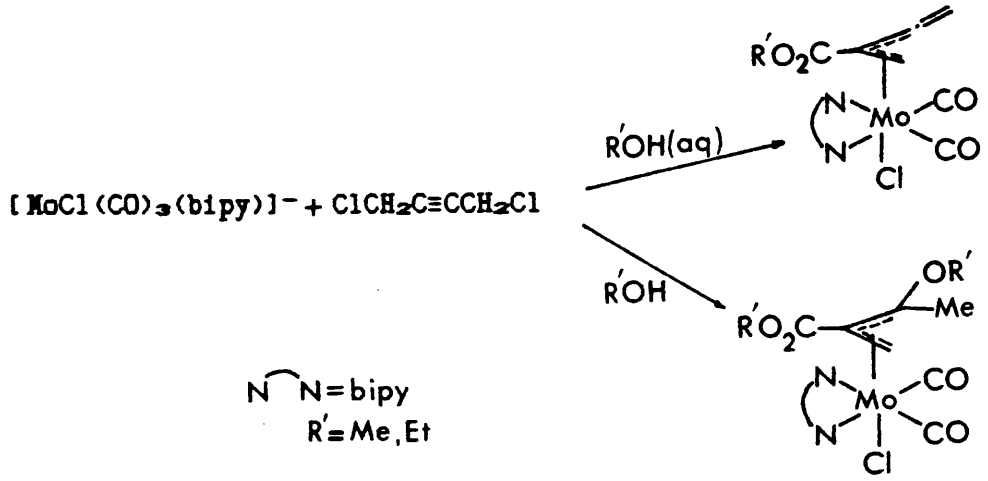

This type of alkoxycarbonylation reaction had been observed previously [194] between σ-propargylic complexes $M(CO)_3(\sigma\text{-}CH_2\text{-}C{\equiv}CR')Cp$ (M=Mo or W, R'=H, Me or Ph) and water, alcohols or thiols RXH, yielding η^3-allyl complexes $M(CO)_2(\eta^3\text{-}CH_2{=}C(COXR){=}C(H)(R'))Cp$ or σ-vinyl complexes $\overline{M\text{-}C(CH_3)=CH\text{-}C(OR')=O}(CO)_2Cp$. Substitution of one CO group by PPh_3 increased the asymmetry of the molecule and reaction of the alkyne in the presence of RXH resulted in the isolation of two diastereoisomers of $Mo(CO)(\eta^3\text{-}CH_2{=}C(COXR){=}C(H)(Me))(PPh_3)Cp$ [195]. Such types of complex are also accessible [326] via protonation of related Mo or Fe complexes $M(CO)_3(\sigma\text{-}CH_2\text{-}C{\equiv}CC(OH)(R')(R''))Cp$ ($R'\neq R''$) by HBF_4 at low temperature followed by dehydration to yield the cationic cumulene complexes $[M(CO)_3(\eta^2\text{-}CH_2{=}C{=}C{=}C(R')(R''))Cp]^+$, which subsequently undergo nucleophilic attack by methoxide to form the η^3-allylic ester complexes illustrated below (B=OMe). The presence of diethylamine or ethylamine in the latter reaction yielded related amide complexes (B=NEt_2 or NHEt) and the dissimilar R' and R" groups (R',R"=Me or Ph) led to geometric Fe isomers of type 1 and 2 below, and Mo isomers of type

1. A further product was isolated from reactions involving $HNEt_2$ in which double addition of amine had occurred, however it was unclear whether the second addition had occurred via the η^3-butadienyl complex.

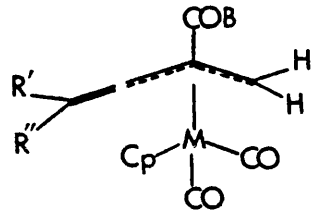

isomers of type 1

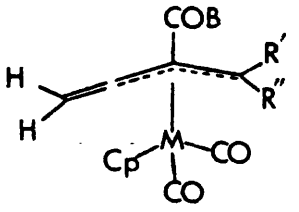

isomers of type 2

These results suggested that the presence of amines or thiols in reactions of $[MoCl(CO)_3(bipy)]^-$ and $ClCH_2C{\equiv}CCH_2Cl$ in MeOH might yield related η^3-bonded allylic complexes. The work in this chapter describes the reactions of methanolic solutions of $[WCl(CO)_3bipy]^-$ and of $[MoCl(CO)_3phen]^-$ towards $ClCH_2C{\equiv}CCH_2Cl$ and examines the influence of water or tertiary amines in such systems. The reactivity of methanolic solutions of $[MoCl(CO)_3(bipy)]^-$ with $ClCH_2C{\equiv}CCH_2Cl$ in the presence of primary or secondary amines RR'NH or thiols R'SH is reported, an order of reactivity for a range of primary and secondary amines is obtained, the heptafluorobutyrate derivatives of the amido complexes prepared and the molecular structure of $Mo(CO)_2(\eta^3\text{-}CH_2{=}C(CONHMe){=}C{=}CH_2)(bipy)(O_2CC_3F_7)$ confirmed by an X-ray diffraction study.

6.2 EXPERIMENTAL

Details of physical techniques and solvents used appear in Appendix 1. The starting materials $Ph_4P[MCl(CO)_3L_2]$ (M=Mo or W, L_2=2,2'-bipyridyl (bipy) or 1,10-phenanthroline (phen)) were prepared from $M(CO)_4L_2$ and Ph_4PCl using reaction conditions described by White et al [271]. The amines RR'NH (R=R'=Me, Et or Pr^n, R=H, R'=Me, Et, Pr^n, Ph, CH_2Ph, $CH_2CH=CH_2$ or $CH_2C\equiv CH$) and the thiols RSH (R=Et, Bu^n or Ph) were all obtained from commercial sources and used without further purification.

PREPARATION OF $MCl(CO)_2(\eta^3-CH_2{=}C(CO_2Me){=}C(OMe)(Me))L_2$ (M=Mo, L_2=phen, M=W, L_2=bipy).

A stirred suspension of $Ph_4P[MCl(CO)_3L_2]$ (1.0mmol) in a 1:1 mixture of anhydrous methanol and THF (10cm^3) was cooled to -10°C and 1,4-dichlorobut-2-yne (0.15cm^3, 1.0mmol) added dropwise. After 0.5hr the mixture was allowed to warm to room temperature and stirred for a further 0.5hr (M=Mo) or 8hr (M=W). Addition of petroleum ether (10cm^3) and cooling (-10°C), yielded the red products, which were filtered, washed with petroleum ether and dried in vacuo.

PREPARATION OF $MCl(CO)_2(\eta^3-CH_2{=}C(CO_2Me){=}C{=}CH_2)L_2$ (M=Mo, L_2=phen, M=W, L_2=bipy).

Dropwise addition of 1,4-dichlorobut-2-yne (0.15cm^3, 1.0mmol) to a stirred suspension of $Ph_4P[MCl(CO)_3L_2]$ (1.0mmol) in methanol (5cm^3) and water (0.5cm^3) at -10°C for 0.5hr, followed by stirring at room temperature for a further 0.5hr (M=Mo) or 8hr (M=W), yielded red solutions. Addition of petroleum ether (10cm^3) and cooling (-10°C) yielded the dark red microcrystalline products. These were filtered, washed with petroleum ether and dried in vacuo.

The molybdenum-phenanthroline complexes were recrystallised from saturated CH_2Cl_2 solutions, but the tungsten complexes were not sufficiently soluble in common solvents for them to be purified by this method.

Table 6.1 Yields and analytical data for complexes $MCl(CO)_2(\eta^3\text{-}CH_2{=}C(CO_2Me){=}C(OMe)(Me))L_2$ and $MCl(CO)_2(\eta^3\text{-}CH_2{=}C(CO_2Me){=}C{=}CH_2)L_2$.

Complex		Yield	Analysis found(calculated)		
M	L_2	%	%C	%H	%N
Complex $MCl(CO)_2(\eta^3\text{-}CH_2{=}C(CO_2Me){=}C(OMe)(Me))L_2$					
Mo	phen	51	49.0(49.4)	3.7(3.7)	5.3(5.5)
W	bipy	67	40.6(39.7)	3.5(3.3)	4.7(4.9)
Complex $MCl(CO)_2(\eta^3\text{-}CH_2{=}C(CO_2Me){=}C{=}CH_2)L_2$					
Mo	phen	60	48.9(50.1)	3.2(3.1)	5.6(5.8)
W	bipy	45	38.7(39.8)	3.1(2.8)	4.8(5.1)

PREPARATION OF $MoCl(CO)_2(\eta^3\text{-}CH_2{=}C(CONRR'){=}C{=}CH_2)L_2$ (L_2=bipy, R=H, R'=H, Me, Et, Pr^n, Ph, CH_2Ph, $CH_2CH{=}CH_2$ or $CH_2C{\equiv}CH$, R=R'=H, Me, Et or Pr^n, L_2=phen, R=R'=Et).

The conditions and reaction times involved in the synthesis of these complexes were dependent upon the nature of the amine involved. The same basic procedures were used, but the amines could be classified into two groups, A and B, depending upon which one of two solvent mixtures was required. The general method of preparation is given below and specific reaction times and conditions are given in Table 6.2.

A suspension of $Ph_4P[MoCl(CO)_3L_2]$ (1.0mmol) in the required solvent mixture (1:1 dry, deoxygenated MeOH and THF ($10cm^3$) for amines in group A, methanol ($10cm^3$) and water ($0.5cm^3$) for amines in group B) was stirred with excess amine RR'NH ($0.5cm^3$) at -10°C. To this mixture 1,4-dichlorobut-2-yne ($0.15cm^3$, 1.0mmol) was added dropwise and the temperature was maintained at -10°C for a specified time (Table 6.2). Stirring for a further period at room temperature produced deep red solutions, which were reduced in volume *in vacuo*. Petroleum ether (40-60°C) ($5cm^3$) was added to the filtered solutions and the required products were isolated upon storage at -10°C. The more soluble orange, microcrystalline products were recrystallised from CH_2Cl_2-petroleum ether (40-60°C) mixtures. Yields and analytical data are contained in Table 6.3.

Table 6.2 Conditions for reaction between $ClCH_2C{\equiv}CCH_2Cl$, amines RR'NH and $Ph_4P[MoCl(CO)_3L_2]$ in methanol.

L_2	R	R'	Reaction time (hr)	
Group A			-10°C	R.T.
bipy	H	Me, Et, Pr^n	0.5	0.5
bipy	Me	Me	0.5	0.5
bipy	Et	Et	0.5	0.5
phen	Et	Et	0.5	0.5
bipy	H	H^	0.5	2d
Group B				
bipy	Pr^n	Pr^n	0.5	1.0
bipy	H	Ph, CH_2Ph	0.5	1.0
bipy	H	$CH_2CH{=}CH_2$	0.5	1.5
bipy	H	$CH_2C{\equiv}CH$	0.5	1.5

^-prepared using aqueous 2M NH_4OH

Table 6.3 Yields and analytical data for complexes

$MoCl(CO)_2(\eta^3\text{-}CH_2{=}C(CONRR'){=}C{=}CH_2)L_2$.

Complex		Yields	Analysis found(calculated)		
R	R'	%	%C	%H	%N
L_2=bipy					
H	H	41	45.8(46.4)	3.2(3.2)	7.2(9.5)
H	Me	59	43.3(47.6)	3.1(3.5)	8.1(9.3)
Me	Me	38	41.8(48.7)	3.4(3.8)	7.7(8.9)
H	Et	72	48.2(48.7)	3.9(3.8)	8.2(8.9)
Et	Et	48	50.5(50.8)	4.4(4.4)	8.3(8.4)
H	Pr^n	48	46.1(49.8)	4.1(4.1)	7.5(8.7)
Pr^n	Pr^n	40	49.3(52.7)	4.1(4.9)	7.2(8.0)
H	Ph	71	54.0(53.5)	4.1(3.4)	7.3(8.1)
H	CH_2Ph	61	50.3(54.3)	3.6(3.7)	7.0(7.9)
H	$CH_2CH{=}CH_2$	87	48.0(50.3)	3.8(3.7)	7.3(8.7)
H	$CH_2C{\equiv}CH$	72	50.2(50.2)	3.3(3.4)	8.4(8.7)
L_2=phen					
Et	Et	43	53.7(53.1)	4.3(4.2)	8.2(8.1)

PREPARATION OF $MoCl(CO)_2(\eta^3\text{-}CH_2{=}C(COSR){=}C{=}CH_2)$bipy (R=Et, Bu^n or Ph).

A suspension of $Ph_4P[MoCl(CO)_3bipy]$ (1.0mmol) in a 1:1 mixture of methanol and THF (10cm^3) was stirred with excess thiol RSH (0.5cm^3) and water (0.5cm^3) at -10°C and 1,4-dichlorobut-2-yne (0.15cm^3, 1.0mmol) added dropwise. The mixture was stirred for 0.5hr and then for a further 48hr at ambient temperature. The dark red powder which precipitated from the solution was filtered, washed with a little cold MeOH and dried *in vacuo*. Purification of the complexes by recrystallisation was prevented by their low solubility in common solvents and this resulted in the poor analytical data given in Table 6.4.

Table 6.4 Yields and analytical data for complexes $MoCl(CO)_2(\eta^3\text{-}CH_2{=}C(COSR){=}C{=}CH_2)bipy$.

Complex R	Yields %	Analysis found(calculated) %C	%H	%N
Et	38	41.2(47.1)	3.2(3.5)	6.7(5.8)
Bu^n	48	42.0(49.1)	3.4(4.0)	6.6(5.4)
Ph	25	41.0(51.8)	3.0(3.2)	6.8(5.3)

PREPARATION OF $Mo(CO)_2(\eta^3\text{-}CH_2{=}C(CONHR'){=}C{=}CH_2)(bipy)(O_2CC_3F_7)$ (R'=Me, Et, Pr^n, Ph or $CH_2CH{=}CH_2$

A solution of silver tetrafluoroborate (0.2g,1.0mmol) in acetone (5cm^3) was added dropwise to a mixture of excess sodium heptafluorobutyrate (250mg) and $MoCl(CO)_2(\eta^3\text{-}CH_2{=}C(CONHR'){=}C{=}CH_2)bipy$ (1.0mmol) in acetone (10cm^3) and stirred at room temperature for 3hr. The orange filtered solution was reduced to low bulk *in vacuo* and added dropwise to stirred petroleum ether (50cm^3). The crude products were isolated in 70-80% yields as orange or yellow microcrystalline powders. Repeated recrystallisation from CH_2Cl_2-petroleum ether mixtures to remove excess $NaO_2CC_3F_7$ resulted in yields below 30% and the analytical data shown in Table 6.5.

Table 6.5 Analytical data for complexes $Mo(CO)_2(\eta^3\text{-}CH_2{=}C(CONHR'){=}C{=}CH_2)(bipy)(O_2CC_3F_7)$.

Complex R'	Analysis found(calculated) %C	%H	%N
Me	41.1(41.8)	2.5(2.5)	6.5(6.6)
Et	34.0(42.8)	2.2(2.8)	4.9(6.5)
Pr^n	43.2(43.7)	3.0(3.0)	6.3(6.4)
Ph	46.8(46.7)	2.7(2.5)	5.9(6.0)
$CH_2CH{=}CH_2$	43.3(43.8)	2.9(2.7)	6.2(6.3)

6.3 RESULTS AND DISCUSSION

6.3.1 COMPLEXES $MCl(CO)_2(\eta^3\text{-}CH_2{=}C(CO_2Me){=}C{=}CH_2)L_2$ AND $MCl(CO)_2(\eta^3\text{-}CH_2{=}C(CO_2Me){=}C(OMe)(Me))L_2$

Reaction of methanolic solutions of $Ph_4P[MCl(CO)_3L_2]$ (M=Mo, L_2=phen, M=W, L_2=bipy) with 1,4-dichlorobut-2-yne in the presence of THF or water yielded dark red, microcrystalline powders which were of limited solubility in alcohols, chlorinated or ketonic solvents. Table 6.6 presents selected infra-red data for these complexes. Two strong ν(CO) modes were attributed to the cis-$M(CO)_2$ moiety and an absorption of medium intensity near 1688cm^{-1} was assigned to the ν(C=O) mode of the ester group, indicating that methoxycarbonylation had occurred.

Table 6.6. Selected infra-red data[a] for complexes $MCl(CO)_2(\eta^3\text{-}CH_2{=}C(CO_2Me){=}C{=}CH_2)L_2$ and $MCl(CO)_2(\eta^3\text{-}CH_2{=}C(CO_2Me){=}C(OMe)(Me))L_2$.

M	L_2	ν(C≡O)	ν(C=O)
Complex $MCl(CO)_2(\eta^3\text{-}CH_2{=}C(CO_2Me){=}C{=}CH_2)L_2$			
Mo	phen	1894, 1972	1690
W	bipy	1880, 1960	1681
Complex $MCl(CO)_2(\eta^3\text{-}CH_2{=}C(CO_2Me){=}C(OMe)(Me))L_2$			
Mo	phen	1868, 1951	1685
W	bipy	1857, 1940	1689

[a]-Measured as Nujol mulls, units of cm^{-1}

The complexes M=Mo, L_2=phen and M=W, L_2=bipy were insufficiently soluble in chlorinated or ketonic solvents for good quality NMR spectra to be obtained.

These results are very similar to those reported by Willis et al for the analogous complexes $MoCl(CO)_2(\eta^3\text{-}CH_2{=}C(CO_2Me){-}C{=}CH_2)$bipy and $MoCl(CO)_2(\eta^3\text{-}CH_2{-}C(CO_2Me){-}C(OMe)(Me))$bipy [325]. In agreement with their observations, the presence of water in all these reactions led to complexes of general formula $MCl(CO)_2(\eta^3\text{-}CH_2{-}C(CO_2Me){-}C{=}CH_2)L_2$, whilst 1:1 mixtures of methanol and THF produced the complexes $MCl(CO)_2(\eta^3\text{-}CH_2{=}C(CO_2Me){-}C(OMe)(Me))L_2$. Thus these reactions are dependent upon solvent composition and a mechanism (Fig. 6.1) has been postulated to account for these two reaction pathways. This involves initial attack of the anion upon the alkyne by an S_N2 process, followed by insertion of a CO group into the metal-allene bond to form a 16-electron species and subsequent addition of methanol across this carbonyl group. It was suggested that water initiated pathway A (Fig. 6.1) by coordinating to the metal centre, whereas in anhydrous conditions pathway B led to addition of methanol across both the inserted carbonyl group and a terminal carbon-carbon double bond.

[Mo] represents $Mo(CO)_2(bipy)Cl$, R=Me

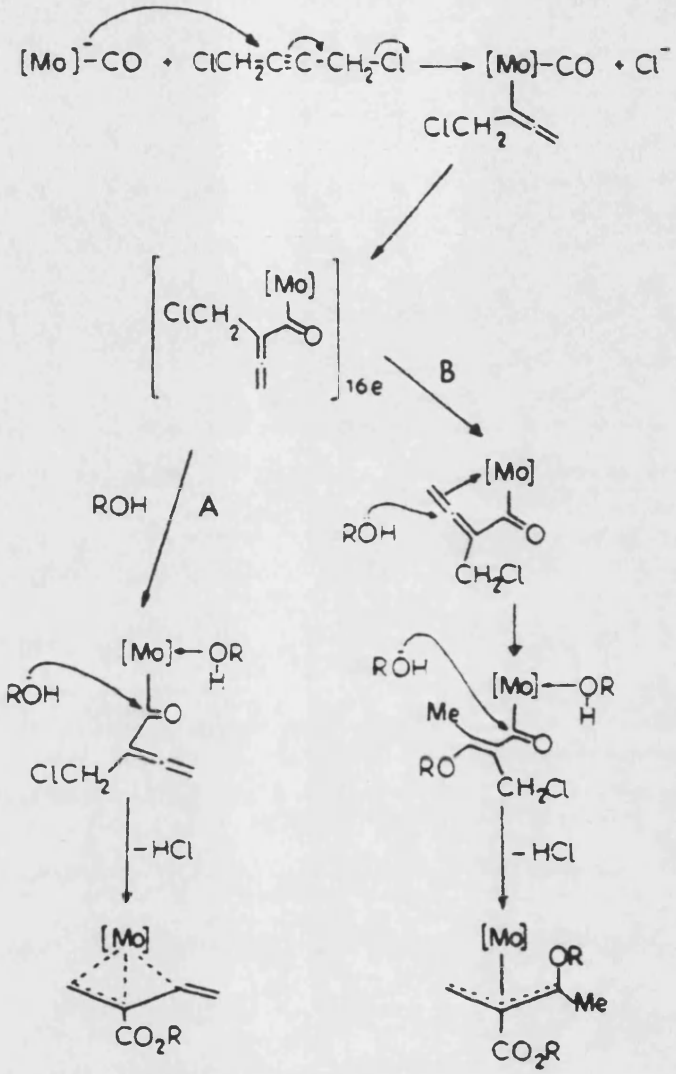

Fig. 6.1 The proposed mechanism for formation of complexes $MoCl(CO)_2(\eta^3\text{-}CH_2{=}C(CO_2Me){=}C{=}CH_2)bipy$ and $MoCl(CO)_2(\eta^3\text{-}CH_2{=}C(CO_2Me){=}C(OMe)(Me))bipy$.

In order to examine the possibility that other electron donor molecules might be used in place of water to initiate pathway A, the author substituted the series of tertiary amines trimethylamine, triethylamine or pyridine (0.5cm³) for water in the reaction of $Ph_4P[MoCl(CO)_3bipy]$ with the alkyne in methanol, using the reaction conditions described in section 6.2. The complex $MoCl(CO)_2(\eta^3\text{-}CH_2\text{-}C(CO_2Me)\text{-}C=CH_2)bipy$ was formed in each case, however as shown in Table 6.8 although all these amines initiated pathway A, reaction times varied. The longer reaction time required for pyridine might be due to its poorer σ-donor property (pKa 5.25), and steric factors are also probably involved due to the bulky bipy group hindering the approach of this larger ligand. The use of aqueous pyridine significantly shortened the reaction time.

Table 6.8 Effect of solvent composition on reaction time.

Solvents	Ratio	Reaction time (hr)	
		-10°C	r.t.
MeOH/H_2O	20:1	0.5	0.5
MeOH/NMe_3	20:1	0.5	0.5
MeOH/NEt_3	20:1	0.5	1.0
MeOH/py	20:1	0.5	3.5
MeOH/py/H_2O	20:1:1	0.5	1.0

On carrying out analogous reactions in the presence of primary or secondary amines R'RNH or thiols R'SH, it was found that a series of new complexes were formed having the general formulae $MoCl(CO)_2(\eta^3\text{-}CH_2\text{-}C(CONRR')\text{-}C=CH_2)L_2$ and $MoCl(CO)_2(\eta^3\text{-}CH_2\text{-}C(COSR')\text{-}C=CH_2)bipy$ in which RR'NH or R'SH, rather than ROH, had added across the inserted CO group. Although reactions of diethylamine with protonated σ-propargylic complexes have been reported to yield double

addition products [326] and Willis has reported the formation of methanol double addition products [325], no evidence was found for related amine double addition products in the systems reported here.

6.3.2 THE COMPLEXES $MoCl(CO)_2(\eta^3\text{-}CH_2{=}C(COSR'){-}C{=}CH_2)bipy$

Addition of 1,4-dichlorobut-2-yne to aqueous methanolic solutions of $Ph_4P[MoCl(CO)_3bipy]$ in the presence of thiols R'SH (R'=Et, Bu^n, Ph) yielded dark red powders of low solubilities which could not be recrystallised. Selected infra-red data for these complexes are presented in Table 6.9, and comparison with the spectral pattern for related complexes $Mo(CO)_2(\eta^3\text{-}CH_2{=}C(COSR){=}C(H)(R'))Cp$ [194] indicates the formation of η^3-butadienyl complexes. Their NMR spectra could not be recorded due to the low solubility of all the complexes, and the broadness of the infra-red spectral bands indicated that the complexes may not be completely pure, consequently reactions involving thiols were not pursued further.

Table 6.9 Infra-red data for $MoCl(CO)_2(\eta^3\text{-}CH_2{=}C(COSR'){=}C{=}CH_2)bipy$.

R'	$\nu(C{\equiv}O)/cm^{-1}$		$\nu(C{=}O)/cm^{-1}$
Et	1953,1936	1875,1842	1690
Bu^n	1954,1937	1873,1840	1693
Ph	1951,1938	1879,1846	1690

Analogous reactions in the presence of amines however resulted in a series of related amido compexes which were of much greater solubility, allowing their structures to be investigated by ^1H and ^{13}C NMR spectroscopy.

6.3.3 COMPLEXES OF GENERAL FORMULA $Mo(CO)_2(\eta^3\text{-}CH_2{=}C(CONRR'){=}C{=}CH_2)L_2X$.

Reactions of methanolic solutions of $Ph_4P[MoCl(CO)_3L_2]$ with 1,4-dichlorobut-2-yne in the presence of amines RR'NH yielded orange, microcrystalline products $MoCl(CO)_2(\eta^3\text{-}CH_2{=}C(CONRR'){-}C{=}CH_2)L_2$, whose solubilities depended upon the nature of R and R'. Related molybdenum-allyl complexes in which the halide ligand has been replaced by perfluorocarboxylate ligands are known to be more soluble in both polar and non-polar solvents [322] and therefore attempts were made to convert the less soluble amido complexes into their heptafluorobutyrate derivatives.

Initial attempts to prepare these products by direct anion exchange using $NaO_2CC_3F_7$ dissolved in acetone were unsuccessful, however chemical extraction of the chloro group by $AgBF_4$ in acetone solutions of $NaO_2CC_3F_7$ resulted in precipitation of AgCl and the formation of the new complexes $Mo(CO)_2(\eta^3\text{-}CH_2{=}C(CONHR'){=}C{=}CH_2)(bipy)(O_2CC_3F_7)$ (R'=Me, Et, Pr^n, Ph or $CH_2CH{=}CH_2$) which were isolated as orange, crystalline solids. Attempts to isolate either the analogous products from $MCl(CO)_2(\eta^3\text{-}CH_2{=}C(CO_2Me){=}C{=}CH_2)bipy$, or the probable intermediate cationic complexes $[Mo(CO)_2(\eta^3\text{-}CH_2{=}C(COB){=}C{=}CH_2)L_2(acetone)]^+$ (B=OMe or NHR') led only to decomposition of the solutions.

INFRA-RED SPECTRA

Selected infra-red data and carbonyl force constants for the complexes $Mo(CO)_2(\eta^3\text{-}CH_2{=}C(CONRR'){=}C{=}CH_2)L_2X$ (X=Cl or $C_3F_7CO_2^-$) are summarised in Table 6.10. The spectra were dominated by the two sharp carbonyl bands expected for such terminal carbonyl stretching modes. Absorptions due to the amide carbonyl group were found in the range 1612 to 1658cm^{-1}, which is slightly higher than values typical for substituted amides [328]. Complexes formed from primary amines exhibited a weak, sharp band for the ν(N-H) stretching mode near 3,400cm^{-1}.

As discussed previously, the bonding mode of the ligands $C_nF_{2n+1}CO_2^-$ can be inferred from the difference between the observed $\nu_{as}(CO_2)$ and $\nu_s(CO_2)$ frequencies for the complex and these data, given in Table 6.10, clearly support a monodentate mode of coordination for the heptafluorobutyrate group in all such complexes. The spectrum of complexes derived from propargylamine exhibited an additional weak, sharp absorption near 3,300cm^{-1} due to the ν(C≡C-H) stretching frequency. Conversion from the chloro to $C_3F_7CO_2^-$ complexes resulted in little change in ν(N-H) or ν(C=O) values, but both ν(C≡O) bands were shifted by 15±5cm^{-1} to higher wavenumber reflecting the different electronegativities of the chloride and heptafluorobutyrate groups.

Table 6.10 Selected infra-red data[a] and calculated force constants for $Mo(CO)_2(\eta^3\text{-}CH_2{=}C(CONRR'){=}C{=}CH_2)L_2X$.

Complex L_2=bipy		ν(C≡O)	ν(C=O)	ν(N-H)	ν(C=C)	$\nu_{as}(CO_2)$	$\nu_s(CO_2)$	Δ	other	Force constants	
NRR'	X									k	k_i
NH_2	Cl	1898,1967	1613m	3,440w	1670w					15.06	0.58
NHMe	Cl	1880,1955	1651m	3,432w	1672w					14.88	0.58
NHMe	$C_3F_7CO_2$	1898,1976	1658m	3,440w	1664sh	1699m	1416w	283		15.17	0.61
NMe_2	Cl	1888,1960	1612m		1688w					14.97	0.56
NHEt	Cl	1889,1963	1651m	3,320w	1670w					15.00	0.58
NHEt	$C_3F_7CO_2$	1897,1973	1649m	3,412w	1672sh	1696m	1418w	278		15.14	0.59
NEt_2	Cl	1890,1958	1608m		1680w					14.97	0.53
$NHPr^n$	Cl	1880,1957	1648m	3,401w	1675w					15.00	0.58
$NHPr^n$	$C_3F_7CO_2$	1899,1969	1648m	3,403w	1677sh	1698m	1418w	280		15.12	0.55
NPr^n_2	Cl	1885,1970	1630m		1666w					15.02	0.65

Table 6.10 continued.

Complex L_2=bipy		ν(C≡O)	ν(C=O)	ν(N-H)	ν(C=C)	$\nu_{as}(CO_2)$	$\nu_s(CO_2)$	Δ	other	Force constants	
NRR'	X									k	k_i
NHPh	Cl	1880,1960	1662m	3,374w	1671w					14.91	0.62
NHPh	$C_3F_7CO_2$	1898,1973	1658m	3,380m	-	1693m	1420w	273		15.15	0.61
NH(CH_2Ph)	Cl	1880,1961	1651m	3,400w	1671w					14.91	0.63
NHCH_2CH=CH_2	Cl	1881,1958	1639m	3,402w	1678w					15.12	0.56
NHCH_2CH=CH_2	$C_3F_7CO_2$	1898,1970	1640m	3,401w	1680sh	1700m	1423w	277		14.90	0.60
NHCH_2C≡CH	Cl	1882,1958	1654m	3,412w	1680w				ν(C≡C-H) 3,270w	15.04	0.58
Complex L_2=phen											
NEt_2	Cl	1876,1960	1615m		1679w					14.88	0.65

^-Measured as Nujol mulls in units of cm^{-1}, -not observed
all bands strong unless otherwise stated.

^1H AND ^{13}C NMR SPECTRA

^1H and ^{13}C NMR spectra for complexes $Mo(CO)_2(\eta^3-CH_2=C(CONHR')=C=CH_2)(bipy)(O_2CC_3F_7)$ or $MoCl(CO)_2(\eta^3-CH_2=C(CONRR')=C=CH_2)L_2$ were recorded in CD_2Cl_2 and pertinent data are presented in Tables 6.11 and 6.12 respectively.

^1H NMR SPECTRA

All the ^1H NMR spectra exhibited two doublets, each integrating for one proton, between 5.4 and 6.5ppm with average coupling constants of 2.2Hz. These were assigned to the uncoordinated terminal $C=CH_2$ moiety. Singlets near 3.9 and 1.9ppm were attributed to the syn and anti protons of a terminal unsubstituted allyl methylene group $-CH_2$. No coupling was observed between these protons although the the ester complexes described by Willis exhibited coupling constants of 1.5Hz. In general resonances due to the amide protons >N-H were observed as broad triplets with coupling constants of ca 5Hz, however for some complexes these were obscured by signals due to CD_2Cl_2 or the higher field methylene doublet. Fig. 6.2 shows that the doublet arising from the methyl group in the methylamine derivative was not appreciably affected by the magnetic anisotropic effect of the bipy ligand, appearing at 1.99ppm. (J=4.95Hz). However the spectrum of the ethylamine product (Fig. 6.3) shows that in addition to an upfield shift of the methyl triplet to 0.5ppm (J=7.2Hz), two signals due to the two methylene protons appear upfield from the free amine position of 3.4ppm, with one clearly being more shielded than the other. This effect was also observed for the n-propylamine complex (Fig. 6.4), again revealing a pair of inequivalent CH_2 protons with one proton significantly upfield from the other (2.10 and 2.65ppm). A second methylene group was assigned to the high field multiplet at 0.95ppm, but here equivalence of the

Table 6.11 ^{1}H NMR data[a] for $Mo(CO)_2(\eta^3\text{-}CH_2\text{-}C(CONRR')\text{-}C\text{=}CH_2)L_2X$.

Complex L_2=bipy		Chemical shift δ(ppm), (multiplicity, coupling constant J in Hz, assignment).					
NRR'	X	H_{syn}	H_{anti}	$=CH_2$	Aliphatic	Aromatic	N-H
NHMe	$C_3F_7CO_2$	3.96s	1.96s	5.79(d,2.2,H)	1.99(d,4.95,H)	7.49-8.95(m,8H)	5.31(q,5.0,H)
				6.31(d,2.2,H)			
NHEt	$C_3F_7CO_2$	3.98s	1.96s	5.80(d,2.2,H)	0.52(t,7.23,3H),2.28(m,2H)	7.51-8.94(m,8H)	5.40(t,H)
				6.32(d,2.2,H)	2.66(m,2H)		
NEt_2	Cl	3.46s	1.89s	6.10(d,2.4,H)	0.53(t,6.41,3H),1.06(t,6.35,3H),	7.40-8.85(m,8H)	
				6.25(d,2.0,H)	2.79(m,H),3.17(m,H),3.77(m,2H)		
$NHPr^n$	$C_3F_7CO_2$	3.99s	1.96s	5.79(d,2.2,H)	0.92(m,7.8,2H),0.62(t,7.8,3H)	7.50-8.92(m,8H)	5.45(t,5.0,H)
				6.31(d,2.2,H)	2.07(m,6.8,H),2.63(m,7.4,H),		
NPr^n_2	Cl	3.37s	1.97s	5.49(d,2.4,H)	0.47(t,7.15,3H),0.98(t,7.16,3H),	7.39-8.83(m,8H)	
				6.08(d,2.4,H)	0.84(m,2H),1.49(m,H),1.86(m,H),		
					2.73(m,H),2.84(m,H),		
					3.34(m,H),3.60(m,H)		

Table 6.11 continued.

Complex L_2=bipy		Chemical shift δ(ppm), (multiplicity, coupling constant J in Hz, assignment).					
NRR'	X	H_{syn}	H_{anti}	$=CH_2$	Aliphatic	Aromatic	N-H
NHPh	$C_3F_7CO_2$	4.06s	2.03s	5.92(d,2.2,H)		6.80-8.90(m,13H)	-
				6.48(d,2.2,H)			
$NHCH_2CH=CH_2$	$C_3F_7CO_2$	3.99s	1.97s	5.80(d,2.2,H)	2.73(m,H),3.31(m,H)	7.50-8.93(m,8H)	5.47(t,5.0,H)
				6.33(d,2.4,H)	4.86(m,H),5.22(m,H)		
L_2=phen							
NEt_2	Cl	3.71s	1.89s	5.62(d,2.2,H)	0.94(brs,6H),2.23(q,H),2.38(m,H)	7.71-9.20(m,8H)	
				6.18(d,2.4,H)	2.79(m,7.03,H),3.68(m,7.04,H)		

^-in CD_2Cl_2 at room temperature, -not observed

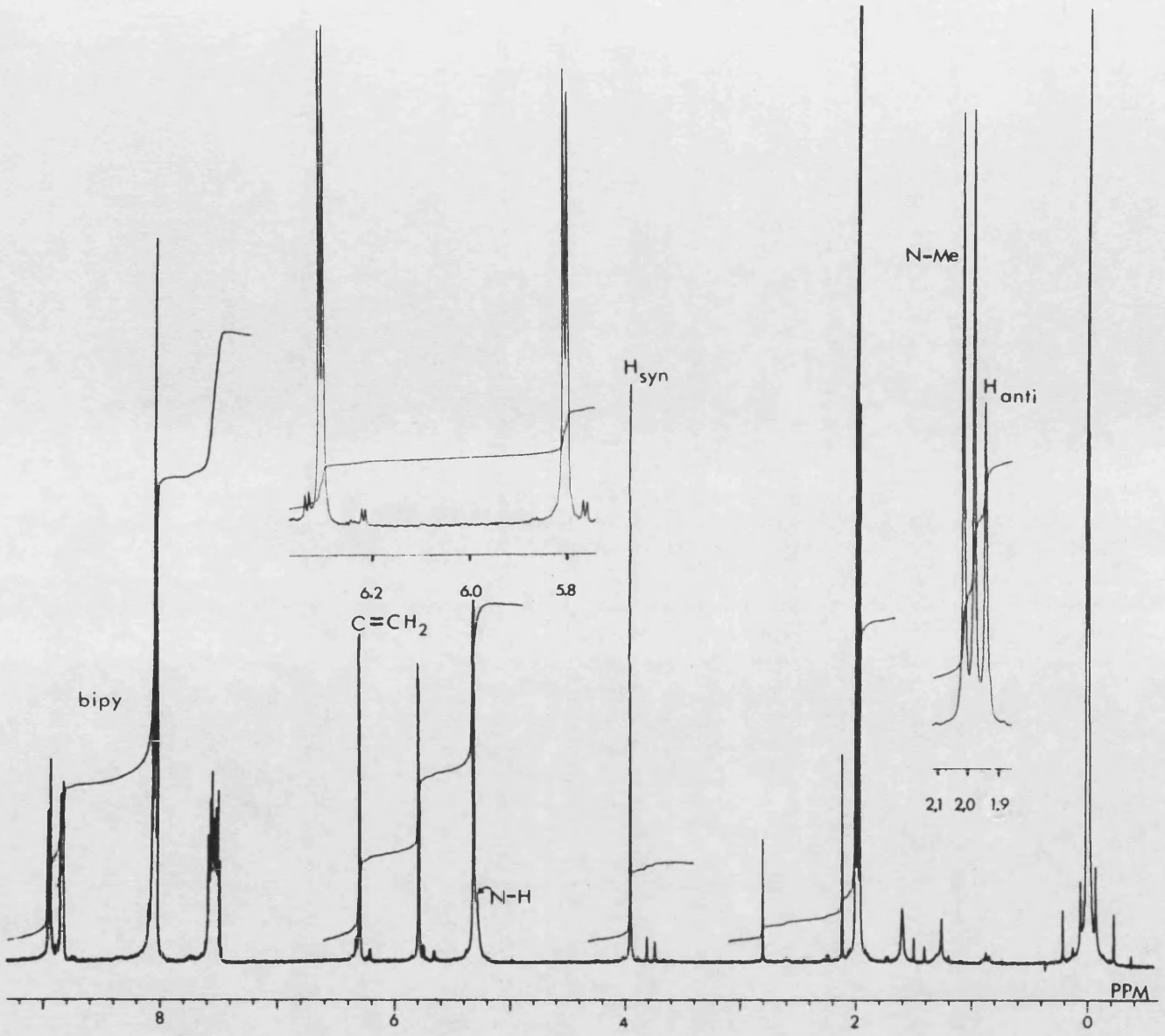

Fig. 6.2 ^{1}H NMR spectrum of $Mo(CO)_2(\eta^3\text{-}CH_2{=}C(CONHMe){-}C{=}CH_2)(bipy)(O_2CC_3F_7)$.

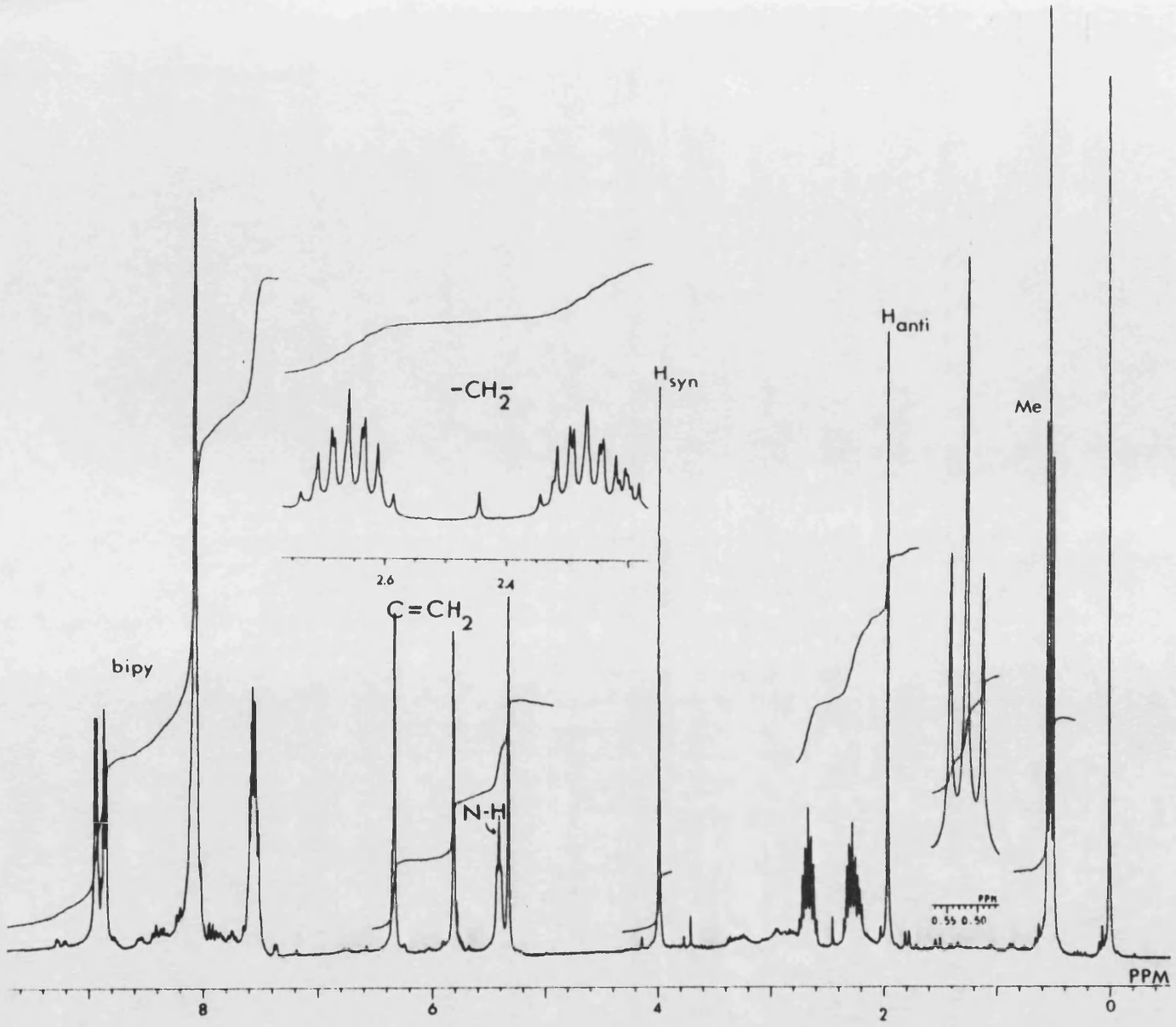

Fig. 6.3 ^{1}H NMR spectrum of $Mo(CO)_2(\eta^3\text{-}CH_2\text{-}C(CONHEt)\text{-}C\text{=}CH_2)(bipy)(O_2CC_3F_7)$.

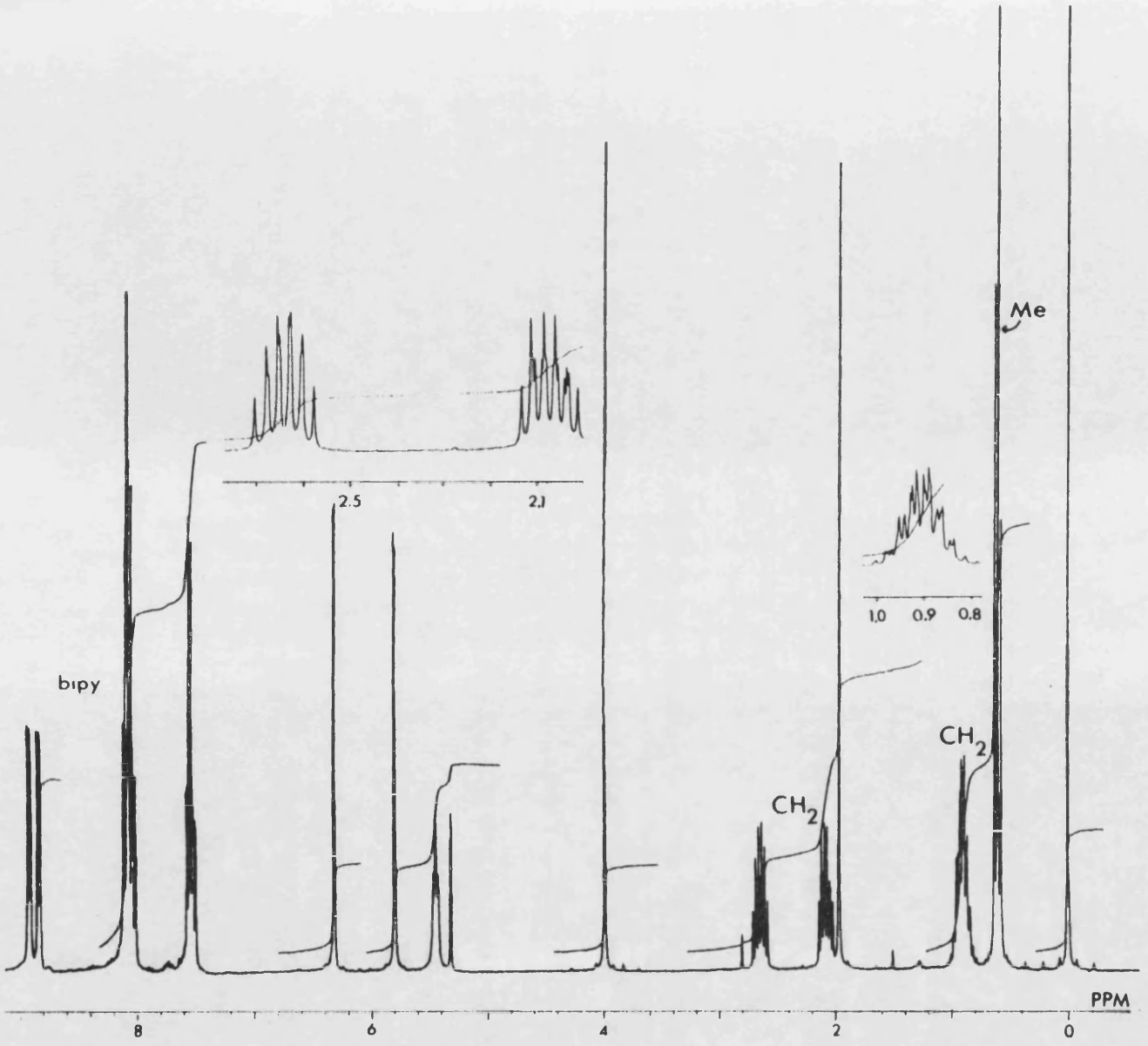

Fig. 6.4 ^{1}H NMR spectrum of $Mo(CO)_2(\eta^3\text{-}CH_2{=}C(CONHPr^n){-}C{=}CH_2)(bipy)(O_2CC_3F_7)$.

protons was apparent. The triplet at 0.62ppm due to the methyl group appeared upfield from the free amine value of 1.0ppm.

The diethylamine and di-n-propylamine complexes resulted in progressively more complex spectra as seen in Figs. 6.5 and 6.6, due to the increasing number of different proton environments. Thus in the spectrum of the diethylamine derivative two methylene protons are differently affected by the proximity of the bipy ligand (3.17 and 3.77ppm). Further upfield another pair of protons appear to be almost equivalent (2.79ppm) whilst triplet resonances at 1.06 and 0.58ppm indicated the two methyl groups were in dissimilar environments. Fig. 6.6 shows part of the expanded spectrum of the di-n-propylamine complex. The two triplets at 0.47 and 0.98ppm were attributed to the two methyl moieties and the remaining spectral pattern revealed two pairs of methylene protons at ca 2.8 and 0.8ppm, and resonances at 1.49, 1.86, 3.34 and 3.60ppm attributable to the four remaining protons. Part of the expanded ^{1}H NMR spectrum of the allylamine derivative is shown in Fig. 6.7. The methylene protons adjacent to the nitrogen of the allylamine group were inequivalent, appearing as two multiplets centred at 2.8 and 3.3ppm, whilst the methine and terminal methylene protons resulted in signals at 5.2 and 4.8ppm respectively, upfield from the free amine values.

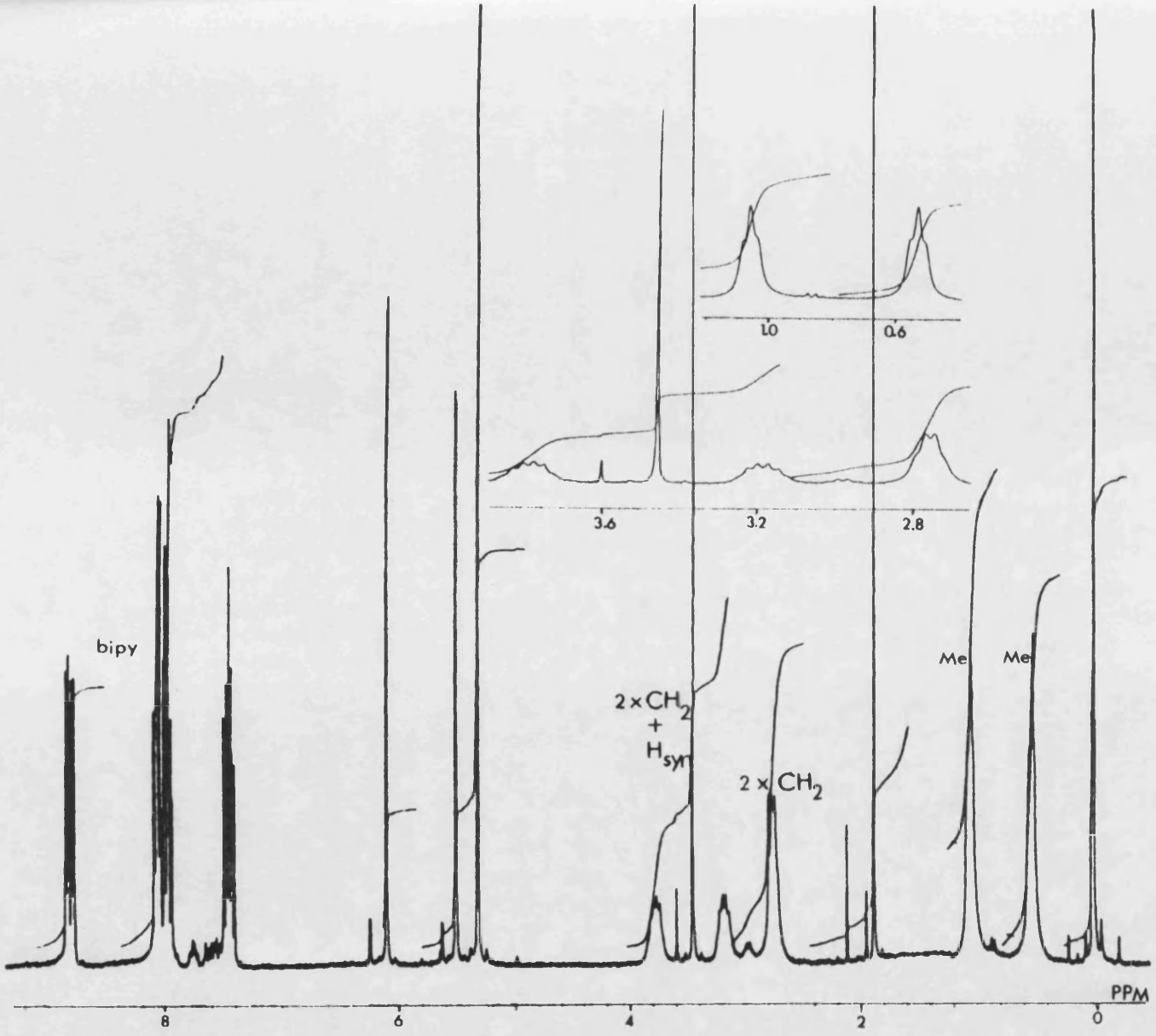

Fig. 6.5 ^{1}H NMR spectrum of $MoCl(CO)_2(\pi^3\text{-}CH_2\text{-}C(CONEt_2)\text{-}C\text{=}CH_2)$bipy.

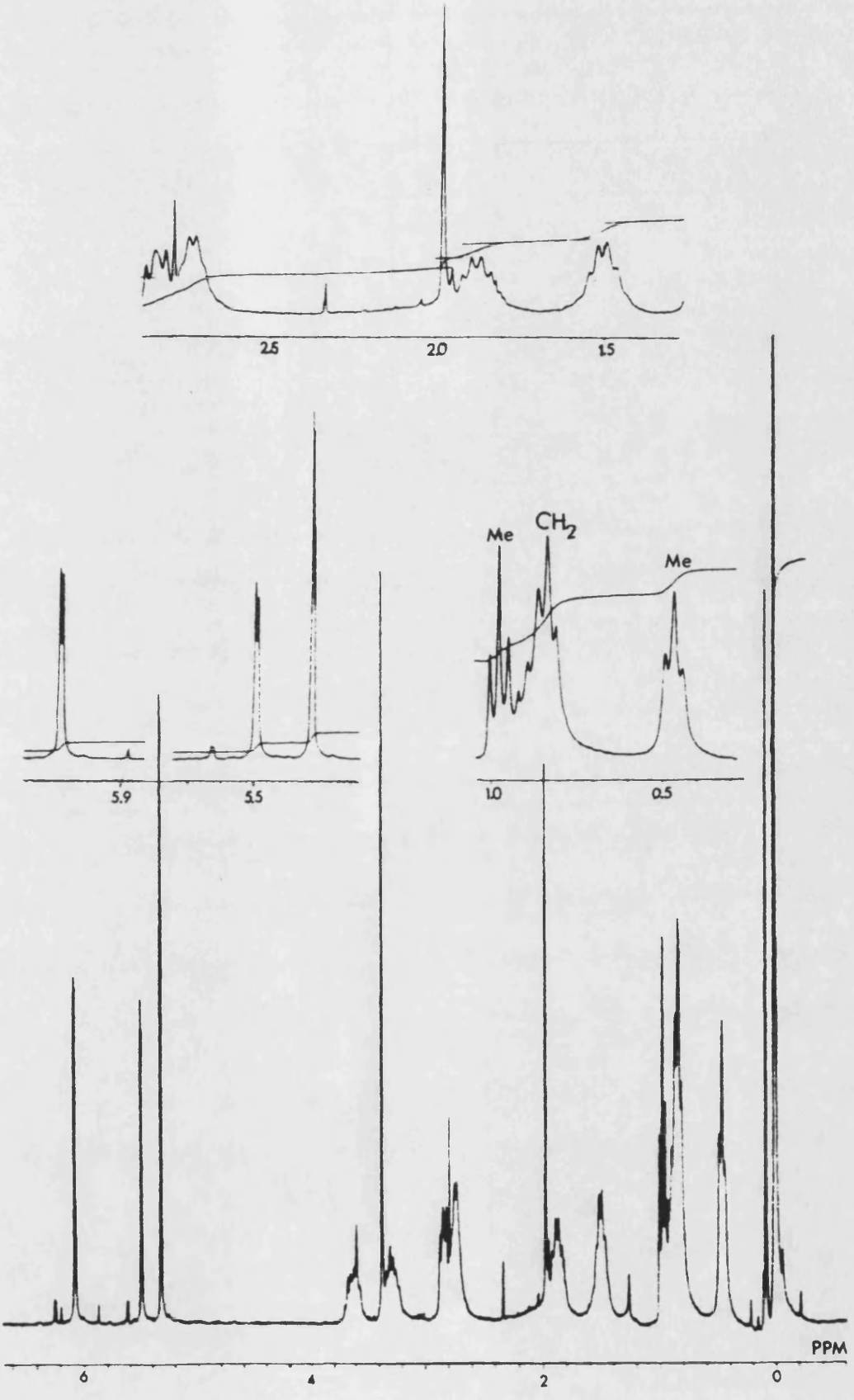

Fig. 6.6 Part of the ^1H NMR spectrum of

$MoCl(CO)_2(\eta^3\text{-}CH_2{=}C(CONPr^n_2){=}C{=}CH_2)bipy$ in CD_2Cl_2.

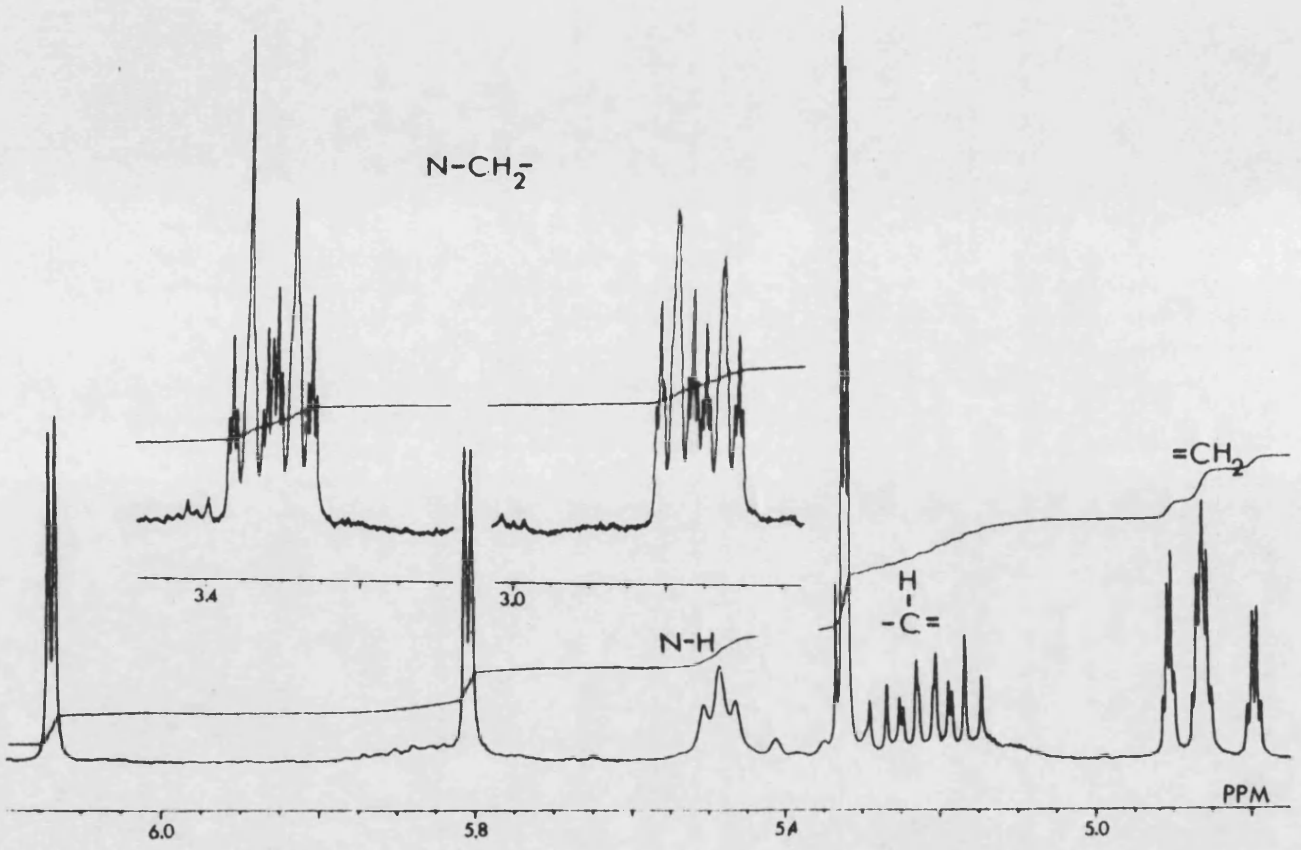

Fig. 6.7 Part of the ^{1}H NMR spectrum of $Mo(CO)_2(\eta^3\text{-}CH_2{=}C(CONHCH_2CH{=}CH_2){-}C{=}CH_2)(bipy)(O_2CC_3F_7)$.

In summary therefore, the chemical shifts of the -CONRR' derivatives show that the amido protons of the R and R' groups are differently influenced by their distance or proximity to the anisotropic effect of the bipy ligand. Thus one set of signals is likely to correspond to the shielded R group closest to the bipy plane, whilst the other arises from the more distant R' group. This accounts for the complex spectra observed for the diethylamine and di-n-propylamine complexes. For the -CONHR' derivatives steric arguements can be used to suggest that the proton adjacent to the amide nitrogen, should be orientated towards the bipy ligand in a structure analogous to that observed for the $-CO_2Me$ complex [325], and molecular models show that for an sp^2 hybridised nitrogen atom with this orientation the adjacent methylene groups will have protons at varying distances from the bipy ligand, so leading to different shielding effects.

This explanation is also consistent with the observed coupling constants. The relationship between the three-bond vicinal coupling constant ^3J and the dihedral angle θ between methylene protons can be shown in a qualitative manner by a plot of J against θ (Fig. 6.8) which suggests that for $\theta>80°$ both J and θ will increase together, whilst for $\theta<80°$ increasing dihedral angles result in lower coupling constants. On the assumption that the amide proton in the CONHEt complex is directed towards the vinylic group as discussed above, then two possible orientations of the ethyl group may be adopted as shown in Fig. 6.9 A and B below.

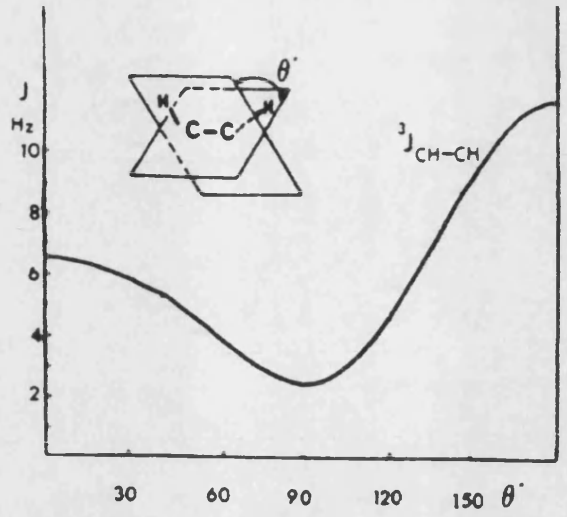

Fig. 6.8 Correlation between coupling constant and dihedral angle.

The two multiplets in Fig. 6.3 which were assigned to the methylene protons of the amido group exhibited coupling constants of 6.60Hz for the higher field multiplet and 6.41Hz for the lower field resonance. In **A** proton H^4 is shielded by bipy and can be assigned to the multiplet at higher field. Since θ_1 and θ_2 cannot both be less than 90° in this configuration, Fig. 6.8 shows that if $J(H^4)>>J(H^5)$ then $\theta_1>\theta_2$ and the methyl group approaches bipy and becomes shielded, in agreement with the observed chemical shift at

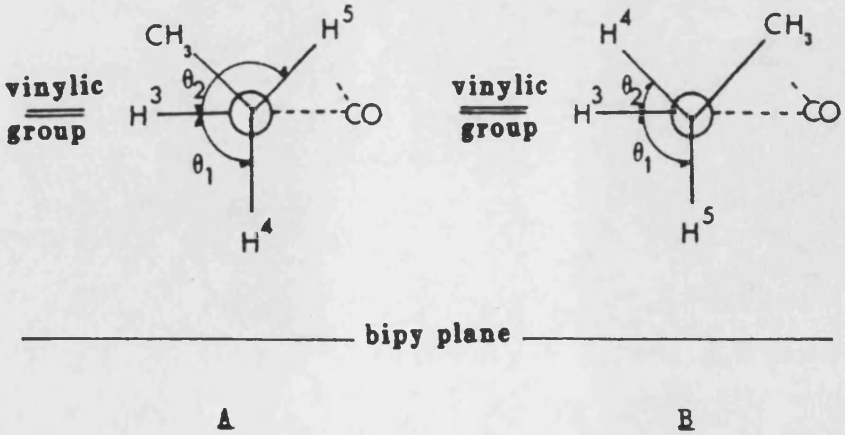

Fig. 6.9 Part of $Mo(CO)_2(\eta^3\text{-}CH_2{=}C(CONHEt){-}C{=}CH_2)(bipy)(O_2CC_3F_7)$.

0.52ppm. Similarly for configuration B, proton H^5 is shielded by bipy and assigned to the higher field multiplet which has the larger coupling constant. Since θ_1 and θ_2 in this orientation must both be less than 120°, then if $J(H^5)>>J(H^4)$ Fig. 6.8 shows that $\theta_1<\theta_2$ and again the CH_3 group approaches bipy and is shielded. Steric arguements might suggest that proximity of an alkyl or aryl group to the vinylic bond would disfavour arrangement A, whilst both bipy and the vinylic bond would present minimum steric strain for long alkyl chains or aromatic groups by the adoption of arrangement B.

The asymmetry within the molecule also creates a chiral centre which may give rise to enantiomeric forms. However on the basis of the NMR and infra-red evidence above, only one orientation of the -CONRR' group with respect to the allyl and vinylic ends of the η^3-butadiene unit is observed. Formation of amide complexes containing substituted, asymmetric R groups would introduce an additional chiral centre to these species and examination of their ^1H NMR spectra should prove interesting.

^{13}C NMR SPECTRA

Table 6.12 contains ^{13}C NMR data measured in CD_2Cl_2 for complexes $Mo(CO)_2(\eta^3\text{-}CH_2{=}C(CONRR'){=}C{=}CH_2)L_2X$ which were assigned to the carbon atoms numbered below by comparison with observed chemical shift values published for $MoCl(CO)_2(\eta^3\text{-}CH_2{=}C(CO_2Me){=}C{=}CH_2)bipy$ [325]. In several cases signals arising from the solvent at ca. 54ppm prevented complete assignment of the spectra.

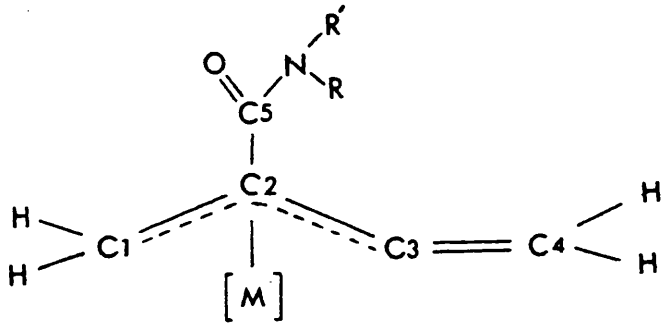

$[M] = Mo(CO)_2L_2X$

Table 6.12 ^{13}C NMR data[a] for $Mo(CO)_2(\eta^3\text{-}CH_2{=}C(CONRR'){=}C{=}CH_2)L_2X$.

R	R'	X	Chemical shift, δ(ppm)					
Complex L_2=bipy			C(1)	C(4)	C(5)	Aliphatics	Aromatics	CO
H	Me	$C_3F_7CO_2$	41.50	106.10	176.35	26.08CH_3	126.38 - 152.74	222.72
H	Et	$C_3F_7CO_2$	52.21	105.62	175.87	14.16CH_3,34.21CH_2	126.02 - 152.32	220.98
Et	Et	Cl	42.27	102.65	174.93	11.16CH_3,49.61CH_2	125.13 - 151.53	221.04
H	Pr^n	$C_3F_7CO_2$	[b]	105.84	176.29	11.39CH_3,22.74CH_2, 41.39CH_2	126.30 - 154.52	220.59
Pr^n	Pr^n	Cl	47.67	102.34	175.3	11.05CH_3,19.45CH_2, 49.29CH_2	125.08 - 154.82	221.49
H	Ph	$C_3F_7CO_2$	51.68	106.43	176.77		125.25 - 153.97	219.65
H	$CH_2CH{=}CH_2$	$C_3F_7CO_2$	41.83	105.78	175.84	57.36CH_2,52.24CH_2	126.12 - 152.29	220.07
Complex L_2=phen								
Et	Et	Cl	40.90	103.39	175.21	12.41CH_3,50.10CH_2	124.52 - 151.88	221.38

[a]-Measured at r.t. in CD_2Cl_2 [b]-Not observed.

6.3.3.1 DISCUSSION

It has been shown that in the reaction of $[MCl(CO)_3L_2]^-$ (L_2=bipy or phen) with 1,4-dichlorobut-2-yne in MeOH, the reaction pathway is dictated by the presence or absence of water or other donor ligands such as pyridine, a tertiary amine or a small primary or secondary amine. The mechanism proposed by Willis et al. involves coordination of water to the metal centre, leading to the formation of $MCl(CO)_2(\eta^3\text{-}CH_2\text{-}C(CO_2Me)\text{=}C\text{=}CH_2)L_2$ exclusively. The role of a non-aqueous donor species might reasonably be expected to parallel that of water and a mechanism for the formation of $MoCl(CO)_2(\eta^3\text{-}CH_2\text{-}C(CONRR')\text{=}C\text{=}CH_2)L_2$ might be postulated in which initial nucleophilic attack of the anion upon the alkyne would be followed by insertion of a CO group and coordination of the donor to the metal centre. In addition formation of the amido complexes in the presence of primary and secondary amines only, suggests that part of this mechanism must involve loss of a proton from these bases. To investigate the effect that the steric and electronic properties of the amines might have in such a mechanism, the reaction of $[MoCl(CO)_3L_2]^-$ with $ClCH_2C\equiv CCH_2Cl$ in methanol has been carried out in the presence of a series of amines HNRR' (R=H, R'=Me, Et, Pr^n, Pr^i, Bu^n, Bu^t, Ph, CH_2Ph, $CH_2CH\text{=}CH_2$ or $CH_2C\equiv CH$ and R=R'=Me, Et, Pr^n, Pr^i, Bu^n or Bu^t), having pka values ranging from 4.6 to 11.0 as shown in Table 6.13. The preformed η^3-butadiene ester complexes failed to react with these amines in alcoholic solutions, indicating that the amido complexes were forming via interaction of the amines with an intermediate.

Table 6.13 pKa values of amines HNRR' [327].

R,R'	H,Me	Me,Me	H,Et	Et,Et	H,Pr^n	Pr^n,Pr^n
pKa	10.66	10.73	10.81	10.49	10.71	10.71

R,R'	H,Pr^i	Pr^i,Pr^i	H,Bu^n	Bu^n,Bu^n	H,Bu^t	Bu^t,Bu^t
pKa	10.63	10.96	10.77	11.39	10.83	10.91

R,R'	H,Ph	Et,Ph	H,CH_2Ph	H,$CH_2CH{=}CH_2$	H,$CH_2C{\equiv}CH$
pKa	4.63	5.12	9.33	9.50	8.15

6.3.3.2 THE INFLUENCE OF AMINE SIZE AND BASICITY

Reactions involving amines R=H, R'=Me, Et or Pr^n and R=R'=Me or Et, proceeded within 1hr to produce the amide products $MoCl(CO)_2(\eta^3\text{-}CH_2{=}C(CONRR'){=}C{=}CH_2)L_2$ with no significant variations in reaction times or yields. However double this reaction time was required for R=H, R'=$CH_2CH{=}CH_2$ or $CH_2C{\equiv}CH$, whilst R=H, R'=Ph or CH_2Ph and R=R'=Pr^n in anhydrous methanol all failed to produce an amide product and yielded only the methanol double addition product. Comparison of the pKa values for these amines (Table 6.13) suggests that these differences in reactivity are related to the size of the amine and not to its electron-donating ability. In the presence of water however, reactions involving $HNPr^n_2$, H_2NPh or H_2NCH_2Ph yielded amides $MoCl(CO)_2(\eta^3\text{-}CH_2{=}C(CONRR'){=}C{=}CH_2)bipy$, suggesting that if the amine molecule is too large it fails to coordinate to the metal centre, but that a small molecule such as water can initiate formation of an intermediate which can then undergo successful attack by these bulky amines to form $MoCl(CO)_2(\eta^3\text{-}CH_2{=}C(CONRR'){=}C{=}CH_2)L_2$. In contrast, the use of water in reactions involving amines R=H, R'=Pr^i, Bu^n or Bu^t and R=R'=Pr^i, Bu^t or HNRR'=HNPh(Et), yielded only

$MoCl(CO)_2(\eta^3\text{-}CH_2{-}C(CO_2Me){-}C{=}CH_2)$bipy showing that even in the presence of this small donor, an intermediate will only react with amines of a certain size. A comparison of the pKa values of primary and secondary amines containing Pr^n, Pr^i, Bu^n and Bu^t groups (Table 6.13), shows that the differences in these reactions appear to be due not to their basicity, but to their relative sizes alone. Thus although these amines fall within the narrow pKa range 10.63 to 10.97, only H_2NPr^n forms an amido complex in anhydrous conditions, $HNPr^n_2$ requires water and all the remaining amines in this group fail to produce amides even in aqueous conditions. The apparent steric control in these reactions was further examined by adding a mixture of H_2NEt, H_2NPr^i and H_2NBu^t (pKa=10.81, 10.63, 10.83 respectively) in the proportions 1:1:1 to aqueous methanolic reactions of $[MoCl(CO)_3bipy]^-$ and $ClCH_2C{\equiv}CCH_2Cl$. Although these amines exhibit very similar pKa values, only the ethylamine-amido product was isolated, again indicating the importance of amine size. These results all indicate that for amines larger than R=H, R'=Pr^n, steric effects are the major controlling factor in these reactions.

6.3.3.3 REACTIONS INVOLVING SMALL AMINES

The amines R=H, R'=Me, Et or Pr^n and R=R'=Me or Et react with $[MoCl(CO)_3L_2]^-$ and $ClCH_2C{\equiv}CCH_2Cl$ in rigorously dried methanol to produce the amide complexes $MoCl(CO)_2(\eta^3\text{-}CH_2{-}C(CONRR'){-}C{=}CH_2)L_2$ without requiring the presence of any additional donor ligand. It might therefore be reasonably assumed that these amines both coordinate to the metal centre and subsequently react with intermediates. Reactions involving mixtures of these amines in 1:1 ratios yielded only one product in each case. The possibility that isolation of the ethylamine-amido complex only from mixtures of H_2NEt and $HNEt_2$ (pKa=10.81 and 10.49) arose from steric considerations

alone was disproved upon forming the dimethylamine-amido complex only from analogous reactions involving 1:1 mixtures of H_2NMe and $HNMe_2$ (pKa=10.66 and 10.73) and clearly indicated that here the relative basicities of the amines were important in determining the reaction product. However isolation of the n-propylamine-amido complex only from reactions involving 1:1 mixtures of $HNMe_2$ and H_2NPr^n (pKa 10.73 and 10.71 respectively), showed that for reactions involving a mixture of amines with similar electron donor abilities, steric factors predominate and dictate the nature of the single product formed. Table 6.14 presents these results in tabular form.

In summary therefore, it has been shown that a small donor is required to initiate formation of the amide complexes and that this may be either water or a small amine (R=H, R'=Me, Et or Pr^n, R=R'=Me or Et). In the presence of such a donor, the relative reactivities of these amines are dependent upon both their electron donating capabilities and their size.

Table 6.14 A summary of reaction products formed by $[MoCl(CO)_2L_2]^-$ and $ClCH_2C{\equiv}CCH_2Cl$ in MeOH with amines HNRR' in aqueous or anhydrous conditions or from mixtures of amines.

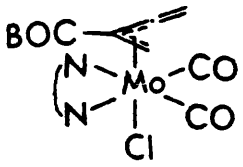

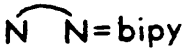

Amine, HNRR'	Other	Product, B
H_2NMe		HNMe
H_2NMe	$HNMe_2$	NMe_2
$HNMe_2$	H_2NPr^n	$HNPr^n$
$HNMe_2$		NMe_2
H_2NEt		HNEt
H_2NEt	$HNEt_2$	HNEt
$HNEt_2$		NEt_2
H_2NPr^n		$HNPr^n$
$HNPr^n{}_2$	H_2O	$NPr^n{}_2$
$H_2NCH_2CH{=}CH_2$	H_2O	$HNCH_2CH{=}CH_2$
$H_2NCH_2C{\equiv}CH$	H_2O	$HNCH_2C{\equiv}CH$
H_2NR (R=Pr^i, Bu^n, Bu^t)	H_2O	OMe
HNR_2 (R=Pr^i, Bu^n, Bu^t)	H_2O	OMe
HNPh(Et)	H_2O	OMe
H_2NR (R=Pr^i, Bu^n, Bu^t)	HNR_2 (R=Pr^i, Bu^n, Bu^t)	^
H_2NR (R=Pr^i, Bu^n, Bu^t)		^
HNR_2 (R=Pr^i, Bu^n, Bu^t)		^
H_2NPh	H_2O	HNPh
H_2NCH_2Ph	H_2O	$HNCH_2Ph$

^ $MoCl(CO)_2(\eta^3\text{-}CH_2{=}C(CO_2Me){=}C(OMe)(Me))bipy$

6.3.3.4 THE MECHANISM

The mechanism proposed by Willis et al. [325] for the formation of $MoCl(CO)_2(\eta^3\text{-}CH_2{=}C(CO_2Me){=}C{=}CH_2)bipy$ and $MoCl(CO)_2(\eta^3\text{-}CH_2{=}C(CO_2Me){=}C(OMe)(Me))bipy$ (Fig. 6.1) involves nucleophilic attack of the anion $[MoCl(CO)_3bipy]^-$ upon 1,4-dichlorobut-2-yne and CO insertion to generate a 16-electron species. At this point two reaction pathways led to either single or double addition of alcohol depending upon whether the donor molecule water or, in its absence, the unsaturated organic moiety itself coordinated to the metal centre. The amido complexes reported in this chapter were all synthesised in the presence of methanol, however the diethylamine product was also isolated in the presence of ethanol or acetonitrile, indicating that these solvents were not chemically involved during the reaction. This was confirmed upon isolation of the amido complexes from reactions of the anion, amine and excess alkyne alone and supports the mechanism shown in Fig. 6.11, in which addition of the amine rather than methanol across the inserted carbonyl group occurs.

In the absence of water Willis isolated double addition products from reactions involving either methanol or ethanol, however for the range of amines examined here no amido double addition products were isolated, and reactions carried out in abhydrous methanol involving large amines such as $HNPr^n_2$ or H_2NCH_2Ph yielded the methanol double addition products only.

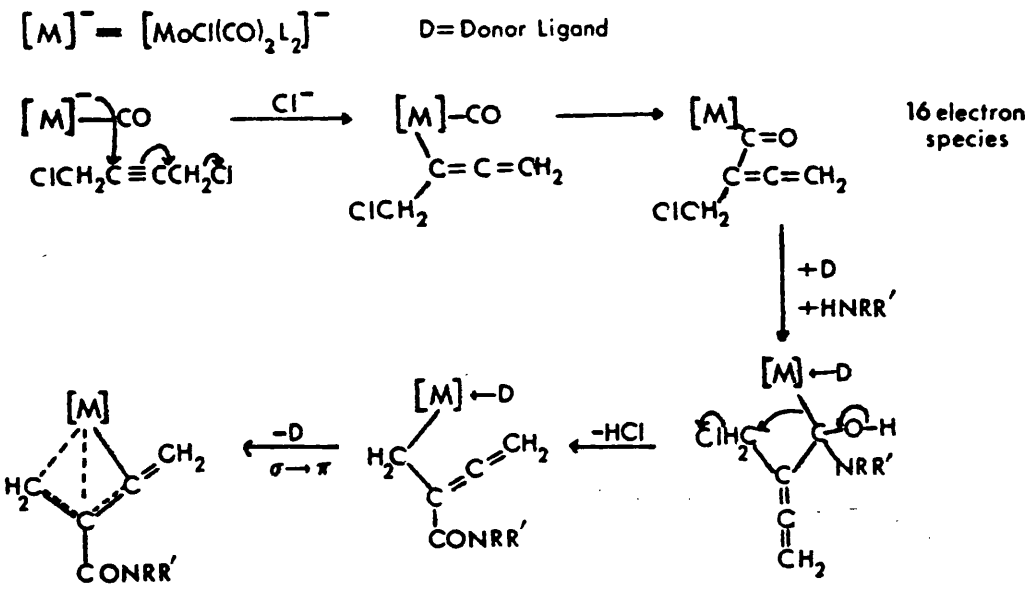

Fig. 6.11 A proposed mechanism for formation of $MoCl(CO)_2(\eta^3\text{-}CH_2{=}C(CONRR'){=}C{=}CH_2)L_2$.

This might be explained by the mechanism in Fig. 6.12, in which the highly reactive allene group generated by nucleophilic attack of the anion upon 1,4-dichlorobut-2-yne is attacked by a migrating amido group attached to the metal centre to form only one product. In such a mechanism a delicate balance might exist between the nucleophilic strength of the amine and its steric property in approaching the congested metal centre, in keeping with the importance of both the relative basicity and size of the amine found in these reactions. Thus in the absence of additional small donors such as water, nucleophilic attack of larger amines upon a coordinated carbonyl group may not occur, and consequently CO insertion into the metal-allene bond of the 16-electron intermediate and alcoholysis generates the ester double addition product.

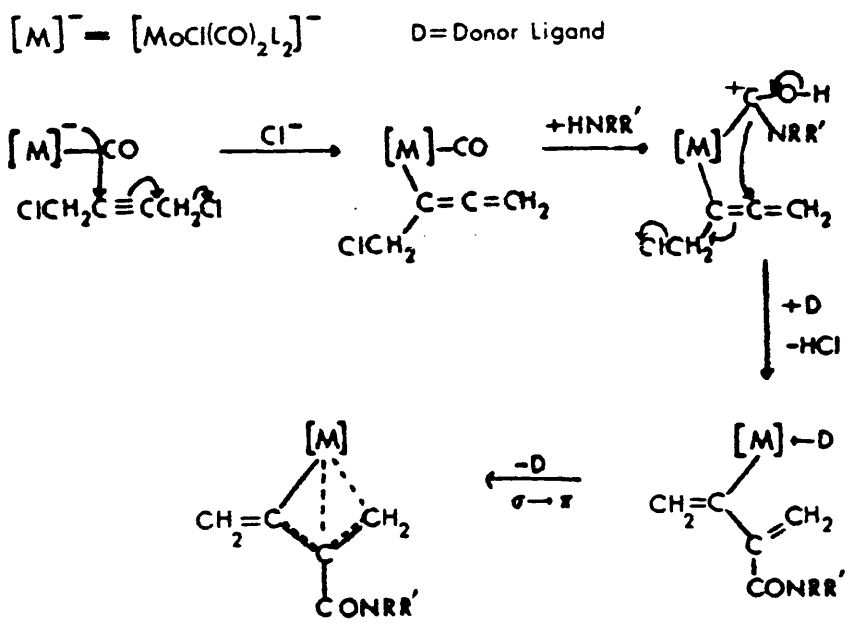

Fig. 6.12 An alternative mechanism.

A related mechanism shown below involves oxidative addition of 1,4-dichlorobut-2-yne to the anion $[MCl(CO)_3L_2]^-$, with loss of a chloride ion to form a cationic η^2-butatriene intermediate. Subsequent aminolysis affords the required amido product.

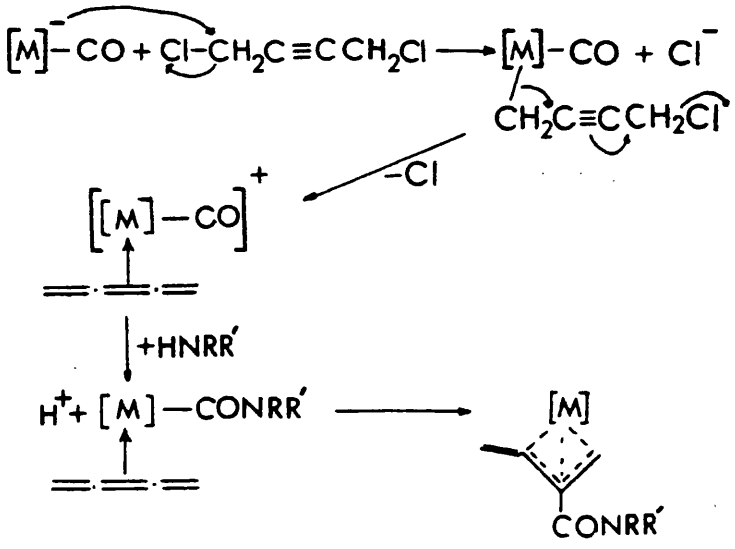

The latter mechanism is similar to that proposed by Giulieri and Benaim for reaction of the cationic cumulene $[Mo(CO)_3(\eta^3\text{-}CH_2{=}C{=}C{=}C(R')(R''))Cp]^+$ (R'≠R''=Me or Ph) with methanol to form $Mo(CO)_2(\eta^3\text{-}CH_2{-}C(CO_2Me){-}C{=}C(R')(R''))Cp$ [326]. Such a mechanism accounts for the absence of amine double addition products in the systems reported here, however attempts to isolate intermediates in these amine reactions which might help to establish the correct mechanism were unsuccessful and must await further investigations.

6.3.5 THE COMPLEXES $Mo(CO)_2(\eta^3\text{-}CH_2{=}C(CONHR'){=}C{=}CH_2)(bipy)(O_2CC_3F_7)$

In order to increase the solubility of the chloro complexes, the halide was extracted with silver tetrafluoroborate in the presence of perfluorocarboxylate anions, to form the title products. These were readily soluble in chlorinated and ketonic solvents and have been fully characterised by IR, ^1H and ^{13}C NMR spectroscopy. Comparison of proton NMR data (Table 6.11) for the more soluble chloro and heptafluorobutyrate complexes reported here, shows no significant chemical shift differences for the terminal syn or anti protons or methylene groups $C{=}CH_2$, indicating that for these species the bonding mode of the η^3-butadienyl ligand does not alter significantly upon anion exchange.

Single crystal X-ray structure determinations [325] of the complexes $MoCl(CO)_2(\eta^3\text{-}CH_2{=}C(CO_2Me){=}C{=}CH_2)bipy$ and $MoCl(CO)_2(\eta^3\text{-}CH_2{=}C(CO_2Me){=}C(OMe)(Me))bipy$ have revealed different orientations of the ester group as shown in Fig. 6.13 and this has been attributed to

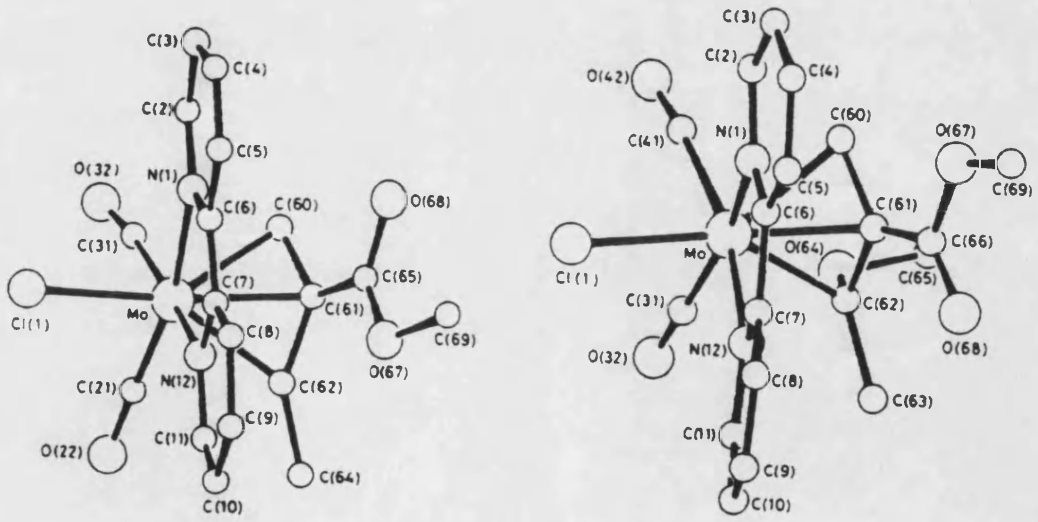

Fig. 6.13 Molecular structures of $MoCl(CO)_2(\eta^3\text{-}CH_2{=}C(CO_2Me){=}C{=}CH_2)bipy$ and $MoCl(CO)_2(\eta^3\text{-}CH_2{=}C(CO_2Me){=}C(OMe)(Me))bipy$.

addition of methanol at two stages in the formation of the latter complex and used as supportive evidence for the two pathways in the proposed mechanism (Fig. 6.1). Since the possible mechanisms proposed for formation of both the ester (B=OMe) and amide (B=NRR') complexes $MoCl(CO)_2(\eta^3\text{-}CH_2{=}C(COB){=}C{=}CH_2)bipy$, as well as their spectroscopic properties were similar in many respects, the same basic mode of bonding of the η^3-butadienyl group appeared to be present in both types of complex. Consequently structures for the amide derivatives were proposed in which the η^3-butadienyl group was orientated over the bipy plane with the -NRR' group directed towards the $C{=}CH_2$ 'tail'. In order to establish the molecular configuration of these complexes unequivocally, a single crystal structure determination of a representative member, namely $Mo(CO)_2(\eta^3\text{-}CH_2{=}C(CONHMe){=}C{=}CH_2)(bipy)(O_2CC_3F_7)$, was undertaken and is reported below. Although complexes $Mo(CO)_2(\eta^3\text{-}RC_3H_4)(bipy)(O_2CC_nF_{2n+1})$ (R=H or Me, n=1,2 or 3) have been previously prepared from their chloro analogues [322], a search using the Cambridge Data Centre files suggests that interest has centred upon trifluoroacetate complexes, and no crystallographic studies of Mo or W metal-allyl heptafluorobutyrate complexes were found. Therefore the following X-ray analysis provides an opportunity to examine both the unusual η^3-butadienyl group and the $C_3F_7CO_2^-$ ligand.

6.3.6 THE SOLID STATE STRUCTURE OF THE COMPLEX $Mo(CO)_2(\eta^3\text{-}CH_2{=}C(CONHMe){=}C{=}CH_2)(bipy)(O_2CC_3F_7)$

The crystal and molecular structure of the title compound were determined in collaboration with Drs. M.F.Mahon and K.C.Molloy at the University of Bath.

A sample of $Mo(CO)_2(\eta^3\text{-}CH_2{=}C(CONHMe){=}C{=}CH_2)(bipy)(O_2CC_3F_7)$ was recrystallised twice from CH_2Cl_2 mixtures at -10°C to produce suitable crystals for X-ray analysis. An orange rectangular crystal of approximate dimensions 0.5x0.4x0.15mm. was selected, mounted on a glass fibre and coated with epoxy resin. This was mounted at random on a Hilger-Watts Y290 four-circle automatic diffractometer which was used to measure diffraction intensities and unit cell dimensions. Graphite filtered molybdenum X-radiation was used and 2,652 independent reflections with $2<\theta<22°$ were measured, of which 2,337 reflections with $I>3\sigma(I)$ were used for subsequent refinement calculations. Backgrounds were measured from plots of background as a function of 2θ and no significant changes were observed in intensities from standard reflections monitored during the experiment. Neither an extinction nor an absorption correction were applied.

Crystal data: $C_{22}F_7H_{16}MoN_3O_6$, M=631.3, Triclinic, a=7.440(3)Å, b=9.727(3)Å, c=17.748(6)Å, α=100.567(26)°, β=94.836(23)°, γ=103.885(24)°, U(unit cell volume)=1214.67Å^3, D_c(calculated density)=1.73gcm^{-3}, Z(number of molecules in the unit cell)=2, F(000)(number of electrons in the unit cell)=628, λ(Mo-K_α)=0.7107Å, μ(Mo-K_α absorption factor)=5.49cm^{-1}, space group $P\bar{1}$ from the successful structure determination.

SOLUTION AND REFINEMENT

The position of the molybdenum atom was obtained by direct methods and subsequent Fourier analyses gave the positions of the remaining non-hydrogen atoms. The hydrogen atoms were not located, but were included in the final refinements at calculated positions for the bipy ligand only. The structure was refined by full-matrix least squares to R=6.38% and R_w=7.23% with a weighting scheme of $W=3.0065/[(\sigma^2(F_o)+0.0010(F_o)^2]$. Calculations were made using the Shelx 76 [121] system of programs at the University of Bath and scattering factors and dispersion corrections were obtained from the International Tables for X-Ray Crystallography [122]. The resulting list of atom positions is given in Appendix 4 and bond lengths and angles appear in Table 6.15. Appendix 4 contains a list of structural factors and thermal parameters.

Fig. 6.14 shows an ORTEP view of the molecule and the atomic numbering scheme used. The central molybdenum atom can be described as heptacoordinate being bonded to two nitrogen atoms of 2,2'-bipyridyl [Mo-N(1) 2.224(8)Å, Mo-N(2) 2.247(8)Å], two carbonyl groups [Mo-C(17) 1.971(13)Å, Mo-C(18) 1.975(13)Å], a monodentate $C_3F_7CO_2$ group and a bidentate substituted η^3-butadienyl system C_6H_8NO. The carbonyl groups are mutually cis with the C(17)-Mo-C(18) bond angle of 82.1(0.5)° comparing well with a value of 84.2° predicted from infra-red ν(CO) intensity measurements. Both metal-carbonyl groups are essentially linear [Mo-C(17)-O(2) 178.1(1.1)°, Mo-C(18)-O(3) 176.5(1.4)°] and the metal-carbon and C-O carbonyl bond lengths [C(17)-O(2) 1.157(14)Å, C(18)-O(3) 1.160(15)Å] are unexceptional. Parameters associated with the two bipyridyl rings compare well with values found for related $MoX(CO)_2(\eta^3$-allyl)bipy structures [240,255] and the two rings of the bipy unit are planar within experimental error, but the crowded metal coordination site is

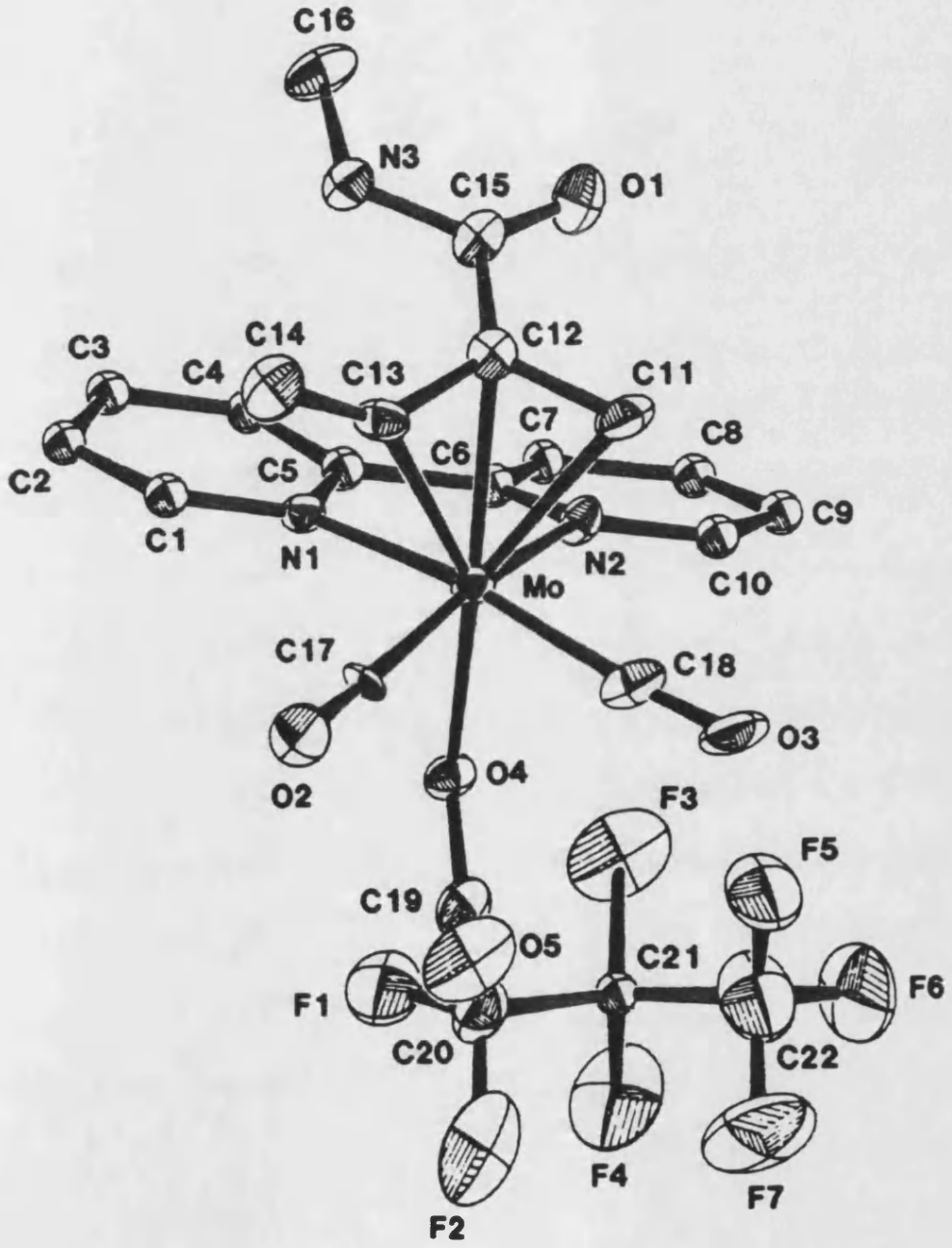

Fig. 6.14

An ORTEP view of $Mo(CO)_2(\eta^3\text{-}CH_2{=}C(CONHMe){=}C{=}CH_2)(bipy)(O_2CC_3F_7)$ with hydrogen atoms omitted for clarity, showing the atomic numbering scheme used.

Table 6.15 Interatomic distances and angles with standard deviations in parentheses for $Mo(CO)_2(\eta^3\text{-}CH_2{=}C(CONHMe){=}C{=}CH_2)(bipy)(O_2CC_3F_7)$.

Coordination Sphere:

Distances (Å):

Mo-O(4)	2.150(7)
Mo-N(1)	2.224(8)
Mo-N(2)	2.247(8)
Mo-C(11)	2.314(13)
Mo-C(12)	2.235(10)
Mo-C(13)	2.200(10)
Mo-C(17)	1.971(13)
Mo-C(18)	1.975(13)

Angles (°):

N(1)-Mo-O(4)	79.3(0.3)	C(17)-Mo-O(4)	89.3(1.4)
N(2)-Mo-O(4)	77.7(0.3)	C(17)-Mo-N(1)	101.9(0.4)
N(2)-Mo-N(1)	74.0(0.3)	C(17)-Mo-N(2)	166.9(0.4)
C(11)-Mo-O(4)	147.6(0.4)	C(17)-Mo-C(11)	109.0(0.5)
C(11)-Mo-N(1)	120.4(0.4)	C(17)-Mo-C(12)	105.4(0.4)
C(11)-Mo-N(2)	83.5(0.4)	C(17)-Mo-C(13)	70.7(0.5)
C(12)-Mo-O(4)	162.0(0.3)	C(18)-Mo-O(4)	88.8(0.4)
C(12)-Mo-N(1)	87.4(0.4)	C(18)-Mo-N(1)	167.4(0.4)
C(12)-Mo-N(2)	87.1(0.3)	C(18)-Mo-N(2)	99.5(0.4)
C(12)-Mo-C(11)	36.2(0.4)	C(18)-Mo-C(11)	68.4(0.5)
C(13)-Mo-O(4)	149.9(0.4)	C(18)-Mo-C(12)	103.2(0.5)
C(13)-Mo-N(1)	83.0(0.3)	C(18)-Mo-C(13)	109.6(0.4)
C(13)-Mo-N(2)	120.3(0.4)		
C(13)-Mo-C(11)	62.4(0.5)		
C(13)-Mo-C(12)	36.8(0.4)		

Carbonyl groups:

Distances (Å):

C(17)-O(2)	1.157(14)
C(18)-O(3)	1.160(15)

Angles (°):

C(18)-Mo-C(17)	82.1(0.5)
Mo-C(17)-O(2)	178.1(1.1)
Mo-C(18)-O(3)	176.5(1.4)

Table 6.15 continued.

Allyl ligand:

Distances (Å):

N(3)-C(16)	1.451(14)
C(11)-C(12)	1.416(17)
C(12)-C(13)	1.399(18)
C(12)-C(15)	1.487(16)
C(13)-C(14)	1.335(18)
C(15)-O(1)	1.208(16)
C(15)-N(3)	1.357(16)

Angles (°):

C(12)-C(11)-Mo	69.9(0.7)
C(11)-C(12)-Mo	74.9(0.7)
C(13)-C(12)-Mo	70.3(0.6)
C(13)-C(12)-C(11)	112.5(1.0)
C(15)-C(12)-Mo	117.3(0.6)
C(15)-C(12)-C(11)	121.4(1.2)
C(15)-C(12)-C(13)	125.8(1.1)
C(12)-C(13)-Mo	73.0(0.6)
C(14)-C(13)-Mo	144.7(1.2)
C(14)-C(13)-C(12)	141.7(1.3)
N(3)-C(15)-O(1)	123.2(1.1)
C(12)-C(15)-O(1)	121.7(1.2)

Heptafluorobutyrate ligand:

Distances (Å):

O(4)-C(19)	1.281(14)	C(21)-F(3)	1.427(22)
C(19)-C(20)	1.554(19)	C(21)-F(4)	1.363(21)
C(19)-O(5)	1.173(15)	C(21)-C(22)	1.393(32)
C(20)-F(1)	1.296(17)	C(22)-F(5)	1.306(22)
C(20)-F(2)	1.294(17)	C(22)-F(6)	1.269(28)
C(20)-C(21)	1.566(28)	C(22)-F(7)	1.480(33)

Table 6.15 continued.

Heptafluorobutyrate ligand:

Angles (°):

C(19)-O(4)-Mo	127.9(0.7)	F(5)-C(22)-C(21)	111.7(2.1)
O(5)-C(19)-O(4)	129.5(1.2)	F(6)-C(22)-C(21)	114.9(2.2)
C(20)-C(19)-O(4)	111.9(1.1)	F(6)-C(22)-F(5)	115.1(2.6)
C(20)-C(19)-O(5)	118.6(1.2)	F(7)-C(22)-C(21)	101.5(2.4)
C(21)-C(20)-C(19)	118.2(1.5)	F(7)-C(22)-F(5)	105.3(2.1)
F(1)-C(20)-C(19)	110.2(1.4)	F(7)-C(22)-F(6)	106.9(2.4)
F(1)-C(20)-C(21)	106.8(1.4)		
F(2)-C(20)-C(19)	111.0(1.1)		
F(2)-C(20)-C(21)	100.5(1.5)		
F(2)-C(20)-F(1)	109.6(1.7)		
C(22)-C(21)-C(20)	120.9(1.8)		
F(3)-C(21)-C(20)	110.3(1.6)		
F(3)-C(21)-C(22)	98.4(2.3)		
F(4)-C(21)-C(20)	110.2(1.9)		
F(4)-C(21)-C(22)	107.7(1.8)		
F(4)-C(21)-F(3)	108.2(1.5)		

Bipyridyl ligand:

Distances (Å):

N(1)-C(1)	1.353(15)	C(6)-C(7)	1.395(16)
C(1)-C(2)	1.340(16)	C(7)-C(8)	1.289(22)
C(2)-C(3)	1.407(18)	C(8)-C(9)	1.358(19)
C(3)-C(4)	1.350(19)	C(9)-C(10)	1.376(18)
C(4)-C(5)	1.396(15)	C(10)-N(2)	1.286(16)
C(5)-N(1)	1.342(13)	N(2)-C(6)	1.351(13)
C(5)-C(6)	1.478(16)		

Angles (°):

C(1)-N(1)-Mo	124.7(0.6)	C(5)-C(6)-N(2)	117.1(0.8)
C(5)-N(1)-Mo	117.0(0.7)	C(7)-C(6)-N(2)	121.5(1.1)
C(5)-N(1)-C(1)	118.0(0.8)	C(7)-C(6)-C(5)	121.4(1.0)
C(2)-C(1)-N(1)	124.1(1.0)	C(8)-C(7)-C(6)	116.9(1.2)
C(3)-C(2)-C(1)	117.6(1.3)	C(9)-C(8)-C(7)	120.9(1.4)
C(4)-C(3)-C(2)	119.7(1.2)	C(10)-C(9)-C(8)	117.1(1.5)
C(5)-C(4)-C(3)	119.5(1.1)	C(9)-C(10)-N(2)	124.8(1.2)
C(4)-C(5)-N(1)	121.1(1.1)	C(6)-N(2)-Mo	115.0(0.7)
C(6)-C(5)-N(1)	116.0(0.8)	C(10)-N(2)-Mo	125.2(0.7)
C(6)-C(5)-C(4)	122.9(0.9)	C(10)-N(2)-C(6)	118.6(0.9)

reflected in a slight distortion of the bipy plane with the two rings intersecting at an angle of 9.6°.

No structures determinations of heptafluorobutyrate complexes are available for direct comparison of bond lengths and angles, but consideration of the relative bond lengths and angles of Mo-O(4) [2.150(7)Å] and Mo-O(5) [3.454Å] and the O(4)-C(19)-O(5) and Mo-O(4)-C(19) bond angles of 129.5(12) and 127.9(0.7)° respectively, confirms the monodentate coordination mode predicted from infrared ν(CO) values. The C_3F_7 unit itself consists of a chain of three carbon atoms [C(20)-C(21)-C(22) 118.2(15)°] with average carbon-fluorine bond lengths of 1.348Å. The CF_3 and two CF_2 groups are in a staggered conformation and dihedral angles within these groups are given in Table 6.16.

Table 6.16 Dihedral angles within the C_3F_7 unit in $Mo(CO)_2(\eta^3\text{-}CH_2{=}C(CONHMe){-}C{=}CH_2)(bipy)(O_2CC_3F_7)$.

Terminal atoms	Angle(°)	Terminal atoms	Angle(°)
F(1)-F(3)	57.45	F(2)-F(3)	172.21
F(1)-F(4)	53.24	F(2)-F(4)	61.52
F(3)-F(5)	64.89	F(4)-F(5)	177.30
F(3)-F(6)	63.53	F(4)-F(6)	58.88
F(3)-F(7)	163.53	F(4)-F(7)	69.90

The bond lengths and angles associated with the η^3-CH_2=C(CONHMe)=C=CH_2 ligand are unusual. The carbon atoms C(11), C(12) and C(13) are bonded to the metal at distances of 2.314(13), 2.235(10) and 2.200(10)Å and comparison of these values with those for other reported Mo-η^3-allyl carbon distances in related complexes (Table 4.2) reveals a relatively short Mo-C(13) distance. The dissimilar bond lengths of C(11)-C(12) [1.416(17)Å], C(12)-C(13) [1.399[18)Å] and C(13)-C(14) [1.335(18)Å] also indicate asymmetric bonding within the unsaturated C_4 unit and an η^3-butadienyl structure may be postulated, whose bonding extremes may be represented by (I) and (II) in Fig. 6.15 below. In general bond lengths and angles within

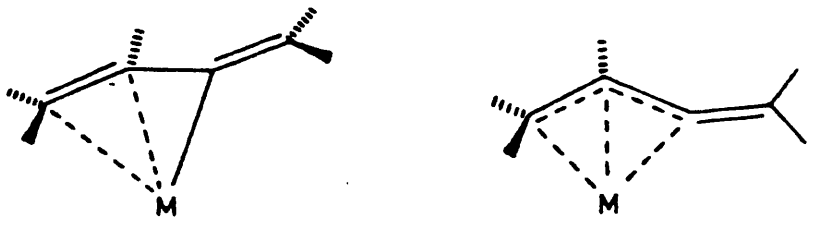

(I) (II)

Fig 6.15 Bonding extremes of the C_6H_8NO unit.

this C_6H_8NO group compare well with dimensions for the analogous ester moiety in $MoCl(CO)_2(\eta^3$-CH_2=C(CO_2Me)=C=CH_2)(bipy) [325]. The CO_2Me and CONHMe substituents show similar conformations with respect to the bipy plane, with both carbonyl groups orientated away from the terminal C=CH_2 group, as shown in Fig. 6.16. The dihedral angle C(16)-N(3)-C(15)-O(1) of -0.73° shows that this area of the C_6H_8NO group is almost planar and the methyl group is held well above the bipy plane [C(16)-C(4) 3.701Å]. The C(11)-C(12)-C(13) angle of 112.5(1.0)° falls well within the range reported for other neutral molybdenum η^3-allyl complexes (Table 4.3).

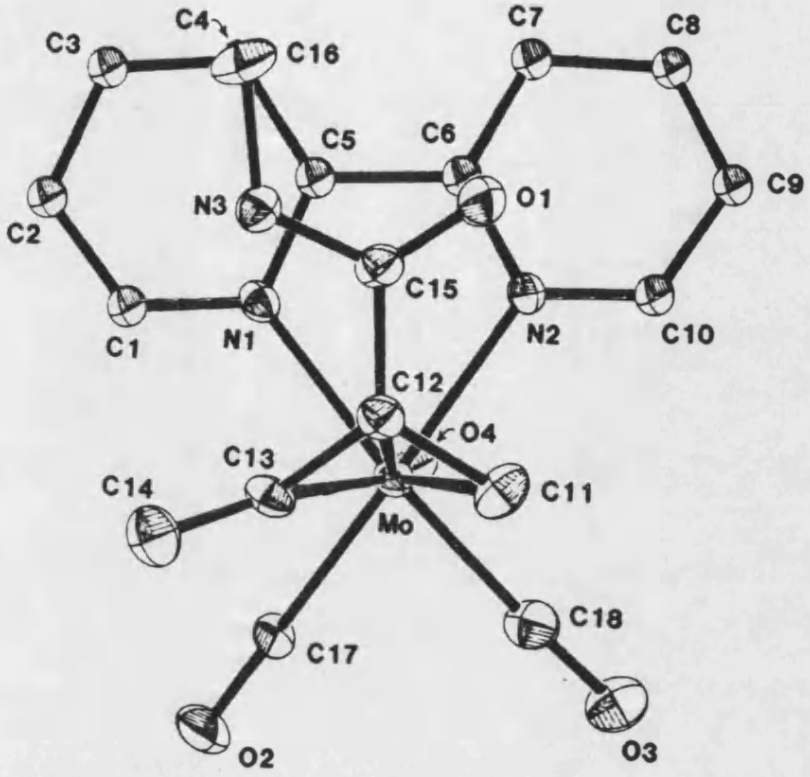

Fig. 6.16 View of the C_6H_6NO ligand above the bipy-Mo-$(CO)_2$ plane.

In contrast to the abnormally long uncoordinated terminal $C=CH_2$ bond length [1.45(0.05)Å] in $MoCl(CO)_2(\eta^3\text{-}CH_2{=}C(CO_2Me){=}C=CH_2)$bipy, the amide complex contains a much shorter terminal $C=CH_2$ bond length [C(13)-C(14) 1.335(18)Å] comparable to the free butadiene distance [1.34Å], and bond lengths for C(11)-C(12) and C(12)-C(13) [1.416(17), 1.399(18)Å] are not significantly different from those found in related η^3-C_3H_5-metal complexes (Table 4.3). Thus overall the bonding of the C_4 unit in the amide complex more closely resembles the η^3-allylic form (II) than (I). This formulation however, does not explain the unusually short Mo-C(13) distance [2.200(10)Å]. Comparison with the average Mo-C(carbonyl) separation [1.973(13)Å] suggests a considerable degree of back-bonding between the metal and C(13). A search using the Cambridge Data Centre files

for crystallographic studies of η^3-butadienyl complexes has revealed only two examples [330,331], both of which were formed via σ-butadienyl precursors containing highly electron withdrawing substituents. Several structural features within the M-C_4 unit of the π-allylidene complex $CpFe(PPh_3)(\eta^3\text{-}CF_2{=}C(CF_3){=}C{=}C(CF_3)_2)$ shown below,

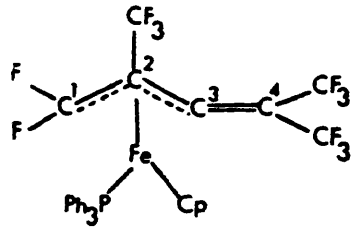

Fe-C^1 1.969(7)Å Fe-C^2 1.981(7)Å Fe-C^3 1.905(6)Å

C^1-C^2 1.426(9)Å C^2-C^3 1.442(8)Å C^3-C^4 1.319(8)Å

are similar to those of the amido structure reported here, with the C^3-C^4 bond showing considerable double bond character compared to C^1-C^2 and C^2-C^3 and an unusually short Fe-C^3 distance. However Bruce et al considered that the unusually short metal-C^3 distance in $CpW(CO)_2(\eta^3\text{-}C(CN)_2{=}C(Ph){=}C{=}C(CN)_2)$ suggested that this complex could be described as a methylenetungstabicyclobutane.

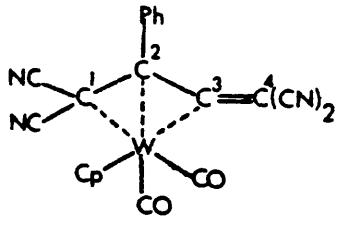

W-C^1 2.285(8)Å W-C^2 2.253(7)Å W-C^3 2.075(8)Å

C^1-C^2 1.480(9)Å C^2-C^3 1.439(9)Å C^3-C^4 1.355(10)Å

Fig. 6.17 shows the crystal packing for $Mo(CO)_2(\eta^3\text{-}CH_2{=}C(CONHMe){=}C{=}CH_2)(bipy)(O_2CC_3F_7)$ and illustrates the unit cell which

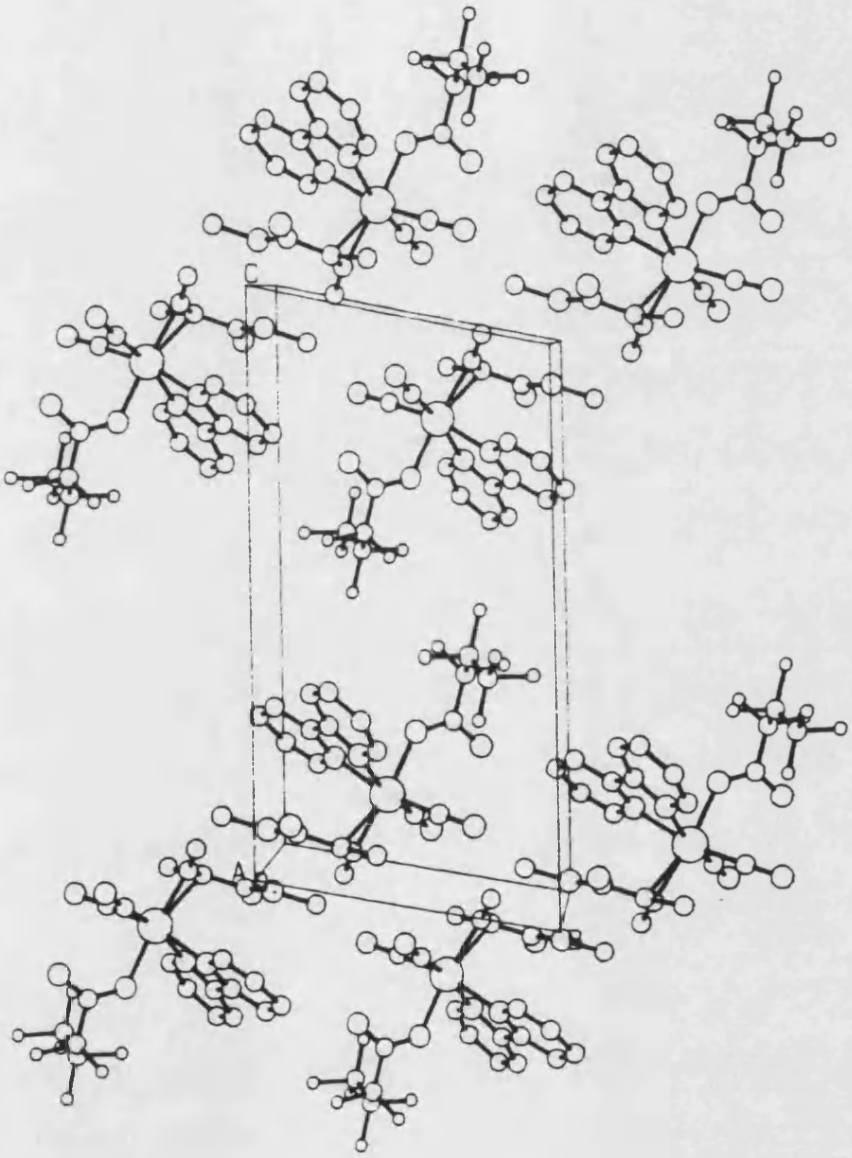

Fig. 6.17 The crystal packing and unit cell of

$Mo(CO)_2(\eta^3\text{-}CH_2{=}C(CONHMe){=}C{=}CH_2)(bipy)(O_2CC_3F_7)$.

contains two molecules related by a centre of inversion. An accurate model of the compound suggested that the geometry might be classified as a CTP with the heptafluorobutyrate oxygen atom in the capping position and the allyl group at the unique edge, as shown in Fig. 6.18.

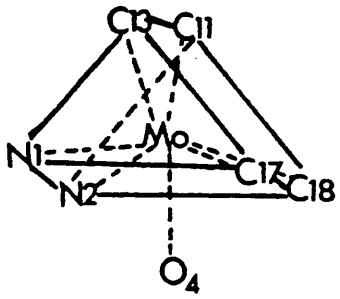

Fig. 6.18 CTP geometry of $Mo(CO)_2(\eta^3\text{-}CH_2{=}C(CONHMe){-}C{=}CH_2)(bipy)(O_2CC_3F_7)$.

APPENDIX 1

APPENDIX 1 PHYSICAL METHODS, REACTION CONDITIONS AND STARTING MATERIALS

1A PHYSICAL METHODS

The methods used to characterise and analyse the complexes discussed in this thesis are described in this section.

1A.1 INFRA-RED SPECTROSCOPY

A Perkin-Elmer 599B spectrometer was used to record IR spectra in the range 4000-650cm^{-1} as Nujol mulls using NaCl discs or as solutions in CH_2Cl_2, MeOH, MeCN or acetone in $1cm^3$ NaCl solution cells, and in the range 650-200cm^{-1} as Nujol mulls between CsI plates. Wavenumber calibration was achieved using a polystyrene film.

1A.2 ULTRA-VIOLET SPECTROSCOPY

Absorbance spectra of the samples as solutions in CH_2Cl_2 were measured using a Cecil CE 595 Double Beam spectrophotometer with 1cm path length silica cells.

1A.3 ^1H AND ^{13}C NMR SPECTROSCOPY

^1H and ^{13}C NMR spectra were obtained with a Jeol GX 270 MHz FT spectrometer, using solutions of the samples in $(CD_3)_2CO$, CD_3OD, CD_2Cl_2, CD_3CN or D_2O, and utilising the associated variable temperature controller when required. The internal standard for ^1H and ^{13}C spectra was TMS.

1A.4 MASS SPECTROSCOPY

Mass spectra were recorded on a VG 70-70E instrument and a DS 2025 data system. FAB positive ion spectra were obtained on samples dispersed in glycerol using xenon as the fast atom beam. The isotope pattern of Mo or W showed the presence of metal-containing fragments and results of ion abundances are reported relative to the most

abundant metal-containing species which is taken as being equal to 100% abundance.

1A.5 CONDUCTIVITY MEASUREMENTS

Conductance measurements at 295K were made on a Wayne-Kerr Autobalance bridge on 10^{-3}M solutions, using rigorously dried solvents. The cell constant was calculated using a standard aqueous 0.1M KCl solution.

1A.6 ELEMENTAL ANALYSIS

Carbon, hydrogen, nitrogen and halogen analyses were carried out by either Butterworth Laboratories Ltd., Teddington, Middlesex or by Analytical Services, School of Chemistry, University of Bath.

1B SOLVENTS AND GENERAL REACTION CONDITIONS

Solvents were purified by distillation if necessary, and then dried for 24hr with molecular sieve 4A before storing over fresh sieves and de-gassed with dry, oxygen-free nitrogen prior to use. All reactions were carried out under an atmosphere of dry nitrogen gas unless otherwise stated.

1C REAGENTS AND STARTING MATERIALS

Purchased reagents were used as received without further purification. Some starting materials were prepared in the laboratory as outlined in the relevant experimental sections.

REFERENCES

REFERENCES

1 D.J.Bevan and R.J.Mawby, J. Chem. Soc., Dalton Trans., 1980, 1904

2 J.W.Faller, D.A.Haitko, R.D.Adams and D.F.Chodosh, J. Am. Chem. Soc., 1979, 101, 865

3 B.J.Brisdon and A.A.Woolf, J. Chem. Soc., Dalton Trans., 1978, 291

4 B.J.Brisdon, D.A.Edwards, K.E.Paddick and M.G.B.Drew, J. Chem. Soc., Dalton Trans., 1980, 1317

5 S.Trofimenko, J. Am. Chem. Soc., 1969, 91, 3183

6 A.J.Deeming, M.T.P. Int. Rev. Sci., Inorg. Chem. Ser., 1974, 9, 275

7 R.J.Jernigan and G.R.Dobson, Inorg. Chem., 1972, 11, 81

8 J.W.McDonald and F.Basolo, Inorg. Chem., 1971, 10, 492

9 M.M.Memering and G.R.Dobson, Inorg. Chem., 1973, 12, 2490

10 M.W.Anker, R.Colton and I.B.Tomkins, Aust. J. Chem., 1979, 20, 9

11 R.Colton and I.B.Tomkins, Aust. J. Chem., 1966, 19, 1143

12 R.Colton and I.B.Tomkins, Aust. J. Chem., 1966, 19, 1519

13 R.Colton and C.J.Rix, Aust. J. Chem., 1969, 22, 305

14 M.G.B.Drew, B.J.Brisdon and A.G.Buttery, Acta Cryst., 1982, B38, 1598

15 F.A.Cotton, L.R.Falvello and J.H.Meadows, Inorg. Chem., 1985, 24, 514

16 J.R.Moss and B.L.Shaw, J. Chem. Soc. (A), 1970, 595

17 M.W.Anker, R.Colton and I.B.Tomkins, Rev. Pure and Appl. Chem. (Australia), 1968, 18, 23

18 J.Lewis and R.Whyman, J. Chem. Soc. (A), 1967, 77

19 A.D.Westland and N.Muriithi, Inorg. Chem., 1972, 11, 2971

20 P.K.Baker, S.G.Fraser and E.M.Keys, J. Organomet. Chem., 1986, 309, 319

21 P.K.Baker and S.G.Fraser, Inorg. Chim. Acta, 1986, 116, L1

22 P.K.Baker and S.G.Fraser, Inorg. Chim. Acta, 1986, 116, L3

23 P.K.Baker and S.G.Fraser, Polyhedron, 1986, 5, 1381

24 P.K.Baker and S.G.Fraser, J. Organomet. Chem., 1987, 329, 209

25 L.Bencze, J. Organomet. Chem., 1972, 37, C37

26 P.Umland and H.Vahrenkamp, Chem. Ber., 1982, 115, 3565

27 J.B.Johnson and W.G.Klemperer, J. Am. Chem. Soc., 1977, 99, 7132

28 M.Bigorgne, J. Inorg. Nucl. Chem., 1964, 26, 107

29 R.J.Angelici and C.M.Ingemason, Inorg. Chem., 1969, 8, 83

30 C.A.Tolman, J. Am. Chem. Soc., 1970, 92, 2953

31 E.W.Abel, M.A.Bennett and G.Wilkinson, J. Chem. Soc., 1959, 2323

32 W.D.Horrocks Jr. and R.C.Taylor, Inorg. Chem., 1963, 2, 723

33 W.A.Graham, Inorg. Chem., 1968, 6, 1731

34 R.J.Angelici and M.D.Malone, Inorg. Chem., 1967, 6, 1731

35 J.H.Plastas, J.M.Stewart, H.S.Preston and S.O.Grim, Inorg. Chem., 1972, 11, 161

36 J.H.Plastas, J.M.Stewart and S.O.Grim, J. Am. Chem. Soc., 1969, 91, 4326

37 C.A.Tolman, Chem. Rev., 1977, 313

38 J.A.Bowden and R.Colton, Aust. J. Chem., 1972, 25, 17

39 M.G.B.Drew, Prog. Inorg. Chem., 1977, 23, 67

40 R.J.Gillespie, Can. J. Chem., 1960, 38, 818

41 D.Britton, Can. J. Chem., 1963, 41, 1632

42 T.A.Claxton and G.C.Benson, Can. J. Chem., 1966, 44, 157

43 H.B.Thompson and L.S.Bartell, Inorg. Chem., 1968, 7, 488

44 E.L.Muetterties and L.J.Guggenburger, J. Am. Chem. Soc., 1974, 96, 1748

45 W.A.Dollase, Acta Cryst., 1974, A30, 513

46 M.G.B.Drew, J.Chem. Soc., Chem. Commun., 1972, 626

47 M.G.B.Drew, J.Chem. Soc., Chem. Commun., 1972, 1329

48 M.G.B.Drew and J.D.Wilkins, J. Chem. Soc., Dalton Trans., 1974, 1654

49 S.J.Lippard and D.F.Lewis, Inorg. Chem., 1972, 11, 621

50 D.L.Lewis and S.J.Lippard, J. Am. Chem. Soc., 1975, 97, 2697

51 S.J.Lippard, E.B.Drayer and C.T.Lam, Inorg. Chem., 1979, 18, 1904

52 M.G.B.Drew and A.P.Wolters, J. Chem. Soc., Chem. Commun., 1972, 457

53 M.G.B.Drew, J.D.Wilkins and A.P.Wolters, J. Chem. Soc., Chem. Commun., 1972, 1278

54 H.P.M.M.Ambrosius, J.H.Noordik and G.J.A.Ariaans, J. Chem. Soc., Chem. Commun., 1980, 832

55 R.M.Foy, D.L.Kepert, C.L.Raston and A.H.White, J. Chem. Soc., Dalton Trans., 1980, 440

56 M.G.B.Drew and J.D.Wilkins, J. Chem. Soc., Dalton Trans., 1977, 557

57 M.G.B.Drew and J.D.Wilkins, J. Chem. Soc., Dalton Trans., 1977, 194

58 M.G.B.Drew, A.W.Johans and A.P.Wolters, J. Chem. Soc., Chem. Commun., 1971, 819

59 M.G.B.Drew and C.J.Rix, J. Organomet. Chem., 1975, 102, 457

60 A.L.Beauchamp, F.Belanger-Gariepy and S.Arabi, Inorg. Chem., 1985, 24, 1860

61 P.D.Brotherton, J.M.Epstein, A.H.White and S.B.Wild, Aust. J. Chem., 1974, 27, 2667

62 J.L.Templeton and B.C.Ward, Inorg. Chem., 1980, 19, 1753

63 L.Mihichuk, M.Pizzey, B.Robertson and R.Barton, Can. J. Chem., 1986, 64, 991

64 G.Lawless, G.McNally, A.R.Manning, D.Cunningham and P.McArdle, Polyhedron, 1986, 5, 1741

65 J.L.Templeton and B.C.Ward, J. Am. Chem. Soc., 1981, 103, 3743

66 J.Chatt, M.Kubota, G.J.Leigh, F.C.March, R.Mason and D.J.Yarrow, J. Chem. Soc., Chem. Commun., 1974, 1033

67 S.Arabi, C.Berthelot, J.Barry, B.Chaudret and N.J.Taylor, Polyhedron, 1986, 5, 1785

68 M.G.B.Drew and J.D.Wilkins, J. Chem. Soc., Dalton Trans., 1975, 1984

69 D.L.Kepert, Prog. Inorg. Chem., 1979, 25, 41

70 M.G.B.Drew and R.Mandyczewsky, J. Chem. Soc., Chem. Commun., 1970, 292

71 F.C.Bradley, E.H.Wong, E.J.Gabe, F.L.Lee and Y.Lepage, Polyhedron, 1987, 6, 1103

72 M.G.B.Drew, A.P.Wolters and I.B.Tomkins, J. Chem. Soc., Dalton Trans., 1977, 974

73 P.D.Brotherton, J.M.Epstein, A.H.White and S.B.Wild, Aust. J. Chem., 1974, 27, 2667

74 E.N.Cradwick and D.Hall, J. Organomet. Chem., 1970, 25, 91

75 F.A.Cotton, L.R.Falvello and R.Poli, Polyhedron, 1987, 6, 1135

76 M.G.B.Drew and A.P.Wolters, Acta Cryst., 1977, B33, 1027

77 W.R.Cullen and L.M.Mihichuk, Can. J. Chem., 1976, 54, 2548

78 R.Colton, Coord. Chem. Rev., 1971, 6, 269

79 R.Colton and J.Kevekordes, Aust. J. Chem., 1982, 35, 895

80 A.Mawby and G.E.Pringle, J. Inorg. Nucl. Chem., 1072, 34, 517

81 R.Hoffmann, B.F.Beier, E.L.Muetterties and A.R.Rossi, Inorg. Chem., 1977, 16, 511

82 M.R.Snow and F.L.Wimmer, Aust. J. Chem., 1976, 29, 2349

83 J.A.Connor, E.J.James, C.Overton and N.El Murr, J. Chem. Soc., Dalton Trans., 1984, 255

84 R.Colton, G.R.Scollary and I.B.Tomkins, Aust. J. Chem., 1968, 21, 15

85 M.G.B.Drew, I.B.Tomkins and R.Colton, Aust. J. Chem., 1970, 23, 2517

86 P.Umland and H.Vahrenkamp., Chem. Ber., 1982, 115, 3565

87 M.W.Anker, R.Colton and I.B.Tomkins, Aust. J. Chem., 1968, 21, 1143

88 M.W.Anker, R.Colton and I.B.Tomkins, Aust. J. Chem., 1968, 21, 1159

89 M.W.Anker, R.Colton and I.B.Tomkins, Aust. J.Chem., 1971, 24, 1157

90 M.H.Chisholm, J.C.Huffman and R.L.Kelly, J. Am. Chem. Soc., 1979, 101, 7615

91 J.L.Templeton and B.C.Ward, J. Am. Chem. Soc., 1980, 102, 6568

92 F.A.Cotton and J.H.Meadows, Inorg. Chem., 1984, 23, 4688

93 P.Kubácek and R.Hoffmann, J. Am. Chem. Soc., 1981, 103, 4320

94 L.Bencze, A.Kraut-Vass and L.Prókai, J. Chem. Soc., Chem. Commun., 1985, 911

95 L.Bencze and A.Kraut-Vass, J. Mol. Catal., 1984, 28, 369

96 R.Colton and I.B.Tomkins, Aust. J. Chem., 1966, 19, 1143

97 R.O.Day, W.H.Batschelet and R.D.Archer, Inorg. Chem., 1980, 19, 2113

98 P.Venkateswarlu, J. Chem. Phys., 1951, 19, 293

99 W.J.Geary, Coord. Chem. Rev., 1971, 7, 81

100 F.A.Cotton and C.S.Kraihanzel, J. Am. Chem. Soc., 1962, 84, 4432

101 R.Colton and G.R.Scollary, Aust. J. Chem., 1968, 21, 1427

102 R.S.Herrick and J.L.Templeton, Inorg. Chem., 1986, 25, 1270

103 J.A.Broomhead and C.G.Young, Aust. J. Chem., 1982, 35, 277

104 G.J.J.Chen, R.O.Yelton and J.W.McDonald, Inorg. Chim. Acta, 1977, 22, 249

105 R.Colton and G.G.Rose, Aust. J. Chem., 1970, 23, 1111

106 S.J.N.Burgmayer and J.L.Templeton, Inorg. Chem., 1985, 24, 2224

107 J.L.Templeton, R.S.Herrick and J.R.Morrow, Organometallics, 1984, 3, 535

108 R.S.Herrick, S.J.N.Burgmayer and J.L.Templeton, Inorg Chem., 1983, 22, 3275

109 B.Huang, M.Sc. Thesis, University of Bath, 1987

110 J.L.Templeton and B.C.Ward, J. Am. Chem. Soc., 1980, 102, 3288

111 P.B.Winston, S.J.N.Burgmayer and J.L.Templeton, Organometallics, 1983, 2, 167

112 R.S.Herrik and J.L.Templeton, Organometallics, 1982, 1, 842

113 P.K.Baker and E.M.Keys, Inorg. Chim. Acta, 1986, 116, L49

114 P.B.Winston, S.J.N.Burgmayer, T.L.Tonker and J.L.Templeton, Organometallics, 1986, 5, 1707

115 J.L.Davidson and G.Vasapollo, J. Chem. Soc., Dalton Trans.,

1985, 2239

116 J.L.Templeton, R.S.Herrick and J.R.Morrow, Organometallics, 1984, 3, 535

117 J.L.Davidson and G.Vasapollo, Polyhedron, 1983, 12, 305

118 P.K.Baker and S.G.Keys, Polyhedron, 1986, 5, 1233

119 J.L.Templeton, P.B.Winston and B.C.Ward, J. Am. Chem. Soc., 1981, 103, 7713

120 SHELX 86, Program for Crystal Structure Determination, G.M.Sheldrick, University of Goetingen, 1986

121 SHELX 76, Package for Crystal Structure Determination, G.M.Sheldrick, University of Cambridge

122 International Tables for X-Ray Crystallography, Vol. 1, 3rd. Edn., Kynoch Press, Birmingham, England, 1969.

123 L.Ricard, R.Weiss, W.E.Newton, G.J.J.Chen and J.W.McDonald, J. Am. Chem. Soc., 1978, 100, 1318

124 B.Capelle, A.L.Beauchamp, M.Dartiguenave and Y.Dartiguenave, J. Chem. Soc., Chem. Commun., 1982, 566

125 B.Capelle, A.L.Beauchamp, M.Dartiguenave and Y.Dartiguenave, J. Am. Chem. Soc., 1983, 105, 4662

126 K.A.Mead, H.Morgan and P.Woodward, J. Chem. Soc., Dalton Trans., 1983, 271

127 T.E.Sloan and A.Wojcicki, Inorg. Chem., 1968, 7, 1268

128 R.A.Bailey, S.L.Kozak, T.W.Michelsen and W.N.Mills, Coord. Chem. Rev., 1971, 6, 407

129 A.H.Norbury, Adv. Inorg. Chem. Radiochem., 1975, 17, 231

130 R.Colton and G.R.Scollary, Aust. J. Chem., 1968, 21, 1435

131 J.Granifo and H.Müller, J.Chem. Soc., Dalton Trans., 1973, 1891

132 E.Carmona, K.Doppert, J.M.Marin, M.L.Poveda, L.Sánchez and R.Sánchez-Delgardo, Inorg. Chem., 1984, 23, 530

133 M.Julve and O.Kahn, Inorg. Chimica Acta, 1983, 76, L39

134 T.R.Felthouse, E.J.Laskowski and D.N.Hendrickson, Inorg. Chem., 1977, 16 1077

135 J.Fujita, A.E.Martell and K.Nakamoto, J. Chem. Phys., 1962, 36, 324

136 J.Fujita, A.E.Martell and K.Nakamoto, J. Chem. Phys., 1962, 36, 331

137 H.D.Hausen, K.Mertz and J.Weidlein, J Organomet. Chem., 1974, 67, 7

138 M.Hashimoto, T.Ozeki, H.Ichida, Y.Sasaki, K. Matsumoto and T.Kudo, Chem. Soc. Japan, Chem. Lett., 1987, 1873

139 G.B.Deacon and R.J.Phillips, Coord. Chem. Rev., 1980, 33, 227

140 C.D.Garner and B.Hughes, Adv. Inorg. Chem. Radiochem., 1975, 17, 1

141 V.Riera, F.J.Arnaiz and G.G.Herbosa, J. Organomet. Chem., 1986, 315, 51

142 S.Arabi, C.Berthelot, J.Barry, F.Bélanger-Gariepy and A.L.Beauchamp, Inorg. Chim. Acta., 1986, 120, 159

143 S.F.A.Kettle and R.Mason, J. Organomet. Chem., 1966, 5, 573

144 P.W.N.M.Van Leeuwen and A.P.Praat, J. Organomet. Chem., 1970, 21, 501

145 I.H.Hillier and R.M.Canadine, Disc. Farad. Soc., 1969, 47, 27

146 L.A.Fedorov, Russ. Chem. Rev., Engl. Transl., 1970, 39, 655

147 G.Wilke, Angew. Chem., Int. Ed., Engl., 1963, 2, 105

148 G.Wilke, B.Bogdanovic, P.Hardt, P.Heimbach, W.Keim, M.Kroner, W.Oberkirch, K.Tanaka, E.Steinrucke, D.Walter and H.Zimmermann, Angew. Chem., Int. Ed., Engl., 1966, 5, 151

149 R.Baker, Chem. Rev., 1973, 487

150 H.Heimbach, P.W.Jolly and G.Wilke, Adv. Organomet. Chem., 1970, 8, 29

151 C.E.H.Bawn, D.G.T.Cooper and A.M.North, Polymer, 1966, 7, 113

152 M.I.Lobach, B.D.Babitskii and V.A.Kormer, Russ. Chem. Rev., Engl. Trans., 1967, 36, 476

153 J.J.Rooney and G.Webb, J. Catalysis, 1964, 3, 488

154 M.A.Schroeder and M.S.Wrighton, J. Am. Chem. Soc., 1976, 98, 551

155 J.Müller, W.Holzinger and H.Menig, Angew. Chem., Int. Ed., Engl., 1976, 15, 702

156 E.O.Sherman and M.Olsen, J. Organomet. Chem., 1979, 172, C13

157 H.J.Clase, A.J.Clelland and M.J.Newlands, J. Organomet. Chem., 1975, 93, 231

158 S.Siegel and G.Perot, J. Chem. Soc., Chem. Commun., 1978, 114

159 M.G.B.Drew and L.S.Pu, Acta Cryst., 1977, B33, 1207

160 G.Raper and W.S.McDonald, J.Chem.Soc., Dalton Trans., 1972, 265

161 M.I.Bruce and M.L.Williams, J.Organomet. Chem., 1985, 288, C55

162 L.Brammer, M.Green, A.G.Orpen, K.E.Paddick and D.R.Saunders, J. Chem. Soc., Dalton Trans., 1986, 657

163 W.E.Carroll, M.Green, A.G.Orpen, C.J.Schraverien, I.D.Williams and A.J.Welch, J.Chem. Soc., Dalton Trans., 1986, 1021

164 M.L.H.Green, J. Organomet. Chem., 1980, 200, 119

165 R.D.W.Kemmitt and A.W.G.Platt, J. Chem. Soc., 1986, 1603

166 F.A.Cotton and M.D.LaPrade, J. Am. Chem. Soc., 1968, 90, 5418

167 G.Hutter, H.H.Brintzinger, L.G.Bell, P.Friedrich, V.Bejenke and D.Neugebauer, J. Organomet. Chem., 1978, 145, 329

168 M.D.Fryzuk, Inorg. Chem., 1982, 21, 2134

169 M.L.H.Green, L.C.Mitchard and W.E.Silverthorn, J. Chem. Soc., Dalton Trans., 1973, 1952

170 H.Lehmkuhl, Y.Tsein, E.Janssen and R.Mynott, Chem. Ber., 1983, 116, 2426

171 A.J.Pearson, Metallo-Organic Chemistry, 1985, 201

172 J.P.Candlin, A.H.Mawby and H.Thomas, Ger. Patent 2 313 947

173 A.N.Nesmeyanov and A.Z.Rubezhov, J. Organomet. Chem., 1979, 164, 259

174 A.S.Ivanov and A.Z.Rubezhov, Izv. Akad. Nauk. SSSR, Ser. Khim., 1979, 1349

175 C.G.Hull and M.H.B.Stiddard, J. Organomet. Chem., 1967, 9, 519

176 M.G.B.Drew, B.J.Brisdon and A.Day, J. Chem. Soc., Dalton Trans., 1981, 1310

177 H.D.Murdoch and E.Weiss, Helv. Chim. Acta, 1962, 45, 1927

178 E.O.Fischer and G.Bürger, Z. Naturforschg., 1961, 16, 77

179 A.J.Deeming and B.L.Shaw, J. Chem. Soc. (A), 1971, 376

180 R.G.Hayter, J. Organomet. Chem., 1968, 13, P1

181 J.Y.Merour, C.Charrier, J.Benaim, J.L.Roustan and D.Commereuc, J. Organomet. Chem., 1972, 39, 321

182 K.Stanley and D.W.McBride, Can. J. Chem., 1975, 53, 2537

183 G.F.Griffin, Ph.D. Thesis, University of Bath 1976

184 R.D.W.Kemmitt, Inorg. Chem. React. Mech., 1972, 19, 117

185 A.J.Deeming, M.T.P. Int. Rev. Sci., Inorg. Chem. Ser., 1972, 19, 117

186 P.K.Wong, K.S.Y.Lau and J.K.Stille, J. Am. Chem. Soc., 1974, 96, 5956

187 R.G.Pearson, Fortchr. Chem. Forsch., 1973, 4, 76

188 J.A.Labinger, A.V.Kramer and J.A.Osborn, J. Am. Chem. Soc., 1973, 95, 7908

189 J.Rousche and G.R.Dobson, J. Organomet. Chem., 1978, 150, 239

190 J.A.Kaduk, A.T.Poulos and J.A.Ibers, J. Organomet. Chem., 1977, 127, 245

191 P.L.Timms and T.W.Turney, Adv. Organomet. Chem., 1977, 15, 33

192 K.J.Klabunde and J.S.Roberts, J. Am. Chem. Soc., 1977, 99, 2509

193 M.I.Bruce, M.Z.Iqbal and F.G.A.Stone, J. Organomet. Chem., 1969, 20, 161

194 C.Charrier, J.Collin, J.Y.Merour and J.L.Roustan, J. Organomet. Chem., 1978, 162, 57

195 P.Cadiot, J.Collin and J.L.Roustan, J. Organomet. Chem., 1978, 162, 67

196 M.Botrill and M.Green, J. Chem. Soc., Dalton Trans., 1979, 820

197 Y.Tatsuno, T.Yoshida and S.Otsuka, Inorg. Synth., 1979, 19, 220

198 P.Powell, J. Organomet. Chem., 1981, 206, 229

199 D.H.Gibson and R.L.Vannhme, J. Am. Chem. Soc., 1972, 94, 5090

200 B.F.G.Johnson, J.Lewis and D.J.Yarrow, J. Chem. Soc., Dalton Trans., 1972, 2084

201 D.F.Pollock and P.M.Maitlis, J. Organomet. Chem., 1971, 26, 407

202 M.L.H.Green, J.Knight and J.A.Segal, J. Chem. Soc., Dalton Trans., 1977, 2189

203 S.G.Davies, M.L.H.Green and D.M.P.Mingos, Tetrahedron, 1978, 34, 3047

204 H.B.Jonassen, R.T.Stearns and J.Kenttamaa, J. Am. Chem. Soc., 1958, 80, 2586

205 S.D.Robinson and B.L.Shaw, J. Chem. Soc. (A), 1963, 4806

206 A.N.Nesmeyanov, G.G.Aleksandrov, N.G.Bokaii, I.B.Zlotina, Y.T.Struchkov and N.E.Kolobova, J. Organomet. Chem., 1976, 11, C9

207 T.E.Bauch and W.P.Giering, J. Organomet. Chem., 1976, 114, 165

208 M.Green and R.I.Hancock, J. Chem. Soc. (A), 1968, 109

209 N.M.Boag, M.Green, J.L.Spencer and F.G.A.Stone, J. Organomet. Chem., 1977, 127, C51

210 W.R.McClelland, H.H.Hoehn, H.N.Cripps, E.L.Muetterties and B.W.Howk, J. Am. Chem. Soc., 1961, 83, 1601

211 T.Luh and C.Wong, J. Organomet. Chem., 1985, 287, 231

212 H.Alper, H.des Abbayes and D.des Roches, J. Organomet. Chem., 1976, 121, C31

213 W.Hieber, J.Sedlmeier and W.Abeck, Chem. Ber., 1953, 86, 700

214 D.H.Gibson, W.L.Hsu and D.S.Lin, J. Organomet. Chem., 1979, 172, C7

215 B.E.Mann, R.Pietropaolo and B.L.Shaw, J. Chem. Soc., Dalton Trans., 1973, 2390

216 H.S.Gutowsky, M.Karplus and D.M.Grant, J. Chem. Phys., 1959, 31, 1278

217 L.M.Jackman and F.A.Cotton, (Eds.), Dynamic NMR spectroscopy, Academic Press, London, 1975

218 K.Vrieze and H.C.Volger, J. Organomet. Chem., 1967, 9, 537

219 J.W.Faller, D.A.Haitko, R.D.Adams and D.F.Chodosh, J. Am. Chem. Soc., 1979, 101, 865

220 B.J.Brisdon and A.A.Woolf, J. Chem. Soc., Dalton Trans., 1978, 291

221 R.S.Cahn, C.Ingold and V.Prelog, Ang. Chem. Int. Ed. Engl., 1966, 5, 385

222 J.W.Faller and M.J.Incorvia, Inorg. Chem., 1968, 7, 840

223 J.W.Faller and A.M.Rosan, J. Am. Chem. Soc., 1976, 98, 3388

224 J.K.Becconsall and S.O'Brien, J. Chem. Soc., Chem. Commun., 1966, 720

225 J.Powell and B.L.Shaw, J. Chem. Soc. (A), 1968, 583

226 H.C.Clark and J.E.H.Ward, Can. J. Chem., 1974, 52, 570

227 P.Powell, J. Organomet. Chem., 1977, 129, 175

228 A.Oudeman and T.S.Sorenson, J. Organomet. Chem., 1978, 156, 259

229 D.H.Gibson and T.S.Ong, J. Organomet. Chem., 1978, 155, 221

230 R.L.Phillips and R.J.Puddephatt, J. Chem. Soc., Dalton Trans., 1978, 1736

231 V.Franke and E.Weiss, J. Organomet. Chem., 1978, 153, 39

232 L.A.Churlyaeva, M.I.Lobach, G.P.Kondratenkov and V.A.Kormer, J. Organomet. Chem., 1972, 39, C23

233 J.W.Emsley, J.Feeney and L.H.Sutcliffe, High Resolution NMR Spectroscopy, Pergamon Press, London, 1965

234 K.Shobatake and K.Nakamoto, J. Am. Chem. Soc., 1970, 92, 3339

235 D.M.Adams and A.Squire, J. Chem. Soc. (A), 1970, 1808

236 D.C.Andrews and G.Davidson, J. Chem. Soc., Dalton Trans., 1972, 126, 1381

237 D.C.Andrews and G.Davidson, J. Organomet. Chem., 1973, 55, 383

238 G.Paliani, A.Poletti, G.Cardaci, S.M.Murgia and R.Catallotti, J. Organomet. Chem., 1973, 60, 157

239 A.E.Smith, Acta Cryst., 1965, 18, 331

240 R.H.Fenn and A.J.Graham, J. Organomet. Chem., 1972, 37, 137

241 C.F.Putnik, J.J.Welter, G.D.Stucky, M.J.D'Aniello, B.A.Sosinsky, J.F.Kirner and E.L.Muetterties, J. Am. Chem. Soc., 1978, 100, 4107

242 M.R.Churchill and T.A.O'Brien, Inorg. Chem., 1967, 6, 1386

243 W.E.Oberhansli and L.F.Dahl, J. Organomet. Chem., 1965, 3, 43

244 B.J.Brisdon, D.A.Edwards, K.E.Paddick and M.G.B.Drew, J. Chem. Soc., Dalton Trans., 1980, 1317

245 J.A.Kaduk, A.T.Poulos and J.A.Ibers, J. Organomet. Chem., 1977, 127, 245

246 T.G.Hewitt, J.J.DeBoer and K.Anzenhofer, Acta Cryst., 1970, B26, 1244

247 M.R.Churchill and S.O'Brian, J. Chem. Soc., Chem. Commun., 1968, 246

248 R.B.Helmholdt, F.Jellinek, H.A.Martin and A.Vos, Rec. Trav. Chim. Pays-Bas., 1967, 86, 1263

249 A.Streitwieser, Jr., Molecular Orbital Theory for Organic Chemists, Wiley and Sons, London, 1961

250 M.M.Rohmer, J.Demuynck and A.Veillard, Theoret. Chim. Acta, 1974, 36, 93

251 D.A.Brown and A.Owens, Inorg. Chimica Acta, 1971, 5, 675

252 M.D.Curtis and O.Eisenstein, Organometallics, 1984, 3, 887

253 N.W.Murrall and A.J.Welch, J. Organomet. Chem., 1986, 301, 109

254 J.W.Faller, D.F.Chodosh and D.Katahira, J. Organomet. Chem., 1980, 187, 227

255 A.J.Graham and R.H.Fenn, J. Organomet. Chem., 1969, 17, 405

256 A.J.Graham and R.H.Fenn, J. Organomet. Chem., 1970, 25, 173

257 F.Dewans, J.Dewailly, J.Meunier-Piret and P.Piret, J. Organomet. Chem., 1974, 76, 53

258 M.G.B.Drew and G.F.Griffin, Acta Cryst., 1979, B35, 3036

259 A.J.Graham, D.Akrigg and B.Sheldrick, Cryst. Struct. Commun., 1976, 5, 891

260 A.J.Graham, D.Akrigg and B.Sheldrick, Cryst. Struct. Commun., 1977, 6, 253

261 M.Boyer, J.C.Daran and Y.Jeannin, J. Organomet. Chem., 1980, 190, 177

262 F.A.Cotton, B.A.Frenz and A.G.Stanislowski, Inorg. Chimica Acta, 1973, 7, 503

263 F.A.Cotton, C.A.Murillo and B.R.Stults, Inorg. Chimica Acta, 1977, 22, 75

264 E.M.Holt, S.L.Holt and K.J.Watson, J. Chem. Soc., Dalton Trans., 1973, 2444

265 K.R.Breakell, S.J.Rettig, D.L.Singbeil, A.Storr and J.Trotter, Can. J. Chem., 1978, 56, 2099

266 K.R.Breakell, S.J.Rettig, A.Storr and J.Trotter, Can. J. Chem., 1979, 59, 139

267 K.S.Chong, S.J.Rettig, A.Storr and J.Trotter, Can. J. Chem. 1979, 57, 1335

268 F.A.Cotton, B.A.Frenz and C.A.Murillo, J. Am. Chem. Soc., 1975, 97, 2118

269 M.G.B.Drew, B.J.Brisdon and M.Cartwright, Inorg. Chim. Acta, 1979, 36, 127

270 C.A.Kosky, P.Ganis and G.Avitabile, Acta Cryst., 1971, B27, 1859

271 B.J.Brisdon, D.A.Edwards and J.W.White, J. Organomet. Chem. 1978, 156, 427

272 M.F.Perpiñán and A.Santos, J. Organomet. Chem., 1981, 221, 63

273 B.J.Brisdon and G.F.Griffin, J. Chem. Soc., Dalton Trans., 1975, 1999

274 H.D.Murdoch and R.Henzi, J. Organomet. Chem., 1966, 5, 552

275 H.T.Dieck and H.Friedel, J. Organomet. Chem., 1968, 14, 375

276 A.A.T.Hsieh and B.O.West, Inorg. Chem., 1974, 13, 2453

277 C.E.Holloway, J.D.Kelly and M.H.B.Stiddard, J. Chem. Soc. (A), 1969, 931

278 B.J.Brisdon, J. Organomet. Chem., 1977, 125, 225

279 G.Doyle, J. Organomet. Chem., 1977, 132, 243

280 K.A.Connor and R.Walton, Inorg. Chem., 1986, 25, 4423

281 A.E.Sánchez-Peláez, M.F.Perpiñán and A.Santos, J. Organomet. Chem., 1985, 296, 367

282 M.J.M.Campbell, E.Morrison, V.Rogers and P.K.Baker, Inorg. Chim. Acta, 1987, 127, L17

283 P.K.Baker, M.J.M.Campbell and M.V.White, Inorg. Chimica Acta, 1985, 98, L27

284 R.G.Hayter, J. Organomet. Chem., 1968, 13, P1

285 E.O.Fischer and H.Werner, Z. Chem., 1962, 2, 181

286 M.D.Curtis and N.A.Fotinos, J. Organomet. Chem., 1984, 272, 43

287 F.Hohmann, J. Organomet. Chem., 1977, 137, 315

288 H.Friedel, I.W.Renk and H.T.Dieck, J. Organomet. Chem., 1971, 26, 247

289 H.T.Dieck and H.Friedel, J. Chem. Soc., Chem. Commun., 1969, 411

290 F.Hohmann and H.T.Dieck, J. Organomet. Chem., 1975, 85, 47

291 B.J.Brisdon and K.E.Paddick, J. Organomet. Chem., 1978, 149, 113

292 R.B.King and M.S.Saran, Inorg. Chem., 1974, 13, 2453

293 J.W.Faller and A.M.Rosan, J. Am. Chem. Soc., 1976, 98, 3388

294 N.A.Bailey, J.A.McCleverty, W.G.Kita, A.J.Murray, B.E.Mann and N.W.J.Walker, J. Chem. Soc., Chem. Commun., 1974, 592

295 J.W.Faller and K.H.Chao, J. Am. Chem. Soc., 1983, 105, 3893

296 J.W.Faller, K.H.Chao and H.H.Murrey, Organometallics, 1984, 3, 1231

297 B.M.Trost and M.Lautens, J. Am. Chem. Soc., 1982, 104, 5543

298 B.J.Brisdon and M.Cartwright, J. Organomet. Chem., 1979, 164, 83

299 K.E.Hill, Ph.D. Thesis, University of Bath, 1982

300 B.J.Brisdon, D.A.Edwards and K.E.Paddick, Trans. Met. Chem., 1981, 6, 83

301 B.J.Brisdon, K.A.Connor and R.A.Walton, Organometallics, 1983, 2, 1159

302 M.S.Bailey, B.J.Brisdon, D.W.Brown and K.M.Stark, Tetrahedron Lett., 1983, 24, 3037

303 S.M.Nelson and J.Rodgers, J. Chem. Soc. (A), 1968, 272

304 M.C.Ganorkar and M.H.B.Stiddard, J. Chem. Soc. (A), 1965, 5346

305 D.P.Madden, M.M.DaMota and S.M.Nelson, J. Chem. Soc. (A), 1970, 790

306 B.J.Brisdon and A.J.Floyd, J. Organomet. Chem., 1985, 288, 305

307 V.F.Bystrov, S.L.Portnova, V.I.Tsetlin, V.T.Ivanov and Y.A.Ovchinnilov, Tetrahedron, 1969, 25, 493

308 P.Meakin, S.Trofimenko and J.P.Jesson, J. Am. Chem. Soc., 1972, 94, 5677

309 J.L.Calderon, F.A.Cotton and A.Shaver, J. Organomet. Chem., 1972, 38, 105

310 B.J.Brisdon and M.Cartwright, University of Bath, unpublished observations.

311 B.M.Trost and T.R.Verhoeven, Comprehensive Organomet. Chem., 1982, 8, 779

312 B.M.Trost, Tetrahedron, 1977, 33, 2615

313 J.Tsuji, Organic Synthesis with Palladium Compounds, Springer-Verlag, New York, 1980

314 B.M.Trost, Pure Appl. Chem., 1981, 53, 2357

315 B.M.Trost and M.Hung, J. Am. Chem. Soc., 1984, 106, 6837 and refs. therein

316 I.Minami, I.Shimizu and J.Tsuji, J. Organomet. Chem., 1985, 296, 269

317 B.M.Trost and T.R.Verhoeven, J. Am. Chem. Soc., 1976, 98, 630

318 S.G.Davies, M.L.H.Green and D.M.P.Mingos, Tetrahedron, 1978, 34, 3047

319 B.M.Trost and M.H.Hung, J. Am. Chem. Soc., 1983, 105, 7757

320 B.M.Trost and M.Lautens, J. Am. Chem. Soc., 1983, 105, 3343

321 B.M.Trost and M.Lautens, Organometallics, 1983, 2, 1687

322 B.J.Brisdon and A.Day, J. Organomet. Chem., 1981, 221, 279

323 F.Dewans and D.Morel, J. Mol. Catal., 1978, 3, 403

324 B.J.Brisdon, D.W.Brown, C.R.Willis and M.G.B.Drew, J. Chem. Soc., Dalton Trans., 1986, 2405

325 M.G.B.Drew, B.J.Brisdon, D.W.Brown and C.R.Willis, J. Chem. Soc., Chem. Commun., 1986, 1510

326 F.Giulieri and J.Benaim, Nouv. J. Chim., 1985, 9, 335

327 Handbook of Chemistry and Physics, The Chemical Rubber Co., 52nd. Edn., 1971, D-117

328 D.Dolphin and A.Wick, Tabulation of IR Spectral Data, Wiley Interscience, 1977

329 F.J.Fañanás and H.Hoberg, J. Organomet. Chem., 1984, 275, 249

330 A.N.Nesmeyanov, N.E.Kolobova, I.B.Zlotina, B.V.Lokshin, I.F.Leshcheva, G.K.Znobina and K.N.Anisimov, J. Organomet. Chem., 1976, 110, 339

331 M.I.Bruce, T.W.Hambley, M.R.Snow and A.G.Swincer, Organometallics, 1985, 4, 494

APPENDIX 2

ANISOTROPIC AND ISOTROPIC THERMAL PARAMETERS FOR

$Mo(CO)(PMePh_2)_2Br_2(MeC{\equiv}CMe)$.

The thermal parameters were terms U_{ij} of

$$\exp(-2\pi^2(U_{11}h^2a^{*2}+U_{22}k^2b^{*2}+U_{33}l^2c^{*2}+2U_{12}hka^*c^*+2U_{33}k(b^*c^*))$$

Atom	U_{11} (or U_{iso})	U_{22}	U_{33}	U_{23}	U_{13}	U_{12}
Mo	0.0449(8)	0.0433(9)	0.0414(11)	0.0000(8)	-0.0027(9)	0.0067(8)
Br(1)	0.0731(13)	0.0664(13)	0.0536(15)	0.0033(11)	-0.0097(11)	0.0241(32)
Br(2)	0.0892(15)	0.0757(14)	0.0530(16)	-0.0181(10)	0.0166(12)	-0.0058(13)
P(1)	0.0441(26)	0.0549(29)	0.0499(36)	-0.0010(26)	-0.0034(26)	0.0058(23)
P(2)	0.0511(29)	0.0477(28)	0.0356(35)	0.0038(21)	0.0032(23)	0.0054(23)
O(1)	0.0885(10)	0.0949(11)	0.0419(11)	-0.0069(81)	0.0021(81)	0.0141(87)
C(1)	0.0700(62)					
C(2)	0.0523(51)					
C(3)	0.0651(75)					
C(4)	0.0832(65)					
C(5)	0.0833(69)					
C(6)	0.0824(67)					
C(7)	0.0719(59)					
C(8)	0.0542(49)					
C(9)	0.0649(57)					
C(10)	0.0831(66)					
C(11)	0.0747(63)					
C(12)	0.0864(69)					
C(13)	0.0705(60)					
C(14)	0.0596(53)					
C(15)	0.0459(46)					
C(16)	0.0618(54)					
C(17)	0.0778(65)					
C(18)	0.0725(62)					
C(19)	0.0601(53)					
C(20)	0.0586(52)					
C(21)	0.0401(43)					
C(22)	0.0450(46)					
C(23)	0.0576(52)					
C(24)	0.0600(53)					
C(25)	0.0625(56)					
C(26)	0.0639(58)					
C(27)	0.0571(14)	0.0237(10)	0.0961(21)	0.0007(12)	0.0038(12)	0.0149(84)
C(28)	0.0277(95)	0.0426(11)	0.0621(16)	0.0009(97)	-0.0122(93)	0.0090(81)
C(29)	0.0370(10)	0.0645(12)	0.0620(16)	0.0051(11)	0.0023(11)	0.0030(94)
C(30)	0.0886(16)	0.0884(16)	0.0564(18)	0.0244(12)	-0.0406(13)	-0.0034(13)
C(31)	0.0546(12)	0.0803(14)	0.0871(19)	-0.0100(12)	0.0250(12)	0.0359(11)

ATOMIC COORDINATES (x10⁴) FOR Mo(CO)(PMePh₂)₂Br₂(MeC≡CMe) WITH ESTIMATED STANDARD DEVIATIONS IN PARENTHESES

Atom	X	Y	Z
Mo	1296(0)	477(1)	1541(1)
Br(1)	1784(1)	-1120(2)	1993(1)
Br(2)	1247(1)	928(2)	3247(1)
P(1)	1971(1)	1592(4)	1587(4)
P(2)	695(1)	-814(3)	1857(3)
O(1)	1464(4)	-419(12)	-300(10)
C(1)	2336(6)	1351(15)	2492(14)
C(2)	2329(5)	1525(14)	677(12)
C(3)	2392(6)	533(15)	279(14)
C(4)	2694(7)	446(18)	-396(16)
C(5)	2888(7)	1357(17)	-693(16)
C(6)	2839(7)	2331(17)	-312(16)
C(7)	2545(6)	2420(16)	387(15)
C(8)	1827(5)	2994(13)	1679(13)
C(9)	1668(6)	3502(15)	946(14)
C(10)	1546(7)	4606(17)	1017(16)
C(11)	1586(6)	5071(16)	1799(15)
C(12)	1748(7)	4576(18)	2561(16)
C(13)	1863(6)	3504(16)	2515(14)
C(14)	742(6)	-1489(14)	2897(13)
C(15)	594(5)	-1946(12)	1138(12)
C(16)	173(6)	-2347(14)	1091(14)
C(17)	118(6)	-3255(17)	585(15)
C(18)	454(6)	-3724(15)	106(15)
C(19)	852(6)	-3304(15)	197(13)
C(20)	939(6)	-2411(14)	686(13)
C(21)	179(5)	-157(12)	1902(11)
C(22)	37(5)	310(12)	1117(12)
C(23)	-357(6)	807(14)	1092(13)
C(24)	-622(6)	784(14)	1839(13)
C(25)	-477(6)	344(15)	2563(13)
C(26)	-81(6)	-127(15)	2609(14)
C(27)	1413(6)	-96(13)	414(17)
C(28)	1011(5)	1404(14)	640(14)
C(29)	906(5)	1718(14)	1454(15)
C(30)	941(7)	1677(17)	-291(14)
C(31)	677(6)	2549(16)	1893(14)

Observed and calculated structural factors for

$Mo(CO)(PMePh_2)_2Br_2(MeC{\equiv}CMe)$

H	K	L	10FO	10FC
4	0	0	4195	-4499
6	0	0	1513	1771
8	0	0	945	973
12	0	0	630	-717
16	0	0	4092	4157
18	0	0	754	-826
20	0	0	2547	-2584
22	0	0	1399	1379
24	0	0	758	751
26	0	0	809	-887
28	0	0	587	-622
30	0	0	730	752
32	0	0	482	509
4	1	0	1819	1884
6	1	0	3455	3565
8	1	0	1182	1169
10	1	0	2114	-2173
14	1	0	1548	1632
20	1	0	724	728
24	1	0	560	560
26	1	0	986	-929
30	1	0	678	736
32	1	0	555	-555
0	2	0	4160	4430
4	2	0	3286	-3471
6	2	0	3157	2988
8	2	0	3704	3668
10	2	0	2543	-2423
12	2	0	1931	-2029
14	2	0	1187	1164
16	2	0	1926	1975
20	2	0	1424	-1437
22	2	0	687	745
24	2	0	747	777
30	2	0	447	409
2	3	0	1724	-1934
4	3	0	751	553
6	3	0	5567	5588
8	3	0	932	863
10	3	0	5769	-5723
14	3	0	1380	1507
16	3	0	844	-896
18	3	0	821	-731
22	3	0	807	759
26	3	0	1804	-1896
28	3	0	496	524
30	3	0	946	1002
32	3	0	419	-443
0	4	0	2368	-2376
2	4	0	1813	1801
4	4	0	1306	1233
8	4	0	2808	2862
10	4	0	1270	-1219
14	4	0	1791	1886
16	4	0	880	-957
20	4	0	918	965
28	4	0	451	-304
2	5	0	1321	-1407
4	5	0	397	348
6	5	0	2893	2939
8	5	0	1544	-1592
10	5	0	1142	-1197
12	5	0	649	659
14	5	0	1556	1571
16	5	0	366	-227
18	5	0	1682	-1771
22	5	0	1674	1798
24	5	0	1008	-1082
26	5	0	527	-631
28	5	0	464	433
0	6	0	1246	-1301
4	6	0	1601	1613
6	6	0	703	662
8	6	0	661	-710
10	6	0	1101	1065
12	6	0	1118	1193
16	6	0	1617	-1694
20	6	0	1533	1604
2	7	0	1949	-1979
4	7	0	1844	1895
6	7	0	493	-600
10	7	0	880	879
12	7	0	919	-960
14	7	0	483	405
18	7	0	924	-980
20	7	0	924	860
22	7	0	402	401
24	7	0	659	-724
28	7	0	536	448
2	8	0	509	-610
4	8	0	987	1055
6	8	0	823	852
8	8	0	1076	-1059
10	8	0	558	509
12	8	0	1255	1284
14	8	0	1090	-1134
16	8	0	757	-744
18	8	0	689	742
6	9	0	695	-615
10	9	0	557	572
0	10	0	665	-748
4	10	0	392	228
6	10	0	396	459
8	10	0	855	-891
12	10	0	486	490
14	10	0	579	-561
18	10	0	555	505
2	11	0	715	676
4	11	0	1009	-1061
8	11	0	377	371
16	11	0	375	-239
4	12	0	462	405
6	12	0	581	-578
8	12	0	468	-499
2	1	1	5133	-5641
3	1	1	885	-996
4	1	1	1057	1053
5	1	1	432	-430
6	1	1	2647	2715
7	1	1	681	782
8	1	1	1217	1038
10	1	1	2410	-2138
11	1	1	321	-265
14	1	1	2486	2533
15	1	1	943	972
16	1	1	768	-763
18	1	1	3297	-3327
19	1	1	1006	-993
20	1	1	902	900
21	1	1	384	560
22	1	1	1373	1420
26	1	1	458	-430
29	1	1	446	438
31	1	1	365	344
3	2	1	499	683
5	2	1	1857	-1847
6	2	1	2000	1967
7	2	1	1928	1831
8	2	1	5673	-5599
10	2	1	326	260
11	2	1	1081	-1034
14	2	1	1227	-1233
15	2	1	773	-771
16	2	1	514	-568
20	2	1	487	-498
24	2	1	962	-1051
25	2	1	369	-352
28	2	1	1491	1538
30	2	1	619	-615
1	3	1	1157	1185
2	3	1	1332	1255
7	3	1	839	-853
8	3	1	2033	2096
9	3	1	1938	1969
10	3	1	423	-432
11	3	1	374	409
12	3	1	1833	-1842
13	3	1	1221	-1275
14	3	1	556	602
15	3	1	1081	1149
16	3	1	841	-831
18	3	1	548	-485
19	3	1	555	-518
20	3	1	363	268
21	3	1	336	-374
22	3	1	375	478
23	3	1	639	737
0	4	1	2287	-2151
1	4	1	595	676
2	4	1	854	-805
3	4	1	814	818
4	4	1	2871	2864
5	4	1	337	433
7	4	1	345	421
8	4	1	3070	-3199
9	4	1	1187	-1125
10	4	1	1333	1308
12	4	1	2689	2676
13	4	1	444	499
14	4	1	492	-514

Observed and calculated structural factors for

$Mo(CO)(PMePh_2)_2Br_2(MeC{\equiv}CMe)$

H	K	L	10FC	10FO	H	K	L	10FC	10FO	H	K	L	10FC	10FO	H	K	L	10FC	10FO
15	4	1	603	600	9	6	1	746	-762	16	8	1	679	-668	3	0	2	1470	-1448	26	1	2	562	638
16	4	1	1362	-1340	10	6	1	499	455	17	8	1	770	-813	4	0	2	2900	2842	0	2	2	3211	-3168
17	4	1	366	-239	11	6	1	397	-338	18	8	1	545	462	5	0	2	1587	1364	1	2	2	408	-456
20	4	1	997	1042	12	6	1	321	333	19	8	1	354	-242	6	0	2	3050	-3026	2	2	2	1247	-1269
21	4	1	515	485	13	6	1	335	261	1	9	1	357	-426	7	0	2	2301	-2137	3	2	2	466	-486
22	4	1	574	-634	15	6	1	634	688	3	9	1	570	583	8	0	2	2663	2360	4	2	2	496	402
24	4	1	1092	-1144	16	6	1	1037	-1034	4	9	1	534	510	9	0	2	610	769	5	2	2	2339	2268
25	4	1	535	-513	17	6	1	744	-766	5	9	1	533	530	10	0	2	517	-492	7	2	2	590	543
26	4	1	612	590	19	6	1	615	-632	6	9	1	710	-710	11	0	2	1042	790	8	2	2	707	-658
28	4	1	543	592	20	6	1	945	957	8	9	1	451	-450	12	0	2	450	592	9	2	2	1635	-1575
30	4	1	385	-280	21	6	1	841	916	9	9	1	614	-655	13	0	2	1118	-1012	10	2	2	672	-592
1	5	1	504	500	22	6	1	835	-940	10	9	1	960	1007	14	0	2	796	771	13	2	2	1298	1240
2	5	1	2908	2997	24	6	1	554	-653	11	9	1	821	869	16	0	2	3655	-3533	16	2	2	841	-766
4	5	1	1706	-1648	25	6	1	682	-620	12	9	1	720	-801	17	0	2	2012	-2043	17	2	2	802	-855
5	5	1	880	-970	26	6	1	695	711	13	9	1	435	361	18	0	2	327	-145	19	2	2	355	-390
6	5	1	583	-633	1	7	1	404	-403	14	9	1	501	-554	20	0	2	2276	2357	20	2	2	779	698
7	5	1	823	865	2	7	1	1023	1025	15	9	1	568	-624	21	0	2	497	474	21	2	2	797	845
8	5	1	458	494	3	7	1	505	-507	16	9	1	946	1016	22	0	2	383	-229	24	2	2	570	-538
9	5	1	1032	990	4	7	1	552	551	0	10	1	637	698	23	0	2	719	-836	25	2	2	504	-548
10	5	1	840	-796	6	7	1	1485	-1520	2	10	1	441	-392	25	0	2	582	-629	26	2	2	526	494
11	5	1	970	-994	9	7	1	588	540	6	10	1	783	820	29	0	2	647	692	1	3	2	575	-465
12	5	1	486	560	10	7	1	811	924	9	10	1	406	-231	31	0	2	458	-364	3	3	2	1065	-1001
13	5	1	332	-373	11	7	1	382	405	10	10	1	406	288	1	1	2	386	495	6	3	2	3092	-3037
14	5	1	628	-689	12	7	1	555	-652	13	10	1	486	481	2	1	2	1056	1083	7	3	2	1094	-1040
15	5	1	624	613	14	7	1	889	-929	14	10	1	440	-447	3	1	2	1089	1213	9	3	2	1168	-1117
16	5	1	675	-787	16	7	1	539	519	1	11	1	377	-411	5	1	2	717	-767	10	3	2	3529	3389
18	5	1	1742	1746	18	7	1	807	741	3	11	1	443	466	7	1	2	1252	1098	11	3	2	1383	1458
22	5	1	692	-764	22	7	1	449	-421	5	11	1	470	485	8	1	2	750	-702	12	3	2	564	-546
27	5	1	382	-383	0	8	1	1141	-1185	6	11	1	374	-423	10	1	2	2404	2236	13	3	2	620	-550
0	6	1	1698	-1843	1	8	1	1250	-1400	7	11	1	749	-794	11	1	2	446	511	14	3	2	1263	-1265
1	6	1	774	-872	2	8	1	451	487	9	11	1	565	-604	14	1	2	1001	-822	16	3	2	549	586
2	6	1	581	517	3	8	1	944	-901	10	11	1	606	584	16	1	2	916	864	17	3	2	1042	1071
4	6	1	1417	1488	7	8	1	456	512	11	11	1	365	286	17	1	2	982	986	21	3	2	744	-702
5	6	1	820	939	8	8	1	1018	990	15	11	1	412	-296	19	1	2	340	-213	22	3	2	554	-467
6	6	1	1141	-1258	11	8	1	715	-727	0	12	1	590	478	21	1	2	638	-524	26	3	2	850	898
7	6	1	687	739	15	8	1	503	529	6	12	1	443	437	25	1	2	404	-421	27	3	2	699	779

Observed and calculated structural factors for

$Mo(CO)(PMePh_2)_2Br_2(MeC{\equiv}CMe)$

H	K	L	10FO	10FC
30	3	2	472	-506
31	3	2	447	-504
0	4	2	2256	2304
1	4	2	344	-221
2	4	2	2498	-2336
3	4	2	2184	-2083
4	4	2	1032	-984
6	4	2	386	533
7	4	2	1789	1040
8	4	2	585	-652
9	4	2	2529	-2565
11	4	2	1046	-978
12	4	2	477	449
13	4	2	1481	1436
14	4	2	596	-667
15	4	2	338	-308
16	4	2	983	1058
17	4	2	765	-749
19	4	2	353	-349
20	4	2	878	-827
23	4	2	572	483
25	4	2	539	-572
27	4	2	384	-314
1	5	2	862	-881
2	5	2	1575	1576
3	5	2	768	838
4	5	2	733	-756
5	5	2	771	824
6	5	2	1712	-1735
7	5	2	2352	-2278
8	5	2	341	318
10	5	2	428	453
11	5	2	1653	1634
15	5	2	899	-838
17	5	2	847	-855
18	5	2	594	559
19	5	2	836	839
22	5	2	700	-680
23	5	2	1281	-1285
24	5	2	694	628
0	6	2	1580	1511
1	6	2	878	-895
2	6	2	429	378
3	6	2	352	-254
4	6	2	1735	-1734
5	6	2	552	632
27	7	2	501	508
3	8	2	612	598
4	8	2	433	-435
6	8	2	743	-704
7	8	2	974	-876
8	8	2	413	443
9	8	2	505	476
12	8	2	895	-911
13	8	2	1272	-1330
14	8	2	675	604
17	8	2	704	758
18	8	2	416	-373
1	9	2	1057	-1089
3	9	2	853	874
5	9	2	729	699
6	9	2	464	506
8	9	2	359	-261
9	9	2	551	-588
11	9	2	670	613
12	9	2	383	-334
15	9	2	1105	-1121
17	9	2	637	-561
19	9	2	405	376
0	10	2	675	-690
1	10	2	1000	959
3	10	2	828	815
5	10	2	899	-917
7	10	2	1041	-1110
9	10	2	1088	1139
11	10	2	910	878
12	10	2	416	-419
13	10	2	943	-916
14	10	2	419	493
17	10	2	592	683
2	11	2	504	-262
3	11	2	707	-678
1	1	3	2346	-2451
5	1	3	1546	-1494
7	1	3	1216	1245
8	1	3	843	839
9	1	3	940	935
10	1	3	1464	-1362
11	1	3	825	-719
12	1	3	355	484
13	1	3	726	652
14	1	3	407	521
15	1	3	1326	-1358
17	1	3	722	-761
19	1	3	1493	1480
22	1	3	455	-371
23	1	3	751	-786
25	1	3	532	582
26	1	3	494	-447
27	1	3	487	448
29	1	3	411	-372
31	1	3	567	-483
0	2	3	2259	-2356
1	2	3	2682	-2622
3	2	3	1595	-1489
5	2	3	621	-595
6	2	3	1273	-1136
7	2	3	763	-899
19	2	3	1823	-1784
20	2	3	611	568
21	2	3	737	649
22	2	3	644	-630
24	2	3	350	144
27	2	3	476	455
28	2	3	397	-419
29	2	3	678	-713
2	3	3	1040	-957
3	3	3	558	-628
5	3	3	2303	2198
7	3	3	1370	-1479
8	3	3	976	-950
9	3	3	1742	-1842
11	3	3	1595	1524
13	3	3	311	254
15	3	3	787	-820
17	3	3	701	-662
18	3	3	887	-872
19	3	3	890	870
21	3	3	615	664
22	3	3	537	511
23	3	3	666	-646
24	3	3	400	-396
27	3	3	404	328
0	4	3	1090	-1040

Observed and calculated structural factors for

$Mo(CO)(PMePh_2)_2Br_2(MeC{\equiv}CMe)$

H	K	L	10FO	10FC	H	K	L	10FO	10FC	H	K	L	10FO	10FC	H	K	L	10FO	10FC	H	K	L	10FO	10FC
1	4	3	361	-339	9	6	3	1393	1398	4	9	3	626	-639	11	0	4	494	-428	9	2	4	1187	1128
3	4	3	546	489	11	6	3	702	660	5	9	3	1233	-1265	12	0	4	2578	2491	11	2	4	315	-281
4	4	3	312	265	12	6	3	418	494	7	9	3	829	829	14	0	4	1135	-1102	12	2	4	1214	1205
5	4	3	1633	-1624	13	6	3	847	-894	9	9	3	1101	1119	16	0	4	1413	-1335	13	2	4	313	297
6	4	3	704	-696	14	6	3	715	-706	11	9	3	1232	-1222	17	0	4	1179	1164	14	2	4	556	-585
7	4	3	812	-741	15	6	3	1180	-1182	13	9	3	486	-386	18	0	4	812	777	16	2	4	790	-736
9	4	3	1739	1766	17	6	3	824	848	15	9	3	1381	1397	20	0	4	566	554	17	2	4	701	730
13	4	3	663	-607	19	6	3	623	598	16	9	3	425	-507	21	0	4	1047	-1015	18	2	4	456	406
15	4	3	499	497	21	6	3	1446	-1462	18	9	3	672	586	23	0	4	422	443	20	2	4	858	853
16	4	3	572	-504	25	6	3	1006	1061	19	9	3	547	-487	24	0	4	770	-730	21	2	4	514	-472
20	4	3	442	418	27	6	3	378	-231	20	9	3	378	-294	27	0	4	676	-734	24	2	4	835	-848
21	4	3	832	-795	1	7	3	410	397	3	10	3	824	857	28	0	4	872	897	25	2	4	437	364
23	4	3	366	343	3	7	3	369	398	6	10	3	413	-400	30	0	4	661	-761	1	3	4	2869	-2768
25	4	3	1005	1025	5	7	3	779	-851	7	10	3	783	-735	32	0	4	620	-599	2	3	4	2776	2657
2	5	3	1584	-1512	11	7	3	673	-714	9	10	3	404	365	2	1	4	1704	1899	3	3	4	2076	2003
4	5	3	409	417	13	7	3	842	821	12	10	3	374	-299	3	1	4	2175	2110	5	3	4	356	-379
5	5	3	1570	1644	15	7	3	395	536	13	10	3	665	-708	4	1	4	993	-1035	6	3	4	1940	-1896
6	5	3	537	-534	25	7	3	393	-313	17	10	3	447	353	5	1	4	904	-693	7	3	4	514	490
7	5	3	1338	-1288	0	8	3	394	-380	1	11	3	570	607	6	1	4	668	-606	8	3	4	1166	1102
8	5	3	492	-488	1	8	3	2447	2468	3	11	3	1054	-1078	7	1	4	699	-696	9	3	4	705	624
9	5	3	2844	-2854	2	8	3	426	-376	5	11	3	601	-594	11	1	4	438	353	10	3	4	1105	1099
10	5	3	417	467	3	8	3	1295	1379	7	11	3	1396	1358	13	1	4	319	348	11	3	4	1231	-1361
11	5	3	1569	1563	5	8	3	1340	-1434	9	11	3	846	800	14	1	4	708	-679	13	3	4	337	266
13	5	3	667	708	8	8	3	818	-860	11	11	3	1094	-1049	15	1	4	781	783	14	3	4	1333	-1292
14	5	3	402	288	10	8	3	351	-447	13	11	3	517	-587	17	1	4	1304	-1292	15	3	4	473	484
15	5	3	759	-777	11	8	3	831	779	15	11	3	571	566	21	1	4	781	737	16	3	4	468	551
16	5	3	527	480	13	8	3	1332	-1329	1	12	3	609	-645	22	1	4	591	-490	17	3	4	1501	-1487
18	5	3	710	-765	14	8	3	356	-351	5	12	3	590	587	23	1	4	547	-469	18	3	4	992	1000
25	5	3	803	-796	15	8	3	1128	-1126	3	13	3	616	-582	26	1	4	392	415	19	3	4	835	758
27	5	3	744	800	17	8	3	1635	1660	4	13	3	431	363	27	1	4	477	-368	20	3	4	375	-340
29	5	3	584	549	19	8	3	443	493	5	0	4	1165	-1245	0	2	4	635	-586	21	3	4	472	500
0	6	3	331	255	21	8	3	723	-767	6	0	4	1171	-998	1	2	4	995	942	22	3	4	602	-583
1	6	3	2204	2125	25	8	3	439	238	7	0	4	4269	3851	3	2	4	886	880	24	3	4	656	680
3	6	3	1608	1620	1	9	3	911	885	8	0	4	2156	-2087	4	2	4	1881	1810	26	3	4	484	481
5	6	3	2774	-2752	2	9	3	567	575	9	0	4	2433	-2254	6	2	4	422	348	27	3	4	499	-505
8	6	3	1438	-1470	3	9	3	753	-772	10	0	4	410	-303	8	2	4	1840	-1885	31	3	4	489	327

Observed and calculated structural factors for

$Mo(CO)(PMePh_2)_2Br_2(MeC{\equiv}CMe)$

H	K	L	10FC	10FO	H	K	L	10FC	10FO	H	K	L	10FC	10FO
0	4	4	-494	459	5	6	4	211	400	7	8	4	1287	1255
1	4	4	-308	405	5	5	4	-600	643	8	8	4	444	417
2	4	4	-309	415	5	4	4	323	387	9	8	4	-621	621
3	4	4	1783	1814	6	6	4	570	632	11	8	4	-321	401
6	4	4	-262	331	6	4	4	957	1018	12	8	4	-649	648
7	4	4	-2259	2295	7	6	4	-668	705	13	8	4	936	1056
9	4	4	2240	2246	7	4	4	-692	723	16	8	4	672	690
11	4	4	917	907	8	6	4	-1026	971	17	8	4	-485	489
13	4	4	-1604	1583	8	4	4	1000	1010	20	8	4	-407	380
18	4	4	-166	355	9	6	4	860	837	22	8	4	360	376
19	4	4	515	495	10	6	4	-351	411	1	9	4	793	808
20	4	4	574	538	11	6	4	1365	1354	2	9	4	407	378
23	4	4	-524	583	12	6	4	-451	435	3	9	4	-413	528
27	4	4	618	551	13	6	4	-199	345	5	9	4	-1006	901
29	4	4	-505	564	20	6	4	-446	494	9	9	4	337	462
2	5	4	-662	602	21	6	4	383	468	11	9	4	-525	580
3	5	4	1293	1225	23	6	4	-434	471	13	9	4	-483	491
4	5	4	-1199	1235	25	6	4	504	489	15	9	4	1116	1122
5	5	4	-290	354	27	6	4	625	597	17	9	4	243	395
6	5	4	-662	602	1	7	4	1803	1761	19	9	4	-729	680
7	5	4	-1970	1935	2	7	4	964	977	0	10	4	618	639
8	5	4	1115	1050	3	7	4	-2395	2386	3	10	4	-728	753
10	5	4	317	322	6	7	4	-791	785	4	10	4	-643	570
11	5	4	-546	447	7	7	4	764	786	5	10	4	812	694
12	5	4	-1115	1097	10	7	4	1000	1010	6	10	4	563	519
13	5	4	-421	336	12	7	4	-323	342	7	10	4	975	960
14	5	4	-1158	1156	13	7	4	-1440	1381	8	10	4	524	515
16	5	4	308	396	14	7	4	-481	489	9	10	4	-1065	1084
17	5	4	759	740	15	7	4	1108	1103	11	10	4	-789	771
18	5	4	765	766	16	7	4	780	807	12	10	4	-460	442
19	5	4	-523	534	17	7	4	1003	1085	13	10	4	1419	1297
20	5	4	-424	428	19	7	4	-1264	1261	16	10	4	421	378
22	5	4	-468	473	23	7	4	951	858	17	10	4	-516	445
23	5	4	995	1026	0	8	4	1416	1427	18	10	4	-300	397
24	5	4	546	621	3	8	4	-845	856	1	11	4	-444	510
25	5	4	-494	517	4	8	4	-726	738	3	11	4	598	591

H	K	L	10FC	10FO	H	K	L	10FC	10FO	H	K	L	10FC	10FO
5	11	4	-443	555	9	2	5	-635	685					
11	11	4	-507	462	10	2	5	736	827					
1	12	4	-604	594	12	2	5	-2245	2337					
4	12	4	-405	416	13	2	5	420	406					
5	12	4	851	898	14	2	5	-842	475					
8	12	4	497	441	15	2	5	-1411	1375					
9	12	4	-684	632	16	2	5	1339	1395					
11	12	4	-234	399	17	2	5	885	888					
3	1	5	-1737	1412	18	2	5	-842	768					
5	1	5	1589	1567	19	2	5	1529	1524					
6	1	5	-697	2845	20	2	5	-703	710					
7	1	5	1112	767	21	2	5	-756	819					
8	1	5	-2173	1232	22	2	5	315	372					
9	1	5	1905	2216	24	2	5	1000	974					
10	1	5	1394	1874	26	2	5	-346	407					
11	1	5	542	1445	27	2	5	-498	565					
13	1	5	1372	463	28	2	5	-721	704					
14	1	5	1717	2894	1	3	5	574	687					
16	1	5	-657	1412	2	3	5	599	581					
18	1	5	1717	1781	3	3	5	800	726					
19	1	5	-583	617	4	3	5	173	304					
20	1	5	-1048	598	5	3	5	-1646	1806					
22	1	5	697	1112	6	3	5	-1299	1391					
24	1	5	-906	886	8	3	5	557	641					
25	1	5	994	985	9	3	5	646	708					
26	1	5	-599	659	10	3	5	1448	1433					
30	1	5	2646	2641	11	3	5	-1302	1338					
0	2	5	2228	2259	12	3	5	-860	852					
1	2	5	-786	811	14	3	5	-382	336					
2	2	5	368	313	15	3	5	481	499					
4	2	5	-2709	3035	17	3	5	-457	462					
5	2	5	-1787	1955	18	3	5	854	877					
6	2	5	965	978	22	3	5	-752	781					
8	2	5	478	545	23	3	5	-351	400					
9	2	5	1248	1282	24	3	5	583	660					
					0	4	5	2356	2380					

Observed and calculated structural factors for

$Mo(CO)(PMePh_2)_2Br_2(MeC{\equiv}CMe)$

H	K	L	10FC	10FO	H	K	L	10FC	10FO	H	K	L	10FC	10FO
1	4	5	1333	1584	1	6	5	-1574	-1584	16	8	5	655	713
3	4	5	1600	1321	4	6	5	-1273	-1321	17	8	5	-693	-660
4	4	5	2106	2177	5	6	5	954	885	18	8	5	-538	-524
6	4	5	748	668	7	6	5	-353	-358	19	8	5	-442	-398
8	4	5	3038	3006	8	6	5	1646	1595	21	8	5	499	435
9	4	5	912	-897	12	6	5	-875	970	2	9	5	-1372	1364
10	4	5	840	-775	13	6	5	-442	506	4	9	5	414	405
12	4	5	1638	-1608	14	6	5	406	475	5	9	5	743	747
13	4	5	370	-313	15	6	5	883	930	6	9	5	677	671
14	4	5	426	368	16	6	5	650	649	9	9	5	-681	690
15	4	5	433	-361	17	6	5	-573	516	10	9	5	-420	457
16	4	5	1638	1618	20	6	5	-786	792	11	9	5	840	858
17	4	5	861	892	21	6	5	604	544	14	9	5	719	813
19	4	5	687	709	22	6	5	682	635	15	9	5	-455	455
20	4	5	1627	-1609	24	6	5	468	429	16	9	5	-681	640
22	4	5	880	836	26	6	5	-463	511	3	10	5	-352	373
24	4	5	851	811	2	7	5	-1192	1174	5	10	5	-400	474
26	4	5	550	-651	3	7	5	-559	534	7	10	5	455	454
1	5	5	499	-418	5	7	5	569	569	13	10	5	627	656
2	5	5	792	-785	6	7	5	1614	1630	3	11	5	488	446
3	5	5	567	604	7	7	5	719	721	4	11	5	312	391
4	5	5	316	322	10	7	5	-1163	1219	6	11	5	570	493
5	5	5	1533	-1512	12	7	5	999	949	7	11	5	-576	568
6	5	5	1015	1034	13	7	5	-632	600	8	11	5	-597	603
7	5	5	1359	1329	14	7	5	515	571	11	11	5	396	439
9	5	5	1936	1895	15	7	5	-421	504	13	11	5	198	380
10	5	5	439	-343	18	7	5	-632	689	14	11	5	556	510
11	5	5	1782	-1773	22	7	5	532	548	1	12	5	526	532
13	5	5	652	-683	0	8	5	781	722	7	12	5	281	417
14	5	5	734	703	1	8	5	-1364	1350	7	0	6	-2188	1865
17	5	5	797	-761	3	8	5	-692	715	8	0	6	1266	1125
18	5	5	538	-507	5	8	5	718	608	9	0	6	1324	1208
22	5	5	428	409	8	8	5	-323	363	11	0	6	1443	1536
25	5	5	636	710	9	8	5	574	571	12	0	6	-2678	2848
27	5	5	422	-420	14	8	5	331	357	13	0	6	-2470	2629
0	6	5	1276	1244	15	8	5	811	876	14	0	6	839	877

H	K	L	10FC	10FO	H	K	L	10FC	10FO	H	K	L	10FC	10FO
15	2	6	637	615	6	3	6	-303	400	1	5	7	-1574	-1584
16	2	6	-674	-693	7	3	6	-727	748	2	5	7	1273	1321
17	2	6	2947	3081	9	3	6	3476	3451	3	5	7	-954	-885
18	2	6	-1409	1410	10	3	6	444	474	4	5	7	353	358
20	2	6	-1753	1670	11	3	6	392	327	5	5	7	-1646	-1595
21	2	6	249	411	12	3	6	-983	945	6	5	7	875	970
22	2	6	243	388	13	3	6	2079	2193	7	5	7	442	506
23	2	6	-470	364	14	3	6	721	732	8	5	7	-406	-475
24	2	6	836	849	15	3	6	-488	475	9	5	7	-883	-930
25	2	6	443	520	16	3	6	1155	1100	10	5	7	650	649
26	2	6	694	702	17	3	6	-657	657	11	5	7	573	516
27	2	6	-686	607	18	3	6	-987	980	12	5	7	-840	-792
28	2	6	-766	771	19	3	6	592	524	13	5	7	604	544
29	2	6	438	406	20	3	6	-724	767	14	5	7	682	635
30	2	6	1191	1096	21	3	6	1224	1220	15	5	7	468	429
6	1	6	674	713	22	3	6	701	689	16	5	7	-463	511
7	1	6	-1508	1573	23	3	6	-1100	1150	17	5	7	-1192	1174
10	1	6	1162	1175	26	3	6	497	424	18	5	7	-559	534
11	1	6	-461	480	30	3	6	-1013	1092	19	5	7	569	569
12	1	6	-791	787	0	4	6	919	889	20	5	7	1614	1630
13	1	6	1390	1439	1	4	6	-640	659	21	5	7	719	721
14	1	6	-939	973	2	4	6	-424	412	22	5	7	-1163	1219
15	1	6	517	564	3	4	6	999	949	23	5	7	-632	600
16	1	6	-670	675	4	4	6	515	571	24	5	7	-421	504
17	1	6	653	583	5	4	6	-632	689	25	5	7	718	608
18	1	6	-668	636	6	4	6	532	548	26	5	7	-323	363
19	1	6	2213	2326	7	4	6	-2367	2425	27	5	7	574	571
20	1	6	975	1024	8	4	6	-807	829	28	5	7	331	357
21	1	6	-1375	1369	9	4	6	-578	533	29	5	7	811	876
22	1	6	616	690	10	4	6	1443	1536	30	5	7	-1609	1627
23	1	6	-1308	1327	11	4	6	-2678	2848	31	5	7	836	880
24	1	6	2269	2317	12	4	6	-2470	2629	32	5	7	-811	-851
25	1	6	-968	986	13	4	6	1324	1208	33	5	7	-651	-550
26	1	6	1324	1327	14	4	6	877	839	34	5	7	-418	499
27	1	6	-1100	1150	15	4	6	839	877	35	5	7	-785	792
28	1	6	497	424	16	4	6	-1013	1092	36	5	7	604	567
29	1	6	-640	659	17	4	6	-424	412	37	5	7	322	316
30	1	6	1244	1276	18	4	6	811	876	38	5	7	-1512	1533
31	1	6	-1034	1015	19	4	6	1329	1359	39	5	7	1034	1015
32	1	6	1618	1638	20	4	6	-1608	1638	40	5	7	1329	1359
33	1	6	892	861	21	4	6	709	687	41	5	7	1895	1936
34	1	6	-1609	1627	22	4	6	-313	370	42	5	7	-343	439
35	1	6	836	880	23	4	6	368	426	43	5	7	-1773	1782
36	1	6	811	851	24	4	6	-361	433	44	5	7	-683	652
37	1	6	-651	550	25	4	6	1618	1638	45	5	7	703	734
38	1	6	-418	499	26	4	6	892	861	46	5	7	-761	797
39	1	6	-785	792	27	4	6	709	687	47	5	7	-507	538
40	1	6	604	567	28	4	6	-1609	1627	48	5	7	409	428
41	1	6	322	316	29	4	6	836	880	49	5	7	710	636
42	1	6	-1512	1533	30	4	6	-811	851	50	5	7	-420	422
43	1	6	1034	1015	31	4	6	1329	1359	51	5	7	1244	1276

Observed and calculated structural factors for

$Mo(CO)(PMePh_2)_2Br_2(MeC{\equiv}CMe)$

H	K	L	10FO	10FC
4	4	6	476	451
5	4	6	727	-731
7	4	6	1490	1463
8	4	6	609	618
9	4	6	465	-470
10	4	6	627	-591
11	4	6	328	-289
13	4	6	747	715
15	4	6	535	-591
16	4	6	703	-719
19	4	6	556	581
21	4	6	766	-751
23	4	6	419	437
2	5	6	1775	-1738
5	5	6	1058	-1006
6	5	6	1872	1866
7	5	6	371	472
8	5	6	437	-476
9	5	6	602	545
10	5	6	1702	-1645
11	5	6	819	-808
12	5	6	394	460
14	5	6	801	785
15	5	6	841	817
16	5	6	447	474
18	5	6	1146	-1075
19	5	6	368	-324
20	5	6	787	799
22	5	6	909	862
24	5	6	843	-807
26	5	6	411	-441
28	5	6	535	461
0	6	6	1710	-1710
1	6	6	471	491
4	6	6	1118	1091
5	6	6	434	544
7	6	6	614	668
8	6	6	1060	-1032
9	6	6	1337	-1282
10	6	6	631	693
11	6	6	682	-708
12	6	6	508	641
13	6	6	465	430
14	6	6	402	-473
16	6	6	1325	-1324
18	6	6	447	-404
20	6	6	952	958
3	7	6	670	-683
3	7	6	854	832
4	7	6	355	329
5	7	6	555	-563
6	7	6	382	-300
7	7	6	520	441
9	7	6	930	926
11	7	6	543	-541
14	7	6	824	822
15	7	6	643	645
17	7	6	850	-814
18	7	6	423	-405
0	8	6	1107	-1125
1	8	6	1000	-989
4	8	6	858	857
5	8	6	786	817
6	8	6	365	404
8	8	6	892	-887
12	8	6	614	525
14	8	6	522	-603
15	8	6	476	435
18	8	6	470	493
20	8	6	406	298
21	8	6	416	370
22	8	6	393	-266
5	10	6	454	522
7	10	6	496	304
8	10	6	410	-447
12	10	6	548	567
14	10	6	402	-465
17	10	6	439	-470
3	12	6	426	-491
6	1	7	532	824
7	1	7	958	1127
8	1	7	407	-430
9	1	7	1514	1516
10	1	7	1250	-1137
11	1	7	1605	-1629
12	1	7	404	-322
14	1	7	1647	1602
15	1	7	1500	1486
18	1	7	1956	-1947
20	1	7	354	465
22	1	7	900	890
23	1	7	421	375
25	1	7	585	590
27	1	7	692	-681
0	2	7	1332	-1351
1	2	7	1825	-1846
3	2	7	495	-522
4	2	7	1917	1991
5	2	7	1411	1365
7	2	7	1181	-1088
8	2	7	2319	-2318
9	2	7	447	537
12	2	7	2055	1929
13	2	7	365	-243
14	2	7	851	833
15	2	7	552	-510
16	2	7	813	-787
21	2	7	618	-680
24	2	7	510	-496
25	2	7	895	928
28	2	7	635	635
1	3	7	1091	-1025
3	3	7	1456	-1392
4	3	7	545	-532
5	3	7	1163	1128
7	3	7	940	-971
10	3	7	682	-693
11	3	7	736	658
12	3	7	358	-219
13	3	7	351	-276
14	3	7	917	928
17	3	7	363	-262
18	3	7	684	-660
19	3	7	843	843
23	3	7	681	-698
0	4	7	1044	-1035
1	4	7	664	675
2	4	7	692	-705
3	4	7	2319	2200
4	4	7	735	740
5	4	7	376	-274
6	4	7	2288	-2296
8	4	7	1016	-1029
9	4	7	515	537
10	4	7	1166	1172
12	4	7	729	660
13	4	7	466	572
15	4	7	509	-436
17	4	7	416	-351
19	4	7	594	-621
20	4	7	429	388
26	4	7	956	918
1	5	7	2114	2080
2	5	7	891	-879
3	5	7	503	480
5	5	7	594	-580
6	5	7	575	-575
9	5	7	680	613
11	5	7	769	-745
14	5	7	637	610
17	5	7	1166	1163
18	5	7	401	-424
19	5	7	605	-551
22	5	7	506	363
23	5	7	780	-830
0	6	7	565	544
2	6	7	925	-918
3	6	7	574	569
4	6	7	462	-544
6	6	7	1674	1693
7	6	7	1149	-1140
9	6	7	380	542
10	6	7	688	-661
11	6	7	1279	1251
13	6	7	571	-428
15	6	7	753	-739
17	6	7	428	390
20	6	7	429	-412
25	6	7	600	612
2	7	7	644	582
4	7	7		

Observed and calculated structural factors for

$Mo(CO)(PMePh_2)_2Br_2(MeC{\equiv}CMe)$

H	K	L	10FC	10FO
6	7	7	742	-775
7	7	7	713	-711
10	7	7	746	735
11	7	7	651	527
12	7	7	644	-661
14	7	7	397	-368
15	7	7	416	309
18	7	7	401	331
22	7	7	494	-487
0	8	7	460	-488
1	8	7	346	-285
2	8	7	468	536
3	8	7	400	-424
5	8	7	596	586
6	8	7	440	-385
7	8	7	487	488
8	8	7	1195	1208
9	8	7	744	-720
11	0	8	703	-747
13	0	8	1482	1393
16	0	8	1280	-1233
17	0	8	1378	-1330
19	0	8	880	888
20	0	8	1195	1225
23	0	8	378	370
24	0	8	384	348
29	0	8	678	669
10	1	8	1237	1380
11	1	8	393	-356
13	1	8	669	583
14	1	8	695	-618
15	1	8	390	-348
24	1	8	424	-294
27	1	8	395	199
0	2	8	476	-383
3	2	8	796	-825
4	2	8	525	510
5	2	8	621	580
7	2	8	814	775
9	2	8	1123	-1043
11	2	8	459	-416
13	2	8	948	909
17	2	8	516	-430
20	2	8	433	437
21	2	8	705	693
25	2	8	575	-565
1	3	8	323	-247
3	3	8	1336	1341
4	3	8	649	645
6	3	8	1859	-1847
7	3	8	549	-535
8	3	8	351	-313
10	3	8	2079	2115
14	3	8	469	-434
4	4	8	493	-429
5	4	8	827	-920
6	4	8	852	844
8	4	8	562	-453
9	4	8	744	739
11	4	8	2014	1951
16	4	8	985	-948
17	4	8	393	-313
20	4	8	369	-327
1	4	8	790	-820
3	4	8	1500	1440
4	4	8	735	716
5	4	8	731	-760
6	4	8	395	485
7	4	8	401	-425
9	4	8	879	927
10	4	8	1069	1103
11	4	8	442	445
13	4	8	541	-590
15	4	8	710	-746
16	4	8	818	875
18	4	8	605	-557
20	4	8	1006	-916
0	5	8	681	630
1	5	8	650	-566
2	5	8	1171	1151
4	5	8	903	-869
5	5	8	372	405
6	5	8	648	-651
14	5	8	1319	1338
17	5	8	508	-509
21	5	8	940	803
1	5	8	386	-254
3	5	8	723	-735
5	5	8	1522	1477
1	6	8	862	-830
4	6	8	1054	-919
5	6	8	394	484
6	6	8	566	-539
8	6	8	441	-438
9	6	8	518	618
11	6	8	548	-539
16	6	8	1036	1083
17	6	8	459	-435
20	6	8	475	-520
1	7	8	640	-707
3	7	8	865	808
4	7	8	545	-508
5	7	8	864	910
6	7	8	1040	1036
7	7	8	709	-658
9	7	8	791	-827
10	7	8	1340	-1367
11	7	8	1440	1478
13	7	8	603	580
15	7	8	1086	-1134
16	7	8	409	-413
19	7	8	686	669
20	7	8	386	-289
0	8	8	740	-718
1	8	8	757	735
2	8	8	414	392
4	8	8	415	485
5	8	8	617	-623
6	8	8	415	-413
8	8	8	536	489
9	8	8	464	457
12	8	8	544	-606
13	8	8	492	-456
16	8	8	508	545
18	8	8	429	504
19	8	8	483	413
6	9	8	473	489
7	9	8	574	-498
9	9	8	490	-439
10	9	8	408	-544
11	9	8	596	582
15	9	8	398	-369
0	10	8	830	-826
1	10	8	1014	930
2	10	8	380	160
4	10	8	425	499
5	10	8	714	-666
11	10	8	527	488
13	10	8	686	-601
4	11	8	681	518
10	1	9	1187	-1532
11	1	9	461	510
12	1	9	889	981
14	1	9	396	352
15	1	9	763	-769
16	1	9	555	-494
18	1	9	409	423
19	1	9	410	316
26	1	9	632	-623
0	2	9	1974	-2121
1	2	9	516	595
2	2	9	543	718
3	2	9	624	-874
6	2	9	743	-837
7	2	9	586	712
8	2	9	1215	1371
9	2	9	354	-215
12	2	9	737	-703
13	2	9	495	448
16	2	9	661	-601
18	2	9	415	393
19	2	9	464	-411

Observed and calculated structural factors for

$Mo(CO)(PMePh_2)_2Br_2(MeC{\equiv}CMe)$

H	K	L	10FO	10FC
20	2	9	648	619
22	2	9	419	-441
1	3	9	499	-518
2	3	9	1289	-1288
4	3	9	358	430
5	3	9	437	492
6	3	9	645	783
7	3	9	1229	-1141
11	3	9	830	804
14	3	9	352	385
15	3	9	424	-501
17	3	9	416	-415
18	3	9	681	-705
19	3	9	649	516
22	3	9	589	580
23	3	9	621	-586
0	4	9	1215	-1204
4	4	9	622	627
5	4	9	622	-637
9	4	9	407	524
10	4	9	556	524
16	4	9	737	-707
20	4	9	457	476
21	4	9	762	-817
1	5	9	455	-447
2	5	9	1465	-1494
3	5	9	1117	1068
4	5	9	779	762
7	5	9	822	-823
9	5	9	593	-616
10	5	9	663	589
11	5	9	413	425
12	5	9	405	-369
13	5	9	722	706
14	5	9	679	610
18	5	9	860	-828
19	5	9	520	437
22	5	9	516	456
23	5	9	425	-455
0	6	9	368	-356
1	6	9	396	410
2	6	9	491	-583
3	6	9	896	828
4	6	9	999	962
5	6	9	380	-461
6	6	9	622	594
7	6	9	795	-732
8	6	9	1659	-1646
9	6	9	1181	1112
12	6	9	1110	1098
13	6	9	1002	-1035
14	6	9	643	-677
16	6	9	425	-347
17	6	9	581	668
18	6	9	447	504
1	7	9	423	-337
10	7	9	466	352
13	7	9	472	443
1	8	9	1080	1051
3	8	9	560	606
4	8	9	654	596
5	8	9	749	-715
7	8	9	624	-681
8	8	9	1029	-1000
11	8	9	535	565
12	8	9	878	872
13	8	9	769	-803
17	8	9	668	629
1	9	9	603	658
2	9	9	1016	1025
3	9	9	980	-973
4	9	9	530	-602
6	9	9	371	-307
7	9	9	456	371
9	9	9	370	193
11	9	9	455	-329
12	9	9	475	386
14	9	9	647	-557
15	9	9	565	495
1	10	9	371	229
3	10	9	386	283
5	10	9	378	-233
6	10	9	508	-409
1	11	9	563	538
2	11	9	440	537
3	11	9	700	-655
14	0	10	939	-881
15	0	10	617	652
16	0	10	431	-405
18	0	10	1029	1022
19	0	10	362	-403
20	0	10	367	-372
22	0	10	495	-557
23	0	10	497	367
24	0	10	608	-515
25	0	10	597	-519
12	1	10	441	482
18	1	10	673	684
20	1	10	410	-505
21	1	10	524	373
0	2	10	615	-672
8	2	10	948	-1285
10	2	10	661	726
11	2	10	448	-475
12	2	10	1054	1056
14	2	10	504	-526
16	2	10	569	-608
20	2	10	600	635
22	2	10	434	-440
24	2	10	430	-496
1	3	10	954	-999
2	3	10	1997	2068
3	3	10	370	362
4	3	10	638	-625
5	3	10	541	565
7	3	10	386	-366
8	3	10	390	368
14	3	10	779	-787
15	3	10	584	-595
17	3	10	656	-600
18	3	10	1313	1294
19	3	10	433	465
20	3	10	611	-675
21	3	10	503	400
22	3	10	598	-625
24	3	10	479	515
0	4	10	1411	-1376
1	4	10	477	443
2	4	10	426	369
3	4	10	508	554
4	4	10	988	958
5	4	10	709	-769
6	4	10	518	-579
7	4	10	576	-480
9	4	10	611	618
10	4	10	434	420
11	4	10	470	402
14	4	10	558	583
16	4	10	716	-682
20	4	10	862	839
22	4	10	478	-464
24	4	10	441	-365
1	5	10	478	-423
2	5	10	648	590
4	5	10	499	433
6	5	10	1471	-1461
7	5	10	458	422
8	5	10	553	509
10	5	10	1330	1317
12	5	10	476	-509
13	5	10	351	-189
14	5	10	859	-807
16	5	10	612	620
18	5	10	686	803
22	5	10	707	-698
0	6	10	810	-819
1	6	10	561	615
5	6	10	603	-690
7	6	10	386	-371
8	6	10	945	948
9	6	10	530	549
10	6	10	573	-559
11	6	10	587	628
15	6	10	438	-472
1	7	10	603	624
2	7	10	508	476
3	7	10	684	-725
5	7	10	618	-640
6	7	10	1034	-1057
10	7	10	1164	1178
13	7	10	574	-547
14	7	10	785	-731
16	7	10	580	602
19	7	10	533	-416
0	8	10	1169	1120
4	8	10	738	-812
6	8	10	699	763
8	8	10	391	355
14	8	10	402	-226
16	8	10	406	552

Observed and calculated structural factors for

$Mo(CO)(PMePh_2)_2Br_2(MeC{\equiv}CMe)$

H	K	L	10FC	10FC
1	9	10	394	414
2	9	10	362	113
3	9	10	372	-320
5	9	10	556	-426
11	9	10	461	-405
0	10	10	1235	1260
1	10	10	446	-473
2	10	10	440	-372
3	10	10	387	-373
4	10	10	719	-615
7	10	10	410	338
14	1	11	1006	-1137
16	1	11	720	375
20	1	11	554	-573
22	1	11	500	-439
11	2	11	425	248
13	2	11	424	-322
15	2	11	556	-642
16	2	11	1172	1043
17	2	11	848	734
18	2	11	445	-286
19	2	11	524	723
20	2	11	724	-766
22	2	11	507	474
2	3	11	682	714
3	3	11	407	423
6	3	11	818	-921
8	3	11	776	867
14	3	11	455	-549
18	3	11	314	303
22	3	11	664	-664
0	4	11	1045	980
1	4	11	807	760
2	4	11	370	-153
3	4	11	784	947
4	4	11	1564	-1555
7	4	11	445	-414
9	4	11	827	963
10	4	11	383	-392
12	4	11	865	-890
13	4	11	632	-724
15	4	11	527	-448
16	4	11	997	955
17	4	11	638	638
19	4	11	651	500
20	4	11	1139	-1009
22	4	11	626	551
5	5	11	608	-676
5	5	11	506	-356
7	5	11	871	773
9	5	11	939	970
10	5	11	1001	-964
11	5	11	492	-537
12	5	11	618	490
13	5	11	396	-456
16	5	11	436	-315
2	6	11	593	535
4	6	11	635	-713
5	6	11	355	278
9	6	11	1062	1092
12	6	11	1273	-1280
14	6	11	605	704
2	7	11	542	-531
6	7	11	986	936
7	7	11	570	582
3	7	11	549	-579
10	7	11	493	-502
13	7	11	410	-392
0	8	11	477	247
3	8	11	417	355
9	8	11	1103	-1101
4	9	11	607	618
6	9	11	426	309
13	0	12	448	-491
21	0	12	414	-436
14	1	12	402	452
17	1	12	481	324
19	1	12	649	-705
10	1	12	421	-481
12	2	12	447	-611
13	2	12	643	-780
15	2	12	308	-425
16	2	12	429	462
17	2	12	390	391
21	2	12	482	-347
1	3	12	1125	1167
2	3	12	1404	-1583
3	3	12	962	-1191
4	3	12	653	768
5	3	12	492	-699
6	3	12	677	990
10	3	12	442	-490
13	3	12	475	-541
14	3	12	654	630
15	3	12	826	311
17	3	12	662	664
18	3	12	813	-862
19	3	12	734	-801
20	3	12	579	459
6	4	12	434	443
7	4	12	520	470
8	4	12	610	-527
0	4	12	393	-386
1	4	12	377	-396
4	4	12	568	509
2	5	12	392	-446
5	5	12	668	-581
6	5	12	1013	1017
7	5	12	803	804
9	5	12	384	302
10	5	12	1027	-987
11	5	12	677	-662
12	5	12	464	347
14	5	12	482	420
15	5	12	760	715
2	6	12	491	-505
4	6	12	819	772
5	6	12	435	502
7	6	12	449	358
8	6	12	887	-835
9	6	12	697	-706
12	6	12	445	445
14	6	12	383	-412
10	7	12	450	-310
12	7	12	402	305
0	8	12	678	-646
4	8	12	567	532
5	8	12	447	486
6	8	12	471	-354
9	8	12	451	-316
18	1	13	487	-398
19	1	13	537	-324
15	2	13	423	633
16	2	13	391	-475
17	2	13	631	-714
3	3	13	404	-564
17	3	13	473	429
0	4	13	651	-740
1	4	13	725	-695
3	4	13	885	-928
5	4	13	708	635
6	4	13	385	-255
8	4	13	575	-510
9	4	13	468	-536
13	4	13	550	545
17	4	13	593	-612
3	5	13	498	-505
4	5	13	464	345
6	5	13	675	-642
9	5	13	436	-541
10	5	13	493	494
14	5	13	397	-338
0	6	13	389	419
3	6	13	628	-690
7	6	13	573	549
9	6	13	718	-786
13	6	13	917	820
2	7	13	542	484
3	7	13	381	238
7	7	13	621	-628
9	3	14	427	234
4	4	14	572	-646
5	4	14	394	500
12	4	14	419	-532
2	5	14	511	-510
5	5	14	534	676
11	5	14	614	601
0	6	14	458	511
2	5	15	526	-497
3	5	15	636	618

APPENDIX 3

ANISOTROPIC AND ISOTROPIC THERMAL PARAMETERS FOR [$W(CO)_2(\eta^3\text{-}C_3H_5)bpma]PF_6$.

The thermal parameters were terms U_{ij} of

$\exp(-2\pi^2(U_{11}h^2a^{*2}+U_{22}k^2b^{*2}+U_{33}l^2c^{*2}+2U_{12}hka^*c^*+2U_{33}k(b^*c^*))$

Atom	U_{11} (or U_{iso})	U_{22}	U_{33}	U_{23}	U_{13}	U_{12}
W(1)	0.0443(4)	0.0212(3)	0.0317(3)	0.0014(2)	0.0093(2)	0.0006(2)
O(1)	0.0813(36)					
O(2)	0.0749(34)					
N(1)	0.0361(26)					
N(2)	0.0335(26)					
N(3)	0.0348(26)					
C(1)	0.0453(37)					
C(2)	0.0563(42)					
C(3)	0.0554(41)					
C(4)	0.0606(44)					
C(5)	0.0558(42)					
C(6)	0.0491(39)					
C(7)	0.0567(42)					
C(8)	0.0556(41)					
C(9)	0.0432(35)					
C(10)	0.0333(31)					
C(11)	0.0438(35)					
C(12)	0.0384(33)					
C(13)	0.0369(33)					
C(14)	0.0550(41)					
C(15)	0.0603(44)					
C(16)	0.0613(45)					
C(17)	0.0475(37)					
P(1)	0.0402(23)	0.0365(21)	0.0441(23)	0.0037(17)	0.0061(18)	-0.0012(17)
F(1)	0.0614(62)	0.0685(61)	0.0518(52)	0.0074(45)	-0.0013(44)	0.0038(47)
F(2)	0.0575(61)	0.0699(61)	0.0671(59)	-0.0215(47)	0.0176(47)	-0.0043(46)
F(3)	0.0669(64)	0.0496(55)	0.0912(69)	0.0192(49)	0.0034(52)	-0.0225(46)
F(4)	0.0572(59)	0.0889(69)	0.0474(50)	0.0041(48)	-0.0033(43)	0.0023(49)
F(5)	0.0591(64)	0.1132(82)	0.0648(59)	-0.0255(58)	0.0201(48)	0.0132(56)
F(6)	0.0887(72)	0.0436(53)	0.0868(67)	-0.0026(49)	0.0138(56)	-0.0175(50)
W(2)	0.0382(4)	0.0327(4)	0.0358(4)	-0.0008(3)	0.0052(3)	-0.0039(3)
O(3)	0.0818(37)					
O(4)	0.0772(35)					
N(4)	0.0388(27)					
N(5)	0.0418(28)					
N(6)	0.0382(27)					
C(18)	0.0533(41)					
C(19)	0.0523(40)					
C(20)	0.0557(41)					
C(21)	0.0519(39)					
C(22)	0.0648(47)					
C(23)	0.0529(40)					
C(24)	0.0571(42)					
C(25)	0.0629(45)					
C(26)	0.0601(44)					

ANISOTROPIC AND ISOTROPIC THERMAL PARAMETERS FOR [$W(CO)_2(\eta^3\text{-}C_3H_5)bpma]PF_6$.

Atom	U_{11} (or U_{iso})	U_{22}	U_{33}	U_{23}	U_{13}	U_{12}
C(27)	0.0395(34)					
C(28)	0.0509(40)					
C(29)	0.0485(38)					
C(30)	0.0437(35)					
C(31)	0.0586(43)					
C(32)	0.0512(39)					
C(33)	0.0531(40)					
C(34)	0.0396(34)					
P(2)	0.0490(27)	0.0607(28)	0.0488(24)	-0.0039(21)	0.0082(20)	-0.0140(21)
F(7)	0.0676(85)	0.2923(22)	0.0759(80)	0.0259(10)	-0.0107(64)	-0.0276(10)
F(8)	0.0826(81)	0.2057(14)	0.0560(63)	-0.0361(74)	0.0272(56)	-0.0643(86)
F(9)	0.2894(23)	0.0611(81)	0.1859(15)	0.0291(90)	0.1129(15)	-0.0170(11)
F(10)	0.0648(82)	0.2568(19)	0.0908(87)	-0.0615(10)	0.0071(64)	0.0064(93)
F(11)	0.0922(78)	0.0817(69)	0.0561(57)	-0.0074(50)	0.0338(53)	-0.0097(58)
F(12)	0.2182(17)	0.0784(88)	0.1511(12)	-0.0304(85)	0.0878(12)	-0.0239(98)

ATOMIC COORDINATES (x10⁴) FOR [W(CO)₂(η³-C₃H₅)bpma]PF₆ WITH ESTIMATED STANDARD DEVIATIONS IN PARENTHESES

Atom	X	Y	Z
W(1)	576(0)	589(0)	1995(1)
O(1)	-1459(11)	875(7)	688(8)
O(2)	1808(10)	845(6)	563(7)
N(1)	380(9)	-500(5)	1732(6)
N(2)	-280(8)	164(5)	2985(6)
N(3)	1887(9)	110(5)	2881(6)
C(1)	-702(12)	762(7)	1188(9)
C(2)	1344(13)	749(8)	1116(10)
C(3)	-223(13)	1592(8)	2286(9)
C(4)	1666(14)	1545(8)	2228(10)
C(5)	877(13)	1521(8)	2717(9)
C(6)	930(13)	-809(8)	1190(9)
C(7)	905(13)	-1506(8)	1100(9)
C(8)	340(13)	-1884(8)	1596(9)
C(9)	-228(12)	-1571(7)	2148(8)
C(10)	-196(11)	-870(6)	2186(8)
C(11)	-1863(12)	-468(7)	2713(8)
C(12)	472(11)	94(7)	3759(8)
C(13)	1581(11)	-106(7)	3597(8)
C(14)	2303(13)	-486(8)	4151(9)
C(15)	3305(14)	-657(8)	3972(10)
C(16)	3616(14)	-426(8)	3256(10)
C(17)	2871(12)	-46(7)	2712(9)
P(1)	642(0)	3134(0)	314(0)
F(1)	1501(7)	2984(4)	1105(5)
F(2)	-172(7)	3433(5)	878(5)
F(3)	1173(8)	3862(4)	273(6)
F(4)	-217(7)	3287(5)	-472(5)
F(5)	1449(8)	2836(6)	-246(5)
F(6)	111(8)	2418(4)	389(6)
W(2)	4545(0)	1547(0)	9224(0)
O(3)	5373(11)	1858(6)	7609(8)
O(4)	5808(10)	219(6)	9028(7)
N(4)	4021(9)	2581(5)	9549(6)
N(5)	4254(9)	1455(6)	10527(7)
N(6)	6014(9)	1967(5)	9983(6)
C(18)	5322(13)	721(8)	9098(9)
C(19)	5051(13)	1752(8)	8233(9)
C(20)	3332(13)	637(8)	9012(9)
C(21)	2817(13)	1284(8)	8865(9)
C(22)	3093(14)	1645(9)	8170(10)
C(23)	4132(13)	3143(8)	9060(9)
C(24)	3958(13)	3787(8)	9341(9)
C(25)	3798(14)	3877(9)	10146(10)
C(26)	37029(14)	3318(8)	10637(10)
C(27)	3851(11)	2672(7)	10312(8)
C(28)	3644(13)	2046(8)	10783(9)
C(29)	5337(12)	1379(8)	11065(9)
C(30)	6673(11)	2402(7)	9665(8)
C(31)	7492(13)	2739(8)	10197(10)

ATOMIC COORDINATES (x10⁴) FOR [W(CO)₂(η^3-C_3H_5)bpma]PF_6 WITH ESTIMATED STANDARD DEVIATIONS IN PARENTHESES

Atom	X	Y	Z
C(32)	7588(12)	2627(8)	11026(9)
C(33)	6922(13)	2182(8)	11334(9)
C(34)	6114(11)	1863(7)	10773(8)
P(2)	3336(0)	5669(0)	1725(0)
F(7)	2156(10)	5670(9)	1244(7)
F(8)	3806(9)	5623(7)	909(6)
F(9)	3443(17)	6447(6)	1746(10)
F(10)	4514(10)	5650(9)	2208(7)
F(11)	2837(8)	5702(5)	2540(5)
F(12)	3273(15)	4878(6)	1745(9)

Observed and calculated structural factors for

$[W(CO)_2(\eta^3\text{-}C_3H_5)bpma]PF_6$

H	K	L	10FO	10FC
3	1	0	3634	-3409
4	1	0	1435	1416
5	1	0	1517	-1565
6	1	0	923	979
1	2	0	2862	2807
2	2	0	477	-480
3	2	0	1338	1206
5	2	0	765	-729
6	2	0	512	-473
7	2	0	1631	-1603
8	2	0	1140	-1202
9	2	0	923	-1035
10	2	0	362	-394
2	3	0	1866	-1726
3	3	0	1424	-1367
4	3	0	1719	-1510
5	3	0	2310	-2224
6	3	0	791	-762
7	3	0	881	-851
0	3	0	437	498
1	3	0	461	451
2	3	0	457	435
0	4	0	1860	-1749
1	4	0	1987	1834
2	4	0	2425	-2260
3	4	0	1713	1636
4	4	0	483	-485
5	4	0	768	685
7	4	0	684	-666
8	4	0	478	494
9	4	0	1109	-1000
10	4	0	527	541
11	4	0	925	-963
12	4	0	629	585
1	5	0	1870	1640
2	5	0	3936	-3621
3	5	0	582	-513
4	5	0	3987	-3682
5	5	0	384	314
6	5	0	3473	-3280
7	5	0	599	559
8	5	0	1729	-1648
9	5	0	663	668
12	5	0	805	798
0	6	0	1178	1050
1	6	0	3043	-2943
2	6	0	2182	2133
3	6	0	1660	-1595
4	6	0	1238	1171
5	6	0	392	454
6	6	0	359	273
7	6	0	1534	1516
8	6	0	324	-301
9	6	0	1177	1163
11	6	0	1266	1201
12	6	0	598	-607
1	7	0	650	-546
2	7	0	936	-926
3	7	0	1077	-1129
4	7	0	667	-603
5	7	0	1718	-1635
6	7	0	424	451
7	7	0	1315	-1227
8	7	0	816	760
10	7	0	541	618
11	7	0	924	967
12	7	0	362	352
0	8	0	3702	-3311
1	8	0	2420	-2227
2	8	0	2059	-1923
3	8	0	1261	-1269
5	8	0	646	662
6	8	0	827	782
7	8	0	1804	1740
8	8	0	1548	1449
9	8	0	1241	1143
10	8	0	1060	1024
11	8	0	710	716
1	9	0	372	-393
2	9	0	1533	1529
3	9	0	646	-685
4	9	0	1478	1405
5	9	0	700	-728
6	9	0	1466	1401
7	9	0	542	-514
8	9	0	810	711
0	10	0	4130	-3919
1	10	0	321	364
2	10	0	3091	-2991
3	10	0	420	-469
4	10	0	1397	-1323
5	10	0	459	436
6	10	0	821	809
8	10	0	1648	1567
9	10	0	469	-433
10	10	0	1512	1449
11	10	0	373	-375
1	11	0	392	311
3	11	0	2546	2461
4	11	0	591	-616
5	11	0	2887	2786
6	11	0	318	-319
7	11	0	1436	1477
10	11	0	484	-510
11	11	0	411	-356
0	12	0	1477	1500
1	12	0	886	-947
2	12	0	816	793
3	12	0	505	-460
4	12	0	767	746
6	12	0	477	455
7	12	0	726	711
9	12	0	898	827
1	13	0	384	305
2	13	0	1596	1573
3	13	0	1417	1339
4	13	0	1357	1343
5	13	0	1283	1208
6	13	0	956	884
7	13	0	499	492
8	13	0	422	452
0	14	0	1957	1891
2	14	0	563	614
4	14	0	362	288
5	14	0	663	-605
8	14	0	946	-886
2	15	0	1396	1411
4	15	0	2207	2228
6	15	0	1460	1437
7	15	0	567	-558
8	15	0	830	752
9	15	0	638	-635
0	16	0	668	635
1	16	0	2148	2195
3	16	0	1540	1558
4	16	0	513	-418
5	16	0	346	-242
6	16	0	508	-508
7	16	0	1263	-1320
8	16	0	379	-421
2	17	0	701	-663
3	17	0	614	689
4	17	0	676	-733
5	17	0	501	530
6	17	0	742	-825
7	17	0	505	525
0	18	0	1272	1284
1	18	0	867	888
2	18	0	817	804
3	18	0	473	491
6	18	0	423	-441
2	19	0	616	-657
3	19	0	517	-456
4	19	0	931	-901
0	20	0	1285	1255
2	20	0	1009	1025
-7	1	1	554	552
-6	1	1	1326	1421
-5	1	1	463	592
-4	1	1	2336	2383
-2	1	1	5074	4894
2	1	1	834	-834
3	1	1	3021	-3012
4	1	1	820	-904
5	1	1	1960	-1915
6	1	1	2330	-2516
7	1	1	279	130
8	1	1	1738	-1907
9	1	1	480	556
-11	2	1	535	688
-9	2	1	1752	1936
-8	2	1	289	-236
-7	2	1	3278	3220
-5	2	1	2146	2056
-4	2	1	348	-322
-2	2	1	1212	-1073
-1	2	1	1194	-1341
1	2	1	3053	-2875
2	2	1	2083	2090
3	2	1	1328	-1475

Observed and calculated structural factors for

$[W(CO)_2(\eta^3\text{-}C_3H_5)bpma]PF_6$

H	K	L	10FO	10FC
4	2	1	1876	1987
5	2	1	2229	-2165
6	2	1	1622	1539
7	2	1	843	-879
8	2	1	1475	1540
9	2	1	492	552
11	2	1	892	955
12	2	1	440	-554
-12	3	1	507	456
-11	3	1	1133	-1182
-10	3	1	358	292
-9	3	1	954	-941
-8	3	1	686	774
-7	3	1	659	608
-5	3	1	2111	1936
-4	3	1	818	-866
-3	3	1	3001	2865
-2	3	1	1006	-866
-1	3	1	4857	4586
0	3	1	1820	-1747
1	3	1	2436	2460
2	3	1	990	-1026
3	3	1	369	308
5	3	1	1249	-1202
7	3	1	1999	-1894
8	3	1	807	727
9	3	1	1444	-1484
10	3	1	1006	1058
11	3	1	802	-770
12	3	1	854	885
-10	4	1	1252	1285
-8	4	1	2469	2442
-7	4	1	391	357
-6	4	1	2892	2726
-5	4	1	565	-483
-4	4	1	763	740
-2	4	1	1513	-1383
0	4	1	4256	-4036
1	4	1	2734	-2559
2	4	1	3314	-3131
4	4	1	2887	-2647
5	4	1	2128	2033
6	4	1	1110	-1149
7	4	1	1612	1607
8	4	1	1038	1021
9	4	1	1337	1341
10	4	1	1389	1415
11	4	1	607	668
12	4	1	1185	1195
-11	5	1	335	351
-10	5	1	440	386
-9	5	1	545	621
-8	5	1	294	208
-6	5	1	497	-446
-4	5	1	1015	-911
-2	5	1	567	-527
-1	5	1	1777	-1717
0	5	1	988	-1046
1	5	1	2799	-2554
2	5	1	540	578
3	5	1	1312	1178
4	5	1	479	464
5	5	1	599	562
8	5	1	356	305
9	5	1	528	527
12	5	1	369	-369
-10	6	1	805	901
-9	6	1	544	550
-8	6	1	1229	1172
-6	6	1	1910	1799
-4	6	1	688	731
-3	6	1	1720	-1584
-2	6	1	637	-657
-1	6	1	1340	-1369
0	6	1	1833	-1849
1	6	1	1323	-1193
2	6	1	2280	-2095
4	6	1	1821	-1770
5	6	1	843	855
6	6	1	362	-333
7	6	1	1204	1249
8	6	1	1211	1137
9	6	1	610	639
10	6	1	651	611
11	6	1	343	321
12	6	1	533	467
-11	7	1	1189	1097
-9	7	1	686	658
-7	7	1	424	-419
-6	7	1	1075	-956
-5	7	1	2661	-2601
-4	7	1	349	-383
-3	7	1	4105	-3893
-1	7	1	3319	-3096
0	7	1	905	891
1	7	1	2802	-2656
2	7	1	984	1003
3	7	1	398	419
4	7	1	1546	1463
5	7	1	2216	2135
6	7	1	329	242
7	7	1	1862	1874
8	7	1	565	-527
9	7	1	1616	1568
10	7	1	1108	-1025
11	7	1	439	446
12	7	1	828	-791
-11	8	1	422	478
-10	8	1	395	-414
-9	8	1	1276	1214
-8	8	1	826	-790
-7	8	1	1751	1655
-6	8	1	1479	-1399
-5	8	1	1190	1095
-4	8	1	1285	-1188
-3	8	1	1508	1417
-2	8	1	482	-460
-1	8	1	759	-637
0	8	1	1049	1000
1	8	1	2763	-2582
2	8	1	1128	1081
3	8	1	2463	-2402
4	8	1	1642	1646
5	8	1	1707	-1674
6	8	1	1598	1563
7	8	1	739	-697
8	8	1	312	344
11	8	1	439	401
-10	9	1	1224	1205
-7	9	1	527	-484
-6	9	1	1052	-1014
-5	9	1	661	-577
-4	9	1	2442	-2336
-2	9	1	3543	-3476
-1	9	1	638	693
0	9	1	2457	-2309
1	9	1	786	802
2	9	1	502	504
3	9	1	2587	2492
4	9	1	2075	1983
5	9	1	1459	1465
6	9	1	2333	2242
8	9	1	1462	1393
9	9	1	331	-374
10	9	1	610	581
11	9	1	841	-784
-10	10	1	545	-550
-9	10	1	744	-755
-8	10	1	373	-328
-7	10	1	1199	-1137
-5	10	1	371	-348
-1	10	1	460	465
0	10	1	909	916
1	10	1	1682	1660
2	10	1	522	-531
3	10	1	1301	1338
4	10	1	631	-612
5	10	1	355	-246
6	10	1	713	-746
8	10	1	626	-577
9	10	1	526	-488
-10	11	1	543	484
-8	11	1	457	401
-6	11	1	1122	-1010
-4	11	1	1981	-1926
-3	11	1	1082	-1027
-2	11	1	2079	-2084
-1	11	1	360	-452
0	11	1	819	-850
3	11	1	576	520
4	11	1	761	801
5	11	1	1100	1081
6	11	1	1300	1253
8	11	1	1157	1151
10	11	1	460	424
-9	12	1	1471	-1430
-7	12	1	2015	-1972
-5	12	1	2171	-2103
-3	12	1	557	-521
-2	12	1	1104	1041

Observed and calculated structural factors for

$[W(CO)_2(\eta^3\text{-}C_3H_5)bpma]PF_6$

H	K	L	10FO	10FC
-1	12	1	700	633
0	12	1	1601	1641
1	12	1	3055	2944
3	12	1	2798	2761
4	12	1	604	-517
5	12	1	1034	1013
6	12	1	801	-811
8	12	1	1236	-1220
9	12	1	873	-801
10	12	1	581	-657
-10	13	1	795	-856
-7	13	1	331	-342
-5	13	1	932	-996
-4	13	1	891	822
-3	13	1	1521	-1500
-2	13	1	2588	2494
-1	13	1	1008	-1041
0	13	1	1834	1761
1	13	1	731	-674
2	13	1	408	346
3	13	1	910	-826
6	13	1	782	-812
7	13	1	859	920
8	13	1	1206	-1133
9	13	1	1052	1027
10	13	1	620	-576
-8	14	1	1281	-1293
-6	14	1	1660	-1692
-5	14	1	486	498
-4	14	1	1020	-1060
-3	14	1	1013	996
-2	14	1	908	884
-1	14	1	534	515
0	14	1	1818	1335
2	14	1	1907	1934
4	14	1	1652	1625
-1	12	2	1155	-1132
0	12	2	347	359
1	12	2	1070	-1147
3	12	2	567	-571
4	12	2	723	-743
5	12	2	591	-523
6	12	2	404	423
8	12	2	1316	1303
9	12	2	544	521
10	12	2	1600	1623
-10	13	2	722	690
-7	13	2	961	902
-5	13	2	801	-792
-4	13	2	798	-716
-3	13	2	719	-763
-2	13	2	1079	-1076
-1	13	2	768	-803
0	13	2	943	-958
1	13	2	417	-419
2	13	2	367	-324
3	13	2	376	414
6	13	2	274	200
7	13	2	338	274
8	13	2	783	820
9	13	2	487	505
10	13	2	656	663
-8	14	2	1368	1406
-6	14	2	821	792
-5	14	2	1866	1906
-4	14	2	336	348
-3	14	2	1644	1664
-2	14	2	816	-759
-1	14	2	552	571
0	14	2	965	-996
2	14	2	604	-617
4	14	2	714	-765
-10	12	1	1509	-1516
-4	12	1	349	-438
-3	12	1	1178	-1177
-1	12	1	784	831
0	12	1	705	-742
1	12	1	670	656
2	12	1	822	-875
3	12	1	398	-394
4	12	1	1006	-1039
6	12	1	1483	-1480
7	12	1	842	765
9	12	1	1071	-1112
-5	13	1	793	814
-4	13	1	1401	1442
-3	13	1	1634	1655
-2	13	1	930	983
-1	13	1	695	-730
0	13	1	551	-627
1	13	1	803	-850
2	13	1	434	-467
3	13	1	664	-646
6	13	1	944	-910
7	13	1	841	-943
8	13	1	1545	-1540
9	13	1	365	-441
10	13	1	1346	-1371
-8	14	1	939	-1038
-6	14	1	2200	2247
-5	14	1	3123	-3174
-4	14	1	3704	-3685
-3	14	1	2461	-2451
-2	14	1	2918	-2917
-1	14	1	2164	2066
0	14	1	2571	-2662
2	14	1	1933	2022
4	14	1	349	295
-10	12	2	343	-520
-4	12	2	1027	-1089
-3	12	2	601	517
-1	12	2	2015	-2160
0	12	2	3342	-3565
2	12	2	2846	2873
3	12	2	2296	-2274
4	12	2	2530	2564
5	12	2	673	-673
6	12	2	1240	1285
7	12	2	278	155
9	12	2	785	757
-5	13	2	458	604
-4	13	2	476	-601
-3	13	2	536	709
-2	13	2	801	833
-1	13	2	1119	1188
0	13	2	633	677
1	13	2	1915	1852
2	13	2	2214	-2388
3	13	2	4760	-4782
6	13	2	2254	-2346
7	13	2	1084	-1062
8	13	2	2994	-3054
9	13	2	298	-269
10	13	2	1957	-1981
-8	14	2	821	724
-6	14	2	1213	1254
-5	14	2	605	651
-4	14	2	853	638
-3	14	2	371	298
-2	14	2	403	479
-1	14	2	474	598
0	14	2	562	658
2	14	2	894	995
4	14	2	805	770
-9	13	2	1479	1493
-6	13	2	2076	2050
-5	13	2	968	927
-3	13	2	1053	1057
-2	13	2	729	776
-1	13	2	635	-619
0	13	2	690	658
1	13	2	341	-353
2	13	2	347	241
3	13	2	1013	1020
4	13	2	854	-836
5	13	2	1968	1896
6	13	2	1037	-1011
7	13	2	2469	2349
8	13	2	2355	-2162
9	13	2	857	833
10	13	2	1232	-1193
-8	14	2	796	743
-6	14	2	315	364
-5	14	2	509	-433
-4	14	2	756	689
-3	14	2	1263	-1183
-2	14	2	1243	1208
-1	14	2	1243	-1200

Observed and calculated structural factors for

$[W(CO)_2(\eta^3\text{-}C_3H_5)bpma]PF_6$

H	K	L	10FO	10FC
8	4	2	997	1057
9	4	2	762	-831
10	4	2	685	622
11	4	2	502	-531
-12	5	2	1325	1269
-10	5	2	2081	1949
-8	5	2	2111	2054
-7	5	2	1066	-1028
-6	5	2	780	720
-5	5	2	1766	-1677
-4	5	2	1462	-1364
-3	5	2	1883	-1857
-2	5	2	2356	-2286
-1	5	2	930	-848
0	5	2	3484	-3344
1	5	2	989	1007
2	5	2	1406	-1463
3	5	2	3198	3105
4	5	2	726	-627
5	5	2	3558	3478
6	5	2	1028	945
7	5	2	1205	1197
8	5	2	725	692
10	5	2	700	612
11	5	2	1080	-1079
-12	6	2	427	-484
-10	6	2	765	-728
-9	6	2	543	-514
-8	6	2	608	-580
-7	6	2	2064	-1996
-6	6	2	421	-393
-5	6	2	2477	-2363
-4	6	2	1683	1633
-3	6	2	1753	-1701
-2	6	2	2415	2396
-1	6	2	1149	-1098
0	6	2	1021	1133
1	6	2	629	689
2	6	2	2182	1991
3	6	2	2037	2050
5	6	2	1464	1383
6	6	2	1816	-1805
7	6	2	1202	1174
8	6	2	2075	-2002
9	6	2	376	427
10	6	2	1388	-1384
12	6	2	457	-459
-11	7	2	448	395
-9	7	2	1397	1315
-8	7	2	681	-632
-7	7	2	1350	1345
-6	7	2	1012	-896
-5	7	2	289	282
-3	7	2	1603	-1503
-2	7	2	342	-212
-1	7	2	1871	-1904
0	7	2	649	618
1	7	2	877	-871
2	7	2	1767	1581
3	7	2	392	-431
4	7	2	1507	1569
6	7	2	1236	1255
7	7	2	320	303
8	7	2	607	554
9	7	2	509	473
11	7	2	563	446
-9	8	2	692	-726
-8	8	2	951	-913
-7	8	2	1590	-1534
-6	8	2	1449	-1402
-5	8	2	1966	-1918
-4	8	2	559	-538
-3	8	2	581	-545
-2	8	2	317	310
0	8	2	2305	2214
1	8	2	2080	1999
2	8	2	3216	2828
3	8	2	2226	2091
4	8	2	1334	1299
5	8	2	702	709
6	8	2	306	177
8	8	2	595	-600
10	8	2	1100	-1053
11	8	2	654	-674
-11	9	2	493	528
-10	9	2	620	-561
-9	9	2	359	373
-8	9	2	404	-580
-7	9	2	430	407
-6	9	2	567	-563
-5	9	2	522	463
-4	9	2	836	-726
-3	9	2	303	302
-1	9	2	523	-544
0	9	2	1668	1483
1	9	2	305	-375
2	9	2	1453	1458
3	9	2	1665	-1595
4	9	2	450	442
5	9	2	973	-890
6	9	2	305	-203
8	9	2	626	-660
10	9	2	475	-530
-11	10	2	586	-459
-9	10	2	742	-738
-8	10	2	1481	-1422
-7	10	2	810	-751
-6	10	2	2520	-2458
-4	10	2	3027	-2902
-3	10	2	1167	1176
-2	10	2	1165	-1174
-1	10	2	2774	2678
0	10	2	836	771
1	10	2	2525	2449
2	10	2	1618	1504
3	10	2	1141	1048
4	10	2	1198	1160
5	10	2	982	-902
6	10	2	1090	1118
7	10	2	1795	-1778
8	10	2	459	478
9	10	2	1962	-1870
11	10	2	1012	-1033
-11	11	2	1204	-1167
-9	11	2	1503	-1447
-8	11	2	759	727
-7	11	2	806	-799
-6	11	2	1028	986
-5	11	2	728	662
-4	11	2	2140	2070
-3	11	2	1791	1748
-2	11	2	1840	1811
-1	11	2	2654	2688
0	11	2	823	-845
1	11	2	2301	2349
2	11	2	2193	-2129
3	11	2	589	540
4	11	2	2126	-2039
6	11	2	2013	-1863
7	11	2	589	-571
8	11	2	455	-485
9	11	2	1027	-1003
10	11	2	456	474
-10	12	2	395	-402
-8	12	2	427	-415
-7	12	2	876	-848
-5	12	2	1051	-974
-4	12	2	716	701
-3	12	2	1161	-1099
-2	12	2	1037	1001
-1	12	2	323	-339
0	12	2	707	714
2	12	2	986	1015
3	12	2	864	941
5	12	2	964	971
6	12	2	637	-572
7	12	2	531	491
8	12	2	584	-589
10	12	2	609	-558
-10	13	2	849	-825
-9	13	2	645	-616
-8	13	2	529	-556
-6	13	2	383	328
-5	13	2	1382	1342
-4	13	2	1475	1415
-3	13	2	1615	1575
-2	13	2	2045	2051
-1	13	2	1082	1088
0	13	2	1134	1082
1	13	2	466	492
3	13	2	1044	-1084
4	13	2	911	-843
5	13	2	1484	-1511
6	13	2	1389	-1409
7	13	2	717	-765
8	13	2	871	-849
-9	14	2	344	281
-8	14	2	547	557
-6	14	2	1008	977
-4	14	2	837	848

Observed and calculated structural factors for

$[W(CO)_2(\eta^3\text{-}C_3H_5)bpma]PF_6$

H	K	L	10FO	10FC
-3	14	2	1062	-1030
-1	14	2	1053	-1016
0	14	2	753	-721
1	14	2	1232	-1303
2	14	2	384	-318
3	14	2	861	-867
4	14	2	401	-473
5	14	2	467	427
6	14	2	410	-398
7	14	2	895	866
9	14	2	765	777
-9	15	2	457	374
-8	15	2	1068	-974
-7	15	2	558	479
-6	15	2	709	-654
-5	15	2	756	761
-4	15	2	514	533
-3	15	2	509	538
-2	15	2	1319	1316
0	15	2	1535	1575
1	15	2	566	-571
2	15	2	1299	1322
3	15	2	1137	-1132
4	15	2	406	414
5	15	2	1349	-1351
6	15	2	455	-366
7	15	2	898	-933
8	15	2	498	-537
-8	16	2	513	523
-7	16	2	1539	1502
-5	16	2	1926	1898
-4	16	2	398	-338
-3	16	2	1534	1532
-2	16	2	894	-948
-1	16	2	482	425
0	16	2	1490	-1511
1	16	2	599	-640
2	16	2	1067	-1121
3	16	2	1147	-1189
4	16	2	557	-527
5	16	2	1087	-1052
6	16	2	624	681
7	16	2	816	-812
-7	17	2	587	-446
-6	17	2	395	477
-4	17	2	428	429
-1	17	2	339	484
0	17	2	536	-552
1	17	2	528	522
2	17	2	993	-984
3	17	2	823	868
4	17	2	814	-782
-6	18	2	1011	1021
-5	18	2	624	607
-4	18	2	583	660
-1	18	2	944	-949
0	18	2	997	-1019
1	18	2	1073	-1051
2	18	2	1114	-1143
3	18	2	926	-943
4	18	2	805	-771
-5	19	2	500	-561
-4	19	2	404	-465
-3	19	2	561	-590
-2	19	2	846	-860
-1	19	2	370	-408
0	19	2	543	-596
3	19	2	493	590
-3	20	2	650	-575
-2	20	2	535	549
-1	20	2	876	-894
1	20	2	775	-817
2	20	2	416	-419
3	20	2	374	-230
-7	1	3	282	-280
-6	1	3	1279	1444
-5	1	3	815	-907
-4	1	3	553	-581
-3	1	3	2216	-2399
-1	1	3	3323	-3657
0	1	3	1204	-1236
1	1	3	2042	-2128
2	1	3	2081	-2084
4	1	3	458	-409
5	1	3	2067	2132
6	1	3	985	1095
7	1	3	1878	1950
9	1	3	1384	1397
-9	2	3	661	742
-8	2	3	1665	-1805
-6	2	3	1789	-1864
-5	2	3	1288	-1417
-4	2	3	480	-503
-3	2	3	1748	-1801
-2	2	3	1955	2118
-1	2	3	2265	-2488
0	2	3	3446	3539
1	2	3	1061	1006
2	2	3	2242	2463
3	2	3	366	477
4	2	3	2710	2740
5	2	3	1024	-1055
6	2	3	421	318
8	2	3	1267	-1278
9	2	3	480	475
10	2	3	1485	-1502
12	2	3	1100	-1203
-12	3	3	380	366
-9	3	3	980	1025
-8	3	3	835	-831
-7	3	3	1657	1638
-6	3	3	1607	-1628
-5	3	3	1578	1524
-4	3	3	2462	-2406
-3	3	3	1972	2009
-2	3	3	1769	-1939
-1	3	3	1114	1182
0	3	3	1415	1344
1	3	3	591	-652
2	3	3	615	634
3	3	3	1471	-1536
4	3	3	2538	2485
5	3	3	1648	-1625
6	3	3	3004	3074
7	3	3	1089	-1152
8	3	3	1586	1658
9	3	3	663	-646
10	3	3	658	703
-12	4	3	651	710
-11	4	3	525	-516
-9	4	3	1438	-1394
-7	4	3	2078	-2057
-6	4	3	1268	-1245
-5	4	3	1911	-1818
-4	4	3	1472	-1372
-3	4	3	613	541
-2	4	3	799	-866
1	4	3	1945	1900
2	4	3	424	537
3	4	3	3405	3182
4	4	3	1495	1489
5	4	3	1116	1029
6	4	3	558	431
8	4	3	308	-261
9	4	3	803	-804
10	4	3	337	241
11	4	3	1368	-1369
-6	5	3	386	354
-4	5	3	420	364
-3	5	3	426	418
-2	5	3	770	735
-1	5	3	403	379
0	5	3	684	713
1	5	3	785	797
4	5	3	1064	-1011
5	5	3	289	193
6	5	3	894	-901
-12	6	3	929	865
-9	6	3	787	-789
-8	6	3	551	-475
-7	6	3	1439	-1415
-6	6	3	1324	-1334
-5	6	3	1117	-1114
-4	6	3	1030	-1007
-3	6	3	790	-798
-2	6	3	837	-868
-1	6	3	1034	1054
1	6	3	2204	2140
2	6	3	411	385
3	6	3	2456	2319
4	6	3	964	1026
5	6	3	1065	1071
6	6	3	675	626
8	6	3	429	-470
9	6	3	868	-940
10	6	3	537	-491
11	6	3	1212	-1262
-12	7	3	991	-946
-11	7	3	682	-726
-10	7	3	530	-541

Observed and calculated structural factors for

[W(CO)$_2$(η^3-C$_3$H$_5$)bpma]PF$_6$

H	K	L	10FO	10FC	H	K	L	10FO	10FC	H	K	L	10FO	10FC	H	K	L	10FO	10FC	H	K	L	10FO	10FC
-9	7	3	1777	-1660	-11	9	3	1050	-1040	-9	11	3	433	-437	-3	13	3	844	-903	8	15	3	921	904
-7	7	3	1534	-1520	-10	9	3	1165	-1142	-8	11	3	539	-594	-2	13	3	1086	987	-6	16	3	374	430
-6	7	3	1728	1696	-9	9	3	774	-729	-7	11	3	571	551	0	13	3	453	453	-4	16	3	434	383
-5	7	3	1120	-1111	-8	9	3	1612	-1613	-6	11	3	436	-430	2	13	3	773	-794	-2	16	3	369	288
-4	7	3	3006	2907	-6	9	3	432	-422	-5	11	3	819	809	3	13	3	900	936	1	16	3	596	-614
-3	7	3	1014	891	-5	9	3	2054	1954	-3	11	3	825	847	4	13	3	1186	-1138	3	16	3	746	-734
-2	7	3	3213	3171	-4	9	3	531	502	-2	11	3	363	258	5	13	3	931	910	5	16	3	385	-297
-1	7	3	1176	1239	-3	9	3	3406	3312	-1	11	3	914	875	6	13	3	909	-885	-7	17	3	857	814
0	7	3	2226	2114	-2	9	3	1348	1423	0	11	3	891	848	7	13	3	856	791	-6	17	3	591	-550
1	7	3	2584	2374	-1	9	3	3195	3103	1	11	3	799	742	8	13	3	1015	-1018	-4	17	3	1441	-1429
3	7	3	356	357	0	9	3	1679	1652	3	11	3	546	-519	9	13	3	395	425	-3	17	3	481	-607
4	7	3	2176	-2162	1	9	3	1772	1702	5	11	3	762	-750	-9	14	3	867	898	-2	17	3	1769	-1793
5	7	3	394	290	2	9	3	1970	1791	7	11	3	755	-836	-7	14	3	1257	1206	-1	17	3	889	-956
6	7	3	3298	-3280	3	9	3	1462	-1430	9	11	3	759	-749	-6	14	3	708	750	0	17	3	1304	-1317
8	7	3	2129	-2144	4	9	3	1115	1042	-10	12	3	933	884	-5	14	3	1289	1291	1	17	3	722	-743
10	7	3	881	-890	5	9	3	2240	-2213	-8	12	3	1138	1128	-4	14	3	1222	1259	4	17	3	1286	1262
-12	8	3	702	-631	6	9	3	435	-488	-7	12	3	1016	923	-2	14	3	1121	1147	6	17	3	1695	1713
11	8	3	990	996	7	9	3	2050	-2107	-6	12	3	1440	1371	-1	14	3	1541	-1557	-4	18	3	673	-712
10	8	3	924	-871	8	9	3	600	-538	-5	12	3	1025	986	0	14	3	521	472	-2	18	3	894	-929
-9	8	3	921	866	9	9	3	1509	-1510	-4	12	3	520	536	1	14	3	2774	-2744	-1	18	3	756	837
-8	8	3	1097	-1110	-10	10	3	487	446	-3	12	3	965	911	3	14	3	2230	-2196	0	18	3	641	-632
-7	8	3	461	437	-8	10	3	720	735	-2	12	3	1110	-1110	4	14	3	714	-756	1	18	3	1382	1463
-6	8	3	423	-402	-7	10	3	937	880	-1	12	3	1252	1294	5	14	3	823	-829	2	18	3	577	-581
-3	8	3	744	-741	-6	10	3	929	982	0	12	3	2532	-2504	6	14	3	633	-602	3	18	3	1273	1272
-2	8	3	1750	1687	-5	10	3	1367	1241	2	12	3	1980	-1992	9	14	3	1127	1134	-5	19	3	920	-981
-1	8	3	1241	-1190	-4	10	3	873	849	3	12	3	610	-590	-9	15	3	653	660	-3	19	3	1310	-1369
0	8	3	3243	2956	-2	10	3	704	-695	4	12	3	1956	-1912	-7	15	3	528	550	-1	19	3	1149	-1178
1	8	3	1161	-1195	-1	10	3	526	567	6	12	3	488	-467	-4	15	3	1350	-1391	0	19	3	471	-514
2	8	3	2232	2157	0	10	3	1006	-1031	7	12	3	403	-370	-2	15	3	1671	-1655	2	19	3	528	-537
3	8	3	1483	-1487	2	10	3	1253	-1234	8	12	3	760	765	-1	15	3	1134	-1168	3	19	3	508	509
4	8	3	1242	1178	3	10	3	757	-740	10	12	3	1024	1015	0	15	3	535	-553	4	19	3	560	-479
7	8	3	582	565	4	10	3	1347	-1311	-8	13	3	595	601	1	15	3	865	-885	-3	20	3	672	-656
8	8	3	718	-724	8	10	3	816	790	-7	13	3	929	-865	4	15	3	755	789	0	20	3	1263	1231
9	8	3	695	678	10	10	3	634	590	-6	13	3	1271	1268	5	15	3	373	436	2	20	3	1360	1381
10	8	3	998	-1044	-11	11	3	493	-380	-5	13	3	1311	-1259	6	15	3	1280	1307	-5	0	4	3278	-3599
11	8	3	629	644	-10	11	3	520	-533	-4	13	3	1489	1442	7	15	3	375	455	-3	0	4	2355	-2339

Observed and calculated structural factors for

$[W(CO)_2(\eta^3\text{-}C_3H_5)bpma]PF_6$

H	K	L	10FO	10FC
-1	0	4	551	433
0	0	4	567	-488
1	0	4	3390	3576
2	0	4	390	354
3	0	4	3824	3879
5	0	4	3543	3566
6	0	4	948	-967
8	0	4	667	-733
9	0	4	499	-244
11	0	4	901	-935
-6	1	4	372	385
-5	1	4	690	-719
-4	1	4	1898	1940
-3	1	4	841	-784
-2	1	4	3060	3140
-1	1	4	776	-868
0	1	4	819	928
1	1	4	1826	-1914
2	1	4	361	354
3	1	4	1591	-1542
4	1	4	721	-777
6	1	4	1643	-1730
7	1	4	618	638
8	1	4	1319	-1314
9	1	4	690	721
10	1	4	969	-904
11	1	4	512	538
-8	2	4	806	-809
-7	2	4	617	-620
-6	2	4	2027	-2147
-5	2	4	1305	-1321
-4	2	4	2973	-2953
-3	2	4	1314	-1364
-2	2	4	1353	-1381
-1	2	4	590	-529
0	2	4	560	-638
2	2	4	760	676
3	2	4	1527	1402
4	2	4	863	931
5	2	4	3766	3935
6	2	4	1560	1541
7	2	4	743	705
9	2	4	313	-342
12	2	4	671	-722
-12	3	4	428	-665
-10	3	4	959	-1021
-9	3	4	1213	-1329
-8	3	4	1330	-1367
-7	3	4	1254	-1250
-6	3	4	525	-435
-5	3	4	314	-176
-4	3	4	1203	1257
-3	3	4	1998	2083
-2	3	4	2730	2946
-1	3	4	1940	1952
0	3	4	1750	1876
1	3	4	410	336
2	3	4	1428	1419
5	3	4	543	-513
6	3	4	2003	-2048
7	3	4	1106	-1177
8	3	4	756	-740
9	3	4	888	-889
10	3	4	764	-768
12	3	4	398	-398
-11	4	4	357	424
-10	4	4	625	-554
-9	4	4	709	704
-8	4	4	1126	-1095
-7	4	4	1204	1190
-6	4	4	1423	-1428
-5	4	4	370	476
-4	4	4	1333	-1332
-3	4	4	365	522
-2	4	4	918	-923
-1	4	4	444	-403
0	4	4	772	829
1	4	4	1261	-1202
-9	6	4	918	-879
-8	6	4	1271	1249
-7	6	4	1095	-1093
-6	6	4	2419	2344
-5	6	4	337	-405
-4	6	4	2542	2505
-2	6	4	929	902
-1	6	4	1033	997
0	6	4	909	-965
2	6	4	2924	-2796
4	6	4	2933	-2951
5	6	4	323	310
6	6	4	1745	-1753
8	6	4	720	-634
9	6	4	690	683
-12	7	4	673	-602
-10	7	4	1045	-999
-8	7	4	785	-753
-4	7	4	1342	1343
-3	7	4	707	-647
-2	7	4	2234	2120
-1	7	4	338	303
0	7	4	1886	1809
1	7	4	470	405
2	7	4	645	696
3	7	4	291	-180
4	7	4	595	-557
6	7	4	1101	-1114
7	7	4	826	-876
8	7	4	453	379
9	7	4	562	-609
10	7	4	506	494
11	7	4	481	-388
-12	8	4	618	-658
-11	8	4	355	308
-9	8	4	806	880
-8	8	4	352	376
-6	8	4	294	-241
-5	8	4	1347	-1263
-4	8	4	2094	-1993
-3	8	4	1527	-1458
-2	8	4	2324	-2237
-1	8	4	748	-769
0	8	4	461	-452
1	8	4	450	-464
2	8	4	377	378
4	8	4	728	730
5	8	4	432	398
6	8	4	635	636
-11	9	4	615	594
-10	9	4	341	-314
-9	9	4	487	449
-7	9	4	387	-311
-5	9	4	998	-964
-4	9	4	769	-711
-3	9	4	1149	-1138
-1	9	4	1337	-1376
0	9	4	1300	1290
1	9	4	1822	-1665
2	9	4	489	508
3	9	4	628	-666
4	9	4	375	326
5	9	4	304	318
7	9	4	792	787
8	9	4	702	-682
9	9	4	500	519

Observed and calculated structural factors for

$[W(CO)_2(\eta^3\text{-}C_3H_5)bpma]PF_6$

H	K	L	10FO	10FC
10	9	4	532	-521
10	10	4	729	-741
-9	10	4	961	995
-8	10	4	651	-645
-7	10	4	2095	2029
-5	10	4	2665	2555
-4	10	4	510	505
-3	10	4	1830	1940
-2	10	4	542	495
1	10	4	2670	-2591
2	10	4	324	-303
3	10	4	2723	-2760
5	10	4	2523	-2451
7	10	4	1417	-1418
8	10	4	716	638
10	10	4	381	472
11	11	4	390	-232
10	11	4	1400	1378
-9	11	4	371	395
-8	11	4	1182	1157
-7	11	4	648	674
-5	11	4	476	458
-4	11	4	1658	-1622
-3	11	4	559	568
-2	11	4	3033	-2960
0	11	4	2615	-2493
2	11	4	1765	-1714
3	11	4	786	735
5	11	4	392	367
6	11	4	1786	1743
8	11	4	1563	1569
10	11	4	1161	1122
10	12	4	350	252
-9	12	4	451	-410
-8	12	4	850	816
-6	12	4	1531	1468
-4	12	4	1425	1431
-2	12	4	558	492
0	12	4	418	-398
2	12	4	1477	-1423
3	12	4	748	686
4	12	4	1008	-993
5	12	4	366	398
6	12	4	726	-748
7	12	4	396	337
-10	13	4	615	510
-9	13	4	1137	1113
-8	13	4	925	900
-7	13	4	660	647
-6	13	4	477	376
-4	13	4	907	-867
-3	13	4	971	-996
-2	13	4	1446	-1410
-1	13	4	2044	-2031
0	13	4	1514	-1524
1	13	4	1753	-1749
2	13	4	1085	-1020
5	13	4	628	740
6	13	4	777	751
7	13	4	1177	1214
8	13	4	593	630
9	13	4	805	962
-9	14	4	623	-562
-6	14	4	504	484
-7	14	4	839	-898
-5	14	4	645	-676
-4	14	4	392	-400
-3	14	4	911	-914
0	14	4	499	-538
1	14	4	857	851
3	14	4	1080	1086
4	14	4	553	579
5	15	4	1061	1093
7	14	4	775	819
9	14	4	374	-316
-9	15	4	745	751
-7	15	4	826	814
-5	15	4	838	-898
-3	15	4	1674	-1709
-1	15	4	1925	-1965
1	15	4	1649	-1603
2	15	4	362	299
3	15	4	581	-569
4	15	4	492	443
5	15	4	471	502
7	15	4	896	889
-8	16	4	1352	-1241
-6	16	4	2156	-2117
-4	16	4	1841	-1816
-3	16	4	465	-439
0	16	4	772	787
2	16	4	1653	1644
4	16	4	2064	2074
6	16	4	1185	1231
7	16	4	430	-348
-6	17	4	354	-114
-5	17	4	480	384
-4	17	4	485	-493
-3	17	4	666	676
-2	17	4	767	-768
-1	17	4	470	516
0	17	4	849	-869
1	17	4	421	482
2	17	4	580	-582
-6	18	4	713	-781
-5	18	4	1275	-1308
-4	18	4	907	-899
-3	18	4	973	-1045
-2	18	4	497	-543
0	18	4	371	287
1	18	4	788	827
2	18	4	779	751
3	18	4	1021	1071
4	18	4	723	725
5	18	4	930	911
-3	19	4	828	823
-1	19	4	1169	1195
0	19	4	456	457
1	19	4	916	903
2	19	4	397	336
1	20	4	642	604
-8	1	5	465	-542
-7	1	5	1685	-1866
-5	1	5	534	-556
-4	1	5	810	847
-3	1	5	330	331
-2	1	5	394	430
-1	1	5	3361	3542
1	1	5	3150	3307
2	1	5	1032	1000
3	1	5	3108	3060
4	1	5	360	317
5	1	5	1273	1359
6	1	5	1096	-1156
7	1	5	821	-866
8	1	5	588	-576
9	1	5	935	-979
10	1	5	475	-444
11	1	5	921	-930
-9	2	5	345	296
-8	2	5	323	289
-7	2	5	330	-324
-6	2	5	1603	1656
-5	2	5	615	-667
-4	2	5	2825	3020
-2	2	5	2702	2824
-1	2	5	1443	-1482
0	2	5	937	926
1	2	5	1344	-1362
2	2	5	521	-561
3	2	5	959	-944
4	2	5	1697	-1637
6	2	5	1876	-1922
8	2	5	1430	-1439
9	2	5	1172	1271
10	2	5	577	-581
11	2	5	875	860
-12	3	5	556	-699
-11	3	5	518	570
-10	3	5	1488	-1591
-9	3	5	458	572
-8	3	5	2000	-2072
-6	3	5	1789	-1838
-5	3	5	434	411
-2	3	5	1216	1252
-1	3	5	300	-358
0	3	5	1944	2020
1	3	5	608	-663
2	3	5	2232	2348
3	3	5	1670	-1662
4	3	5	1083	1014
5	3	5	2112	-2133
6	3	5	545	-561
7	3	5	1213	-1258
8	3	5	469	-486
9	3	5	318	-262
10	3	5	972	-997
-11	4	5	1367	-1383
-8	4	5	354	340
-7	4	5	1641	1633

Observed and calculated structural factors for

$[W(CO)_2(\eta^3\text{-}C_3H_5)bpma]PF_6$

H	K	L	10FO	10FC
-6	4	5	868	871
-5	4	5	3613	3717
-4	4	5	878	970
-3	4	5	4094	4129
-1	4	5	1959	1973
0	4	5	831	-842
1	4	5	735	712
2	4	5	1488	1402
3	4	5	2538	2469
5	4	5	2658	2707
7	4	5	1834	1861
8	4	5	779	837
9	4	5	345	-362
10	4	5	1047	1035
12	5	5	331	297
10	5	5	449	447
-8	5	5	750	701
-6	5	5	423	-341
-5	5	5	722	-765
-3	5	5	1165	-1220
-2	5	5	480	-378
0	5	5	369	-473
1	5	5	672	-682
6	5	5	914	897
7	5	5	715	727
8	5	5	465	452
11	6	5	848	-782
-7	6	5	685	681
-5	6	5	1833	1832
-4	6	5	890	874
-3	6	5	2162	2261
-1	6	5	984	962
0	6	5	561	-629
2	6	5	1297	-1280
3	6	5	1321	-1336
4	6	5	1037	-1028
H	K	L	10FO	10FC
5	6	5	1847	-1862
6	6	5	472	-460
7	6	5	1415	-1425
9	6	5	338	-375
10	6	5	642	563
-12	7	5	758	744
-10	7	5	1213	1192
-8	7	5	2309	2317
-7	7	5	362	-363
-6	7	5	1936	1899
-3	7	5	526	-539
-2	7	5	1855	-1920
-1	7	5	367	-375
0	7	5	3106	-3130
2	7	5	2473	-2451
3	7	5	743	751
4	7	5	1787	-1762
5	7	5	723	757
6	7	5	426	344
7	7	5	1275	1333
8	7	5	650	705
9	7	5	719	755
10	7	5	977	996
-12	8	5	709	-703
-11	8	5	504	505
-10	8	5	560	-575
-8	8	5	440	382
-7	8	5	626	-586
-6	8	5	1322	1310
-5	8	5	1374	-1275
-4	8	5	1804	1776
-3	8	5	1523	-1520
-2	8	5	1303	1449
-1	8	5	1140	-1217
0	8	5	1100	1052
1	8	5	990	-950
H	K	L	10FO	10FC
2	8	5	324	297
3	8	5	512	-459
4	8	5	1023	-1010
5	8	5	1053	1031
6	8	5	1495	-1465
7	8	5	1192	1165
8	8	5	1063	-1099
9	8	5	879	794
10	8	5	664	-673
-11	9	5	1116	1140
-9	9	5	2091	2020
-8	9	5	347	329
-7	9	5	1854	1862
-5	9	5	1010	1027
-4	9	5	483	-465
-3	9	5	834	-833
-2	9	5	1086	-1036
-1	9	5	2313	-2346
0	9	5	1487	-1456
1	9	5	3403	-3345
3	9	5	2297	-2280
5	9	5	1113	-1075
6	9	5	1000	956
7	9	5	375	435
8	9	5	555	533
9	9	5	1151	1168
-10	10	5	584	563
-6	10	5	729	-692
-4	10	5	1055	-1102
-3	10	5	396	-382
-2	10	5	1298	-1308
0	10	5	363	-324
1	10	5	902	849
2	10	5	462	416
3	10	5	661	601
4	10	5	1173	1108
H	K	L	10FO	10FC
6	10	5	739	794
8	10	5	537	494
-9	11	5	867	845
-8	11	5	443	336
-7	11	5	1051	1050
-4	11	5	594	-570
-3	11	5	793	-843
-2	11	5	682	-662
-1	11	5	1912	-1945
0	11	5	676	-644
1	11	5	1566	-1514
3	11	5	634	-600
4	11	5	320	397
6	11	5	793	963
7	11	5	517	514
8	11	5	857	840
9	11	5	580	612
-10	12	5	855	817
-6	12	5	2139	-2062
-5	12	5	531	-547
-4	12	5	2568	-2543
-3	12	5	479	-447
-2	12	5	1901	-1850
-1	12	5	667	636
0	12	5	697	-742
1	12	5	1358	1326
2	12	5	1309	1227
3	12	5	1026	1040
4	12	5	1956	1910
5	12	5	547	520
6	12	5	1214	1218
8	12	5	542	587
9	12	5	861	-868
-10	13	5	621	589
-9	13	5	1137	-1125
-8	13	5	843	830
H	K	L	10FO	10FC
-7	13	5	927	-924
-6	13	5	1011	956
-5	13	5	341	-475
-4	13	5	879	915
-3	13	5	607	615
-1	13	5	1510	1555
0	13	5	1125	-1102
1	13	5	1319	1362
2	13	5	1183	-1157
3	13	5	1408	1402
4	13	5	1243	-1250
5	13	5	780	842
6	13	5	658	-635
7	14	5	859	-812
-5	14	5	1541	-1571
-3	14	5	1804	-1812
-1	14	5	1596	-1529
0	14	5	382	473
1	14	5	402	-383
2	14	5	866	826
3	14	5	1246	1262
4	14	5	408	429
5	14	5	1482	1464
7	14	5	1215	1253
8	14	5	486	-487
9	15	5	1137	-1066
-6	15	5	1026	-1004
-3	15	5	422	412
-2	15	5	749	704
-1	15	5	740	810
0	15	5	1128	1155
1	15	5	338	327
2	15	5	1361	1408
6	15	5	426	-447
7	15	5	510	-547
-2	16	5	358	211

Observed and calculated structural factors for

$[W(CO)_2(\eta^3\text{-}C_3H_5)bpma]PF_6$

H	K	L	10FO	10FC
2	16	5	464	397
3	16	5	358	389
-6	17	5	1179	-1144
-3	17	5	398	301
-2	17	5	985	1031
-1	17	5	659	627
0	17	5	1729	1781
1	17	5	420	497
2	17	5	1733	1743
4	17	5	791	749
-5	17	5	634	-683
-5	18	5	1094	1084
-4	18	5	664	-568
-3	18	5	1337	1390
-2	18	5	671	-670
-1	18	5	791	824
0	18	5	503	-500
1	18	5	398	344
3	18	5	524	-526
-3	19	5	380	368
-2	19	5	427	550
-1	19	5	1333	1377
0	19	5	375	377
1	19	5	1552	1583
3	19	5	1026	1119
-8	0	6	558	643
-7	0	6	365	-337
-6	0	6	2380	2437
-5	0	6	1484	1522
-4	0	6	2132	2163
-3	0	6	4436	4519
-2	0	6	587	-631
-1	0	6	3897	3979
0	0	6	2705	-2727
1	0	6	2057	2104
2	0	6	2594	-2613
3	0	6	3600	-3615
4	0	6	1932	-1933
5	0	6	1346	-1361
7	0	6	2184	-2214
9	0	6	953	-1040
10	0	6	882	-896
11	0	6	429	-466
-9	1	6	340	409
-8	1	6	1179	1266
-6	1	6	2005	2184
-5	1	6	920	-912
-4	1	6	1777	1959
-3	1	6	1671	-1767
-2	1	6	1304	1396
-1	1	6	2964	-2071
0	1	6	362	-359
1	1	6	794	-858
2	1	6	1715	-1761
3	1	6	373	399
4	1	6	1335	-1402
5	1	6	807	838
6	1	6	492	-485
7	1	6	1669	1681
8	1	6	442	-385
9	1	6	1030	1029
10	2	6	892	-1037
11	2	6	349	423
-12	3	6	504	571
-11	3	6	731	742
-10	3	6	1172	1240
-9	3	6	1464	1477
-8	3	6	1853	1875
-7	3	6	2482	2643
-6	3	6	305	279
-5	3	6	873	979
-4	3	6	504	-534
-3	3	6	1562	-1499
-2	3	6	921	-998
-1	3	6	998	-1030
0	3	6	489	-503
1	3	6	709	-792
2	3	6	622	-741
3	3	6	334	-406
4	3	6	616	637
5	3	6	591	596
6	3	6	307	390
7	3	6	845	917
8	3	6	1571	1589
-8	4	6	633	664
-7	4	6	1412	1432
-6	4	6	999	978
-5	4	6	1098	1082
-4	4	6	1333	-1422
-3	4	6	2325	-2311
-2	4	6	1902	-1944
-1	4	6	821	-818
0	4	6	577	-482
1	4	6	1112	1189
2	4	6	439	493
3	4	6	960	948
4	4	6	626	612
5	4	6	569	526
6	4	6	590	-584
7	4	6	716	702
8	4	6	700	-746
9	4	6	805	892
-12	5	6	834	-816
-11	5	6	1059	1078
-10	5	6	284	339
-9	5	6	543	517
-8	5	6	1463	1412
-7	5	6	323	-301
-6	5	6	1770	1810
-5	5	6	1089	-1104
-4	5	6	2255	2285
-3	5	6	829	-934
-2	5	6	1419	1485
-1	5	6	1149	-1162
0	5	6	473	-557
1	5	6	343	-369
2	5	6	323	318
3	5	6	798	-733
4	5	6	579	596
5	5	6	1268	1239
6	5	6	429	399
7	5	6	2164	2226
8	5	6	488	-562
9	5	6	2469	2593
10	5	6	2469	-2521
11	5	6	973	1090
12	5	6	2983	-2978
13	5	6	499	-525
14	5	6	2239	-2194
15	5	6	2460	-2474
16	5	6	1022	-1045
17	5	6	2424	-2428
18	5	6	869	823
19	5	6	1951	-1953
20	5	6	1804	1818
21	5	6	1534	1534
22	5	6	1207	1155
23	6	6	883	876
24	6	6	1351	1311
25	6	6	722	-674
26	6	6	1242	1273
27	6	6	1237	-1207
28	6	6	1068	-1134
-11	6	6	1466	-1503
-10	6	6	2469	-2515
-9	6	6	572	666
-8	6	6	2090	-2127
-7	6	6	1406	1460
-6	6	6	1757	-1744
-5	6	6	1322	1359
-4	6	6	849	849
-3	6	6	507	522
-2	6	6	549	586
-1	6	6	787	-842
0	6	6	499	536
1	6	6	367	-336
2	6	6	463	453
3	6	6	489	463
4	6	6	348	375
5	6	6	1355	1309
6	6	6	675	681
7	6	6	1839	1826
8	6	6	1254	1327
-7	7	6	1418	-1426
-6	7	6	914	-938
-5	7	6	625	-665
-4	7	6	345	-419
-3	7	6	1041	-1048
-2	7	6	805	-745
-1	7	6	392	400
0	7	6	1190	1182
1	7	6	1047	1025
2	7	6	1020	980
3	7	6	943	971
4	7	6	746	797
5	8	6	634	567
6	8	6	1143	-1075
7	8	6	1635	-1638
8	8	6	2200	-2230

Observed and calculated structural factors for

[W(CO)$_2$(η^3-C$_3$H$_5$)bpma]PF$_6$

H	K	L	10FO	10FC	H	K	L	10FO	10FC	H	K	L	10FO	10FC	H	K	L	10FO	10FC	H	K	L	10FO	10FC
-3	8	6	2145	-2138	2	10	6	1975	1983	5	12	6	500	490	1	15	6	1421	1402	2	19	6	421	-474
-2	8	6	1707	-1773	3	10	6	536	-519	-9	13	6	711	-755	2	15	6	645	684	-10	1	7	751	863
-1	8	6	1222	-1220	4	10	6	1802	1808	-8	13	6	1001	-999	3	15	6	1198	1222	-8	1	7	1687	1770
0	8	6	324	-331	5	10	6	361	483	-7	13	6	972	-1008	5	15	6	737	791	-7	1	7	1032	1031
3	8	6	1287	1269	6	10	6	648	689	-6	13	6	748	-826	6	15	6	909	-889	-6	1	7	1081	1118
4	8	6	1262	1249	7	10	6	1039	1032	-5	13	6	730	-785	-7	16	6	780	769	-5	1	7	1950	2000
5	8	6	1834	1821	9	10	6	752	774	-2	13	6	539	536	-6	16	6	415	425	-3	1	7	1086	1106
6	8	6	1425	1403	-10	11	6	353	-379	-1	13	6	1330	1345	-5	16	6	1249	1192	-2	1	7	1097	-1156
7	8	6	1064	1126	-9	11	6	602	-575	0	13	6	1365	1381	-4	16	6	1601	1568	0	1	7	2767	-2781
8	8	6	559	616	-8	11	6	1712	-1676	1	13	6	1203	1206	-3	16	6	991	963	1	1	7	683	-681
-9	9	6	521	-554	-6	11	6	1835	-1825	2	13	6	1462	1425	-2	16	6	2139	2180	2	1	7	2279	-2406
-7	9	6	1279	-1285	-5	11	6	700	635	3	13	6	959	983	0	16	6	1540	1574	3	1	7	471	-476
-6	9	6	589	535	-4	11	6	1471	-1450	4	13	6	491	418	1	16	6	858	-899	4	1	7	667	-697
-5	9	6	1200	-1182	-3	11	6	1198	1187	5	13	6	490	414	2	16	6	529	519	5	1	7	767	-872
-4	9	6	721	730	-2	11	6	647	-609	6	13	6	458	-371	3	16	6	1575	-1621	8	1	7	931	999
-3	9	6	967	-970	-1	11	6	1967	1932	7	13	6	439	-450	4	16	6	590	-663	10	1	7	1465	1483
-2	9	6	673	699	0	11	6	908	850	8	13	6	684	-642	5	16	6	1318	-1341	-10	2	7	1057	1055
0	9	6	605	571	1	11	6	1311	1280	-9	14	6	459	-467	6	16	6	713	-720	-9	2	7	766	-826
1	9	6	479	410	2	11	6	1624	1615	-6	14	6	550	470	-6	17	6	462	-521	-8	2	7	1336	1353
3	9	6	676	752	3	11	6	386	-356	-5	14	6	532	508	-5	17	6	873	866	-7	2	7	1798	-1910
4	9	6	629	-579	4	11	6	1350	1402	-3	14	6	920	874	-4	17	6	755	-777	-6	2	7	407	426
5	9	6	869	915	5	11	6	625	-610	-2	14	6	532	-509	-3	17	6	399	461	-5	2	7	2547	-2689
6	9	6	1097	-1054	6	11	6	1007	1042	-1	14	6	677	685	-2	17	6	621	-604	-3	2	7	2792	-2852
8	9	6	896	-917	7	11	6	1331	-1391	0	14	6	603	-605	3	17	6	621	-649	-2	2	7	757	-788
9	9	6	337	151	9	11	6	1121	-1100	1	14	6	459	544	5	17	6	578	-598	-1	2	7	1357	-1294
10	9	6	634	-586	-10	12	6	702	661	2	14	6	636	-631	-5	18	6	558	552	0	2	7	1385	-1380
-11	10	6	1385	1351	-9	12	6	333	-239	4	14	6	804	-782	-4	18	6	947	900	1	2	7	778	820
-9	10	6	1185	1188	-8	12	6	555	477	6	14	6	368	-482	-3	18	6	943	1032	2	2	7	1033	-1013
-8	10	6	776	-762	-7	12	6	536	-499	7	14	6	513	-388	-2	18	6	752	806	3	2	7	2274	2254
-6	10	6	1231	-1240	-5	12	6	730	-681	-7	15	6	1294	-1306	-1	18	6	739	801	4	2	7	612	-687
-5	10	6	690	-689	-4	12	6	642	-634	-5	15	6	1333	-1401	2	18	6	548	-547	5	2	7	2488	2471
-4	10	6	566	-555	-2	12	6	1189	-1155	-4	15	6	924	866	3	18	6	657	-665	6	2	7	534	-503
-3	10	6	1926	-1973	0	12	6	1310	-1337	-3	15	6	480	-568	4	18	6	907	-893	7	2	7	1593	1642
-1	10	6	2142	-2256	1	12	6	595	631	-2	15	6	1280	1265	-2	19	6	631	-577	9	2	7	439	397
0	10	6	1350	1297	2	12	6	862	-845	-1	15	6	487	541	0	19	6	642	-649	-11	3	7	992	1005
1	10	6	1056	-1104	3	12	6	768	795	0	15	6	1338	1380	1	19	6	645	-629	-10	3	7	850	-929

Observed and calculated structural factors for

$[W(CO)_2(\eta^3\text{-}C_3H_5)bpma]PF_6$

H	K	L	10FO	10FC	H	K	L	10FO	10FC	H	K	L	10FO	10FC	H	K	L	10FO	10FC
-9	3	7	1040	1012	8	4	7	1418	1458	-8	7	7	827	-843	-7	9	7	900	-788	5	11	7	647	671
-7	3	7	781	760	-10	5	7	329	496	-7	7	7	1433	-1458	-6	9	7	1197	-1214	-10	12	7	1193	-1106
-6	3	7	1395	1380	-8	5	7	414	-405	-6	7	7	1254	-1278	-5	9	7	1788	-1782	-8	12	7	1186	-1160
-5	3	7	313	260	-7	5	7	545	-494	-5	7	7	428	-395	-3	9	7	1270	-1293	-7	12	7	567	510
-4	3	7	2062	2174	-6	5	7	505	-597	-4	7	7	1704	-1801	-2	9	7	1387	1452	-6	12	7	531	-572
-3	3	7	1257	-1247	-5	5	7	807	-812	-3	7	7	931	977	0	9	7	2385	2425	-5	12	7	1338	1390
-2	3	7	1735	1035	-4	5	7	477	-499	-2	7	7	1601	-1742	2	9	7	2168	2169	-3	12	7	2247	2336
-1	3	7	2260	-2357	-3	5	7	315	187	-1	7	7	2059	2124	3	9	7	1011	992	-2	12	7	1201	1192
0	3	7	1486	1479	-1	5	7	601	703	1	7	7	3459	3464	4	9	7	1106	1175	-1	12	7	1392	1460
1	3	7	2414	-2466	0	5	7	505	525	2	7	7	665	672	5	9	7	833	777	0	12	7	1596	1636
3	3	7	2091	-2105	1	5	7	1113	1044	3	7	7	1966	1937	8	9	7	1316	-1257	2	12	7	791	810
4	3	7	588	-612	3	5	7	602	714	4	7	7	949	942	-10	10	7	684	-615	3	12	7	1149	-1144
5	3	7	337	-323	4	5	7	754	727	5	7	7	497	363	-8	10	7	510	-424	5	12	7	1844	-1878
6	3	7	915	-870	5	5	7	979	980	6	7	7	818	809	-6	10	7	363	462	7	12	7	1634	-1630
7	3	7	1008	1027	6	5	7	663	648	7	7	7	977	-1003	-5	10	7	925	932	8	12	7	449	-392
8	3	7	539	-514	9	5	7	475	-407	8	7	7	601	601	-3	10	7	1277	1274	-9	13	7	601	-559
9	3	7	1330	1372	-12	6	7	507	521	9	7	7	1347	-1287	-2	10	7	658	743	-8	13	7	492	514
10	3	7	453	-391	-11	6	7	709	783	-9	8	7	829	-837	-1	10	7	460	493	-5	13	7	591	660
-12	4	7	448	432	-10	6	7	516	514	-8	8	7	963	927	0	10	7	546	564	-4	13	7	892	-924
-11	4	7	995	1078	-9	6	7	608	607	-7	8	7	1437	-1392	3	10	7	503	-571	-3	13	7	1122	1182
-10	4	7	620	655	-7	6	7	363	401	-6	8	7	1694	1654	4	10	7	359	-202	-2	13	7	1222	-1182
-9	4	7	1324	1304	-6	6	7	1572	-1573	-5	8	7	1856	-1883	5	10	7	1154	-1117	-1	13	7	989	1060
-7	4	7	1758	1832	-4	6	7	1846	-1843	-4	8	7	864	965	7	10	7	831	-794	0	13	7	1501	-1515
-6	4	7	1648	-1671	-3	6	7	487	-496	-3	8	7	1339	-1355	-10	11	7	417	-386	1	13	7	1011	1006
-4	4	7	2224	-2403	-2	6	7	1530	-1560	0	8	7	666	-630	-8	11	7	770	-767	2	13	7	1038	-1064
-3	4	7	1603	-1671	-1	6	7	1528	-1529	1	8	7	628	599	-7	11	7	899	-868	3	13	7	383	349
-2	4	7	2012	-2080	0	6	7	643	-655	2	8	7	1099	-1182	-6	11	7	604	-632	5	13	7	537	-505
-1	4	7	1154	-1110	1	6	7	874	-813	3	8	7	1126	1118	-5	11	7	1261	-1193	7	13	7	616	-591
0	4	7	838	-836	2	6	7	674	663	4	8	7	1383	-1329	-4	11	7	529	-487	-7	14	7	993	-995
1	4	7	1101	-1086	3	6	7	479	489	5	8	7	1674	1684	-3	11	7	926	-956	-6	14	7	1326	1319
2	4	7	837	866	4	6	7	1942	1966	6	8	7	702	-691	-2	11	7	539	552	-5	14	7	983	-502
3	4	7	659	-697	5	6	7	633	579	7	8	7	1136	1092	0	11	7	1015	1051	-4	14	7	1483	1443
4	4	7	2298	2359	6	6	7	1245	1297	9	8	7	347	368	1	11	7	713	703	-3	14	7	527	578
5	4	7	865	877	8	6	7	916	866	-11	9	7	393	335	2	11	7	1210	1170	-2	14	7	1132	1109
6	4	7	2239	2208	-11	7	7	756	-740	-10	9	7	785	-772	3	11	7	988	1026	-1	14	7	819	820
7	4	7	802	817	-9	7	7	1285	-1316	-8	9	7	1739	-1751	4	11	7	941	953	1	14	7	549	544

Observed and calculated structural factors for

$[W(CO)_2(\eta^3\text{-}C_3H_5)bpma]PF_6$

Observed and calculated structural factors for

$[W(CO)_2(\eta^3\text{-}C_3H_5)bpma]PF_6$

H	K	L	10FO	10FC
-8	8	8	916	-887
-7	8	8	730	-756
-4	8	8	535	529
-3	8	8	1543	1564
-2	8	8	1376	1402
-1	8	8	1828	1385
0	8	8	1335	1310
1	8	8	1021	957
2	8	8	407	317
3	8	8	310	195
5	8	8	937	-364
6	8	8	501	-430
7	8	8	973	-992
8	8	8	604	-593
9	8	8	681	-716
-10	9	8	369	299
-9	9	8	503	-573
-8	9	8	627	624
-7	9	8	752	-733
-6	9	8	824	830
-4	9	8	985	1033
-1	9	8	343	313
0	9	8	920	-907
1	9	8	578	523
2	9	8	1073	-1072
3	9	8	627	650
4	9	8	1023	-1002
6	9	8	822	-819
-10	10	8	1431	-1408
-9	10	8	924	-888
-8	10	8	580	-556
-7	10	8	818	-879
-6	10	8	690	744
-5	10	8	353	-312
-4	10	8	1887	1921
-2	10	8	2954	2977
0	10	8	2421	2475
2	10	8	630	-631
4	10	8	887	-900
6	10	8	1579	-1590
8	10	8	1458	-1491
10	11	8	585	-606
9	11	8	1059	1075
7	11	8	1728	1752
5	11	8	1930	2032
4	11	8	398	445
3	11	8	531	479
2	11	8	733	736
1	11	8	978	-962
1	11	8	2197	-2181
3	11	8	2395	-2427
5	11	8	1568	-1607
6	12	8	494	-494
5	12	8	522	582
3	12	8	1106	1144
1	12	8	1499	1457
0	12	8	413	-462
1	12	8	573	549
5	12	8	602	-606
7	12	8	1005	-977
8	13	8	1006	934
7	13	8	895	935
6	13	8	1125	1129
5	13	8	1213	1202
4	13	8	1108	1067
3	13	8	614	626
1	13	8	685	-690
0	13	8	1146	-1204
1	13	8	1061	-1080
2	13	8	1357	-1390
3	13	8	1150	-1156
4	13	8	963	-966
5	13	8	803	-845
6	13	8	410	-412
7	14	8	412	471
6	14	8	409	-462
4	14	8	821	-809
2	14	8	1449	-1439
0	14	8	594	-660
6	14	8	712	699
6	15	8	1295	1323
4	15	8	772	732
3	15	8	392	307
0	15	8	1156	-1144
1	15	8	400	379
2	15	8	1602	-1582
4	15	8	1374	-1427
6	16	8	464	477
5	16	8	1122	-1091
4	16	8	471	424
3	16	8	1815	-1874
2	16	8	369	-217
1	16	8	1558	-1601
0	16	8	305	-148
1	16	8	1308	-1355
1	17	8	504	-557
1	17	8	674	-776
2	17	8	510	482
3	18	8	630	-680
2	18	8	1144	-1224
1	18	8	721	-761
0	18	8	884	-945
1	18	8	462	-477
-9	1	9	354	350
-8	1	9	819	-757
-7	1	9	321	-338
-6	1	9	1911	-1918
-5	1	9	1415	-1419
-4	1	9	2653	-2652
-3	1	9	370	454
-2	1	9	1624	-1650
-1	1	9	967	981
2	1	9	1673	1779
3	1	9	1383	1444
4	1	9	1750	1740
5	1	9	505	488
6	1	9	1569	1587
7	1	9	466	-439
8	1	9	465	479
9	1	9	631	-647
10	1	9	397	-243
-11	2	9	1038	-1110
-9	2	9	1591	-1644
-8	2	9	472	538
-7	2	9	1829	-1760
-5	2	9	331	-170
-4	2	9	503	-552
-3	2	9	977	985
-2	2	9	379	343
-1	2	9	2109	2200
1	2	9	2582	2604
2	2	9	874	-867
3	2	9	1724	1701
4	2	9	1557	-1593
6	2	9	1148	-1182
7	2	9	870	-915
8	2	9	386	-463
9	2	9	1236	-1282
-8	3	9	564	544
-7	3	9	1236	-1267
-6	3	9	1046	986
-5	3	9	2284	-2317
-4	3	9	1101	1086
-3	3	9	1974	-1996
-2	3	9	912	953
-1	3	9	1424	-1448
0	3	9	316	330
3	3	9	922	962
4	3	9	1132	-1162
5	3	9	1374	1392
6	3	9	1011	-1036
7	3	9	1126	1114
8	3	9	918	-980
9	3	9	571	582
-10	4	9	1249	-1252
-8	4	9	1178	-1239
-6	4	9	643	-630
-5	4	9	544	482
-3	4	9	896	942
-2	4	9	2382	2440
-1	4	9	1199	1228
0	4	9	2506	2513
1	4	9	403	420
2	4	9	1835	1910
3	4	9	826	-802
4	4	9	631	589
5	4	9	1041	-1143
6	4	9	363	-281
7	4	9	720	-607
8	4	9	1182	-1196
-5	5	9	773	822
0	5	9	618	-590
1	5	9	799	-732
2	5	9	307	-323
3	5	9	470	-489
-10	6	9	1099	-1075
-9	6	9	510	-486
-8	6	9	1363	-1430
-7	6	9	496	-522
-6	6	9	641	-645

Observed and calculated structural factors for

$[W(CO)_2(\eta^3\text{-}C_3H_5)bpma]PF_6$

H	K	L	10FO	10FC
-5	6	9	643	638
-4	6	9	663	664
-3	6	9	905	934
-2	6	9	2002	1968
-1	6	9	778	748
0	6	9	1927	1972
1	6	9	624	593
2	6	9	1567	1597
5	6	9	970	-927
6	6	9	712	-694
7	6	9	871	-885
8	6	9	792	-807
9	6	9	523	-503
-11	7	9	364	-464
-10	7	9	347	-386
-9	7	9	344	196
-7	7	9	1753	1801
-5	7	9	2970	2977
-3	7	9	1834	1875
-2	7	9	528	-563
-1	7	9	1097	1117
0	7	9	724	-757
1	7	9	668	-729
2	7	9	738	-779
3	7	9	2012	-2034
4	7	9	437	-336
5	7	9	1864	-1874
6	7	9	367	377
7	7	9	1066	-1069
8	7	9	959	888
-11	8	9	761	-830
-10	8	9	578	585
-9	8	9	1176	-1164
-8	8	9	680	673
-7	8	9	662	-724
-6	8	9	486	594
-5	8	9	520	-541
-3	8	9	361	346
-2	8	9	745	-791
-1	8	9	1598	1573
0	8	9	1413	-1413
1	8	9	1626	1775
2	8	9	1332	-1388
3	8	9	1147	1120
4	8	9	911	-845
5	8	9	562	505
-8	9	9	1042	1055
-7	9	9	600	564
-6	9	9	1732	1771
-5	9	9	714	742
-4	9	9	2534	2516
-2	9	9	2030	2102
-1	9	9	676	-772
0	9	9	363	-395
1	9	9	1187	-1194
2	9	9	1704	-1723
3	9	9	964	-893
4	9	9	1970	-1971
5	9	9	589	-514
6	9	9	1646	-1702
8	9	9	711	-676
-9	10	9	626	632
-8	10	9	393	345
-7	10	9	711	659
-6	10	9	339	127
-3	10	9	847	-849
-2	10	9	793	-757
-1	10	9	1084	-1046
0	10	9	318	-310
1	10	9	1174	-1097
6	10	9	605	603
7	10	9	586	607
-8	10	9	352	438
-6	11	9	515	548
-5	11	9	719	763
-4	11	9	361	294
-3	11	9	1065	1059
-2	11	9	822	780
-1	11	9	429	-325
0	11	9	439	-403
2	11	9	372	-391
4	11	9	767	-775
6	11	9	803	-765
-7	12	9	1291	1267
-7	12	9	1266	1271
-3	12	9	1154	-1122
-2	12	9	378	-371
-1	12	9	1676	-1749
0	12	9	306	239
1	12	9	1600	-1609
2	12	9	507	448
3	12	9	1109	-1022
4	12	9	492	532
6	12	9	819	841
7	12	9	696	714
-8	13	9	470	-468
-7	13	9	450	528
-6	13	9	670	-734
-5	13	9	755	796
-4	13	9	986	-1063
-3	13	9	1375	1360
-2	13	9	581	-630
-1	13	9	1039	1071
2	13	9	393	363
3	13	9	521	-514
4	13	9	578	540
5	13	9	781	-801
6	13	9	944	904
-8	14	9	1222	1269
-6	14	9	612	745
-5	14	9	486	-362
-4	14	9	608	-558
-3	14	9	597	-570
-2	14	9	1937	-1977
-1	14	9	379	-353
0	14	9	2128	-2174
2	14	9	1506	-1510
5	14	9	817	821
-7	15	9	839	-858
-5	15	9	1396	-1396
-4	15	9	381	-416
-3	15	9	921	-891
-1	15	9	469	-467
0	15	9	529	490
2	15	9	533	490
3	15	9	993	977
4	15	9	421	438
5	15	9	738	750
-2	16	9	440	-394
-1	16	9	460	-390
0	16	9	521	-487
-3	17	9	1304	-1367
-1	17	9	523	-559
0	17	9	323	410
1	17	9	538	495
2	17	9	732	746
-10	0	10	1369	-1376
-9	0	10	403	-424
-8	0	10	2065	-2115
-7	0	10	343	-452
-6	0	10	2259	-2309
-5	0	10	1377	1294
-4	0	10	1737	-1775
-3	0	10	2154	2092
-2	0	10	1029	1080
-1	0	10	1511	1490
0	0	10	2193	2271
1	0	10	753	730
2	0	10	1793	1815
3	0	10	961	-1027
4	0	10	1824	1799
5	0	10	1580	-1513
6	0	10	387	473
7	0	10	1374	-1320
9	0	10	838	-829
-11	1	10	720	-723
-10	1	10	725	697
-9	1	10	364	-401
-8	1	10	759	890
-7	1	10	427	488
-5	1	10	954	916
-3	1	10	1006	1043
-2	1	10	668	-708
-1	1	10	1365	1459
0	1	10	1611	-1666
1	1	10	1006	965
2	1	10	1569	-1544
3	1	10	368	313
4	1	10	907	-980
7	1	10	810	-841
8	1	10	588	545
9	1	10	544	-555
-11	2	10	391	-404
-9	2	10	793	-813
-8	2	10	691	-747
-7	2	10	1792	-1837
-6	2	10	420	-346
-5	2	10	652	-585
-2	2	10	1874	1877
-1	2	10	808	875

Observed and calculated structural factors for

$[W(CO)_2(\eta^3\text{-}C_3H_5)bpma]PF_6$

H	K	L	10FO	10FC
0	2	10	1534	1576
1	2	10	1586	1587
2	2	10	836	824
3	2	10	1518	1553
5	2	10	479	455
6	2	10	658	-623
8	2	10	755	-739
9	2	10	358	-410
-11	3	10	590	-622
-9	3	10	414	-325
-8	3	10	541	560
-7	3	10	521	507
-6	3	10	707	832
-5	3	10	1630	1690
-4	3	10	2039	2059
-3	3	10	1138	1120
-2	3	10	651	668
-1	3	10	1329	1349
0	3	10	386	-392
2	3	10	1014	-1033
3	3	10	983	-960
4	3	10	964	-973
5	3	10	815	-844
6	3	10	928	-971
7	3	10	399	-422
-9	4	10	656	-575
-8	4	10	396	350
-7	4	10	947	-963
-6	4	10	893	883
-5	4	10	720	-702
-4	4	10	951	1028
-3	4	10	867	-886
-1	4	10	307	-306
1	4	10	1003	978
2	4	10	519	-488
3	4	10	919	830
4	4	10	940	-985
5	4	10	909	978
6	4	10	962	-976
7	4	10	477	501
8	4	10	428	-401
-10	5	10	1267	-1305
-9	5	10	514	442
-8	5	10	448	-486
-7	5	10	977	1036
-6	5	10	839	872
-5	5	10	814	822
-4	5	10	2378	2364
-2	5	10	2338	2435
-1	5	10	1051	-1083
0	5	10	1444	1467
1	5	10	1903	-1908
3	5	10	2333	-2294
4	5	10	900	-959
5	5	10	887	-845
6	5	10	1058	-1002
8	5	10	818	-803
9	5	10	749	765
-10	6	10	445	405
-9	6	10	1004	1070
-7	6	10	1935	1939
-6	6	10	425	-536
-5	6	10	1701	1697
-4	6	10	913	-957
-3	6	10	499	536
-2	6	10	1501	-1457
-1	6	10	742	-765
0	6	10	678	-634
1	6	10	1418	-1439
2	6	10	428	229
3	6	10	1445	-1437
4	6	10	739	751
5	6	10	776	-768
6	6	10	1250	1225
8	6	10	991	921
-8	7	10	767	765
-7	7	10	350	319
-6	7	10	440	440
-5	7	10	1224	1229
-3	7	10	1175	1253
-1	7	10	761	785
0	7	10	773	-732
2	7	10	1049	-1100
4	7	10	664	-706
5	7	10	575	-615
7	7	10	519	393
8	7	10	833	782
-10	8	10	737	704
-9	8	10	330	334
-8	8	10	1150	1123
-6	8	10	726	771
-4	8	10	1021	1036
-3	8	10	610	-653
-2	8	10	1307	-1456
-1	8	10	1169	-1206
0	8	10	1530	-1534
1	8	10	943	-945
2	8	10	660	-633
3	8	10	610	-676
5	8	10	435	324
6	8	10	601	541
7	8	10	482	441
8	8	10	791	771
-9	9	10	530	-467
-5	9	10	505	-478
-4	9	10	653	-594
-3	9	10	420	478
-2	9	10	718	-790
-5	10	10	394	-429
-4	10	10	849	817
-3	10	10	866	-912
-1	10	10	1394	-1415
0	10	10	1328	-1341
1	10	10	681	-671
2	10	10	1558	-1524
4	10	10	1318	-1336
5	10	10	1263	1238
6	10	10	498	-485
7	10	10	1375	1321
-9	11	10	706	649
-8	11	10	699	-751
-6	11	10	372	-422
-5	11	10	1287	-1336
-4	11	10	634	-587
-3	11	10	1517	-1568
-1	11	10	1675	-1655
0	11	10	1259	1214
1	11	10	924	-935
2	11	10	1182	1260
3	11	10	401	384
4	11	10	1203	1251
5	11	10	791	805
6	11	10	440	526
7	11	10	788	757
-7	12	10	652	692
-6	12	10	458	-507
-5	12	10	604	633
-4	12	10	550	-575
-2	12	10	454	-417
0	12	10	411	-391
1	12	10	510	-474
3	12	10	733	-654
4	12	10	637	595
5	12	10	580	-548
-6	12	10	604	633
-7	13	10	550	-575
-6	13	10	722	-699
-5	13	10	1045	-1044
-4	13	10	1402	-1418
-3	13	10	832	-852
-2	13	10	955	-953
-1	13	10	434	-481
1	13	10	416	441
2	13	10	649	663
3	13	10	1075	1041
4	13	10	973	1010
5	13	10	907	842
-6	14	10	591	-661
-4	14	10	590	-603
-2	14	10	580	534
0	14	10	781	782
1	14	10	735	773
2	14	10	731	733
4	14	10	752	670
5	14	10	458	-511
-6	15	10	610	-567
-5	15	10	460	-501
-4	15	10	1101	-1146
-2	15	10	844	-899
-1	15	10	948	982
0	15	10	586	-572
1	15	10	1295	1262

Observed and calculated structural factors for

$[W(CO)_2(\eta^3\text{-}C_3H_5)bpma]PF_6$

H	K	L	10FO	10FC
3	15	10	1100	1080
-5	16	10	827	-852
-4	16	10	690	699
-2	16	10	1003	1028
-1	16	10	635	640
0	16	10	735	753
1	16	10	1082	1103
-2	17	10	476	505
-1	17	10	569	-609
0	17	10	308	452
-11	1	11	467	-513
-10	1	11	995	-1006
-9	1	11	889	-956
-7	1	11	851	940
-6	1	11	497	-426
-5	1	11	1070	1103
-4	1	11	1296	1246
-3	1	11	960	977
-2	1	11	1522	1536
-1	1	11	859	926
0	1	11	1059	1078
1	1	11	629	-633
2	1	11	562	556
3	1	11	1784	-1757
5	1	11	1343	-1438
6	1	11	551	-513
7	1	11	870	-876
-11	2	11	442	-464
-10	2	11	942	945
-8	2	11	532	514
-7	2	11	1062	1058
-5	2	11	1042	1037
-4	2	11	609	-605
-3	2	11	1548	1539
-2	2	11	2225	-2227
-1	2	11	867	838
0	2	11	1515	-1546
1	2	11	317	-299
2	2	11	1424	-1431
3	2	11	806	-817
4	2	11	574	-539
5	2	11	735	808
6	2	11	1396	1377
-11	3	11	763	-763
-10	3	11	1025	-1099
-9	3	11	851	856
-8	3	11	306	-365
-7	3	11	1003	1172
-6	3	11	1559	1606
-4	3	11	963	932
-3	3	11	582	609
-2	3	11	1343	1308
-1	3	11	623	-572
0	3	11	936	1045
1	3	11	1473	-1557
2	3	11	524	566
3	3	11	1666	-1565
4	3	11	414	482
5	3	11	562	551
6	3	11	902	-1029
-11	4	11	695	665
-10	4	11	422	423
-9	4	11	1235	1231
-8	4	11	1056	1052
-7	4	11	984	1017
-6	4	11	1842	1904
-5	4	11	337	-406
-4	4	11	1246	1203
-3	4	11	1123	-1053
-1	4	11	2271	-2286
0	4	11	764	-765
1	4	11	2450	-2522
2	4	11	925	-886
-10	5	11	972	-997
-9	5	11	837	-820
-8	5	11	1275	1283
-6	5	11	404	-361
-4	5	11	970	-1038
-3	5	11	445	-437
-1	5	11	459	500
0	5	11	508	545
2	5	11	502	565
3	5	11	763	757
-9	6	11	551	540
-8	6	11	687	660
-7	6	11	1118	1153
-6	6	11	877	977
-4	6	11	553	-656
-3	6	11	1437	-1358
-1	6	11	688	-702
1	6	11	1876	-1890
2	6	11	777	-752
3	6	11	742	-705
4	6	11	709	-758
7	6	11	562	551
-9	7	11	935	959
-8	7	11	913	-949
-7	7	11	595	658
-6	7	11	1022	-1016
-5	7	11	363	-358
-4	7	11	1727	-1752
-3	7	11	755	-777
-2	7	11	1140	-1182
-1	7	11	1318	-1348
0	7	11	472	486
1	7	11	701	-725
2	7	11	1041	971
4	7	11	1829	1825
6	7	11	1260	1245
-10	8	11	556	511
-7	8	11	508	525
-5	8	11	911	921
-4	8	11	978	-933
-3	8	11	1158	1107
-2	8	11	1101	-1118
-1	8	11	958	964
0	8	11	1567	-1625
1	8	11	484	554
2	8	11	653	-669
5	8	11	620	-649
6	8	11	512	487
7	8	11	547	-578
-8	9	11	834	843
-7	9	11	677	-753
-5	9	11	1210	-1152
-4	9	11	1038	-1019
-3	9	11	1468	-1532
-2	9	11	1202	-1174
-1	9	11	706	-729
0	9	11	929	-944
1	9	11	730	716
2	9	11	830	-783
3	9	11	1678	1711
5	9	11	1526	1502
7	9	11	779	837
-7	10	11	632	-639
-6	10	11	402	-469
-5	10	11	356	-378
-3	10	11	414	-406
-2	10	11	714	682
0	10	11	708	734
2	10	11	599	572
3	10	11	367	333
4	10	11	374	284
6	10	11	569	-536
-8	11	11	448	373
-7	11	11	540	-525
-5	11	11	888	-903
-4	11	11	708	-696
-3	11	11	733	-735
-2	11	11	977	-1024
-1	11	11	299	-202
0	11	11	853	789
3	11	11	875	882
5	11	11	857	-839
-8	12	11	953	-984
-7	12	11	617	-643
-6	12	11	845	-857
-5	12	11	860	-784
-3	12	11	1935	1931
-2	12	11	1657	1660
0	12	11	1021	1023
1	12	11	1111	1073
2	12	11	423	494
3	12	11	857	831
-7	13	11	828	-794
-6	13	11	605	652
-5	13	11	333	347
1	13	11	1299	-1313
2	13	11	447	549
3	13	11	1229	-1230
4	13	11	459	527
-6	14	11	958	-1012
-4	14	11	713	-777
-3	14	11	904	872
-2	14	11	485	-424
-1	14	11	1374	1374
1	14	11	1386	1362
2	14	11	682	665
3	14	11	543	591
-5	15	11	375	325

Observed and calculated structural factors for

$[W(CO)_2(\eta^3\text{-}C_3H_5)bpma]PF_6$

Observed and calculated structural factors for

[W(CO)$_2$(η^3-C$_3$H$_5$)bpmal]PF$_6$

H	K	L	10FO	10FC
4	2	13	1484	1473
5	2	13	529	-422
6	2	13	840	908
7	2	13	755	-692
-10	3	13	1074	1071
-8	3	13	781	784
-4	3	13	746	-777
-3	3	13	524	491
-2	3	13	1701	-1710
-1	3	13	454	351
0	3	13	1960	-2002
1	3	13	698	704
2	3	13	1137	-1125
3	3	13	601	586
-9	4	13	603	549
-7	4	13	726	-676
-6	4	13	1678	-1684
-5	4	13	414	-385
-4	4	13	1471	-1508
-3	4	13	414	-385
0	4	13	450	434
1	4	13	1415	1316
2	4	13	904	905
3	4	13	1417	1405
5	4	13	1258	1268
-8	5	13	426	-350
-3	5	13	350	-245
-2	5	13	372	349
0	5	13	474	461
2	5	13	913	962
-9	6	13	689	719
-7	6	13	569	-552
-6	6	13	1313	-1292
-5	6	13	403	-423
			1410	-1372

H	K	L	10FO	10FC
-3	6	13	778	-730
-2	6	13	436	242
-1	6	13	377	326
0	6	13	702	659
1	6	13	803	716
2	6	13	704	683
3	6	13	1216	1194
4	6	13	572	510
5	6	13	863	891
-8	7	13	1065	-1041
-4	7	13	1421	1349
-3	7	13	351	246
-2	7	13	1758	1801
0	7	13	1566	1535
2	7	13	1188	1171
3	7	13	578	-590
5	7	13	503	-498
6	7	13	805	-754
-8	8	13	703	-757
-7	8	13	758	756
-6	8	13	1113	-1087
-5	8	13	858	827
-4	8	13	1099	-1146
-3	8	13	542	591
-2	8	13	423	-403
0	8	13	299	273
2	8	13	886	869
3	8	13	366	-341
4	8	13	1240	1178
5	8	13	719	-685
-7	9	13	749	-660
-4	9	13	375	351
-3	9	13	1265	1234
-2	9	13	367	326
-1	9	13	1906	1930
1	9	13	1334	1309

H	K	L	10FO	10FC
3	0	13	415	388
4	0	13	828	-859
5	0	13	429	-482
-9	1	13	606	611
-8	1	13	383	-183
-7	1	13	514	-538
-6	1	13	676	-706
-5	1	13	634	-589
-4	1	13	372	251
0	1	13	952	992
1	1	13	456	420
2	1	13	1024	960
3	1	13	604	551
4	1	13	913	916
5	1	13	1537	1498
-8	2	13	1437	1413
-7	2	13	706	742
-6	2	13	349	-276
-5	2	13	473	-438
-4	2	13	543	-483
-3	2	13	1290	-1342
-2	2	13	503	477
-1	2	13	555	-642
1	2	13	744	706
2	2	13	1113	-1085
3	2	13	508	528
4	2	13	919	-818
5	2	13	636	-589
-8	3	13	744	-683
-7	3	13	709	-617
-6	3	13	1425	-1412
-5	3	13	1988	-1956
-3	3	13	379	363
-2	3	13	1256	-1246
-1	3	13	695	701
0	3	13	1477	1527

H	K	L	10FO	10FC
-1	3	14	1052	1056
0	3	14	1175	1236
2	3	14	915	914
5	3	14	361	-495
6	3	14	454	-488
-4	4	14	766	-715
-3	4	14	810	715
-2	4	14	1044	-1006
-1	4	14	829	770
0	4	14	654	-730
1	4	14	608	625
5	4	14	440	-397
-7	5	14	1325	-1291
-6	5	14	939	867
-5	5	14	671	-686
-4	5	14	1302	1264
-3	5	14	510	459
-2	5	14	1082	1057
-1	5	14	1572	1629
0	5	14	624	645
1	5	14	1564	1529
3	5	14	1307	1324
4	5	14	1192	-1202
-7	6	14	484	445
-6	6	14	951	959
-4	6	14	1094	1137
-3	6	14	427	-414
-2	6	14	1293	1230
-1	6	14	919	-925
0	6	14	828	837
1	6	14	994	-1018
2	6	14	555	-592
3	6	14	434	-377
4	6	14	710	-690
-8	7	14	760	-732
-6	7	14	836	-746

Observed and calculated structural factors for

[W(CO)$_2$(η^3-C$_3$H$_5$)bpma]PF$_6$

H	K	L	10FO	10FC	H	K	L	10FO	10FC	H	K	L	10FO	10FC	H	K	L	10FO	10FC	H	K	L	10FO	10FC
-2	7	14	450	414	-4	12	14	603	553	-5	4	15	605	681	0	9	15	1323	-1303	-5	4	16	675	683
0	7	14	792	791	-3	12	14	517	-462	-4	4	15	903	839	1	9	15	714	-736	-4	4	16	374	-359
2	7	14	731	744	-2	12	14	592	610	-3	4	15	622	750	2	9	15	707	-755	-3	4	16	712	683
3	7	14	417	-376	-1	12	14	430	-351	-1	4	15	576	605	-4	10	15	594	-545	2	4	16	450	475
-7	8	14	496	443	0	12	14	332	356	2	4	15	1398	-1389	-3	10	15	447	-435	-6	5	16	874	825
-6	8	14	1153	1137	-8	1	15	632	-716	4	4	15	1180	-1156	-2	10	15	486	-505	-5	5	16	518	534
-5	8	14	659	624	-7	1	15	1091	-1020	1	5	15	527	-468	-7	0	16	772	-597	-3	5	16	488	401
-4	8	14	935	880	-5	1	15	1046	-981	-6	6	15	869	782	-6	0	16	1370	1272	-2	5	16	1064	-1040
-3	8	14	585	672	-4	1	15	528	390	-5	6	15	625	590	-4	0	16	1845	1791	-1	5	16	363	263
-2	8	14	552	513	-2	1	15	1107	1103	-4	6	15	1015	1005	-2	0	16	1112	1008	0	5	16	1659	-1645
1	8	14	508	-482	-1	1	15	574	599	-3	6	15	1001	1011	2	0	16	780	-701	2	5	16	1454	-1421
2	8	14	742	-737	0	1	15	1392	1367	-2	6	15	422	490	-7	1	16	757	725	-5	6	16	1211	-1157
3	8	14	792	-813	1	1	15	575	580	-1	6	15	733	673	-3	1	16	951	-923	-4	6	16	385	254
4	8	14	775	-683	2	1	15	592	603	2	6	15	1162	-1110	-1	1	16	1018	-979	-3	6	16	1198	-1160
-7	9	14	433	476	3	1	15	912	913	3	6	15	413	-303	0	1	16	354	264	-1	6	16	892	-852
-6	9	14	525	-492	4	1	15	376	-276	-6	7	15	1072	1008	1	1	16	842	-860	-5	7	16	352	166
-5	9	14	422	344	-8	2	15	504	-583	-5	7	15	599	-562	2	1	16	409	418	-1	7	16	784	-777
-4	9	14	579	-562	-7	2	15	1148	1074	-4	7	15	812	821	3	1	16	690	-668	1	7	16	843	-749
-3	9	14	363	211	-5	2	15	1471	1450	-3	7	15	1108	-1154	-7	2	16	349	357	-3	8	16	681	-775
1	9	14	674	-676	-4	2	15	811	820	-1	7	15	1358	-1359	-5	2	16	1036	921	-2	8	16	694	-590
3	9	14	771	-724	-3	2	15	877	817	0	7	15	783	-806	-4	2	16	466	503	-1	8	16	452	-381
-6	10	14	618	620	-2	2	15	1289	1376	1	7	15	886	-919	-3	2	16	1114	1069	0	8	16	322	-247
-5	10	14	1598	1540	0	2	15	931	998	2	7	15	529	-642	-2	2	16	591	554	-4	1	17	803	827
-3	10	14	1700	1680	1	2	15	880	-899	-6	8	15	410	-375	-1	2	16	834	801	0	1	17	702	-670
-2	10	14	391	-506	3	2	15	1363	-1309	-5	8	15	675	662	0	2	16	356	390	-5	2	17	857	-765
-1	10	14	841	739	-8	3	15	659	-583	-2	8	15	687	649	1	2	16	355	236	-3	2	17	1512	-1416
0	10	14	719	-684	-6	3	15	891	-818	-1	8	15	466	-460	3	2	16	528	-507	-1	2	17	1333	-1284
2	10	14	1063	-1077	-5	3	15	747	578	0	8	15	788	728	-6	3	16	567	573	1	2	17	848	-844
3	10	14	457	-417	-4	3	15	895	-951	1	8	15	902	-835	-5	3	16	516	506	-3	3	17	359	389
-5	11	14	512	-503	-3	3	15	1081	1099	2	8	15	717	725	-1	3	16	931	-952	-4	4	17	1475	-1394
-3	11	14	993	-905	-2	3	15	610	-702	-5	9	15	777	723	0	3	16	633	-618	-3	4	17	680	-562
-2	11	14	754	-783	-1	3	15	885	899	-4	9	15	813	-736	1	3	16	1078	-1082	-2	4	17	1672	-1591
-1	11	14	757	-730	4	3	15	722	668	-2	9	15	1302	-1284	3	3	16	817	-816	0	4	17	1038	-1030
0	11	14	1267	-1265	-8	4	15	713	781	-1	9	15	399	-432	-6	4	16	519	-360	-2	5	17	398	278
2	11	14	1060	-993	-6	4	15	1269	1197															

APPENDIX 4

ANISOTROPIC AND ISOTROPIC THERMAL PARAMETERS FOR

$Mo(CO)_2(\pi^3\text{-}CH_2{=}C(CONHMe){=}C{=}CH_2)(bipy)(O_2CC_3F_7)$.

The thermal parameters were terms U_{ij} of

$\exp(-2\pi^2(U_{11}h^2a^{*2}+U_{22}k^2b^{*2}+U_{33}l^2c^{*2}+2U_{12}hka^*c^*+2U_{23}k(b^*c^*))$

Atom	U_{11} (or U_{iso})	U_{22}	U_{33}	U_{23}	U_{13}	U_{12}
Mo	0.0428(8)	0.0318(6)	0.0497(6)	0.0149(4)	-0.0018(4)	0.0031(4)
O(1)	0.0684(76)	0.0705(53)	0.0780(51)	0.0008(41)	-0.0082(53)	0.0315(49)
O(2)	0.0744(79)	0.0706(56)	0.1294(77)	0.0397(54)	-0.0170(67)	0.0215(54)
O(3)	0.1034(87)	0.0372(44)	0.1187(70)	0.0272(43)	0.0033(62)	-0.0121(51)
O(4)	0.0738(64)	0.0338(38)	0.0559(37)	0.0089(30)	0.0137(39)	0.0131(37)
O(5)	0.2246(18)	0.0699(63)	0.1146(76)	0.0266(59)	0.0076(93)	0.0784(90)
N(1)	0.0444(62)	0.0363(42)	0.0468(41)	0.0152(34)	-0.0028(43)	0.0001(39)
N(2)	0.0422(62)	0.0411(44)	0.0453(41)	0.0038(34)	-0.0108(42)	0.0088(40)
N(3)	0.0612(75)	0.0410(49)	0.0612(51)	0.0018(39)	-0.0013(51)	0.0084(49)
C(1)	0.0494(25)					
C(2)	0.0649(31)					
C(3)	0.0733(34)					
C(4)	0.0573(28)					
C(5)	0.0434(24)					
C(6)	0.0431(24)					
C(7)	0.0688(33)					
C(8)	0.0836(39)					
C(9)	0.0752(36)					
C(10)	0.0562(28)					
C(11)	0.0820(11)	0.0820(11)	0.0548(58)	0.0034(48)	0.0131(64)	-0.0069(64)
C(12)	0.0618(92)	0.0583(67)	0.0353(48)	0.0134(45)	0.0030(55)	0.0165(61)
C(13)	0.0600(90)	0.0499(58)	0.0499(55)	0.0293(47)	0.0016(61)	0.0062(56)
C(14)	0.0873(12)	0.0938(95)	0.0555(63)	0.0218(62)	-0.0161(77)	0.0052(84)
C(15)	0.0717(11)	0.0551(68)	0.0376(51)	0.0112(46)	-0.0035(59)	0.0170(67)
C(16)	0.1218(15)	0.0460(63)	0.0740(73)	0.0173(55)	0.0080(83)	0.0137(76)
C(17)	0.0315(74)	0.0459(59)	0.0790(69)	0.0305(53)	0.0219(59)	0.0052(51)
C(18)	0.0898(11)	0.0461(67)	0.0588(63)	0.0177(51)	-0.0168(69)	-0.0032(70)
C(19)	0.0799(12)	0.0627(82)	0.0728(75)	0.0038(65)	0.0143(76)	0.0267(67)
C(20)	0.0891(14)	0.0567(79)	0.1036(10)	-0.0062(75)	0.0252(98)	0.0140(81)
C(21)	0.1153(59)					
C(22)	0.1088(23)	0.2318(31)	0.1007(15)	0.0348(15)	0.0183(15)	0.0164(20)
F(1)	0.2007(17)	0.1618(10)	0.1373(82)	-0.0427(76)	0.0143(88)	0.1117(11)
F(2)	0.1317(11)	0.1674(99)	0.0784(52)	0.0049(57)	0.0272(59)	-0.0150(84)
F(3)	0.2508(18)	0.1139(73)	0.1135(67)	0.0352(57)	0.0245(86)	0.0979(96)
F(4)	0.2087(16)	0.2672(16)	0.0462(43)	-0.0182(63)	-0.0027(66)	-0.0012(13)
F(5)	0.1217(12)	0.2059(12)	0.1061(74)	0.0286(75)	0.0130(71)	-0.0467(93)
F(6)	0.0949(11)	0.2705(18)	0.1704(12)	0.0507(11)	-0.0448(10)	-0.0065(10)
F(7)	0.3177(29)	0.0688(67)	0.3177(216)	0.0348(94)	0.0564(19)	0.0133(11)

ATOMIC COORDINATES (x10⁴) FOR $Mo(CO)_2(\eta^3\text{-}CH_2{=}C(CONHMe){=}C{=}CH_2)(bipy)(O_2CC_2F_7)$

WITH ESTIMATED STANDARD DEVIATIONS IN PARENTHESES

Atom	X	Y	Z
Mo	-706(1)	4334(1)	1809(1)
O(1)	11695(14)	1339(9)	1156(5)
O(2)	6154(15)	5591(10)	1144(6)
O(3)	11915(17)	7307(9)	1683(6)
O(4)	8968(12)	5291(7)	2964(4)
O(5)	8476(25)	7429(11)	2871(7)
N(1)	7641(13)	2405(8)	2179(4)
N(2)	11345(13)	3591(8)	2534(4)
N(3)	8615(15)	283(9)	800(5)
H(1)'	7276(15)	427(9)	596(5)
H(1)	5080(17)	2229(11)	1535(6)
H(2)	3395(21)	85(13)	1914(6)
H(3)	5192(22)	-1172(14)	2698(7)
H(4)	8450(18)	21(12)	3225(6)
H(7)	11024(21)	1193(13)	3705(7)
H(8)	14413(24)	2465(15)	4012(8)
H(9)	15729(24)	4468(14)	3395(7)
H(10)	13652(19)	5173(12)	2490(6)
H(16A)	7399(25)	-1870(12)	802(7)
H(16B)	9294(25)	-1008(12)	1536(7)
H(16C)	9703(25)	-1502(12)	572(7)
C(1)	5818(17)	1749(11)	1921(6)
C(2)	4873(21)	526(13)	2105(6)
C(3)	5870(22)	-146(14)	2568(7)
C(4)	7688(18)	488(12)	2840(6)
C(5)	8576(16)	1770(10)	2630(5)
C(6)	10577(16)	2502(10)	2878(5)
C(7)	11638(21)	2060(13)	3428(7)
C(8)	13523(24)	2781(15)	3600(8)
C(9)	14267(24)	3897(14)	3264(7)
C(10)	13079(19)	4261(12)	2743(6)
C(11)	11286(21)	4073(11)	891(6)
C(12)	9806(18)	2805(11)	796(5)
C(13)	8052(18)	3061(11)	646(6)
C(14)	6498(24)	2607(16)	136(7)
C(15)	10151(21)	1422(12)	935(5)
C(16)	8764(25)	-1112(12)	937(7)
C(17)	7316(17)	5140(11)	1402(6)
C(18)	10896(22)	6225(13)	1726(6)
C(19)	8805(23)	6571(14)	3216(7)
C(20)	9172(26)	7005(14)	4114(9)
C(21)	11181(36)	7159(22)	4524(11)
C(22)	12753(40)	7993(35)	4293(12)
F(1)	8763(24)	8220(14)	4352(6)
F(2)	8200(19)	6011(13)	4419(5)
F(3)	11635(23)	5799(11)	4378(6)
F(4)	11270(25)	7606(17)	5303(4)
F(5)	12791(19)	7617(15)	3551(16)
F(6)	14279(21)	8146(20)	4716(9)
F(7)	12352(36)	9431(13)	4409(11)

Observed and calculated structural factors for

$Mo(CO)_2(\eta^3\text{-}CH_2{=}C(CONHMe){=}C{=}CH_2)(bipy)(O_2CC_3F_7)$

H	K	L	10FO	10FC	H	K	L	10FO	10FC	H	K	L	10FO	10FC	H	K	L	10FO	10FC
1	0	0	1612	1646	1	4	0	73	-78	4	7	0	60	-53	-1	-7	1	126	134	3	-4	1	70	81
3	0	0	406	-401	2	4	0	363	-411	-6	6	0	149	140	0	-7	1	298	299	4	-4	1	252	243
4	0	0	401	-415	3	4	0	390	-384	-5	6	0	110	105	1	-7	1	264	287	5	-4	1	296	277
5	0	0	161	-215	4	4	0	201	-212	-3	6	0	140	-148	2	-7	1	164	166	6	-4	1	109	140
-4	1	0	101	159	5	4	0	216	-197	-2	6	0	332	-327	3	-7	1	227	222	-6	-3	1	79	-100
-3	1	0	67	-99	6	4	0	67	-68	-1	6	0	272	-279	4	-7	1	165	157	-4	-3	1	245	235
-2	1	0	117	-102	-6	5	0	131	-104	0	6	0	225	-216	5	-7	1	191	173	-3	-3	1	292	292
-1	1	0	1192	-1152	-5	5	0	206	-208	1	6	0	56	-56	6	-7	1	108	92	-2	-3	1	455	436
0	1	0	786	-819	-4	5	0	360	-334	-3	6	0	252	230	-4	-6	1	154	136	-1	-3	1	287	292
1	1	0	402	-422	-3	5	0	245	-224	-2	6	0	285	272	-3	-6	1	55	-49	0	-3	1	565	505
2	1	0	385	-386	-2	5	0	449	-454	-1	6	0	244	233	-2	-6	1	108	-109	1	-3	1	427	395
3	1	0	315	-277	-1	5	0	348	-328	0	6	0	90	99	-1	-6	1	273	-291	2	-3	1	100	-108
4	1	0	305	273	2	5	0	554	531	1	6	0	63	85	0	-6	1	91	-107	3	-3	1	651	-575
5	1	0	402	450	3	5	0	128	121	-2	7	0	192	-194	1	-6	1	246	-271	4	-3	1	383	-387
-2	2	0	987	987	4	5	0	102	86	1	-10	1	78	-90	2	-6	1	491	-488	5	-3	1	429	-424
-1	2	0	193	-180	5	5	0	72	66	2	-10	1	111	-91	3	-6	1	380	-401	-5	-2	1	253	-253
0	2	0	227	-221	-6	6	0	150	163	3	-10	1	86	-90	5	-6	1	96	96	-4	-2	1	420	-438
1	2	0	196	150	-5	6	0	200	207	-1	-9	1	125	-141	6	-6	1	80	62	-3	-2	1	695	-670
2	2	0	222	-250	-4	6	0	94	82	0	-9	1	60	-62	7	-6	1	157	164	-2	-2	1	618	-557
3	2	0	152	-100	-3	6	0	78	85	1	-9	1	52	52	-5	-5	1	251	-214	-1	-2	1	791	-746
4	2	0	382	-374	-2	6	0	46	47	2	-9	1	100	107	-3	-5	1	139	163	0	-2	1	438	402
5	2	0	364	-366	-1	6	0	321	-358	3	-9	1	195	203	-2	-5	1	414	422	1	-2	1	879	832
-3	3	0	446	-502	0	6	0	398	-457	4	-9	1	221	192	0	-5	1	178	172	2	-2	1	405	365
-2	3	0	665	-631	1	6	0	240	-230	5	-9	1	205	193	1	-5	1	348	313	3	-2	1	234	229
-1	3	0	68	70	2	6	0	200	-218	-3	-8	1	236	250	2	-5	1	288	318	4	-2	1	184	199
0	3	0	305	-256	3	6	0	233	-216	-2	-8	1	190	177	3	-5	1	317	327	5	-2	1	277	319
1	3	0	357	-343	4	6	0	81	-68	-1	-8	1	171	164	5	-5	1	309	-286	6	-2	1	103	171
2	3	0	303	275	-6	7	0	105	-105	0	-8	1	92	87	6	-5	1	195	-213	-5	-1	1	224	305
3	3	0	261	276	-5	7	0	61	-56	1	-8	1	121	-136	7	-5	1	202	-295	-4	-1	1	385	417
4	3	0	440	396	-4	7	0	78	-82	2	-8	1	267	-250	-6	-4	1	166	168	-3	-1	1	300	317
5	3	0	282	262	-2	7	0	138	142	3	-8	1	371	-349	-5	-4	1	58	73	-2	-1	1	742	751
6	3	0	158	199	-1	7	0	253	249	4	-8	1	255	-231	-3	-4	1	216	-175	-1	-1	1	268	314
-5	4	0	214	285	0	7	0	407	415	5	-8	1	192	-182	-2	-4	1	511	-550	0	-1	1	240	284
-4	4	0	447	447	1	7	0	339	345	6	-8	1	63	-58	-1	-4	1	677	-724	2	-1	1	341	-338
-3	4	0	680	638	2	7	0	273	275	-4	-7	1	180	-175	0	-4	1	469	-596	3	-1	1	667	-656
-1	4	0	220	-199	3	7	0	149	168	-3	-7	1	252	-258	1	-4	1	476	-501	4	-1	1	515	-527

Observed and calculated structural factors for

$Mo(CO)_2(\eta^3\text{-}CH_2\text{-}C(CONHMe)\text{-}C{=}CH_2)(bipy)(O_2CC_3F_7)$

H	K	L	10FO	10FC	H	K	L	10FO	10FC	H	K	L	10FO	10FC	H	K	L	10FO	10FC	H	K	L	10FO	10FC
5	-1	1	163	-192	2	4	1	80	76	-2	8	1	63	46	5	-7	2	126	130	4	-4	2	184	-190
-1	0	1	128	-147	4	4	1	251	-235	0	8	1	142	-151	6	-7	2	155	154	5	-4	2	60	-63
1	0	1	661	572	5	4	1	170	-170	1	8	1	182	-171	-5	-6	2	142	133	6	-4	2	118	137
2	0	1	942	881	6	4	1	198	-186	2	8	1	300	-306	-4	-6	2	354	326	-6	-3	2	133	-193
3	0	1	769	790	-5	5	1	56	-41	-5	9	1	157	-142	-3	-6	2	365	375	-5	-3	2	174	-159
4	0	1	314	330	-4	5	1	357	-356	-4	9	1	209	-188	-2	-6	2	140	134	-4	-3	2	297	-283
5	0	1	301	290	-3	5	1	323	-334	-3	9	1	134	-122	-1	-6	2	51	73	-3	-3	2	376	-372
-1	1	1	115	-81	-2	5	1	276	-291	-1	9	1	71	79	0	-6	2	38	30	-2	-3	2	214	-189
0	1	1	733	-696	-1	5	1	352	-300	0	9	1	204	206	1	-6	2	270	-310	-1	-3	2	836	797
1	1	1	218	-166	1	5	1	179	-134	1	9	1	205	201	2	-6	2	362	-355	0	-3	2	572	540
2	1	1	623	-574	2	5	1	104	94	1-10	2	272	262	3	-6	2	431	-408	1	-3	2	875	829
3	1	1	469	-459	3	5	1	212	191	2-10	2	145	140	4	-6	2	242	-220	2	-3	2	566	541
4	1	1	301	-278	5	5	1	180	151	-1	-9	2	231	-240	5	-6	2	206	-189	3	-3	2	211	203
5	1	1	131	-144	-6	6	1	145	165	0	-9	2	252	-223	6	-6	2	132	-128	5	-3	2	184	-189
6	1	1	87	121	-5	6	1	278	267	1	-9	2	192	-187	7	-6	2	88	-83	-5	-2	2	301	332
-2	2	1	295	368	-4	6	1	395	389	2	-9	2	85	-93	-5	-5	2	325	-285	-4	-2	2	140	125
-1	2	1	433	414	-3	6	1	276	274	3	-9	2	140	-138	-4	-5	2	163	-154	-3	-2	2	192	-180
0	2	1	745	725	-2	6	1	193	203	5	-9	2	160	147	-3	-5	2	248	-242	-2	-2	2	807	-812
1	2	1	423	443	-1	6	1	72	75	-3	-8	2	183	160	-2	-5	2	168	-175	-1	-2	2	914	-914
2	2	1	379	380	0	6	1	76	-61	-2	-8	2	204	215	-1	-5	2	189	136	0	-2	2	734	-726
3	2	1	363	328	2	6	1	179	-160	-1	-8	2	254	274	1	-5	2	373	336	1	-2	2	479	-462
5	2	1	267	-231	3	6	1	59	-57	0	-8	2	217	218	2	-5	2	264	257	2	-2	2	105	-84
6	2	1	162	-188	4	6	1	195	-166	1	-8	2	78	81	3	-5	2	139	140	4	-2	2	101	102
-2	3	1	170	-181	-6	7	1	82	-84	2	-8	2	114	98	4	-5	2	162	148	5	-2	2	210	211
0	3	1	620	-591	-5	7	1	105	-94	3	-8	2	84	-71	5	-5	2	63	42	-5	-1	2	79	-142
1	3	1	695	-731	-4	7	1	208	-188	4	-8	2	93	-92	7	-5	2	66	-102	-4	-1	2	111	130
2	3	1	187	-181	-3	7	1	319	-302	5	-8	2	154	-136	-6	-4	2	204	216	-3	-1	2	377	465
3	3	1	165	-163	-2	7	1	291	-288	6	-8	2	150	-141	-5	-4	2	181	155	-2	-1	2	59	78
4	3	1	57	49	0	7	1	154	169	-4	-7	2	247	-244	-4	-4	2	80	72	-1	-1	2	1526	1422
5	3	1	249	231	1	7	1	205	205	-3	-7	2	384	-386	-3	-4	2	379	355	0	-1	2	1532	1451
6	3	1	146	161	2	7	1	301	322	-2	-7	2	125	-112	-2	-4	2	189	193	1	-1	2	780	722
-4	4	1	174	194	3	7	1	379	346	0	-7	2	59	53	-1	-4	2	296	-341	2	-1	2	499	426
-3	4	1	184	195	-6	8	1	158	166	1	-7	2	80	80	0	-4	2	476	-498	3	-1	2	232	-217
-2	4	1	247	241	-5	8	1	187	171	2	-7	2	158	151	1	-4	2	569	-564	4	-1	2	256	-263
-1	4	1	35	52	-4	8	1	189	170	3	-7	2	228	236	2	-4	2	446	-430	5	-1	2	415	-386
1	4	1	431	461	-3	8	1	175	163	4	-7	2	224	210	3	-4	2	412	-409	0	0	2	591	-611

Observed and calculated structural factors for

$Mo(CO)_2(\eta^3\text{-}CH_2{=}C(CONHMe){=}C{=}CH_2)(bipy)(O_2CC_3F_7)$

H	K	L	10FO	10FC	H	K	L	10FO	10FC	H	K	L	10FO	10FC	H	K	L	10FO	10FC
1	0	2	428	400	3	4	2	273	272	1-10	3	101	110	7 -6	3	180	-180	-3 -2	3 411 361
2	0	2	661	-574	5	4	2	56	-66	2-10	3	180	184	-4 -5	3	266	-233	-2 -2	3 798 802
3	0	2	282	258	-4	5	2	98	76	-1 -7	3	61	-73	-3 -5	3	320	-337	-1 -2	3 140 140
4	0	2	376	361	-3	5	2	240	-219	0 -7	3	66	-70	-2 -5	3	560	-542	0 -2	3 464 -453
5	0	2	469	462	-2	5	2	324	-335	1 -7	3	123	-114	1 -5	3	36	-16	1 -2	3 384 -359
-1	1	2	77	76	-1	5	2	511	-486	2 -7	3	133	-147	2 -5	3	321	320	2 -2	3 1099-1051
-1	1	2	155	143	2	5	2	290	-295	3 -7	3	213	-197	4 -5	3	181	187	3 -2	3 876 -842
2	1	2	66	72	5	5	2	132	120	4 -7	3	197	-180	5 -5	3	151	125	4 -2	3 504 -515
4	1	2	482	-400	-6	6	2	80	-84	5 -7	3	107	-104	6 -5	3	251	235	5 -2	3 83 -93
5	1	2	433	-424	-4	6	2	235	211	-2 -6	3	109	109	7 -5	3	234	250	-2 -1	3 612 -607
6	1	2	201	-232	-3	6	2	222	220	-1 -6	3	131	136	-5 -4	3	218	186	-1 -1	3 398 402
-1	2	2	632	630	-2	6	2	384	399	0 -6	3	287	299	-4 -4	3	115	116	1 -1	3 967 901
0	2	2	280	-259	-1	6	2	508	564	1 -6	3	255	274	-3 -4	3	511	484	2 -1	3 1204 1159
1	2	2	686	667	0	6	2	330	317	2 -6	3	338	318	-2 -4	3	343	350	3 -1	3 954 904
2	2	2	187	206	1	6	2	320	329	3 -6	3	212	203	-1 -4	3	487	506	4 -1	3 250 264
3	2	2	222	246	2	6	2	157	169	6 -6	3	112	-94	0 -4	3	580	639	5 -1	3 128 127
4	2	2	322	232	4	6	2	84	-67	-2 -7	3	132	-140	1 -4	3	90	-90	6 -1	3 82 -86
5	2	2	197	172	-6	7	2	93	101	-1 -7	3	270	-265	2 -4	3	273	-290	-1 0	3 324 -327
6	2	2	85	91	-4	7	2	84	-89	0 -7	3	389	-379	3 -4	3	351	-341	0 0	3 893 -913
-3	3	2	533	620	-3	7	2	247	-262	1 -7	3	368	-376	4 -4	3	506	-472	1 0	3 916 -865
-2	3	2	121	143	-2	7	2	305	-304	2 -7	3	328	-325	5 -4	3	309	-273	2 0	3 418 -430
-1	3	2	116	-122	-1	7	2	229	-231	4 -7	3	199	185	6 -4	3	66	-78	3 0	3 116 104
0	3	2	468	-435	0	7	2	203	-231	5 -7	3	104	87	-6 -3	3	75	-119	6 0	3 227 227
1	3	2	576	-590	1	7	2	71	-85	6 -7	3	145	133	-5 -3	3	182	-179	-1 1	3 1519 1483
2	3	2	406	-401	3	7	2	89	98	-5 -6	3	65	-89	-4 -3	3	446	-383	0 1	3 1061 1031
3	3	2	265	-278	-4	8	2	152	144	-4 -6	3	52	-16	-3 -3	3	479	-441	1 1	3 54 33
4	3	2	231	-236	-3	8	2	333	319	-3 -6	3	160	152	-2 -3	3	423	-389	3 1	3 169 -151
5	3	2	127	-146	-2	8	2	326	318	-2 -6	3	248	266	-1 -3	3	275	-288	5 1	3 366 -329
6	3	2	62	-61	-1	8	2	149	143	-1 -6	3	340	337	1 -3	3	145	145	6 1	3 314 -335
-4	4	2	268	-276	1	8	2	106	-116	0 -6	3	180	228	2 -3	3	712	653	-2 2	3 326 -435
-3	4	2	195	-135	2	8	2	141	-142	1 -6	3	393	455	3 -3	3	665	606	-1 2	3 847 -824
-2	4	2	95	-89	-4	9	2	166	-149	2 -6	3	250	247	4 -3	3	498	471	0 2	3 609 -643
-1	4	2	75	-78	-3	9	2	323	-303	3 -6	3	166	-149	5 -3	3	268	223	1 2	3 38 -58
0	4	2	175	222	-2	9	2	259	-268	4 -6	3	377	-359	6 -3	3	85	-79	3 2	3 86 -77
1	4	2	697	720	-1	9	2	167	-169	5 -6	3	290	-272	-5 -2	3	285	380	4 2	3 296 278
2	4	2	549	541	1	9	2	86	89	6 -6	3	270	-247	-4 -2	3	365	386	5 2	3 232 229

Observed and calculated structural factors for

$Mo(CO)_2(\eta^3\text{-}CH_2{=}C(CONHMe){=}C{=}CH_2)(bipy)(O_2CC_3F_7)$

H	K	L	10FO	10FC	H	K	L	10FO	10FC	H	K	L	10FO	10FC	H	K	L	10FO	10FC
-6	2	3	82	78	4	6	3	176	149	5	-8	4	156	147	2	-4	4	404	401	5	-1	4	512	445
-3	3	3	255	335	-6	7	3	115	116	-4	-7	4	315	312	3	-4	4	328	310	6	-1	4	74	74
-2	3	3	61	-53	-5	7	3	80	70	-3	-7	4	254	244	4	-4	4	349	-331	-1	0	4	292	-281
-1	3	3	97	-92	-4	7	3	141	144	0	-7	4	247	-263	5	-4	4	163	-182	0	0	4	143	-143
0	3	3	748	710	-3	7	3	163	167	1	-7	4	286	-263	6	-4	4	304	-289	1	0	4	272	-245
1	3	3	161	148	-1	7	3	290	-306	2	-7	4	480	-447	7	-4	4	206	-218	2	0	4	175	-185
2	3	3	181	158	0	7	3	257	-267	3	-7	4	377	-342	-5	-3	4	74	97	3	0	4	526	-510
3	3	3	161	-170	1	7	3	286	-294	4	-7	4	240	-226	-3	-3	4	386	-360	4	0	4	431	-424
4	3	3	457	-416	2	7	3	183	-204	5	-7	4	184	-171	-2	-3	4	877	-880	5	0	4	335	-285
5	3	3	210	-205	3	7	3	140	-135	-5	-6	4	212	-195	-1	-3	4	828	-818	6	0	4	125	-113
-3	4	3	136	-144	-5	8	3	126	-119	-4	-6	4	385	-383	0	-3	4	123	-106	-1	1	4	1212	-1166
-2	4	3	226	-238	-4	8	3	120	-112	-3	-6	4	288	-299	1	-3	4	57	-68	0	1	4	232	-218
0	4	3	111	-136	-2	8	3	112	101	-2	-6	4	65	-45	2	-3	4	366	-342	1	1	4	299	275
1	4	3	122	174	-1	8	3	131	137	-1	-6	4	71	83	3	-3	4	50	-28	2	1	4	471	475
2	4	3	338	337	0	8	3	213	178	0	-6	4	299	355	4	-3	4	289	273	3	1	4	553	557
3	4	3	409	382	1	8	3	136	132	1	-6	4	415	441	5	-3	4	286	281	4	1	4	195	183
4	4	3	235	233	2	8	3	234	250	2	-6	4	385	392	6	-3	4	202	188	5	1	4	58	48
5	4	3	146	155	-4	9	3	52	56	3	-6	4	296	289	7	-3	4	167	224	6	1	4	127	-144
-4	5	3	486	474	-3	9	3	81	-73	6	-6	4	127	-113	-4	-2	4	216	213	-2	2	4	461	-486
-3	5	3	382	358	-2	9	3	124	-128	7	-6	4	91	-79	-3	-2	4	472	484	-1	2	4	959	-955
-2	5	3	274	271	-1	9	3	211	-207	-5	-5	4	228	191	-2	-2	4	763	698	0	2	4	307	-293
-1	5	3	91	96	0	9	3	174	-174	-4	-5	4	77	70	-1	-2	4	609	549	1	2	4	257	-245
0	5	3	76	-96	1-10		4	150	-154	-2	-5	4	239	-226	0	-2	4	43	32	2	2	4	111	-108
1	5	3	539	-537	3-10		4	80	61	0	-5	4	212	-216	2	-2	4	388	-348	3	2	4	244	-217
2	5	3	230	-233	-1	-9	4	174	185	1	-5	4	567	-566	3	-2	4	63	-76	4	2	4	76	-69
3	5	3	65	-56	0	-9	4	55	59	2	-5	4	446	-442	4	-2	4	138	-152	6	2	4	95	79
4	5	3	113	-101	3	-9	4	71	69	3	-5	4	150	-173	5	-2	4	286	-250	-3	3	4	114	136
5	5	3	127	-155	4	-9	4	133	-136	5	-5	4	135	115	6	-2	4	132	-136	-2	3	4	192	179
-5	6	3	178	-182	5	-9	4	213	-193	6	-5	4	130	109	7	-2	4	130	-171	-1	3	4	91	95
-4	6	3	244	-237	-3	-8	4	254	-250	7	-5	4	239	235	-3	-1	4	121	-188	0	3	4	459	424
-3	6	3	291	-203	-2	-8	4	164	-173	-6	-4	4	176	-188	-2	-1	4	409	-362	1	3	4	643	656
-2	6	3	166	148	0	-8	4	147	169	-4	-4	4	130	123	-1	-1	4	304	-336	2	3	4	571	569
-1	6	3	357	357	1	-8	4	181	198	-2	-4	4	263	263	0	-1	4	816	769	3	3	4	125	128
0	6	3	408	426	2	-8	4	193	206	-1	-4	4	375	308	2	-1	4	318	291	5	3	4	69	-58
1	6	3	328	305	3	-8	4	278	266	0	-4	4	673	772	3	-1	4	156	132	6	3	4	77	-82
2	6	3			4	-8	4	153	150	1	-4	4	857	872	4	-1	4	481	448	-4	4	4	83	-121

Observed and calculated structural factors for

$Mo(CO)_2(\eta^3\text{-}CH_2{\sim}C(CONHMe){\sim}C{=}CH_2)(bipy)(O_2CC_3F_7)$

H	K	L	10FO	10FC
1	0	5	233	253
2	0	5	267	245
3	0	5	96	-96
4	0	5	254	-218
5	0	5	178	-168
-2	1	5	449	-520
-1	1	5	1684	-1559
0	1	5	297	-285
1	1	5	102	117
2	1	5	498	461
3	1	5	419	366
4	1	5	259	265
5	1	5	166	200
6	1	5	97	119
-2	2	5	816	797
-1	2	5	1073	1065
1	2	5	495	-497
2	2	5	213	-235
3	2	5	347	-350
4	2	5	355	-323
5	2	5	199	-179
6	2	5	57	-48
-3	3	5	435	-544
-2	3	5	63	-43
0	3	5	431	431
1	3	5	500	480
2	3	5	183	169
3	3	5	428	410
4	3	5	298	269
5	3	5	200	180
-4	4	5	265	332
-3	4	5	431	415
-2	4	5	59	-40
-1	4	5	290	-269
0	4	5	326	-375
1	4	5	172	-142
2	4	5	208	-240
3	4	5	119	136
4	4	5	174	148
5	4	5	70	85
-4	5	5	150	146
-3	5	5	88	112
-2	5	5	429	-362
-1	5	5	172	-142
0	5	5	680	-660
1	5	5	208	-240
2	5	5	119	136
3	5	5	174	148
4	5	5	70	85
5	5	5	150	146
6	5	5	88	112
-3	6	5	429	-362
-2	6	5	172	-142
-1	6	5	680	-660
0	6	5	208	-240
1	6	5	119	136
2	6	5	174	148
3	6	5	70	85
4	6	5	150	146
5	6	5	88	112
-4	7	5	429	-362
-3	7	5	172	-142
-2	7	5	680	-660
-1	7	5	208	-240
0	7	5	119	136
1	7	5	174	148
2	7	5	70	85
3	7	5	150	146
4	7	5	88	112
5	7	5	429	-362
-3	8	5	172	-142
-2	8	5	680	-660
-1	8	5	208	-240
0	8	5	119	136
1	8	5	174	148
2	8	5	70	85
3	8	5	150	146
4	8	5	88	112
-4	9	5	429	-362
-3	9	5	172	-142
-2	9	5	680	-660
-1	9	5	208	-240
0	9	5	119	136
1	9	5	174	148
2	9	5	70	85
3	9	5	150	146
4	9	5	88	112
-5	10	5	429	-362
-4	10	5	172	-142
-3	10	5	680	-660
-2	10	5	208	-240
-1	10	5	119	136
0	10	5	174	148
1	10	5	70	85
2	10	5	150	146
3	10	5	88	112
-5	11	5	429	-362
-4	11	5	172	-142
-3	11	5	680	-660
-2	11	5	208	-240
-1	11	5	119	136
0	11	5	174	148
1	11	5	70	85
2	11	5	150	146
3	11	5	88	112
-5	12	5	429	-362
-4	12	5	172	-142
-3	12	5	680	-660
-2	12	5	208	-240
-1	12	5	119	136
0	12	5	174	148
1	12	5	70	85
2	12	5	150	146
3	12	5	88	112
-5	13	5	429	-362
-4	13	5	172	-142
-3	13	5	680	-660
-2	13	5	208	-240
-1	13	5	119	136
0	13	5	174	148
1	13	5	70	85
2	13	5	150	146
3	13	5	88	112
-5	14	5	429	-362
-4	14	5	172	-142
-3	14	5	680	-660
-2	14	5	208	-240
-1	14	5	119	136
0	14	5	174	148
1	14	5	70	85
2	14	5	150	146
3	14	5	88	112
-5	15	5	429	-362
-4	15	5	172	-142
-3	15	5	680	-660
-2	15	5	208	-240
-1	15	5	119	136
0	15	5	174	148
1	15	5	70	85
2	15	5	150	146
3	15	5	88	112
-5	16	5	429	-362
-4	16	5	172	-142
-3	16	5	680	-660
-2	16	5	208	-240
-1	16	5	119	136
0	16	5	174	148
1	16	5	70	85
2	16	5	150	146
3	16	5	88	112
-5	17	5	429	-362
-4	17	5	172	-142
-3	17	5	680	-660
-2	17	5	208	-240
-1	17	5	119	136
0	17	5	174	148
1	17	5	70	85
2	17	5	150	146
3	17	5	88	112
-5	18	5	429	-362
-4	18	5	172	-142
-3	18	5	680	-660
-2	18	5	208	-240
-1	18	5	119	136
0	18	5	174	148
1	18	5	70	85
2	18	5	150	146
3	18	5	88	112
-5	19	5	429	-362
-4	19	5	172	-142
-3	19	5	680	-660
-2	19	5	208	-240
-1	19	5	119	136
0	19	5	174	148
1	19	5	70	85
2	19	5	150	146
3	19	5	88	112
-5	20	5	429	-362
-4	20	5	172	-142
-3	20	5	680	-660
-2	20	5	208	-240
-1	20	5	119	136
0	20	5	174	148
1	20	5	70	85
2	20	5	150	146
3	20	5	88	112
-5	21	5	429	-362
-4	21	5	172	-142
-3	21	5	680	-660
-2	21	5	208	-240
-1	21	5	119	136
0	21	5	174	148
1	21	5	70	85
2	21	5	150	146
3	21	5	88	112
-5	22	5	429	-362
-4	22	5	172	-142
-3	22	5	680	-660
-2	22	5	208	-240
-1	22	5	119	136
0	22	5	174	148
1	22	5	70	85
2	22	5	150	146
3	22	5	88	112
-5	23	5	429	-362
-4	23	5	172	-142
-3	23	5	680	-660
-2	23	5	208	-240
-1	23	5	119	136
0	23	5	174	148
1	23	5	70	85
2	23	5	150	146
3	23	5	88	112
-5	24	5	429	-362
-4	24	5	172	-142
-3	24	5	680	-660
-2	24	5	208	-240
-1	24	5	119	136
0	24	5	174	148
1	24	5	70	85
2	24	5	150	146
3	24	5	88	112
-5	25	5	429	-362
-4	25	5	172	-142
-3	25	5	680	-660
-2	25	5	208	-240
-1	25	5	119	136
0	25	5	174	148
1	25	5	70	85
2	25	5	150	146
3	25	5	88	112
-5	26	5	429	-362
-4	26	5	172	-142
-3	26	5	680	-660
-2	26	5	208	-240
-1	26	5	119	136
0	26	5	174	148
1	26	5	70	85
2	26	5	150	146
3	26	5	88	112
-5	27	5	429	-362
-4	27	5	172	-142
-3	27	5	680	-660
-2	27	5	208	-240
-1	27	5	119	136
0	27	5	174	148
1	27	5	70	85
2	27	5	150	146
3	27	5	88	112
-5	28	5	429	-362
-4	28	5	172	-142
-3	28	5	680	-660
-2	28	5	208	-240
-1	28	5	119	136
0	28	5	174	148
1	28	5	70	85
2	28	5	150	146
3	28	5	88	112
-5	29	5	429	-362
-4	29	5	172	-142
-3	29	5	680	-660
-2	29	5	208	-240
-1	29	5	119	136
0	29	5	174	148
1	29	5	70	85
2	29	5	150	146
3	29	5	88	112
-5	30	5	429	-362
-4	30	5	172	-142
-3	30	5	680	-660
-2	30	5	208	-240
-1	30	5	119	136
0	30	5	174	148
1	30	5	70	85
2	30	5	150	146
3	30	5	88	112
-5	31	5	429	-362
-4	31	5	172	-142
-3	31	5	680	-660
-2	31	5	208	-240
-1	31	5	119	136
0	31	5	174	148
1	31	5	70	85
2	31	5	150	146
3	31	5	88	112
-5	32	5	429	-362
-4	32	5	172	-142
-3	32	5	680	-660
-2	32	5	208	-240
-1	32	5	119	136
0	32	5	174	148
1	32	5	70	85
2	32	5	150	146
3	32	5	88	112
-5	33	5	429	-362
-4	33	5	172	-142
-3	33	5	680	-660
-2	33	5	208	-240
-1	33	5	119	136
0	33	5	174	148
1	33	5	70	85
2	33	5	150	146
3	33	5	88	112
-5	34	5	429	-362
-4	34	5	172	-142
-3	34	5	680	-660
-2	34	5	208	-240
-1	34	5	119	136
0	34	5	174	148
1	34	5	70	85
2	34	5	150	146
3	34	5	88	112
-5	35	5	429	-362
-4	35	5	172	-142
-3	35	5	680	-660
-2	35	5	208	-240
-1	35	5	119	136
0	35	5	174	148
1	35	5	70	85
2	35	5	150	146
3	35	5	88	112
-5	36	5	429	-362
-4	36	5	172	-142
-3	36	5	680	-660
-2	36	5	208	-240
-1	36	5	119	136
0	36	5	174	148
1	36	5	70	85
2	36	5	150	146
3	36	5	88	112
-5	37	5	429	-362
-4	37	5	172	-142
-3	37	5	680	-660
-2	37	5	208	-240
-1	37	5	119	136
0	37	5	174	148
1	37	5	70	85
2	37	5	150	146
3	37	5	88	112
-5	38	5	429	-362
-4	38	5	172	-142
-3	38	5	680	-660
-2	38	5	208	-240
-1	38	5	119	136
0	38	5	174	148
1	38	5	70	85
2	38	5	150	146
3	38	5	88	112
-5	39	5	429	-362
-4	39	5	172	-142
-3	39	5	680	-660
-2	39	5	208	-240
-1	39	5	119	136
0	39	5	174	148
1	39	5	70	85
2	39	5	150	146
3	39	5	88	112
-5	40	5	429	-362
-4	40	5	172	-142
-3	40	5	680	-660
-2	40	5	208	-240
-1	40	5	119	136
0	40	5	174	148
1	40	5	70	85
2	40	5	150	146
3	40	5	88	112
-5	41	5	429	-362
-4	41	5	172	-142
-3	41	5	680	-660
-2	41	5	208	-240
-1	41	5	119	136
0	41	5	174	148
1	41	5	70	85
2	41	5	150	146
3	41	5	88	112
-5	42	5	429	-362
-4	42	5	172	-142
-3	42	5	680	-660
-2	42	5	208	-240
-1	42	5	119	136
0	42	5	174	148
1	42	5	70	85
2	42	5	150	146
3	42	5	88	112
-5	43	5	429	-362
-4	43	5	172	-142
-3	43	5	680	-660
-2	43	5	208	-240
-1	43	5	119	136
0	43	5	174	148
1	43	5	70	85
2	43	5	150	146
3	43	5	88	112
-5	44	5	429	-362
-4	44	5	172	-142
-3	44	5	680	-660
-2	44	5	208	-240
-1	44	5	119	136
0	44	5	174	148
1	44	5	70	85
2	44	5	150	146
3	44	5	88	112
-5	45	5	429	-362
-4	45	5	172	-142
-3	45	5	680	-660
-2	45	5	208	-240
-1	45	5	119	136
0	45	5	174	148
1	45	5	70	85
2	45	5	150	146
3	45	5	88	112
-5	46	5	429	-362
-4	46	5	172	-142
-3	46	5	680	-660
-2	46	5	208	-240
-1	46	5	119	136
0	46	5	174	148
1	46	5	70	85
2	46	5	150	146
3	46	5	88	112
-5	47	5	429	-362
-4	47	5	172	-142
-3	47	5	680	-660
-2	47	5	208	-240
-1	47	5	119	136
0	47	5	174	148
1	47	5	70	85
2	47	5	150	146
3	47	5	88	112
-5	48	5	429	-362
-4	48	5	172	-142
-3	48	5	680	-660
-2	48	5	208	-240
-1	48	5	119	136
0	48	5	174	148
1	48	5	70	85
2	48	5	150	146
3	48	5	88	112
-5	49	5	429	-362
-4	49	5	172	-142
-3	49	5	680	-660
-2	49	5	208	-240
-1	49	5	119	136
0	49	5	174	148
1	49	5	70	85
2	49	5	150	146
3	49	5	88	112
-5	50	5	429	-362
-4	50	5	172	-142
-3	50	5	680	-660
-2	50	5	208	-240
-1	50	5	119	136
0	50	5	174	148
1	50	5	70	85
2	50	5	150	146
3	50	5	88	112
-5	51	5	429	-362
-4	51	5	172	-142
-3	51	5	680	-660
-2	51	5	208	-240
-1	51	5	119	136
0	51	5	174	148
1	51	5	70	85
2	51	5	150	146
3	51	5	88	112
-5	52	5	429	-362
-4	52	5	172	-142
-3	52	5	680	-660
-2	52	5	208	-240
-1	52	5	119	136
0	52	5	174	148
1	52	5	70	85
2	52	5	150	146
3	52	5	88	112
-5	53	5	429	-362
-4	53	5	172	-142
-3	53	5	680	-660
-2	53	5	208	-240
-1	53	5	119	136
0	53	5	174	148
1	53	5	70	85
2	53	5	150	146
3	53	5	88	112
-5	54	5	429	-362
-4	54	5	172	-142
-3	54	5	680	-660
-2	54	5	208	-240
-1	54	5	119	136
0	54	5	174	148
1	54	5	70	85
2	54	5	150	146
3	54	5	88	112
-5	55	5	429	-362
-4	55	5	172	-142
-3	55	5	680	-660
-2	55	5	208	-240
-1	55	5	119	136
0	55	5	174	148
1	55	5	70	85
2	55	5	150	146
3	55	5	88	112
-5	56	5	429	-362
-4	56	5	172	-142
-3	56	5	680	-660
-2	56	5	208	-240
-1	56	5	119	136
0	56	5	174	148
1	56	5	70	85
2	56	5	150	146
3	56	5	88	112
-5	57	5	429	-362
-4	57	5	172	-142
-3	57	5	680	-660
-2	57	5	208	-240
-1	57	5	119	136
0	57	5	174	148
1	57	5	70	85
2	57	5	150	146
3	57	5	88	112
-5	58	5	429	-362
-4	58	5	172	-142
-3	58	5	680	-660
-2	58	5	208	-240
-1	58	5	119	136
0	58	5	174	148
1	58	5	70	85
2	58	5	150	146
3	58	5	88	112
-5	59	5	429	-362
-4	59	5	172	-142
-3	59	5	680	-660
-2	59	5	208	-240
-1	59	5	119	136
0	59	5	174	148
1	59	5	70	85
2	59	5	150	146
3	59	5	88	112
-5	60	5	429	-362
-4	60	5	172	-142
-3	60	5	680	-660
-2	60	5	208	-240
-1	60	5	119	136
0	60	5	174	148
1	60	5	70	85
2	60	5	150	146
3	60	5	88	112
-5	61	5	429	-362
-4	61	5	172	-142
-3	61	5	680	-660
-2	61	5	208	-240
-1	61	5	119	136
0	61	5	174	148
1	61	5	70	85
2	61	5	150	146
3	61	5	88	112
-5	62	5	429	-362
-4	62	5	172	-142
-3	62	5	680	-660
-2	62	5	208	-240
-1	62	5	119	136
0	62	5	174	148
1	62	5	70	85
2	62	5	150	146
3	62	5	88	112
-5	63	5	429	-362
-4	63	5	172	-142
-3	63	5	680	-660
-2	63	5	208	-240
-1	63	5	119	136
0	63	5	174	148
1	63	5	70	85
2	63	5	150	146
3	63	5	88	112
-5	64	5	429	-362
-4	64	5	172	-142
-3	64	5	680	-660
-2	64	5	208	-240
-1	64	5	119	136
0	64	5	174	148
1	64	5	70	85
2	64	5	150	146
3	64	5	88	112
-5	65	5	429	-362
-4	65	5	172	-142
-3	65	5	680	-660
-2	65	5	208	-240
-1	65	5	119	136
0	65	5	174	148
1	65	5	70	85
2	65	5	150	146
3	65	5	88	112
-5	66	5	429	-362
-4	66	5	172	-142
-3	66	5	680	-660
-2	66	5	208	-240
-1	66	5	119	136
0	66	5	174	148
1	66	5	70	85
2	66	5	150	146
3	66	5	88	112
-5	67	5	429	-362
-4	67	5	172	-142
-3	67	5	680	-660
-2	67	5	208	-240
-1	67	5	119	136
0	67	5	174	148
1	67	5	70	85
2	67	5	150	146
3	67	5	88	112
-5	68	5	429	-362
-4	68	5	172	-142
-3	68	5	680	-660
-2	68	5	208	-240
-1	68	5	119	136
0	68	5	174	148
1	68	5	70	85
2	68	5	150	146
3	68	5	88	112
-5	69	5	429	-362
-4	69	5	172	-142
-3	69	5	680	-660
-2	69	5	208	-240
-1	69	5	119	136
0	69	5	174	148
1	69	5	70	85
2	69	5	150	146
3	69	5	88	112
-5	70	5	429	-362
-4	70	5	172	-142
-3	70	5	680	-660
-2	70	5	208	-240
-1	70	5	119	136
0	70	5	174	148
1	70	5	70	85
2	70	5	150	146
3	70	5	88	112
-5	71	5	429	-362
-4	71	5	172	-142
-3	71	5	680	-660
-2	71	5	208	-240
-1	71	5	119	136
0	71	5	174	148
1	71	5	70	85
2	71	5	150	146
3	71	5	88	112
-5	72	5	429	-362
-4	72	5	172	-142
-3	72	5	680	-660
-2	72	5	208	-240
-1	72	5	119	136
0	72	5	174	148
1	72	5	70	85
2	72	5	150	146
3	72	5	88	112
-5	73	5	429	-362
-4	73	5	172	-142
-3	73	5	680	-660
-2	73	5	208	-240
-1	73	5	119	136
0	73	5	174	148
1	73	5	70	85
2	73	5	150	146
3	73	5	88	112
-5	74	5	429	-362
-4	74	5	172	-142
-3	74	5	680	-660
-2	74	5	208	-240
-1	74	5	119	136
0	74	5	174	148
1	74	5	70	85
2	74	5	150	146
3	74	5	88	112
-5	75	5	429	-362
-4	75	5	172	-142
-3	75	5	680	-660
-2	75	5	208	-240
-1	75	5	119	136
0	75	5	174	148
1	75	5	70	85
2	75	5	150	146
3	75	5	88	112
-5	76	5	429	-362
-4	76	5	172	-142
-3	76	5	680	-660
-2	76	5	208	-240
-1	76	5	119	136
0	76	5	174	148
1	76	5	70	85
2	76	5	150	146
3	76	5	88	112
-5	77	5	429	-362
-4	77	5	172	-142
-3	77	5	680	-660
-2	77	5	208	-240
-1	77	5	119	136
0	77	5	174	148
1	77	5	70	85
2	77	5	150	146
3	77	5	88	112
-5	78	5	429	-362
-4	78	5	172	-142
-3	78	5	680	-660
-2	78	5	208	-240
-1	78	5	119	136
0	78	5	174	148
1	78	5	70	85
2	78	5	150	146
3	78	5	88	112
-5	79	5	429	-362
-4	79	5	172	-142
-3	79	5	680	-660
-2	79	5	208	-240
-1	79	5	119	136
0	79	5	174	148
1	79	5	70	85
2	79	5	150	146
3	79	5	88	112
-5	80	5	429	-362
-4	80	5	172	-142
-3	80	5	680	-660
-2	80	5	208	-

Observed and calculated structural factors for

$Mo(CO)_2(\eta^3\text{-}CH_2{=}C(CONHMe){-}C{=}CH_2)(bipy)(O_2CC_3F_7)$

H	K	L	10FO	10FC
1	0	5	514	-530
2	4	5	394	-376
3	4	5	212	-227
4	4	5	163	-167
5	4	5	98	-102
-4	5	5	234	-257
-3	5	5	181	-167
-2	5	5	60	54
-1	5	5	258	218
2	5	5	313	330
3	5	5	148	145
4	5	5	55	48
-6	6	5	65	102
-5	6	5	114	102
-4	6	5	53	61
-2	6	5	119	-116
-1	6	5	233	-258
0	6	5	319	-311
1	6	5	400	-394
2	6	5	168	-162
	6	5	99	-135
-6	7	5	87	-88
-5	7	5	130	140
-3	7	5	297	302
-2	7	5	275	300
-1	7	5	171	175
0	7	5	110	118
1	7	5	55	-55
-4	8	5	121	-105
-3	8	5	174	-156
-2	8	5	200	-213
-1	8	5	182	-164
0	8	5	102	-114
1	8	5	192	181
-3	9	5	122	102
-2	9	5	79	78

H	K	L	10FO	10FC
1-10	-9	6	62	-86
2-10	-9	6	131	-119
0	-9	6	76	86
1	-9	6	210	220
2	-9	6	226	214
3	-9	6	129	141
4	-9	6	210	194
-3	-8	6	102	89
-1	-8	6	84	-100
0	-8	6	187	-193
1	-8	6	342	-357
2	-8	6	302	-308
3	-8	6	223	-200
4	-8	6	135	-140
-4	-7	6	139	-128
-2	-7	6	70	-78
0	-7	6	278	284
1	-7	6	422	424
2	-7	6	570	567
3	-7	6	146	154
5	-7	6	176	-170
6	-7	6	233	-206
-5	-6	6	121	134
-4	-6	6	157	149
-3	-6	6	107	-104
-2	-6	6	196	-191
-1	-6	6	407	-389
0	-6	6	389	-470
1	-6	6	332	-367
2	-6	6	224	-259
3	-6	6	51	-42
4	-6	6	60	60
5	-6	6	96	98
6	-6	6	214	204
-5	-5	6	60	-54
-4	-5	6	63	39

H	K	L	10FO	10FC
-3	-5	6	184	171
-2	-5	6	407	406
0	-5	6	567	574
1	-5	6	369	366
2	-5	6	245	242
3	-5	6	136	-125
4	-5	6	185	-191
5	-5	6	118	-121
6	-5	6	240	-219
7	-5	6	186	-185
-6	-4	6	68	71
-5	-4	6	158	-139
-4	-4	6	203	-190
-3	-4	6	406	-386
-2	-4	6	577	-559
-1	-4	6	255	-244
0	-4	6	177	-175
1	-4	6	83	-70
2	-4	6	136	-127
3	-4	6	218	214
4	-4	6	425	405
5	-4	6	308	268
6	-4	6	449	417
7	-4	6	87	112
-5	-3	6	99	78
-4	-3	6	227	211
-3	-3	6	484	468
-2	-3	6	494	453
-1	-3	6	365	335
0	-3	6	100	112
1	-3	6	40	51
3	-3	6	351	-338
4	-3	6	371	-326
5	-3	6	347	-336
6	-3	6	170	-156
7	-3	6	96	-101

H	K	L	10FO	10FC
-5	-2	6	99	-120
-4	-2	6	231	-256
-3	-2	6	134	-125
-2	-2	6	244	-230
-1	-2	6	182	-203
0	-2	6	365	-335
1	-2	6	318	299
2	-2	6	987	923
3	-2	6	483	465
4	-2	6	650	596
5	-2	6	74	-75
6	-2	6	90	-79
-3	-1	6	200	239
-2	-1	6	57	61
-1	-1	6	209	-193
0	-1	6	137	-137
1	-1	6	810	-780
2	-1	6	702	-664
3	-1	6	521	-530
4	-1	6	348	-347
6	-1	6	61	50
-2	0	6	256	284
1	0	6	67	-47
2	0	6	348	353
3	0	6	349	356
4	0	6	78	86
6	0	6	151	-130
-2	1	6	412	-392
-1	1	6	687	-650
0	1	6	1035	-994
1	1	6	71	-79
2	1	6	306	-292
3	1	6	93	112
4	1	6	66	45
5	1	6	93	68
6	1	6	221	194

H	K	L	10FO	10FC
-3	2	6	113	105
-2	2	6	427	412
-1	2	6	1010	974
0	2	6	375	381
1	2	6	500	519
2	2	6	75	75
3	2	6	46	-52
4	2	6	99	-84
5	2	6	182	-174
6	2	6	164	-164
-3	3	6	273	-269
-2	3	6	754	-710
-1	3	6	493	-473
0	3	6	408	-422
1	3	6	134	-137
2	3	6	100	96
3	3	6	233	239
4	3	6	310	293
5	3	6	197	182
-4	4	6	117	127
-3	4	6	286	265
-2	4	6	251	209
-1	4	6	574	578
0	4	6	232	311
1	4	6	43	-56
2	4	6	204	-206
3	4	6	288	-259
4	4	6	251	-238
5	4	6	145	-147
-4	5	6	194	-198
-3	5	6	120	-125
-2	5	6	73	65
-1	5	6	142	-115
0	5	6	171	-167
2	5	6	177	183
3	5	6	273	273

Observed and calculated structural factors for

$Mo(CO)_2(\eta^3\text{-}CH_2{=}C(CONHMe){=}C{=}CH_2)(bipy)(O_2CC_3F_7)$

H	K	L	10FO	10FC	H	K	L	10FO	10FC	H	K	L	10FO	10FC	H	K	L	10FO	10FC	H	K	L	10FO	10FC
4	5	6	232	245	2	-8	7	61	-65	-5	-4	7	140	122	1	-1	7	221	-204	2	3	7	215	-212
-5	6	6	109	143	3	-8	7	198	-215	-4	-4	7	53	61	2	-1	7	110	-105	3	3	7	213	-231
-4	6	6	254	241	4	-8	7	285	-261	-3	-4	7	50	-48	3	-1	7	160	-148	4	3	7	87	-78
-3	6	6	218	225	5	-8	7	278	-269	-2	-4	7	126	-114	4	-1	7	279	-258	5	3	7	64	72
-2	6	6	151	169	-4	-7	7	230	-205	-1	-4	7	40	-45	5	-1	7	56	-66	-4	4	7	139	-146
-1	6	6	103	121	-3	-7	7	278	-273	0	-4	7	368	-446	6	-1	7	131	-115	-3	4	7	127	122
0	6	6	109	-97	-2	-7	7	222	-218	1	-4	7	577	-549	-2	0	7	747	-716	-2	4	7	467	471
1	6	6	235	-244	-1	-7	7	160	-159	2	-4	7	175	-190	-1	0	7	53	-54	-1	4	7	321	330
2	6	6	261	-276	0	-7	7	64	66	3	-4	7	128	-139	0	0	7	226	214	1	4	7	228	239
3	6	6	148	-155	1	-7	7	87	101	6	-4	7	141	149	1	0	7	397	391	2	4	7	101	119
-6	7	6	102	-102	2	-7	7	229	203	-5	-3	7	152	166	2	0	7	405	381	3	4	7	121	96
-5	7	6	167	-172	3	-7	7	254	241	-4	-3	7	87	77	3	0	7	289	270	-4	5	7	57	45
-4	7	6	108	-107	4	-7	7	233	225	-3	-3	7	280	252	4	0	7	292	278	-3	5	7	82	-70
-3	7	6	108	-113	5	-7	7	176	158	-2	-3	7	487	499	5	0	7	63	82	-2	5	7	289	-278
-2	7	6	67	-71	6	-7	7	57	46	-1	-3	7	294	300	-2	1	7	411	403	-1	5	7	321	-317
-1	7	6	67	45	-4	-6	7	320	301	0	-3	7	248	255	-1	1	7	519	522	0	5	7	441	-350
0	7	6	38	23	-3	-6	7	207	181	2	-3	7	142	134	0	1	7	196	-192	2	5	7	116	-103
1	7	6	109	113	-2	-6	7	116	115	3	-3	7	115	109	1	1	7	448	-432	4	5	7	128	122
2	7	6	55	61	-1	-6	7	59	-48	4	-3	7	52	-64	2	1	7	654	-636	-5	6	7	69	-92
-4	8	6	61	63	0	-6	7	243	-273	5	-3	7	261	-260	3	1	7	425	-426	-4	6	7	74	87
-2	8	6	121	-125	1	-6	7	385	-362	6	-3	7	335	-335	4	1	7	265	-239	-3	6	7	147	134
-1	8	6	113	-112	2	-6	7	371	-340	7	-3	7	159	-178	5	1	7	159	-135	-2	6	7	158	150
0	8	6	136	-123	3	-6	7	259	-248	-4	-2	7	104	-99	-3	2	7	87	134	-1	6	7	197	190
1	8	6	118	-123	4	-6	7	122	-124	-3	-2	7	316	-312	-2	2	7	346	-347	0	6	7	168	165
1	-10	7	118	132	5	-6	7	98	-97	-2	-2	7	874	-837	-1	2	7	96	-85	1	6	7	139	140
-1	-9	7	323	-339	6	-6	7	45	19	-1	-2	7	236	-248	0	2	7	361	355	3	6	7	111	-123
0	-9	7	251	-247	-5	-5	7	218	-198	0	-2	7	92	-104	1	2	7	248	271	-5	7	7	161	-173
1	-9	7	68	-75	-4	-5	7	336	-300	1	-2	7	232	-218	2	2	7	362	363	-4	7	7	207	-185
2	-9	7	285	252	-3	-5	7	82	-61	2	-2	7	186	-182	3	2	7	323	311	-3	7	7	143	-131
3	-9	7	205	216	0	-5	7	470	424	3	-2	7	191	175	4	2	7	332	319	-2	7	7	153	-154
4	-9	7	192	184	1	-5	7	495	501	4	-2	7	264	272	5	2	7	191	168	-1	7	7	111	-115
-3	-8	7	191	192	2	-5	7	603	588	5	-2	7	224	228	-3	3	7	116	124	0	7	7	68	-84
-2	-8	7	271	271	3	-5	7	307	305	6	-2	7	153	117	-2	3	7	317	-318	2	7	7	57	64
-1	-8	7	156	177	4	-5	7	184	184	-3	-1	7	519	564	-1	3	7	234	-193	-4	8	7	170	158
0	-8	7	66	63	5	-5	7	80	89	-2	-1	7	537	511	0	3	7	356	-339	-3	8	7	157	157
1	-8	7	119	-117	-6	-4	7	111	129	0	-1	7	363	-377	1	3	7	225	-213	-2	8	7	93	96

Observed and calculated structural factors for

$Mo(CO)_2(\eta^3\text{-}CH_2\text{-}C(CONHMe)\text{-}C\text{=}CH_2)(bipy)(O_2CC_3F_7)$

H	K	L	10FO	10FC	H	K	L	10FO	10FC	H	K	L	10FO	10FC	H	K	L	10FO	10FC
-1	8	7	55	47	-1	-5	8	281	-241	-1	-2	8	282	-276	-2	2	8	494	-454	-1	7	8	205	-204
-1	-9	8	160	-139	0	-5	8	215	-208	0	-2	8	371	-369	-1	2	8	369	-374	0	7	8	185	-189
0	-9	8	242	-225	1	-5	8	108	97	1	-2	8	496	-491	0	2	8	137	-144	1	7	8	194	-186
1	-9	8	307	-314	2	-5	8	304	285	2	-2	8	329	-322	2	2	8	307	317	-3	8	8	101	96
2	-9	8	123	-117	3	-5	8	498	482	3	-2	8	363	-353	3	2	8	272	275	-2	8	8	234	233
3	-9	8	82	-89	4	-5	8	250	246	4	-2	8	106	-110	4	2	8	363	346	-1	8	8	214	217
-3	-8	8	59	64	5	-5	8	266	251	5	-2	8	249	227	5	2	8	279	310	-1	-9	9	158	165
-2	-8	8	160	150	6	-5	8	138	140	-3	-1	8	100	90	-3	3	8	407	398	0	-9	9	40	32
-1	-8	8	190	196	-6	-4	8	59	83	-2	-1	8	434	424	-2	3	8	683	688	1	-9	9	113	-122
0	-8	8	277	257	-5	-4	8	266	254	-1	-1	8	212	217	-1	3	8	167	168	2	-9	9	279	-285
1	-8	8	105	210	-4	-4	8	263	260	0	-1	8	305	331	0	3	8	157	-151	3	-9	9	254	-256
5	-8	8	175	-167	-3	-4	8	374	334	1	-1	8	513	494	1	3	8	359	-371	-2	-8	9	174	-165
-4	-7	8	69	-55	-2	-4	8	56	62	2	-1	8	281	265	2	3	8	167	-173	-1	-8	9	68	-93
-3	-7	8	200	-175	-1	-4	8	113	-101	4	-1	8	166	-175	3	3	8	253	-244	1	-8	9	191	183
-2	-7	8	231	-232	0	-4	8	137	-159	5	-1	8	166	-144	4	3	8	287	-266	2	-8	9	104	102
-1	-7	8	353	-354	1	-4	8	245	-249	6	-1	8	149	-137	5	3	8	151	-143	3	-8	9	254	250
0	-7	8	235	-253	2	-4	8	291	-277	-2	0	8	373	-343	-4	4	8	257	-245	4	-8	9	225	222
1	-7	8	233	-249	3	-4	8	277	-270	-1	0	8	922	-883	-3	4	8	109	-84	5	-8	9	165	161
2	-7	8	160	-160	4	-4	8	235	-220	0	0	8	829	-823	-2	4	8	100	84	-3	-7	9	115	107
3	-7	8	117	118	5	-4	8	237	-215	1	0	8	557	-573	-1	4	8	107	-115	-1	-7	9	110	-111
4	-7	8	130	127	6	-4	8	162	-174	2	0	8	289	-265	0	4	8	97	120	0	-7	9	296	-294
5	-7	8	271	258	-5	-3	8	166	-180	3	0	8	232	207	2	4	8	157	155	1	-7	9	140	-150
-4	-6	8	172	158	-4	-3	8	355	-327	4	0	8	81	64	3	4	8	286	302	2	-7	9	206	-184
-3	-6	8	197	212	-3	-3	8	165	-147	5	0	8	205	190	4	4	8	212	212	3	-7	9	160	-169
-2	-6	8	228	229	-1	-3	8	44	45	6	0	8	213	181	-4	5	8	197	194	4	-7	9	160	-162
-1	-6	8	383	373	0	-3	8	247	225	-3	1	8	109	94	0	5	8	228	-199	-4	-6	9	78	-69
1	-6	8	254	216	1	-3	8	410	449	-2	1	8	523	526	2	5	8	195	-206	-3	-6	9	117	109
2	-6	8	83	-99	2	-3	8	148	170	-1	1	8	848	824	3	5	8	215	-213	-2	-6	9	202	191
3	-6	8	229	-238	3	-3	8	402	381	0	1	8	678	663	-5	6	8	117	-141	-1	-6	9	360	357
4	-6	8	91	-95	4	-3	8	255	250	1	1	8	435	442	-4	6	8	79	-86	1	-6	9	420	413
5	-6	8	130	-129	5	-3	8	80	91	2	1	8	95	-106	-1	6	8	53	72	2	-6	9	265	270
6	-6	8	176	-162	6	-3	8	44	-47	3	1	8	360	-343	0	6	8	220	209	3	-6	9	124	149
-5	-5	8	82	-79	-5	-2	8	91	130	4	1	8	209	-202	1	6	8	229	244	4	-6	9	120	118
-4	-5	8	125	-125	-4	-2	8	236	293	5	1	8	140	-141	2	6	8	154	158	5	-6	9	74	-67
-3	-5	8	165	-167	-3	-2	8	130	147	6	1	8	155	-140	-3	7	8	72	-85	6	-6	9	142	-135
-2	-5	8	274	-245	-2	-2	8	106	-102	-3	2	8	223	-221	-2	7	8	177	-160	-5	-5	9	178	176

Observed and calculated structural factors for

$Mo(CO)_2(\eta^3\text{-}CH_2{=}C(CONHMe){=}CH_2)(bipy)(O_2CC_3F_7)$

H	K	L	10FO	10FC	H	K	L	10FO	10FC	H	K	L	10FO	10FC	H	K	L	10FO	10FC
-3	-5	9	200	-195	-1	-2	9	146	132	-2	2	9	119	129	1	7	9	165	-172
-2	-5	9	288	-284	0	-2	9	74	-70	-1	2	9	382	-386	0	-9	10	257	254
-1	-5	9	301	-303	2	-2	9	307	-320	0	2	9	298	-297	1	-9	10	121	124
0	-5	9	340	-335	3	-2	9	454	-436	1	2	9	291	-316	3	-9	10	59	-53
1	-5	9	415	-411	4	-2	9	340	-355	2	2	9	223	-215	-2	-8	10	294	-269
2	-5	9	250	-234	5	-2	9	170	-152	3	2	9	70	-76	-1	-8	10	250	-261
4	-5	9	114	128	6	-2	9	90	-77	5	2	9	206	191	0	-8	10	163	-157
5	-5	9	240	238	-3	-1	9	485	-508	-4	3	9	58	55	1	-8	10	94	76
6	-5	9	210	193	-2	-1	9	414	-400	-3	3	9	185	155	2	-8	10	172	160
-5	-4	9	57	-72	-1	-1	9	153	168	-2	3	9	490	466	3	-8	10	54	60
-4	-4	9	158	127	0	-1	9	236	216	-1	3	9	386	357	4	-8	10	165	156
-3	-4	9	449	433	1	-1	9	553	542	0	3	9	217	237	-3	-7	10	298	266
-2	-4	9	367	380	2	-1	9	415	404	1	3	9	42	-30	-2	-7	10	311	310
-1	-4	9	176	175	3	-1	9	328	311	4	3	9	190	-105	-1	-7	10	170	174
0	-4	9	112	118	4	-1	9	63	62	-4	4	9	57	-46	0	-7	10	79	-50
1	-4	9	36	-24	5	-1	9	70	-63	-3	4	9	300	-284	1	-7	10	169	-190
3	-4	9	86	-83	6	-1	9	112	90	-2	4	9	320	-307	2	-7	10	161	-172
4	-4	9	218	-214	-3	0	9	126	141	-1	4	9	286	-283	3	-7	10	185	-170
5	-4	9	213	-179	-2	0	9	105	109	0	4	9	197	-258	4	-7	10	210	-205
6	-4	9	256	-250	-1	0	9	34	18	1	4	9	100	-94	5	-7	10	224	-212
-5	-3	9	207	-207	0	0	9	69	-74	3	4	9	177	183	-4	-6	10	104	-96
-4	-3	9	159	-148	1	0	9	626	-613	4	4	9	161	158	-3	-6	10	80	78
-3	-3	9	403	-392	2	0	9	509	-516	-4	5	9	110	114	-1	-6	10	43	50
-2	-3	9	180	-178	3	0	9	401	-388	-1	5	9	122	90	0	-6	10	286	271
-1	-3	9	402	-395	4	0	9	156	-135	0	5	9	197	178	2	-6	10	319	323
0	-3	9	371	-333	6	0	9	70	89	2	5	9	62	-70	3	-6	10	312	314
1	-3	9	63	73	-3	1	9	68	84	3	5	9	149	-161	4	-6	10	205	194
2	-3	9	107	93	-2	1	9	389	373	-5	6	9	153	-178	5	-6	10	206	193
3	-3	9	465	439	-1	1	9	308	312	-4	6	9	209	-197	-5	-5	10	217	205
4	-3	9	266	250	0	1	9	273	257	-3	6	9	76	-62	-4	-5	10	97	87
5	-3	9	265	250	1	1	9	224	220	0	6	9	46	36	-3	-5	10	196	-198
6	-3	9	156	163	2	1	9	299	291	1	6	9	75	64	-1	-5	10	342	-307
-5	-2	9	143	175	3	1	9	275	260	2	6	9	132	120	0	-5	10	391	-361
-4	-2	9	257	202	4	1	9	330	300	-4	7	9	140	145	1	-5	10	289	-294
-3	-2	9	317	314	-4	2	9	59	76	-3	7	9	70	81	2	-5	10	176	-187
-2	-2	9	456	431	-3	2	9	62	-67	0	7	9	77	-83	3	-5	10	554	-546

Observed and calculated structural factors for

$Mo(CO)_2(\eta^3\text{-}CH_2{*}C(CONHMe){=}C{=}CH_2)(bipy)(O_2CC_3F_7)$

H	K	L	10FO	10FC	H	K	L	10FO	10FC	H	K	L	10FO	10FC	H	K	L	10FO	10FC
-1	-1	10	389	-438	-3	3	10	173	-150	-3	-7	11	162	154	-3	-3	11	193	193	4	0	11	121	-111
0	-1	10	320	-300	-2	3	10	280	-288	-2	-7	11	321	310	0	-3	11	155	-154	5	0	11	158	-145
1	-1	10	398	-376	-1	3	10	45	61	-1	-7	11	306	297	1	-3	11	236	-229	-4	1	11	64	-78
3	-1	10	81	72	0	3	10	192	194	0	-7	11	278	273	2	-3	11	351	-347	-3	1	11	117	-115
4	-1	10	223	305	1	3	10	250	256	5	-7	11	130	-135	3	-3	11	346	-333	-2	1	11	159	-156
5	-1	10	323	283	2	3	10	204	196	-4	-6	11	94	-92	4	-3	11	144	-131	-1	1	11	309	-305
6	-1	10	177	186	3	3	10	183	186	-3	-6	11	180	-101	5	-3	11	156	-158	0	1	11	364	-364
-4	0	10	82	101	4	3	10	130	122	-2	-6	11	190	-174	-5	-2	11	185	-223	1	1	11	247	-262
-3	0	10	424	393	-4	4	10	95	83	-1	-6	11	234	-226	-4	-2	11	283	-292	4	1	11	114	116
-2	0	10	670	650	-1	4	10	123	-127	0	-6	11	221	-242	-3	-2	11	306	-303	5	1	11	231	212
-1	0	10	304	297	1	4	10	149	-152	2	-6	11	57	46	-2	-2	11	110	-105	-3	2	11	129	117
0	0	10	83	80	2	4	10	199	-215	3	-6	11	136	134	-1	-2	11	239	229	-2	2	11	224	205
2	0	10	134	-122	3	4	10	142	-137	4	-6	11	292	298	0	-2	11	274	264	-1	2	11	215	197
3	0	10	165	-157	-3	5	10	227	248	5	-6	11	271	268	1	-2	11	194	208	0	2	11	279	286
4	0	10	110	-126	-2	5	10	156	144	-4	-5	11	182	185	2	-2	11	305	347	2	2	11	96	-93
5	0	10	165	-160	-1	5	10	206	199	-3	-5	11	163	169	3	-2	11	290	280	3	2	11	146	-150
-4	1	10	122	-105	2	5	10	64	80	-2	-5	11	201	189	4	-2	11	207	205	4	2	11	166	-166
-3	1	10	237	-201	-4	6	10	58	-60	-1	-5	11	235	215	5	-2	11	113	109	-4	3	11	161	-156
-1	1	10	330	299	-3	6	10	227	-225	0	-5	11	287	264	-5	-1	11	73	137	-3	3	11	130	-100
0	1	10	246	245	-2	6	10	314	-316	1	-5	11	52	46	-4	-1	11	141	172	-2	3	11	294	-277
1	1	10	115	115	-1	6	10	210	-216	2	-5	11	193	-200	-3	-1	11	259	263	-1	3	11	141	-140
2	1	10	102	108	0	6	10	185	-184	3	-5	11	270	-277	-2	-1	11	75	-74	0	3	11	51	-53
3	1	10	233	225	1	6	10	64	-75	4	-5	11	233	-238	-1	-1	11	95	-85	2	3	11	64	69
4	1	10	201	213	-5	7	10	91	75	5	-5	11	245	-222	0	-1	11	135	-121	3	3	11	181	164
5	1	10	153	153	-2	7	10	160	142	-5	-4	11	130	-120	1	-1	11	454	-453	4	3	11	133	132
-4	2	10	124	171	-1	7	10	176	178	-4	-4	11	208	-212	2	-1	11	387	-389	-4	4	11	129	114
-3	2	10	126	135	0	7	10	167	186	-3	-4	11	186	-190	3	-1	11	346	-344	-3	4	11	238	243
-2	2	10	164	168	0	-9	11	176	158	-2	-4	11	183	-153	5	-1	11	97	107	-2	4	11	50	30
-1	2	10	88	84	1	-9	11	122	144	-1	-4	11	334	-310	-4	0	11	113	-133	1	4	11	45	-36
0	2	10	143	-137	2	-7	11	180	178	1	-4	11	71	64	-3	0	11	63	75	2	4	11	125	-133
1	2	10	281	-268	-2	-8	11	86	-76	2	-4	11	248	301	-2	0	11	197	186	3	4	11	201	-204
2	2	10	289	-308	-1	-8	11	148	-159	3	-4	11	252	256	-1	0	11	334	334	-5	5	11	116	-175
3	2	10	287	-279	0	-8	11	166	-185	4	-4	11	112	110	0	0	11	721	722	-4	5	11	217	-193
4	2	10	187	-169	1	-8	11	198	-169	5	-4	11	134	131	1	0	11	572	565	-3	5	11	113	-110
5	2	10	97	-101	2	-8	11	98	-93	-5	-3	11	241	247	2	0	11	199	200	0	5	11	164	135
-4	3	10	139	-127	3	-8	11	124	-135	-4	-3	11	277	257	3	0	11	67	52	2	5	11	177	179

Observed and calculated structural factors for

$Mo(CO)_2(\eta^3\text{-}CH_2{=}C(CONHMe){=}C{=}CH_2)(bipy)(O_2CC_3F_7)$

H	K	L	10FO	10FC
-4	6	11	73	55
0	6	11	185	-183
1	6	11	198	-186
1	-6	12	231	-243
2	-6	12	191	-173
3	-6	12	167	-159
-3	-7	12	131	-118
-1	-7	12	76	104
0	-7	12	250	254
1	-7	12	235	234
2	-7	12	222	226
3	-7	12	207	199
4	-7	12	201	203
-1	-6	12	241	-228
0	-6	12	179	-199
2	-6	12	252	-256
3	-6	12	194	-173
4	-6	12	113	-118
5	-6	12	55	62
-3	-5	12	103	97
-2	-5	12	192	185
-1	-5	12	257	256
0	-5	12	262	278
1	-5	12	234	239
2	-5	12	90	102
3	-5	12	49	-31
4	-5	12	164	-162
5	-5	12	136	-139
-5	-4	12	117	112
-4	-4	12	51	-50
-3	-4	12	167	-157
-2	-4	12	296	-273
-1	-4	12	356	-338
0	-4	12	453	-474
1	-4	12	342	-336
2	-4	12	98	-104

H	K	L	10FO	10FC
-3	-4	12	127	120
-2	-4	12	162	167
-1	-4	12	176	157
0	-4	12	92	95
1	-3	12	276	261
2	-3	12	294	267
3	-3	12	387	402
4	-3	12	379	377
5	-3	12	169	177
-5	-2	12	108	-94
-4	-2	12	222	-216
-3	-2	12	264	-256
-2	-2	12	250	-253
-1	-2	12	290	-290
0	-2	12	32	-45
1	-2	12	100	103
2	-2	12	152	149
3	-2	12	109	120
4	-2	12	177	207
5	-2	12	293	311
-5	-1	12	95	120
-4	-1	12	131	121
-3	-1	12	291	292
-2	-1	12	251	242
-1	-1	12	67	-71
0	-1	12	109	-103
1	-1	12	139	-134
2	-1	12	143	-150
3	-1	12	294	-303
4	-1	12	123	-112
5	-1	12	75	-132
-5	0	12	162	-173

H	K	L	10FO	10FC
-4	0	12	252	-260
-3	0	12	76	75
-2	0	12	268	239
-1	0	12	167	172
0	0	12	168	177
1	0	12	190	193
2	0	12	274	288
3	0	12	56	46
4	0	12	73	65
5	0	12	109	110
-4	1	12	75	62
-3	1	12	92	-89
-2	1	12	100	-92
-1	1	12	175	-102
0	1	12	152	-159
1	1	12	293	-306
2	1	12	179	-168
3	1	12	103	-81
4	2	12	127	136
-1	2	12	195	177
0	2	12	271	268
1	2	12	231	235
2	2	12	105	102
3	2	12	112	-107
-4	3	12	55	-40
-3	3	12	88	-92
-2	3	12	186	-189
-1	3	12	146	-153
0	3	12	179	-177
1	3	12	54	-66
2	3	12	84	-87
3	3	12	127	102
-4	4	12	170	151
-3	4	12	210	211
-2	4	12	179	178
-1	4	12	70	97

H	K	L	10FO	10FC
-4	5	12	160	-153
-3	5	12	312	-317
-2	5	12	224	-199
-3	6	12	119	114
-2	6	12	122	128
-1	6	12	98	124
0	6	12	69	74
-1	-8	13	234	239
0	-8	13	190	198
1	-8	13	64	46
-2	-7	13	189	-170
-1	-7	13	132	-124
0	-7	13	79	-80
1	-7	13	183	167
2	-7	13	102	110
3	-7	13	161	178
4	-7	13	207	204
-3	-6	13	208	187
-2	-6	13	117	114
-1	-6	13	80	72
0	-6	13	37	-27
2	-6	13	239	-246
3	-6	13	228	-245
4	-6	13	274	-282
-4	-5	13	233	-221
-3	-5	13	103	-92
-2	-5	13	91	-97
1	-5	13	159	161
2	-5	13	269	268
3	-5	13	122	129
4	-5	13	93	86
-4	-4	13	129	120
-3	-4	13	110	95
-2	-4	13	90	88
-1	-4	13	77	-60
0	-4	13	289	-275

H	K	L	10FO	10FC
1	-4	13	311	-312
2	-4	13	337	-343
3	-4	13	109	-101
4	-4	13	70	-69
-5	-3	13	107	-104
-4	-3	13	159	-158
-3	-3	13	144	-148
-1	-3	13	289	281
0	-3	13	457	429
1	-3	13	382	379
2	-3	13	207	209
3	-3	13	93	95
-4	-2	13	75	72
-2	-2	13	144	-121
-1	-2	13	211	-199
0	-2	13	347	-370
1	-2	13	190	-197
2	-2	13	202	-199
3	-2	13	51	-39
5	-2	13	102	104
-3	-1	13	134	127
-2	-1	13	259	243
-1	-1	13	264	273
0	-1	13	269	266
1	-1	13	169	177
2	-1	13	65	61
4	-1	13	165	-172
-4	0	13	184	-175
-3	0	13	291	-272
-2	0	13	106	-113
-1	0	13	93	-65
0	0	13	173	-179
1	0	13	168	175
2	0	13	243	243
3	0	13	224	223
3	1	13	201	195

Observed and calculated structural factors for

$Mo(CO)_2(\eta^3\text{-}CH_2{=}C(CONHMe){=}CH_2)(bipy)(O_2CC_3F_7)$

H	K	L	10FO	10FC
-2	1	13	88	78
0	1	13	46	-38
2	1	13	64	-43
3	1	13	98	-91
4	1	13	159	-161
-4	2	13	122	-123
-3	2	13	222	-248
-2	2	13	206	-214
0	2	13	66	79
1	2	13	72	76
2	2	13	170	177
3	2	13	65	66
-4	3	13	65	71
-3	3	13	85	83
-2	3	13	116	114
0	3	13	89	-83
1	3	13	201	-220
2	3	13	245	-253
3	3	13	155	-159
-4	4	13	153	-121
-3	4	13	226	-233
-1	4	13	147	139
1	4	13	247	257
2	4	13	162	160
-4	5	13	96	96
0	5	13	239	-156
0	6	14	167	184
-8	8	14	228	259
-2	7	14	52	-48
-1	7	14	119	-128
0	7	14	256	-239
1	7	14	194	-108
2	7	14	149	-109
3	7	14	71	-73
-3	6	14	64	49
-2	6	14	111	98

H	K	L	10FO	10FC
-1	-6	14	268	260
1	-6	14	113	83
2	-6	14	54	53
3	-6	14	60	-55
4	-6	14	113	-103
-3	-5	14	192	-172
-2	-5	14	293	-273
-1	-5	14	222	-228
0	-5	14	183	-188
1	-5	14	64	-65
3	-5	14	79	87
4	-5	14	125	139
-4	-4	14	101	100
-3	-4	14	204	177
-2	-4	14	242	242
-1	-4	14	307	304
0	-4	14	324	328
2	-4	14	182	-184
3	-4	14	174	-176
4	-4	14	189	-186
-5	-3	14	102	-90
-4	-3	14	197	-179
-3	-3	14	179	-165
-2	-3	14	77	-66
-1	-3	14	60	-50
0	-3	14	42	-37
1	-3	14	70	69
2	-3	14	134	137
3	-3	14	116	129
4	-3	14	216	215
-5	-2	14	122	128
-4	-2	14	193	197
0	-2	14	138	-145
1	-2	14	158	-162
2	-2	14	172	-161
3	-2	14	177	-170

H	K	L	10FO	10FC
-4	-2	14	149	-152
-5	-1	14	95	-116
-4	-1	14	90	-86
-3	-1	14	65	-51
-1	-1	14	102	115
0	-1	14	127	135
1	-1	14	170	176
2	-1	14	310	332
3	-1	14	289	288
4	-1	14	113	117
-5	0	14	82	111
-4	0	14	157	163
-3	0	14	64	63
-2	0	14	194	-195
-1	0	14	182	-201
0	0	14	140	-152
1	0	14	183	-191
2	0	14	239	-235
3	0	14	50	-70
4	0	14	77	94
-2	1	14	127	120
-1	1	14	209	202
0	1	14	264	267
1	1	14	202	199
2	1	14	70	68
3	1	14	150	-154
4	2	14	160	-145
-3	2	14	234	-220
-2	2	14	222	-223
-1	2	14	214	-207
0	2	14	171	-161
1	2	14	64	-64
-4	3	14	176	159
-3	3	14	127	119
-2	3	14	145	148
-1	3	14	105	106

H	K	L	10FO	10FC
0	3	14	119	121
-4	4	14	93	-83
-3	4	14	171	-151
-2	4	14	177	-171
-1	4	14	87	-86
0	4	14	39	31
1	4	14	94	118
-3	5	14	161	156
-2	5	14	98	91
-1	5	14	63	35
0	-7	15	110	-119
1	-7	15	199	-226
2	-7	15	154	-174
-2	-6	15	98	-104
-1	-6	15	92	89
2	-6	15	166	168
3	-6	15	82	75
-1	-5	15	143	-152
0	-5	15	51	-65
1	-5	15	258	-269
2	-5	15	196	-192
3	-5	15	163	-166
-3	-4	15	53	41
-2	-4	15	138	134
-1	-4	15	203	187
0	-4	15	259	270
1	-4	15	202	220
2	-4	15	142	153
-4	-3	15	61	-69
-3	-3	15	198	-186
-2	-3	15	183	-169
-1	-3	15	255	-242
0	-3	15	175	-176
1	-3	15	66	-75
3	-3	15	92	87
4	-3	15	123	127

H	K	L	10FO	10FC
-4	-2	15	194	190
-3	-2	15	298	272
-2	-2	15	211	192
-1	-2	15	139	136
1	-2	15	45	-52
3	-2	15	116	-125
4	-2	15	79	-93
-5	-1	15	65	-62
-4	-1	15	163	-163
-3	-1	15	140	-120
-2	-1	15	141	-121
-1	-1	15	53	-50
0	-1	15	77	74
1	-1	15	103	97
2	-1	15	147	154
3	-1	15	104	102
-5	0	15	85	112
-4	0	15	150	142
-3	0	15	134	144
-2	0	15	59	53
-1	0	15	64	-68
0	0	15	48	-30
1	0	15	134	-139
2	0	15	111	-110
3	0	15	190	-213
-5	1	15	72	-89
-4	1	15	171	-175
-3	1	15	181	-186
-2	1	15	110	-122
-1	1	15	58	-65
0	1	15	69	76
1	1	15	185	190
2	1	15	198	218
3	1	15	87	81
-4	2	15	101	89
-2	2	15	98	-93

Observed and calculated structural factors for

$Mo(CO)_2(\eta^3\text{-}CH_2{=}C(CONHMe){-}C{=}CH_2)(bipy)(O_2CC_3F_7)$

H	K	L	10FO	10FC
-1	2	15	162	-179
0	2	15	158	-157
1	2	15	175	-179
2	2	15	133	-126
-2	3	15	95	91
-1	3	15	184	184
0	3	15	172	188
1	3	15	183	180
-2	4	15	95	-88
-1	4	15	103	-94
0	4	15	92	-115
0	-6	16	47	45
2	-6	16	90	100
-2	-5	16	135	131
1	-5	16	98	-102
2	-5	16	114	-124
3	-5	16	160	-163
-3	-4	16	81	-72
1	-4	16	202	196
2	-4	16	181	191
3	-4	16	205	215
-4	-3	16	60	57
-3	-3	16	47	-58
-1	-3	16	125	-126
1	-3	16	171	-175
2	-3	16	132	-132
3	-3	16	104	-100
-2	-2	16	86	82
-1	-2	16	229	233
0	-2	16	212	211
1	-2	16	154	163
2	-2	16	142	149
-3	-1	16	61	-52
-2	-1	16	165	-155
-1	-1	16	243	-250
0	-1	16	160	-148
1	-1	16	123	-127
2	-1	16	57	-47
-3	0	16	111	105
-2	0	16	139	132
-1	0	16	51	50
0	0	16	93	86
1	0	16	87	93
-4	1	16	124	-111
-3	1	16	183	-182
-2	1	16	159	-149
-1	1	16	183	-179
0	1	16	170	-169
2	1	16	67	55
-4	2	16	140	143
-3	2	16	124	133
-2	2	16	112	121
-1	2	16	140	157
0	2	16	69	67
1	2	16	58	-46
-3	3	16	94	-105
-2	3	16	92	-98
0	3	16	52	62
-1	-5	17	141	160
0	-5	17	52	54
1	-5	17	92	99
2	-5	17	71	79
-2	-4	17	179	-172
-1	-4	17	46	-55
-3	-3	17	173	161
-2	-3	17	136	121
-1	-3	17	161	161
1	-3	17	55	-48
2	-3	17	137	-146
-3	-2	17	91	-81
-2	-2	17	91	-90
-1	-2	17	108	-96
0	-2	17	52	-40
1	-2	17	120	127
2	-2	17	184	196
0	-1	17	85	-96
1	-1	17	171	-188
2	-1	17	149	-173
-3	0	17	65	-61
-1	0	17	77	-83
0	0	17	122	118
1	0	17	166	176
-2	1	17	143	-147
-1	1	17	146	-143
-2	-1	18	152	142
-1	-1	18	137	150
0	-1	18	58	-63
-2	0	18	127	-121
-1	0	18	91	-89
0	1	17	161	-164
1	1	17	116	-112
-2	2	17	149	142
-1	2	17	180	188
0	2	17	107	98
-1	-4	18	55	-63
0	-4	18	116	-119
1	-4	18	139	-132
-2	-3	18	86	77
-1	-3	18	96	95
0	-3	18	124	120
1	-3	18	115	124
-2	-2	18	203	-167
-1	-2	18	212	-199
0	-2	18	100	-100
1	-2	18	53	-34
-2	-1	18	152	142
-1	-1	18	137	150
0	-1	18	58	-63
-2	0	18	127	-121
-1	0	18	91	-89